



精工锻造的钉砧使钳口压力增强且一致
三点控制系统确保缝钉排列整齐，成型良好
独有金色钉仓，提供1.8mm 成钉高度

60
Echelon

45
Echelon



腔镜直线型切割吻合器和钉仓 (商品名: ECHELON 60)
注册证号: 国食药监械(进)字2011第3220273号

腔镜直线型切割吻合器和钉仓 (商品名: ECHELON 45)
注册证号: 国食药监械(进)字2009第3651686号

广告批准文号:

强生(上海)医疗器械有限公司
地址: 上海市徐汇区虹桥路355号城开国际大厦4楼
邮编: 200030
电话: 021-22058888
传真: 021-22058868
网址: www.jjmc.com.cn
生产企业地址: Ethicon Endo-Surgery, LLC



JOURNAL of THORACIC DISEASE



www.jthoracdis.com



Published by



The Official Publication of



Indexed in
PubMed, SCI

Aims and Scope

The *Journal of Thoracic Disease* (JTD, J Thorac Dis, pISSN: 2072-1439; eISSN: 2077-6624) was founded in Dec 2009, indexed in Pubmed/Pubmed Central in Dec 2011, and Science Citation Index (SCI) on Feb 4, 2013. It is published quarterly (Dec 2009- Dec 2011), bimonthly (Jan 2012- Dec 2013), and monthly (Jan 2014-), and openly distributed worldwide. JTD publishes manuscripts that describe new findings in the field to provide current, practical information on the diagnosis and treatment of conditions related to thoracic disease (lung disease, cardiac disease, breast disease and esophagus disease). Original articles are considered most important and will be processed for rapid review by the members of Editorial Board. Clinical trial notes, Cancer genetics reports, Epidemiology notes and Technical notes are also published. Case reports implying new findings that have significant clinical impact are carefully processed for possible publication. Review articles are published in principle at the Editor's request. There is no fee involved throughout the publication process. The acceptance of the article is based on the merit of quality of the manuscripts. All the submission and reviewing are conducted electronically so that rapid review is assured.

The Official Publication of:

- ❖ Guangzhou Institute of Respiratory Disease (GIRD)
- ❖ China State Key Laboratory of Respiratory Disease
- ❖ First Affiliated Hospital of Guangzhou Medical University
- ❖ Society for Thoracic Disease (STD)

Endorsed by:

- ❖ International COPD Coalition (ICC)

Editorial Correspondence

HK office:

Daoyuan Wang.

Pioneer Bioscience Publishing Company

Room 604, 6/F Hollywood Center, 77-91 Queen's road, Sheung Wan, Hong Kong.

Guangzhou office:

Guangqiao Zeng, MD

Guangzhou Institute of Respiratory Disease & The First Affiliated Hospital of Guangzhou Medical University.

No. 151, Yanjiang Rd, Guangzhou 510120, China.

Email: jtd@thebpc.org

www.jthoracdis.com

Note to NIH Grantees

Pursuant to NIH mandate, Pioneer Bioscience Publishing Company will post the accepted version of contributions authored by NIH grant-holders to PubMed Central upon acceptance. This accepted version will be made publicly available 2 months after publication. For further information, see www.thebpc.org

Conflict of Interest Policy for Editors

The full policy and the Editors' disclosure statements are available online at: www.jthoracdis.com

Disclaimer

The Publisher and Editors cannot be held responsible for errors or any consequences arising from the use of information contained in this journal; the views and opinions expressed do not necessarily reflect those of the Publisher and Editors, neither does the publication of advertisements constitute any endorsement by the Publisher and Editors of the products advertised.

Cover image:

Postoperative pulmonary computed tomography (CT) revealed no anastomotic stricture at 1 month after surgery. (See P1487 in this issue).

For submission instructions, subscription and all other information visit www.jthoracdis.com

© 2014 Pioneer Bioscience Publishing Company

Editor-in-Chief

Nanshan Zhong, MD
*Academician, Chinese Academy of Engineering,
 Guangzhou Institute of Respiratory Disease,
 Guangzhou, China*

Deputy Editors-in-Chief

Jin-Shing Chen, MD, PhD
Taipei, Taiwan
 Rongchang Chen, MD, PhD
Guangzhou, China
 Yi-Jen Chen, MD, PhD
Duarte, USA
 Kwun Fong, MBBS (Lon), FRACP, PhD
Brisbane, Australia

Associate Editors

Hatem A Azim Jr, MD
Brussels, Belgium
 Kazuaki Takabe, MD, PhD, FACS
Richmond, United States
 Gary Y. Yang, MD
Loma Linda, United States

Section Editor (Surgical Video)

Yaxing Shen, MD
Shanghai, China

Executive Editor-in-Chief

Jianxing He, MD, FACS
*The First Affiliated Hospital of Guangzhou
 Medical University, Guangzhou, China*

Lawrence Grouse, MD, PhD
Gig Harbor, USA
 Shahzad G. Raja, MBBS, MRCSEd, FRCSEd
 (C-Th)
London, United Kingdom
 Gaetano Rocco, MD, FRCS (Ed), FETCS,
 FCCP
Naples, Italy

Paul Zarogoulidis, MD, PhD
Thessaloniki, Greece
 Junya Zhu, MS, MA
Boston, United States

Section Editor

(Systematic Review and Meta-analysis)
 Zhi-De Hu, M.M Jinan, China
 Wan-Jie Gu, MSc Nanning, China
 Zhi-Rui Zhou, MD Changchun, China

**Executive Editor-in-Chief
(Cardiovascular Surgery)**

Tristan D. Yan, BSc, MBBS, MS, MD, PhD
*Department of Cardiothoracic Surgery, Royal
 Prince Alfred Hospital, University of Sydney,
 Sydney, Australia; The Collaborative Research
 (CORE) Group, Sydney, Australia*

Editorial Co-Directors & Executive Editors

Guangqiao Zeng, MD
Guangzhou, China
 Daoyuan Wang, MD
Guangzhou, China

Statistical Editors

Jiqian Fang, PhD
Guangzhou, China
 Baoliang Zhong, MD, PhD
Hong Kong, China

Section Editor

(Cancer Registry, Prevention and Control)
 Wanqing Chen, MD
Beijing, China

Editorial Board

Peter J Barnes, DM, DSc, FRCP,
 FCCP, FMedSci, FRF
 J. Patrick Barron, MD
 Luca Bertolaccini, MD, PhD
 Alessandro Brunelli, MD
 Peter Calverley, MD
 Weiguo Cao, MD
 Stephen D. Cassivi, MD, MSc,
 FRCS, FACS
 Mario Cazzola, MD
 Joe Y Chang, MD, PhD
 Kian Fan Chung, MD, DSc, FRCP
 Henri G. Colt, MD, FCCP
 Thomas A. D'Amico, MD
 Giovanni Dapri, MD, FACS, FASMB
 Keertan Dheda, MBBCh,
 FCP(SA), FCCP, PhD(Lond),
 FRCP(Lond)
 Peter V. Dicpinigaitis, MD
 Leonardo M. Fabbri
 Wentao Fang, MD
 Yoshinosuke Fukuchi, MD, PhD
 Diego Gonzalez-Rivas, MD, FECS
 Cesare Gridelli, MD

Tomas Gudbjartsson, MD, PhD
 Henrik Jessen Hansen, MD
 Don Hayes, Jr, MD, MS, Med
 Andrea Imperatori, MD
 Mary Sau Man Ip, MBBS(HK),
 MD(HK), FRCP (London,
 Edinburgh, Glasgow), FHKCP,
 FHKAM, FAPSR, FCCP
 Rihard S. Irwin, MD, Master FCCP
 Ki-Suck Jung, MD, PhD
 Markus Krane, MD
 Alexander Sasha Krupnick, MD
 Hyun Koo Kim, MD, PhD
 Anand Kumar, MD
 Aseem Kumar, PhD
 Y. C. Gary Lee, MBChB, PhD,
 FCCP, FRCP, FRACP
 Mario Leoncini, MD
 Hui Li, MD
 Min Li, PhD, Professor
 Tianhong Li, MD, PhD
 Wenhua Liang, MD
 Yang Ling, MD
 Deruo Liu, MD
 Lunxu Liu, MD

Hui-Wen Lo, PhD
 Kevin W. Lobdell, MD
 Jiade J. Lu, MD, MBA
 Wei-Guo Ma, MD
 Giovanni Mariscalco, MD, PhD
 Doug McEvoy, MBBC, FRACP
 Walter McNicholas, MD, FRCPI,
 FRCPC, FCCP
 Michael T. Milano, MD, PhD
 John D. Mitchell, MD
 Alyn H. Morice, MD
 Akio Niimi, MD, PhD
 Antonio Passaro, MD
 Georgios Plataniotis, MD, PhD
 David Price, M.B B.Chir, MA,
 DRCOG, FRCGP
 Gui-bin Qiao, MD, PhD
 Klaus F. Rabe, MD, PhD
 Dominik Rüttinger, MD, PhD, FACS
 Sundeep Salvi, MD, DNB, PhD,
 FCCP
 Martin Schweiger, MD
 Suresh Senan, MD
 Alan Dart Loon Sihoe, MBBChir,
 MA (Cantab), FRCSEd (CTh),

FCSHK, FHKAM (Surgery), FCCP
 Charles B. Simone, II, MD
 Yong Song, MD, PhD
 Joerg S. Steier, MD (D), PhD (UK)
 Xiaoning Sun, MD, PhD
 Lijie Tan, MD, Vice Chief
 Kenneth WT Tsang, MD, FRCP
 Mark I. van Berge Henegouwen,
 MD, PhD
 Federico Venuta, MD
 Ko Pen Wang, MD, FCCP
 Qun Wang, MD, FRCS
 Yi-Xiang Wang, MD
 Zheng Wang, MD
 Bryan A. Whitson, MD, PhD
 Yunlong Xia, MD, PhD
 Jin Xu, MS
 Stephen C. Yang, MD
 Kazuhiro Yasufuku, MD, PhD
 Xiuyi Zhi, MD
 Ming Zhong, MD
 Caicun Zhou, MD, PhD
 Qinghua Zhou, MD
 Zhi-hua Zhu, MD, PhD

Journal Club Director

Bing Gu, MD

Editorial Assistants

Maria Karina, MD, PhD,
 FRCP
 Parag Prakash Shah, PhD

Senior Editors

Grace S. Li (Corresponding
 Editor)
 Eunice X. Xu
 Elva S. Zheng
 Nancy Q. Zhong

Science Editors

Melanie C. He
 Tina C. Pei
 Molly J. Wang
 Rui Wang

Executive Copyeditor

Eudora Liu

Executive Typesetting Editor

Jian Li

Production Editor

Emily M. Shi

Table of Contents

Editorial

- 1374 **Precise and fast video assisted thoracoscopic bronchial sleeve resection**

Chia-Chuan Liu

- 1376 **Comment on He *et al.*, VATS bronchial sleeve resection**

David R. Jones

Meet the Professor

- 1378 **Prof. Jose Luis López-Campos: effective management of COPD**

Rebecca Wong

Original Article

- 1380 **Quantifying the expression of tumor marker genes in lung squamous cell cancer with RNA sequencing**

Lin Wang, Cheng Zhan, Yongxing Zhang, Jun Ma, Junjie Xi, Wei Jiang, Yu Shi, Qun Wang

- 1388 **Prevalence and risk factors of aortic aneurysm in patients with chronic obstructive pulmonary disease**

Katsutoshi Ando, Norihiro Kaneko, Tokubide Doi, Masahiro Aoshima, Kazubisa Takahashi

- 1396 **Analysis of the molecular and clinicopathologic features of surgically resected lung adenocarcinoma in patients under 40 years old**

Ting Ye, Yunjian Pan, Rui Wang, Haichuan Hu, Yang Zhang, Hang Li, Lei Wang, Yibua Sun, Haiquan Chen

- 1403 **Differences in distribution and drug sensitivity of pathogens in lower respiratory tract infections between general wards and RICU**

Ruoxi He, Bailing Luo, Chengping Hu, Ying Li, Ruichao Niu

- 1411 **Experimentation with aerosol bosentan, pirfenidone, treprostinil and sildenafil**

Haidong Huang, Paul Zarogoulidis, Sofia Lampaki, John Organtzis, Dimitris Petridis, Konstantinos Porpodis, Antonis Papaiwannou, Vasilis Karageorgiou, Georgia Pitsiou, Ioannis Kioumis, Wolfgang Hobenforst-Schmidt, Qiang Li, Kaid Darwicbe, Lutz Freitag, Aggeliki Rapti, Konstantinos Zarogoulidis

- 1420 **Factors affecting tumor recurrence after curative surgery for NSCLC: impacts of lymphovascular invasion on early tumor recurrence**

Chanyeong Park, In Jae Lee, Seung Hun Jang, Jae Woong Lee

- 1429 **The role of red blood cell distribution width in mortality and cardiovascular risk among patients with coronary artery diseases: a systematic review and meta-analysis**

Chang Su, Li-Zhen Liao, Yan Song, Zhi-Wei Xu, Wei-Yi Mei

- 1441 Correlations between brachial endothelial function and cardiovascular risk factors: a survey of 2,511 Chinese subjects**
Ping-Ting Yang, Hong Yuan, Ya-Qin Wang, Xia Cao, Liu-Xin Wu, Zhi-Heng Chen
- 1452 Analysis on minimally invasive diagnosis and treatment of 49 cases with solitary nodular ground-glass opacity**
Hu Zhang, Jing Duan, Zhi-Jun Li, Zheng-Fu He, Zhou-Miao Chen, Yong Xu, Wei-Wen Ye, Ou Wu
- 1458 Hypoxia induces cardiac fibroblast proliferation and phenotypic switch: a role for caveolae and caveolin-1/PTEN mediated pathway**
Yao Gao, Ming Chu, Jian Hong, Jingping Shang, Di Xu
- 1469 The association of lipopolysaccharide and inflammatory factors with hepatopulmonary syndrome and their changes after orthotopic liver transplantation**
Huimin Yi, Yuling An, Haijin Lv, Xuxia Wei, Xiaomeng Yi, Genshu Wang, Yang Yang, Guibua Chen, Shubong Yi
- 1476 Nonspecific interstitial pneumonia and usual interstitial pneumonia: comparison of the clinicopathologic features and prognosis**
Xia Li, Chang Chen, Jinfu Xu, Jinming Liu, Xianghua Yi, Xiwen Sun, Jingyun Shi

Surgical Technique

- 1482 The experience of using Endo GIA™ Radial Reload with Tri-Staple™ Technology for various lung surgery**
Toshinari Ema
- 1485 Non-intubated complete thoracoscopic bronchial sleeve resection for central lung cancer**
Wenlong Shao, Kevin Phan, Xiaotong Guo, Jun Liu, Qinglong Dong, Jianxing He

Special Report

- 1489 Chinese expert consensus on molecularly targeted therapy for advanced non-small cell lung cancer (2013 edition)**
Guoming Wu, Caicun Zhou, Chunxue Bai, Guisheng Qian

Review Article

- 1499 Microsatellite alteration in multiple primary lung cancer**
Cheng Shen, Xin Wang, Long Tian, Guowei Che
- 1506 Experimental studies in the bronchial circulation. Which is the ideal animal model?**
Christophoros Kotoulas, Ioannis Panagiotou, Panteleimon Tsipas, Maria Melacrinou, Dimitrios Alexopoulos, Dimitrios Dougenis
- 1513 L-BLP25 as a peptide vaccine therapy in non-small cell lung cancer: a review**
Wenjie Xia, Jie Wang, Youtao Xu, Feng Jiang, Lin Xu

Case Report

E209 Emergency operation of a patient with spontaneous rupture and massive hemorrhage of pleural solitary fibrous tumor

Feng Shao, Rusong Yang, Yanqing Pan

E212 Caution for acute submassive pulmonary embolism with syncope as initial symptom: a case report

Sheng-Yu Wang, Hui Chen, Li-Gai Di

E217 Rapid growing huge teratoma: complete surgical resection

Dobun Kim, Si-Wook Kim, Jong-Myeon Hong

E220 The challenging management of lung choriocarcinoma

Lasba Gvinianidze, Nikolaos Panagiotopoulos, Wen Ling Woo, Elaine Borg, David Lawrence

E223 Primary mucoepidermoid carcinoma of the thymus presenting with myasthenia gravis

Wen Ling Woo, Nikolaos Panagiotopoulos, Lasba Gvinianidze, Ian Proctor, David Lawrence

E226 Right ventricle inflow obstructing mass proven to be a synovial sarcoma

Guang-Won Seo, Sang-Hoon Seol, Pil-Sang Song, Dong-Kie Kim, Ki-Hun Kim, Woo Gyeong Kim, Yeon Mee Kim, Sun Ju Oh, Hee-Jae Jun, Doo-Il Kim

E230 Chondrosarcoma of the anterior chest wall: surgical resection and reconstruction with titanium mesh

Elçin Ersöz, Serdar Evman, Levent Alpay, Mustafa Akyıl, Mustafa Vayvada, Deniz Gürer, Serkan Bayram, Çağatay Tezel

E234 Large cell carcinoma on the bullous wall detected in a specimen from a patient with spontaneous pneumothorax: report of a case

Toshinari Ema

E237 A huge neoplasm occupying the right hemithorax in a pregnancy

Mei Yang, Cheng Shen, Heng Du, Yun Wang, Guowei Che

E242 Primary intravascular large B-cell lymphoma of the lung: a review and case report

Yanfan Chen, Cheng Ding, Quan Lin, Kaiyan Yang, Yuping Li, Shaoxian Chen

Precise and fast video assisted thoracoscopic bronchial sleeve resection

Chia-Chuan Liu^{1,2}

¹Faculty of medicine, School of Medicine, National Yang-Ming University, Taipei 112, Taiwan; ²Division of Thoracic Surgery, Department of Surgery, Koo-Foundation Sun Yat-Sen Cancer Center, Taipei, Taiwan

Correspondence to: Chia-Chuan Liu, MD. Division of Thoracic Surgery, Department of Surgery, Koo-Foundation Sun Yat-Sen Cancer Center, 125 Lih-Der Road, Pei-Tou District, Taipei 112, Taiwan. Email: gcliu@kfsyscc.org.

Abstract: Surgical management for lung cancer is basically a destructive one. The lung parenchyma removed is in the balance between the purpose of curative resection and the preservation of patient's lung function. Bronchial sleeve has been alternatively developed to achieve the same purpose, but through a different way—to save back healthy lung tissue through reconstruction of the central airway. Sleeve resection had been done with open technique for years, and just like the other thoracic operations, has continuously evolved into the era of minimally invasive surgery in spite of its difficulty. With rapid advancement and availability in technology—high resolution 3-D dynamic chest computed tomography (CT), PET-CT, and endobronchial ultrasound (EBUS), these tools are very helpful for us to have more precise tumor staging, and suitable for preoperative surgical planning. Under magnified 3-D endoscopic view and modified endoscopic suturing method, re-anastomosis of the airway could be easier and quicker, which would facilitate this innovative operation to accumulate experience in the not too distant future.

Keywords: Video assisted thoracoscopic surgery (VATS); bronchial sleeve resection

Submitted Aug 07, 2014. Accepted for publication Aug 11, 2014.

doi: 10.3978/j.issn.2072-1439.2014.08.39

View this article at: <http://dx.doi.org/10.3978/j.issn.2072-1439.2014.08.39>

Lung cancer surgery is fundamentally a destructive operative approach. From pneumonectomy to lobectomy and/or sub-lobar resection, the effort is directed towards removal of relevant lung tissue in order to preserve more functional capacity for the patients. With the lung cancer localized in the central region of the lung, a bi-lobectomy or even pneumonectomy is traditionally performed. As a result, lots of healthy lung distal to the tumor would be sacrificed; yet a sleeve resection procedure has emerged as another standard treatment of choice with similar oncological results, but with much better pulmonary reserve. In this particular type of surgery, it is no longer considered entirely destructive, but also reconstructive, and therefore it comes with the issues concerning technique and complications associated with the reconstruction procedure.

A successful sleeve resection is surgically challenging. The keys to success include an accurate preoperative configuration of tumor invasiveness and intra-operative

delicate technique both for resection and reconstruction, especially the suturing technique on the bronchial anastomosis with major pulmonary vessels nearby. Accordingly, a sleeve resection was ranked high on the top skill-demanding surgery, and often being done in open surgery in the past. In the recently published articles by Dr. He's series (1,2), the technique for sleeve resection has evolved from open to hybrid and eventually video assisted thoracoscopic surgery (VATS); while the bronchoplasty sites varied from bronchus to half carina, and all these operations achieved satisfactory perioperative outcomes.

Endoscopic suturing technique is particularly important in sleeve resection. It is not uncommon to notice that in a thoracic training program, there are very limited opportunities for laparoscopic skills, especially the endoscopic suturing. In spite of this limitation, the thoracic surgeons often use a utility incision on the chest wall which allows the space for using traditional instruments; however,

endoscopic suturing sometimes works very well especially in a narrow space, as found in single port technique. Moreover, a modified traditional needle holder with extracorporeal ties may also work well. The traditional telescopic interrupted suturing is feasible and applicable via an open technique in the past. With the advanced experience from lung transplantation, a continuous suturing is now considered as an easier and less time-consuming way of doing the bronchial anastomosis as shown in Dr He's series. Through this technique, surgeons no longer need to pass the needle into the anastomosis site with so many threads nearby. The anastomosis related complications such as leakage or stenosis are also low. Another characteristic part of bronchial sleeve operation—covering the anastomosis site with muscle flap or pedicled pericardial flap, is controversial; as some surgeons consider sleeve resections without muscle flap are safe even after neoadjuvant therapy (3). The tissue glue or mesh is not yet well proven in protecting the anastomosis; however, its usage has been applied around the anastomosis during operation, and also used for managing anastomosis leakage after operation (4).

What have we achieved from transforming an open bronchoplastic procedure into a complete VATS technique? The benefits are like other VATS procedures for the patient, e.g., reduction of trauma and less pain, rapid regain of daily activities, and ability to receive adjuvant treatment whenever indicated; however, from the oncological point of view, a meticulous preoperative staging and a careful resection and reconstruction cannot be overemphasized. With advancement in technology, a dynamic high-resolution 3-D CT enables us to do accurate preoperative simulation for the patients (5), and an EBUS with magnified endoscopic view can detect tumor invasiveness inside the tracheobronchial tree before surgery. Many magnified 3-D image video systems available on the market would enable the surgeons to regain the distance difference lost in the traditional 2-D image system—just like the 3-D image

equipped in a robotic system, but the cost is much lower. The total operation time could even be shortened if we use continuous suturing and absorbable sealing material such as tissue glue, without muscle flap wrapping around the anastomosis in selected cases. In summary, VATS bronchial sleeve resection could be done with a precise surgical planning; and it is possible to shorten the operation time with modified instruments and suturing techniques. We look forward to anticipate a good long-term oncological results and higher utilization rates of this technique within the chest surgery society in the future.

Acknowledgements

Disclosure: The author declares no conflict of interest.

References

1. He J, Shao W, Cao C, et al. Long-term outcome of hybrid surgical approach of video-assisted minithoracotomy sleeve lobectomy for non-small-cell lung cancer. *Surg Endosc* 2011;25:2509-15.
2. Xu X, Chen H, Yin W, et al. Thoracoscopic Half Carina Resection and Bronchial Sleeve Resection for Central Lung Cancer. *Surg Innov* 2014;21:481-6.
3. Storelli E, Tutic M, Kestenholz P, et al. Sleeve resections with unprotected bronchial anastomoses are safe even after neoadjuvant therapy. *Eur J Cardiothorac Surg* 2012;42:77-81.
4. Kamiyoshihara M, Nagashima T, Igai H, et al. Video-assisted thoracic lobectomy with bronchoplasty for lung cancer, with special reference to methodology. *Interact Cardiovasc Thorac Surg* 2011;12:534-8.
5. Saji H, Inoue T, Kato Y, et al. Virtual segmentectomy based on high-quality three-dimensional lung modelling from computed tomography images. *Interact Cardiovasc Thorac Surg* 2013;17:227-32.

Cite this article as: Liu CC. Precise and fast video assisted thoracoscopic bronchial sleeve resection. *J Thorac Dis* 2014;6(10):1374-1375. doi: 10.3978/j.issn.2072-1439.2014.08.39

Comment on He *et al.*, VATS bronchial sleeve resection

David R. Jones

Thoracic Surgery, Memorial Sloan Kettering Cancer Center, New York, New York, USA

Correspondence to: David R. Jones, MD. Professor & Chief, Thoracic Surgery, Memorial Sloan Kettering Cancer Center, 1275 York Avenue, Box 7, New York, NY 10065, USA. Email: jonesd2@mskcc.org.

Submitted Aug 21, 2014. Accepted for publication Sep 12, 2014.

doi: 10.3978/j.issn.2072-1439.2014.10.13

View this article at: <http://dx.doi.org/10.3978/j.issn.2072-1439.2014.10.13>

Video-assisted thoracic surgery (VATS) lobectomy has become the standard of care for resection of early-stage non-small cell lung cancer. The results of nearly all studies to date suggest that patients return to work sooner, have less postoperative pain, and are able to initiate and complete adjuvant therapies more expeditiously, compared with open thoracotomy (1,2). It remains an open question how often VATS can be routinely applied for several situations, including postinduction anatomic resections, bronchial sleeve resections, and pulmonary arterioplasties. In this paper from the First Affiliated Hospital of Guangzhou Medical University, Dr. He and colleagues retrospectively report their experience with VATS bronchial sleeve resection in 20 highly selected patients. No patient who needed a pulmonary arterioplasty was included, and only one patient had induction therapy. During the study period of 22 months, VATS bronchial sleeve resection composed 41% of the total number of sleeve resections (n=49) performed. The majority of sleeve resections were of the right upper lobe (n=11, 55%), with the remaining lobes having at least one sleeve resection.

Like most surgeons who are adopting new surgical techniques, the authors modified their bronchial anastomotic technique from a partial interrupted (n=8, 40%) to a continuous running approach (n=12, 60%). Not surprisingly, there was a decrease in the time it took to complete the anastomosis. From a technical perspective, a continuous suture approach is the easiest to perform when doing the procedure using VATS. This limits the number of sutures that need to be tied and significantly decreases the tangling of the sutures. The procedure setup is best when two separate traction sutures are placed in each cut end of the bronchi and exit the chest through separate 3-mm stab wounds. This reduces anastomotic tension, perhaps

the most critical element in creating the anastomosis. I favor the use of the Carter Thomason device to grasp and remove the ends of the sutures. Once the traction sutures are in place, the anastomosis can begin. In the authors' description, it is unclear why the sutures used for the interrupted technique were absorbable monofilament, while the continuous suture approach used a single nonabsorbable suture. We would favor an absorbable monofilament suture regardless of approach. It is also not stated how many of the bronchial anastomoses were telescoped *vs.* end-to-end. This is an important point, as it is an indirect measure of how often there is a significant size discrepancy between the bronchi that necessitates a telescoped approach. To decrease the incidence of anastomotic stricture formation, I prefer to perform an end-to-end approach on nearly all sleeve resections, and I find that with thoughtful suture placement, this is possible. At the conclusion of the procedure, I also perform an intraoperative bronchoscopy to remove secretions and inspect the anastomotic integrity and assess the diameter of the anastomosis.

The authors had excellent results in this highly selected group of patients. There were no early anastomotic complications and no conversions to an open procedure. The operative times and listed morbidities were also very reasonable. No patient had their sleeve reconstruction covered with vascularized soft tissue; in cases where adjuvant radiation may be considered (i.e., pN2 disease), I recommend coverage with a pericardial fat pad flap that is easily harvested thoracoscopically.

What is not explicitly stated, but inferred from the paper, is who is a good candidate for a VATS bronchial sleeve resection. Typically, patients without induction therapy, with no need for a pulmonary arterioplasty or double sleeve resection, and with a favorable body habitus are the best

candidates for this approach. There are reports of patients who have had a bronchial sleeve resection who have larger tumors or have had induction therapy, but these are highly selective case reports.

In conclusion, this is an encouraging report of a selected group of patients who had a VATS bronchial sleeve resection performed for lung cancer. The operations were performed by skilled VATS surgeons, and their outcomes were very good. The important points regarding this VATS approach, including patient selection, technical modifications to facilitate the successful completion of the anastomosis, and the use of a continuous suture, are all well made by the authors. Future studies will need to continue to improve the technical aspects of the procedures (i.e., reticulating VATS instruments) and minimally invasive

techniques to address bronchial size mismatches.

Acknowledgements

Disclosure: The author declares no conflict of interest.

References

1. Xu X, Chen H, Yin W, et al. Thoracoscopic half carina resection and bronchial sleeve resection for central lung cancer. *Surg Innov* 2014;21:481-6.
2. Nakanishi R, Shinohara S, Yamashita T, et al. Advances in the use of video-assisted thoracoscopic lobectomy in lung cancer: sleeve bronchoplasty and arterioplasty. *Lung Cancer Manage* 2014;3:287-95.

Cite this article as: Jones DR. Comment on He *et al.*, VATS bronchial sleeve resection. *J Thorac Dis* 2014;6(10):1376-1377. doi: 10.3978/j.issn.2072-1439.2014.10.13

Prof. Jose Luis López-Campos: effective management of COPD

Submitted Sep 06, 2014. Accepted for publication Oct 10, 2014.

doi: 10.3978/j.issn.2072-1439.2014.10.07

View this article at: <http://dx.doi.org/10.3978/j.issn.2072-1439.2014.10.07>

Prof. Jose Luis López-Campos (Figure 1) is an expert in respiratory medicine, pulmonology, chronic obstructive pulmonary disease (COPD) and pulmonary rehabilitation. He works as a respiratory physician at Virgen del Rocío University Hospital and an associate professor of Medicine at Seville University. He is also the secretary of the Group 5.2 Monitoring Airway Diseases of the European Respiratory Society (ERS). We had an interview with Prof. López-Campos during the ERS course on “Environmental respiratory diseases” in Guangzhou. In this interview, Prof. López-Campos has shared with us the relation between environment and COPD, the pharmacological treatment and multidimensional approaches for COPD.



Figure 1 Professor Jose Luis López-Campos.

JTD: *As we know, you have given an impressive lecture in the ERS course on “Environmental respiratory diseases”. Would you like to share with us about the key points that you addressed in your lecture? I think those who could not attend this conference will be glad to learn your views via our interview.*

Prof. López-Campos: In the lecture, my idea was to give a global and updated view on the pharmacological treatment for COPD. As you know, the Global Initiative for Obstructive Lung Disease (GOLD) strategy has changed considerably in the last few years. Accordingly, the therapeutic approach has also changed with the aim to get closer to a more patient-centered medicine. This new conception of the disease as a complex multidimensional disease makes us consider other variables apart from FEV₁. It follows that old treatment strategies based on lung function will have to change with this new vision of the disease.

COPD is a chronic obstructive disease in which long-acting bronchodilators are the pillar for pharmacological treatment. Additionally, inhaled steroids can help decreasing the number of exacerbations if not adequately controlled by a long-acting bronchodilator. However, once the initial treatment has been established the progression of this treatment is not so well defined. Intensification of treatment depends on which aspect of the disease we need

to improve: symptoms, lung function or exacerbations. Double bronchodilation is the preferred option if we want to impact on lung function or chronic symptoms. However, inhaled steroids should be use if we want to impact on exacerbation rate beyond that achieved by a long-acting bronchodilator.

JTD: *In this conference, environment is an important topic. What do you think of the correlation between environment and COPD?*

Prof. López-Campos: The relation between environment and COPD is extremely important. COPD is a multigenetic disease in which many genes participate. The different expressions of these genes interplay with the environment exposure to cause the final disease phenotype. It is well known that tobacco is the main environmental factor to develop COPD. However, biomass exposure is also a recognized risk factor for COPD. Chronic exposure to biomass smoke can also be related with a progressively decreased lung function. Different studies are starting to investigate on the different clinical expression of COPD associated with non-tobacco smoke with some interesting findings.

JTD: *I am quite interested in your article entitled “Patient-centered medicine for COPD management: multidimensional approaches versus the phenotype-based medicine”. Would you like to share with us about the concepts of patient-centered medicine and multidimensional approaches?*

Prof. López-Campos: COPD has been traditionally considered a relentlessly progressive disease in which the deterioration of lung function is associated with an increase in symptoms and exacerbations. However, we now know that this paradigm does not reflect the reality of the disease which is far more complex. Accordingly several initiatives have been established in the last years for a more personalized medicine. So far three main approaches have been proposed in order to address the complexity of COPD as well as to develop appropriate diagnostic, prognostic and therapeutic strategies for the disease. These are the use of independent, clinically relevant variables, the use of multidimensional indices, and the so-called clinical phenotypes. All these three initiatives have pros and cons which are reviewed in the article you mention. Although these approaches are not perfect, they represent the first step towards patient-centered medicine for COPD. In the near-future, these different approaches should converge in one strategy to focus on the better management of COPD patients.

JTD: *And how to achieve the ideal patient-centered goal, as we know medicines currently are expensive but probably not with good efficacy?*

Prof. López-Campos: I have to disagree. Inhaled medicines for COPD have proven to have a good efficacy, with an adequate safety profile and have also showed to be cost-effective. COPD is an expensive disease. However, the greatest expenditure associated with the disease is not pharmacological treatment, but exacerbations and admissions. Interestingly, inhaled treatments for COPD decrease exacerbations, and so the reduce the cost associated with the disease. In this context, the best way to achieve an ideal patient-centered medicine is to consider the clinical expression of the particular case we are dealing with and modify treatment accordingly. In this strategy several key clinical manifestations in which we can impact with treatment must be selected to guide treatment.

JTD: *For the best of patients, the multidisciplinary therapy is getting more and more attention. What do you think of this?*

Prof. López-Campos: COPD is a complex disease with multisystem consequences. It follows that a

multidisciplinary team should provide a better care. Apart from pulmonologists, some COPD patients may also benefit from rehabilitators and physiotherapist, nutrition specialist and several other medical specialties to treat comorbidities including cardiovascular and non-cardiovascular. Of especial interest is a timely correct psychiatric intervention for those patients with anxiety and depression.

JTD: *In your presentation, the new medication like QVA149, which is a combination of LABA and LAMA, seems getting promising outcomes. While many COPD patients in Western countries were associated with obesity or overweight, could new medication or more treatments enhance the cardiovascular risk? And other medication such as statins, could bring direct or indirect benefit for patients. For such kind of research, could you give some suggestions?*

Prof. López-Campos: A LABA-LAMA combination is becoming available in several countries. This double bronchodilation has shown to improve lung function importantly and consequently symptoms. The safety profile of these combinations seems to be adequate and no clinical trial has yet given any alarm sign.

Another question is the relationship of nutritional abnormalities (under or overweight). We know that underweight is a risk factor for mortality in COPD. However, obesity is also relevant, since it has been associated with decreased lung-function measures in population-based studies. Additionally it is a risk factor for several other diseases. It follows that a good nutrition scheme is key for a correct COPD management and recommendations should be given to patients and professional advice should be seek if needed.

The relationship of statins and COPD is a matter of debate. There are some articles highlighting the potential role of statins in reducing mortality, exacerbations or different clinical outcomes. However, the evidence is not consistent. So in my opinion this constitutes an interesting line for research.

JTD: *Thank you very much!*

Acknowledgements

Disclosure: The author declares no conflict of interest.

(Science Editor: Rebecca Wong, JTD, jtd@thebpc.org)

Cite this article as: Wong R. Prof. Jose Luis López-Campos: effective management of COPD. *J Thorac Dis* 2014;6(10):1378-1379. doi: 10.3978/j.issn.2072-1439.2014.10.07

Quantifying the expression of tumor marker genes in lung squamous cell cancer with RNA sequencing

Lin Wang*, Cheng Zhan*, Yongxing Zhang*, Jun Ma, Junjie Xi, Wei Jiang, Yu Shi, Qun Wang

Department of Thoracic Surgery, Zhongshan Hospital, Fudan University, Shanghai 200032, China

*These authors contributed equally to this work.

Correspondence to: Qun Wang. Department of Thoracic Surgery, Zhongshan Hospital, 180 Fenglin Rd, Shanghai 200032, China.

Email: wang.qun@zs-hospital.sh.cn; Yu Shi. Department of Thoracic Surgery, Zhongshan Hospital, 180 Fenglin Rd, Shanghai 200032, China.

Email: shi.yu@zs-hospital.sh.cn.

Background: We measured the expression of some commonly used tumor markers with RNA sequencing (RNA-Seq) to identify any that might be useful for the evaluation of squamous cell lung cancer and identify possible correlations between these tumor markers and any clinical characteristics.

Methods: RNA-Seq was performed on five pairs of squamous-cell lung cancer and normal tissues and another 39 squamous-cell lung cancer tissues obtained by our department between September and December, 2012. The expression of 13 commonly used tumor markers was determined.

Results: All of the patients in our study were male. The expressions of CA125, CYFRA21-1, NSE and SCC increased in tumor samples and there were statistically significant differences between squamous cell lung cancer and normal tissues ($P=0.008$, $P<0.001$, $P<0.001$, $P=0.001$). The expression of $\beta 2M$ and CA15-3 was reduced in squamous cell carcinoma relative to normal tissues and there was no significant difference in the expression of other tumor markers, including AFP, AFU, CT, FER and HE4.

Conclusions: CA125, CYFRA21-1, NSE and SCC may be appropriate tumor markers for squamous cell lung cancer.

Keywords: RNA sequencing (RNA-Seq); tumor marker; squamous cell lung cancer

Submitted May 22, 2014. Accepted for publication Aug 07, 2014.

doi: 10.3978/j.issn.2072-1439.2014.08.27

View this article at: <http://dx.doi.org/10.3978/j.issn.2072-1439.2014.08.27>

Introduction

Lung cancer is the most commonly diagnosed cancer as well as the leading cause of cancer-related death. This disease accounted for 13% (1.6 million) of total cancer cases and 18% (1.4 million) of deaths caused by cancer in 2008 (1). Squamous-cell lung cancer, one of the most common types of lung cancer, typically originates in the large airways and represents approximately 20-30% of lung cancer cases in recent years (2). The overall survival of early stage patients is quite good, but most patients are diagnosed at an advanced stage when there are fewer curative opportunities. Therefore, early diagnosis is the key to improve patient outcomes for squamous-cell lung cancer.

Tumor markers have been widely applied in cancer diagnosis over the last two decades due to convenience, low cost, reproducibility and non-invasiveness. Most previous studies have focused on tumor marker levels in the serum. Here, we studied the expression of several commonly used tumor-marker genes in tumor and normal tissues. Squamous-cell lung cancer and adenocarcinoma are so different from each other (3). Therefore, we measured the expression of some commonly used tumor markers in squamous-cell lung cancer tissues using RNA sequencing (RNA-Seq) to screen for genes that may be suitable tumor markers in squamous cell lung cancer. We then investigated possible correlations between these tumor markers and clinical characteristics.

Materials and methods

Ethics statement

This study was approved by the Ethics Committee of Zhongshan Hospital, Fudan University {Approved No. 2011-219[2]}. Written informed consent was obtained from each patient participating in this study.

Tissue samples and clinicopathological characteristics

Samples were obtained from patients with squamous-cell lung cancer who underwent surgical resection between September and December, 2012 at Zhongshan Hospital, Fudan University, Shanghai, China. Clinicopathological characteristics were recorded for all patients. Normal lung specimens were resected at least 3 centimeters away from the tumor margin, while tumor samples were carefully extracted from the center of squamous-cell carcinoma. All samples were flash frozen in liquid nitrogen after removal and then saved at -80°C . Part of each sample was paraffin embedded, HE stained and checked by an experienced pathologist to make ensure that no cancer cell existed in the normal tissues and more than 80% of cells in every tumor sample were squamous carcinoma. Finally, five matched pairs of normal tissue samples and lung squamous-cell carcinoma tissues and another 39 lung squamous-cell carcinoma tissues were obtained. These samples were then used in RNA-Seq.

RNA preparation

Total RNA from each sample was extracted with Trizol (Invitrogen, Carlsbad, CA, USA), re-dissolved in DEPC-treated water and quantified using NanoVue Plus spectrophotometry (GE Healthcare, Fairfield, CT, USA). RNA integrity was evaluated using agarose gel electrophoresis, and DNA contamination was eliminated using gDNA Eraser (Takara, Tokyo, Japan) according to the manufacturer's guidelines.

RNA sequencing (RNA-Seq)

The mRNA component of total RNA was converted into a library of template molecules suitable for sequencing using TruSeq[®] RNA Sample Preparation Kit v2 (Illumina, San Diego, CA, USA) according to the manufacturer's guidelines. mRNA was purified and fragmented and first and second strand cDNA was synthesized. RNA was then subjected to end repair, 3' end adenylation, ligation of

adapters, PCR amplification of cDNA libraries procedure, among others. Sequencing was then performed using a Genome Analyzer II (Illumina, San Diego, CA, USA) according the manufacturer's recommendation. Sequence analysis was performed using Galaxy software (<http://galaxyproject.org>) to calculate the reads per kilobase of exon model per million mapped reads (RPKM) of every transcript. Then the RPKM of all transcripts from each gene were added up to evaluate that gene's expression. Each sample was sequenced twice and the average of the RPKM value of each gene was adopted to reflect its expression level.

Statistical analysis

The RPKM data derived from RNA-Seq were analyzed using SPSS for windows, version 20 (IBM, Armonk, NY, USA). The mean of the RPKM was used to evaluate the gene expression level. The expression profiles of tumor marker genes in normal samples were compared with paired tumor samples using the paired *t*-test and *t*-test for comparing genes' expressions between normal and all tumor samples. Spearman correlation analysis was used to identify correlations between the expression of tumor marker gene expression and clinicopathological characteristics, and Pearson correlation analysis was used to identify correlations between CA125, CYFRA21-1, NSE and SCC.

Results

Patient clinicopathological characteristics

The clinicopathological characteristics of all 44 patients are listed in *Table 1*. All of the patients in our study were male, because most squamous-cell lung cancers occur in older male patients. Female patients accounted for only 7.8% (104/1,320) of squamous-cell lung cancer in our department from 2005-1-1 to 2011-12-31. In our study, none of the patients were at N3 or M1 stage, because these patients were not suitable for radical surgical resection. No patients were in stage IV for the same reason.

Expression profiles of commonly used tumor markers

We evaluated 13 commonly used tumor markers, including β 2M, AFP, AFU, CA125, CA15-3, CEA, CT, CYFRA21-1, FER, HE4, NSE, PSA and SCC. Their full names, encoding genes and functions are presented in *Table 2*. We listed all encoding genes and expression profiles for tumor

Table 1 The clinicopathological characteristics of all 44 patients

Clinicopathological characteristics	No.
No.	44
Gender	
Male	44
Female	0
Age	
≥60	26
<60	18
Smoking status	
Yes	23
No	21
Primary tumor	
T1	15
T2	19
T3	6
T4	4
Regional lymph nodes	
N0	29
N1	8
N2	7
N3	0
Metastasis	
M0	44
M1	0
Differentiation	
Well differentiated	8
Moderately differentiated	18
Poorly differentiated	18
TNM stage	
I	23
II	12
III	9
IV	0

markers that are encoded by more than one gene, with the exception of CEA. CEA is encoded by a group of genes, including at least 12 carcinoembryonic antigen-related cell adhesion molecule genes and 11 pregnancy-specific beta-1-glycoprotein genes, so we listed the four most highly expressed genes. The expression of PSA was too low to be detected in most of our samples, so it is not listed in *Table 3*.

The expression of CA125, CYFRA21-1, NSE and

SCC increased in tumor samples, and there was statistical significance in the difference between squamous cell lung cancer and normal tissues for these genes. While CEA was produced by the co-expression of multiple genes, only expression from some of these genes produced statistical significance. The expression of β 2M and CA15-3 was lower in squamous cell carcinoma relative to normal tissues, and there was statistical significance in these differences. There is no statistical significance in the expression of the other tumor markers tested, including AFP, AFU, CT, FER and HE4 (*Table 3*).

Correlation analyses between the expression of four tumor marker genes and patient clinicopathological characteristics

We calculated the correlation between the expression of four tumor marker genes (CA125, CYFRA21-1, NSE and SCC) and patient clinicopathological characteristics, including age, smoking status, size of primary tumor, condition of regional lymph nodes, differentiation and TNM stage. Statistical significance only existed for differences in NSE across different T stages.

The expression levels of NSE and SCC tended to increase with increasing TNM stage, but changes did not reach statistical significance (*Table 4*). Increasing sample numbers may achieve statistical significance, however. There were no obvious correlations in the expression profiles of CA125, CYFRA21-1, NSE and SCC (*Table 5*).

Discussion

Lung cancer is the leading cancer site in males and accounts for 11% of total female cancer deaths in developing countries (1). Squamous-cell lung cancer is one of the most common subtypes of lung cancer. Most squamous-cell lung cancer occurs in male patients who smoke, and this disease is often diagnosed at an advanced and inoperable stage (4). Although considerable progress has been made in the early diagnosis and treatment of lung cancer, outcomes are typically not satisfactory. Because most squamous-cell lung cancers originate in the main bronchus, they are difficult to detect with imageological examination. The evaluation of serum tumor markers could provide an important supplementary examination method for diagnosis when disease manifestations are not obvious and imageological examination is negative (5,6). Therefore, there is significant clinical significance for the research of serum tumor markers in squamous cell

Table 2 The full names, code genes and functions of common tumor makers

Name	Full name	Gene	Function
β 2M	β 2-microglobulin	<i>B2M</i>	The heavy chain of the major histocompatibility complex (MHC) class I
AFP	α -fetoprotein	<i>AFP</i>	The fetal counterpart of serum albumin
AFU	α -L-fucosidase	<i>FUCA1 and FUCA2</i>	A enzyme involved in the degradation of fucose-containing glycoproteins and glycolipids
CA125	Carbohydrate antigen 125	<i>MUC16</i>	A glycoprotein located in cell membrane
CA15-3	Carbohydrate antigen 15-3	<i>MUC1</i>	A glycoprotein located in cell membrane
CEA	Carcinoembryonic antigen	<i>A group of CEACAs and PSGs</i>	A glycoprotein functioned as immunoglobulin and cell adhesion molecule
CT	Calcitonin	<i>CALCA</i>	A hormone involved in the regulation of calcium and phosphorus
CYFRA21-1	Cytokeratin 19 fragments	<i>KRT19</i>	Fragments of cytokeratins 19
FER	Ferritin	<i>FTL and FTH1</i>	An intracellular iron storage protein
HE4	Human epididymis protein 4	<i>WFDC2</i>	A protein possibly involved in sperm maturation
NSE	Neuron-specific enolase	<i>ENO2</i>	An isoenzyme of enolase involved in glycolysis and gluconeogenesis
PSA	Prostate specific antigen	<i>KLK3</i>	A protease present in seminal plasma
SCC	Squamous cell carcinoma antigen	<i>SERPINB3</i>	A member of the serine protease inhibitors

Table 3 The expression profiles of tumor maker genes in normal samples, paired tumor samples and all tumor samples

Name	Gene	Normal samples	Paired tumor samples	P value	All tumor samples	P value
β 2M	<i>B2M</i>	3,941 \pm 1,259	1,640 \pm 604.5	0.015	2,140 \pm 1,246	0.004
AFP	<i>AFP</i>	0.151 \pm 0.178	0.013 \pm 0.013	0.172	0.153 \pm 0.439	0.987
AFU	<i>FUCA1</i>	31.46 \pm 6.864	17.92 \pm 10.12	0.017	20.42 \pm 12.87	0.067
	<i>FUCA2</i>	20.85 \pm 2.216	14.54 \pm 2.294	0.013	21.57 \pm 8.795	0.857
CA125	<i>MUC16</i>	0.562 \pm 0.434	1.216 \pm 0.714	0.088	2.284 \pm 3.915	0.008
CA15-3	<i>MUC1</i>	475.3 \pm 140.7	195.5 \pm 334.7	0.200	158.3 \pm 194.5	0.001
CEA	<i>CEACAM1</i>	2.138 \pm 0.936	5.282 \pm 3.849	0.175	7.047 \pm 8.263	0.001
	<i>CEACAM5</i>	5.942 \pm 4.120	5.804 \pm 9.735	0.977	52.15 \pm 108.9	0.008
	<i>CEACAM6</i>	116.2 \pm 36.66	10.91 \pm 14.61	0.007	68.40 \pm 119.4	0.382
	<i>CEACAM19</i>	5.622 \pm 1.708	8.163 \pm 5.586	0.251	7.337 \pm 5.705	0.511
CT	<i>CALCA</i>	0.204 \pm 0.058	0.187 \pm 0.178	0.848	1.621 \pm 7.314	0.670
CYFRA21-1	<i>KRT19</i>	353.0 \pm 127.4	1,524 \pm 1,158	0.122	2,193 \pm 1,883	<0.001
FER	<i>FTL</i>	6,233 \pm 1,493	5,866 \pm 4,284	0.868	4,555 \pm 2,659	0.175
	<i>FTH1</i>	3,923 \pm 1,042	3,979 \pm 1,371	0.957	3,498 \pm 1,769	0.603
HE4	<i>WFDC2</i>	167.4 \pm 73.47	136.2 \pm 198.2	0.752	282.7 \pm 406.1	0.533
NSE	<i>ENO2</i>	16.73 \pm 1.366	36.84 \pm 30.54	0.223	39.96 \pm 35.33	<0.001
SCC	<i>SERPINB3</i>	0.795 \pm 0.844	16.68 \pm 15.51	0.076	26.59 \pm 47.62	0.001

Table 4 The correlation analyses between the expressions of tumor marker genes and the clinicopathological characteristics

Characteristics	No.	CA125	P value	CYFRA21-1	P value	NSE	P value	SCC	P value
Gene		<i>MUC16</i>		<i>KRT19</i>		<i>ENO2</i>		<i>SERPINB3</i>	
Age			0.176		0.210		0.375		0.213
≥60	26	1.624±3.015		1,898±1,734		43.90±33.51		19.18±42.76	
<60	18	3.237±4.775		2,619±2,004		34.27±37.07		37.29±52.04	
Smoking status			0.314		0.520		0.700		0.140
Yes	23	2.852±4.119		2,018±1,756		41.93±29.06		36.65±51.38	
No	21	1.662±3.577		2,385±1,995		37.80±41.01		15.57±40.35	
Primary tumor			0.368		0.274		0.003		0.577
T1	15	1.091±2.662		2,127±1,627		28.36±27.48		15.25±33.28	
T2	19	3.039±4.473		2,206±2,186		42.64±34.62		37.33±60.62	
T3	6	2.958±3.496		2,157±1,487		46.96±33.21		16.97±27.52	
T4	4	2.218±4.438		2,433±1,748		60.23±50.28		32.53±31.55	
Regional lymph nodes			0.897		0.792		0.288		0.196
N0	29	1.940±3.147		1,960±1,952		37.06±30.68		24.55±41.68	
N1	8	1.607±1.717		2,886±1,517		57.54±43.53		20.57±42.28	
N2	7	4.486±6.788		2,367±1,750		31.90±36.42		41.93±68.70	
Differentiation			0.708		0.207		0.765		0.361
Well differentiated	8	2.588±3.340		1,967±1,664		35.97±28.64		20.97±32.79	
Moderately differentiated	18	2.414±4.726		1,992±1,583		34.58±30.47		33.57±60.98	
Poorly differentiated	18	2.019±3.162		2,492±2,186		47.11±40.88		22.11±33.55	
TNM stage			0.389		0.757		0.172		0.082
I	23	2.165±2.975		2,186±2,035		34.79±29.56		21.98±40.26	
II	12	2.337±3.117		2,432±1,578		44.03±40.92		26.47±40.16	
III	9	2.517±6.270		1,892±1,807		47.75±38.54		38.53±67.80	

Table 5 The correlation analyses between CA125, CYFRA21-1, NSE and SCC

Name	Gene	Value	CA125	CYFRA21-1	NSE	SCC
CA125	<i>MUC16</i>	R	1	-0.212	-0.005	0.182
		P		0.167	0.976	0.236
CYFRA21-1	<i>KRT19</i>	R	-0.212	1	-0.050	0.134
		P	0.167		0.748	0.386
NSE	<i>ENO2</i>	R	-0.005	-0.050	1	-0.110
		P	0.976	0.748		0.475
SCC	<i>SERPINB3</i>	R	0.182	0.134	-0.110	1
		P	0.236	0.386	0.475	

lung cancer. An elevated level of serum tumor markers is typically caused by the level of these tumor markers in tumor tissues. In this study we performed RNA-Seq on five matched pairs of normal and squamous-cell lung cancer tissues and another 39 squamous-cell lung cancer tissues. Thirteen commonly used tumor marker genes were tested to screen for appropriate tumor markers. Finally, the genes encoding CA125, CYFRA21-1, NSE and SCC were shown to be expressed at higher levels in tumor than in normal tissues. Therefore, they might be suitable as tumor markers for screen squamous-cell lung cancer.

SCC has been implicated in tumor growth, and it also inhibits the apoptosis of tumor cells (7,8). As a commonly used tumor marker, SCC is valuable for the detection of many types of squamous cell carcinoma, including esophageal, head and neck and lung squamous cell carcinoma (9,10). SCC resides in the cytosol of squamous cells and is released into the circulation during squamous cell carcinoma (11). NSE is widely used in the screening in small cell lung cancer (12-14), but its function in squamous cell lung cancer has not been clearly studied. NSE as an enzyme active in glycolysis, and the rate of glycolysis is extremely elevated in tumor proliferation, a phenomenon called the "Warburg effect" (15). We also detected that the level of NSE was significantly higher in tumors than in normal tissues. CYFRA 21-1 is the serum dissolution fragment of cytokeratin 19 (CK19), which is expressed exclusively in epithelial cells and tumors of epithelial origin (16). Previous studies have suggested that CK19 played a part in the aggressive behavior of tumor cells and was connected with the differentiation and invasion of tumor cells (17). Increased serum CYFRA 21-1 is the result not only of cytokeratin release as a consequence of cell lysis or necrosis, but also of the degradation of cytokeratin filaments by activated proteases in tumor cells (18,19). The high level of CYFRA21-1 in patients with squamous cell lung cancer makes this protein the most sensitive of all of the currently studied tumor markers (20). CA125 is also found at a high level in ovarian carcinomas and lung cancer (21,22). Although previous studies have suggested that tumor markers such as CT, Ferritin and HE4 were present at high levels in lung cancer (23-25), they were not found to be elevated in the tumor tissues from our study.

Most previous studies have focused on the detection of tumor markers in the serum. However, few studies have investigated tumor markers in tissue and, in particular, the expression of their encoding genes. To address this shortcoming, we measured the expression of tumor markers

in tissues in our study. In the 13 tumor markers we tested, CA125, CYFRA21-1, NSE and SCC have been commonly used in clinical practice for diagnosis or prognosis of NSCLC (21,26-28). These tumor markers also express at a higher level in tumor samples than in normal samples in our study. Our study also supports their use in clinical practice. Several studies have demonstrated the use of these tumor markers in TNM staging (29-31). We also evaluated any correlations between the expression of the encoding genes of these tumor markers and patient clinicopathological characteristics, but we identified no statistically significant differences. We evaluated whether serum levels of these tumor markers would increase with increasing tumor volume, this being the reason why serum levels for these tumor markers can reflect TNM stages. The outcome of RNA-seq is an expression of unit volume, however, so it may not change with tumor growth.

Squamous cell lung cancer and adenocarcinoma are the two most common histologic subtypes of non-small cell lung cancer. However, these two subtypes are quite different in host susceptibility, clonal evolution, molecular evolution and molecular profiling (3). Previous studies have suggested that the elevated serum SCC percentage is highest in squamous-cell lung cancer, while this percentage is substantially lower in other types (32). NSE expression is higher in squamous-cell lung cancer with neuroendocrine differentiation. The serum CYFRA 21-1 level has been shown to be particularly elevated in squamous cell cancers (28). CA125 has been shown to be substantially expressed in large cell carcinoma and adenocarcinoma, but this protein could not be detected in a squamous lung cell line (33). Therefore, it is not clear whether or not our study can be directly applied to other types of lung cancer, such as adenocarcinoma or large cell lung cancer.

RNA-Seq has emerged as a popular high-throughput technology in recent years. In this technique, transcript levels are quantified in RPKM, which reflects the molar concentration of a transcript normalized by the total read number of the measurement. This normalization avoids common experimental deviations and also facilitates comparisons between multiple genes and samples. As such, RNA-Seq is an ideal method for global gene expression analysis.

Conclusions

Encoding-gene expression for CA125, CYFRA21-1, NSE and SCC was elevating in tumor tissues of squamous-cell lung cancer, while β 2M and CA15-3 were expressed

at a lower level in squamous cell lung cancer tissues. PSA could not be detected in most samples, and there was no significant difference between tumor and normal samples for the others tumor markers evaluated in this study, AFP, AFU, CEA, CT, FER and HE4.

Acknowledgements

Funding: This work was supported by Doctoral Program Foundation of Institutions of Higher Education of China (No. 20110071120066).

Authors' contribution: Qun Wang supervised this study, designed experiments and edited the paper with Yu Shi. Lin Wang, Cheng Zhan and Yongxing Zhang designed and carried out experiments, collected and analyzed data and co-wrote the paper. Jun Ma collected tissues and clinical characteristics of the patients with Junjie Xi and Wei Jiang, they also performed experiments with Yu Shi.

Disclosure: The authors declare no conflict of interest.

References

- Jemal A, Bray F, Center MM, et al. Global cancer statistics. *CA Cancer J Clin* 2011;61:69-90.
- Travis WD. Pathology of lung cancer. *Clin Chest Med* 2011;32:669-92.
- Herbst RS, Heymach JV, Lippman SM. Lung cancer. *N Engl J Med* 2008;359:1367-80.
- Jemal A, Center MM, DeSantis C, et al. Global patterns of cancer incidence and mortality rates and trends. *Cancer Epidemiol Biomarkers Prev* 2010;19:1893-907.
- Ather MH, Abbas F, Faruqui N, et al. Correlation of three immunohistochemically detected markers of neuroendocrine differentiation with clinical predictors of disease progression in prostate cancer. *BMC Urol* 2008;8:21.
- Hinestroza MC, Dickersin K, Klein P, et al. Shaping the future of biomarker research in breast cancer to ensure clinical relevance. *Nat Rev Cancer* 2007;7:309-15.
- Kato H. Expression and function of squamous cell carcinoma antigen. *Anticancer Res* 1996;16:2149-53.
- Suminami Y, Nawata S, Kato H. Biological role of SCC antigen. *Tumour Biol* 1998;19:488-93.
- Mino N, Iio A, Hamamoto K. Availability of tumor-antigen 4 as a marker of squamous cell carcinoma of the lung and other organs. *Cancer* 1988;62:730-4.
- Palermo F, Carniato A, Fede A, et al. Serum SCC-Ag in head and neck squamous cell carcinoma. *Int J Biol Markers* 1990;5:118-20.
- Uemura Y, Pak SC, Luke C, et al. Circulating serpin tumor markers SCCA1 and SCCA2 are not actively secreted but reside in the cytosol of squamous carcinoma cells. *Int J Cancer* 2000;89:368-77.
- Satoh H, Ishikawa H, Kurishima K, et al. Cut-off levels of NSE to differentiate SCLC from NSCLC. *Oncol Rep* 2002;9:581-3.
- Schneider J, Velcovsky HG, Morr H, et al. Comparison of the tumor markers tumor M2-PK, CEA, CYFRA 21-1, NSE and SCC in the diagnosis of lung cancer. *Anticancer Res* 2000;20:5053-8.
- Molina R, Auge JM, Escudero JM, et al. Mucins CA 125, CA 19.9, CA 15.3 and TAG-72.3 as tumor markers in patients with lung cancer: comparison with CYFRA 21-1, CEA, SCC and NSE. *Tumour Biol* 2008;29:371-80.
- Warburg O, Wind F, Negelein E. The metabolism of tumors in the body. *J Gen Physiol* 1927;8:519-30.
- Moll R, Krepler R, Franke WW. Complex cytokeratin polypeptide patterns observed in certain human carcinomas. *Differentiation* 1983;23:256-69.
- Isic Dencic T, Cvejic D, Paunovic I, et al. Cytokeratin19 expression discriminates papillary thyroid carcinoma from other thyroid lesions and predicts its aggressive behavior. *Med Oncol* 2013;30:362.
- Kulpa J, Wójcik E, Reinfuss M, et al. Carcinoembryonic antigen, squamous cell carcinoma antigen, CYFRA 21-1, and neuron-specific enolase in squamous cell lung cancer patients. *Clin Chem* 2002;48:1931-7.
- Sheard MA, Vojtesek B, Simickova M, et al. Release of cytokeratin-18 and -19 fragments (TPS and CYFRA 21-1) into the extracellular space during apoptosis. *J Cell Biochem* 2002;85:670-7.
- Takei Y, Minato K, Tsuchiya S, et al. CYFRA 21-1: an indicator of survival and therapeutic effect in lung cancer. *Oncology* 1997;54:43-7.
- Kimura Y, Fujii T, Hamamoto K, et al. Serum CA125 level is a good prognostic indicator in lung cancer. *Br J Cancer* 1990;62:676-8.
- Dietel M, Arps H, Klapdor R, et al. Antigen detection by the monoclonal antibodies CA 19-9 and CA 125 in normal and tumor tissue and patients' sera. *J Cancer Res Clin Oncol* 1986;111:257-65.
- McKenzie CG, Evans IM, Hillyard CJ, et al. Biochemical markers in bronchial carcinoma. *Br J Cancer* 1977;36:700-7.
- Volpino P, Cangemi V, Caputo V, et al. Clinical usefulness of serum ferritin measurements in lung cancer patients. *J Nucl Med Allied Sci* 1984;28:27-30.

25. Galgano MT, Hampton GM, Frierson HF Jr. Comprehensive analysis of HE4 expression in normal and malignant human tissues. *Mod Pathol* 2006;19:847-53.
26. Vassilakopoulos T, Troupis T, Sotiropoulou C, et al. Diagnostic and prognostic significance of squamous cell carcinoma antigen in non-small cell lung cancer. *Lung Cancer* 2001;32:137-44.
27. Ferrigno D, Buccheri G, Giordano C. Neuron-specific enolase is an effective tumour marker in non-small cell lung cancer (NSCLC). *Lung Cancer* 2003;41:311-20.
28. Stieber P, Hasholzner U, Bodenmüller H, et al. CYFRA 21-1. A new marker in lung cancer. *Cancer* 1993;72:707-13.
29. Molina R, Filella X, Augé JM, et al. Tumor markers (CEA, CA 125, CYFRA 21-1, SCC and NSE) in patients with non-small cell lung cancer as an aid in histological diagnosis and prognosis. Comparison with the main clinical and pathological prognostic factors. *Tumour Biol* 2003;24:209-18.
30. Diez M, Gomez A, Hernando F, et al. Serum CEA, CA125, and SCC antigens and tumor recurrence in resectable non-small cell lung cancer. *Int J Biol Markers* 1995;10:5-10.
31. Foa P, Fornier M, Miceli R, et al. Tumour markers CEA, NSE, SCC, TPA and CYFRA 21.1 in resectable non-small cell lung cancer. *Anticancer Res* 1999;19:3613-8.
32. Sánchez De Cos J, Masa F, de la Cruz JL, et al. Squamous cell carcinoma antigen (SCC Ag) in the diagnosis and prognosis of lung cancer. *Chest* 1994;105:773-6.
33. Homma S, Satoh H, Kagohashi K, et al. Production of CA125 by human lung cancer cell lines. *Clin Exp Med* 2004;4:139-41.

Cite this article as: Wang L, Zhan C, Zhang Y, Ma J, Xi J, Jiang W, Shi Y, Wang Q. Quantifying the expression of tumor marker genes in lung squamous cell cancer with RNA sequencing. *J Thorac Dis* 2014;6(10):1380-1387. doi: 10.3978/j.issn.2072-1439.2014.08.27

Prevalence and risk factors of aortic aneurysm in patients with chronic obstructive pulmonary disease

Katsutoshi Ando¹, Norihiro Kaneko², Tokuhide Doi³, Masahiro Aoshima², Kazuhisa Takahashi¹

¹Department of Respiratory Medicine, Juntendo University Graduate School of Medicine, 2-1-1 Hongo, Bunkyo-Ku, Tokyo 113-8421, Japan;

²Department of Respiratory Medicine, Kameda Medical Center, 929 Higashi-cho, Kamogawa-City, Chiba 296-8602, Japan; ³Fukuoka Clinic, 7-18-11 Umeda, Adachi-Ku, Tokyo 123-0851, Japan

Correspondence to: Katsutoshi Ando, M.D. Department of Respiratory Medicine, Juntendo University Graduate School of Medicine, 2-1-1 Hongo, Bunkyo-Ku, Tokyo 113-8421, Japan. Email: kando@juntendo.ac.jp.

Background: Patients with chronic obstructive pulmonary disease (COPD) manifest an excess of chronic co-morbidities and present a high prevalence of cardiovascular disease such as congestive heart failure and ischemic heart disease. Aortic aneurysm (AA) also shared the risks of those diseases and its rupture is an important cause of death. However, since AA progresses almost silently, the prevalence of AA in patients with COPD remains unclear. The aim of this study was to determine AA prevalence and risk factors in patients with COPD.

Methods: With computed tomography (CT) screening, we tested for AA in 231 COPD patients, and assessed emphysema by Goddard classification and aortic wall calcification in abdominal artery, respectively. We also evaluated that of thoracic artery using our original methods, which we assessed the extent of calcification in the thoracic artery as well as which defined as “aortic calcification index (ACI) in thoracic artery”.

Results: In 231 patients with COPD, 27 (11.7%) had AA determined by CT imaging and another 6 patients with previously diagnosed AA and a history of repaired operation (2.6%). In this total of 33 patients (AA group), the age of 95% confidence interval (CI) was 75.8 to 80.1 years and the prevalence of AA in patients aged 76 to 80 years was 26.8%. A low attenuation area and aortic wall calcification were more severe in the AA group than in the non-AA group, but forced expiratory volume in 1 second (FEV₁) was not significantly different in those patients. The Goddard score of nine and ACI in the thoracic artery of 25.0% were determined to identify the most appropriate cut-off levels for discriminating between AA and non-AA groups.

Conclusions: Our analysis indicated that sizeable under-recognition of AA seems likely in COPD. Especially for patients with severe lung destruction and aortic calcification verifiable by chest CT, abdominal CT would be beneficial for detecting AA.

Keywords: Aortic aneurysm (AA); calcification; chronic obstructive pulmonary disease (COPD); co-morbidity; computed tomography (CT)

Submitted May 23, 2014. Accepted for publication Sep 25, 2014.

doi: 10.3978/j.issn.2072-1439.2014.10.01

View this article at: <http://dx.doi.org/10.3978/j.issn.2072-1439.2014.10.01>

Introduction

Chronic obstructive pulmonary disease (COPD) is one of the leading causes of morbidity and mortality worldwide. The characteristic feature is progressive airflow limitation related to a chronic inflammatory response in the lung (1). Recently, epidemiological studies have demonstrated that COPD

patients manifest an excess of chronic co-morbidities, mainly cardiovascular, which are well-known as important factors that determine prognosis and functional capabilities (2-7). The prevalence of coronary artery diseases and heart failure in patients with COPD has been reported to be associated with airflow obstruction and the extent of emphysema. Moreover, the percentage of cardiovascular-

related mortality is up to twofold higher than in a matched population without COPD (2,3).

Aortic aneurysm (AA) is a common and potentially life-threatening condition. Advanced age and smoking are risk factors that connected with COPD as they are for other cardiovascular diseases. Some studies reveal that COPD is associated with the development of AA and appears to convey an added risk of rupture in patients with small aneurysms (8,9). Furthermore, in the 4-year Understanding Potential Long-Term Impacts on Function with Tiotropium (UPLIFT) trial, AA rupture was reported as one of the common causes of death as well as myocardial infarction and colorectal cancer. That is, the incidence of AA was twice or more as frequent as that of pulmonary embolism or prostate cancer (10). Together, these previous reports suggest that COPD patients, like those with coronary artery disease and heart failure, have a comparatively higher risk of AA than non-COPD smokers. To determine its prevalence and risk factors, we performed the cross-sectional, case-control study in a major Japanese medical institution.

Methods

Patient population and study design

We recruited participants from patients who had a prior diagnosis of COPD and regularly visited the Department of Respiratory Medicine at Kameda Medical Center (Chiba, Japan) between April 2011 and March 2012. The inclusion criteria were: aged >40 years, a smoking history of at least 20 pack-year, and a post-bronchodilator forced expiratory volume in 1 second (FEV₁)/forced vital capacity (FVC) ratio <70% at inclusion. In this study, we also included patients whose AA was previously diagnosed, but excluded patients with a history of lung resection or other significant respiratory diseases. Then, finally, 231 patients were enrolled and underwent CT scanning of the chest, abdomen and pelvis, in addition to the regular COPD workup that including physical examination, pulmonary function testing, and chest radiographs.

The presence of AA was diagnosed by one radiologist and independently confirmed by two pulmonologists (KA and NK) on the basis of CT findings such as its size, length, location and shape, etc. Then, we designated 33 patients whose AA was documented either by our current CT scans (n=27) or former diagnoses (n=6) as “patients with AA (AA group)”, and classified the remaining 198 without AA of 231 patients initially enrolled into a non-AA group. We compared both groups’ backgrounds and CT data. The

study protocol was approved by the ethics committee of Kameda Medical Center, and written informed consent was obtained from each participant.

Pulmonary function tests

Pulmonary function tests were performed according to American Thoracic Society standards, with a Chestac-65V (Chest MI Corp, Tokyo, Japan). FEV₁ for each patient is expressed as a percentage of the predicted value (FEV₁ % predicted), which was calculated based on reference values from the Japanese population (11).

Analyses of CT images

All CT examinations were performed with commercially available CT scanners (X-force SH, Toshiba Medical, Tokyo, Japan), and non-enhanced CT scans were obtained with 5-mm section thickness. The severity of emphysema was visually assessed on CT images of the chest by two pulmonologists (KA and NK), and its extent, the percentage of lung destruction, was classified according to the Goddard scoring system (12): score 0, normal; score 1, ≤25% affected; score 2, <25% and ≤50% affected; score 3, 50% and ≤75% affected; and score 4, >75% affected. Six images were analyzed in three slices, which were obtained from 1 cm above the upper margin of the aortic arch, 1 cm below the carina, and 1 cm above the right diaphragm, and a total score of six images was calculated in each person.

Meanwhile, the aortic calcification index (ACI) was recently reported as a useful marker for evaluating abdominal aortic calcification and in association with the prevalence of cardiovascular disease (13-16). To assess ACI, we selected ten slices from each patient at 1 cm intervals from the common iliac bifurcation upward and calculated the mean percentage of the calcification area (divided into 12 sectors).

Although this index is the accepted method for assessing the abdominal artery, it has never been reported for evaluating the calcification visible in a chest CT. Then, to determine a useful, simple method applicable in routine COPD workups, we posited that calcification in an abdominal artery resembled that in a thoracic artery. Therefore, for each patient, we selected a slice with the most severe aortic wall calcification in thoracic artery, excluding the aortic arch, and a slice in which the aortic arch was longitudinally delineated. ACI (%) measurements in the thoracic artery and aortic arch were then recorded. When the findings were not agreed upon by consensus

Table 1 Status of aortic aneurysm in the enrolled patients

Variables	Diagnosed before this study (n=6) [%]	Diagnosed in this study (n=27) [%]
With a history of repair operation	6 [100]	2 [7]
Site		
Thoracic artery	0	6 [22]*
Abdominal artery	6 [100]	20 [74]*
Iliac artery	0	3 [11]*
Maximum aortic diameter		
<4 cm	0	18 [67]
4-5.5 cm	0	7 [26]
>5.5 cm	2 [33]	2 [7]
Unknown	4 [67]**	0

*, two patients had aortic aneurysm (AA) detected at different sites; one in abdominal and thoracic arteries, and the other in abdominal and common iliac arteries; **, four patients were whose a repair operation was performed before this study and we could not identify the aortic diameter in detail.

between two pulmonologists, the other pulmonologist finally determined its severity.

Statistical analyses

We used the Chi-squared test, paired *t*-test or Mann-Whitney test, as appropriate, to compare the two groups of patients. All data were subjected to Spearman's rank correlation analysis. To determine independent factors associated with AA, we used logistic regression multivariable analysis. We also analyzed Akaike's information criterion (AIC), which is a statistical value known to provide a superior fit, to obtain the most appropriate cut-off level (17,18). A smaller AIC value indicated a more reliable model for predicting the existence of AA. These analyses were performed with SPSS Version 21. Data were expressed as means with standard deviations (SD). For all statistical analyses, a *P* value less than 0.05 was considered significant.

Results

Baseline characteristics

The mean age was 73.3 years (8.7) among the patients, of

whom 94% were men, and 14% were current smokers. The mean FEV₁ was 1.86 liters (83.7% of the predicted value), and patients whose COPD was classified as stage I, II, III, or IV, according to criteria of the GOLD guideline, comprised 59%, 26%, 13% and 2% of patients, respectively. The mean points of Goddard classification for lung damage were 7.4 (6.0). Of the 238 patients, 120 (52%) were given a long-acting inhaled muscarine receptor antagonist (LAMA); 91 (39%) received a long-acting inhaled β_2 -agonist (LABA), for 89 (39%) a corticosteroid inhalant was administered, 76 (33%) had a theophylline compound, and 28 (12%) received oxygen supplementation. As for co-morbidities, on the other hand, 149 patients (65%) had hypertension, 68 (29%) had hyperlipidemia, 42 (18%) had diabetes mellitus, 58 (24%) had cardiovascular disease other than AA, and 16 (7%) had cerebrovascular disease.

In six patients, abdominal AA had already been diagnosed and a repair operation was performed before this study. Meanwhile, our CT screening newly detected AA in 27 patients (*Table 1*), of whom 5 had thoracic AA, 18 had abdominal AA, 2 had common iliac AA, 1 had both thoracic and abdominal AA, and 1 had both abdominal and common iliac AA. Of 33 patients in this overall AA group, the maximal aortic diameter of 18 patients (55%) was less than 4 cm; another 7 (21%) had 4 to 5.5 cm, and 6 (18%) had more than 5.5 cm. Two patients whose AA was detected in our CT screening and who manifested an aortic diameter more than 5.5 cm underwent a repair operation after this study.

ACI in thoracic artery

To assess the reliability of ACI in aortic arch and thoracic artery, we correlated those values with that of the previously established ACI in an abdominal artery (*Figure 1*). Indices for the current patients had strongly positive correlations with ACI in abdominal artery (ACI in aortic arch; $r=0.709$, $P<0.001$; ACI in thoracic artery; $r=0.706$, $P<0.001$).

Patients' characteristics associated with AA

Comparisons of patients' characteristics between the AA group (n=33) and non-AA group (n=198) designated here are shown in *Table 2*. The AA group were older (77.9 *vs.* 72.5 years, $P<0.001$), had a more excessive smoking status (pack-year, 77.4 *vs.* 63.8, $P=0.032$), higher Goddard score (10.8 *vs.* 7.1, $P<0.001$), elevated ACI in aortic arch, thoracic and abdominal arteries (26.0% *vs.* 12.2%, $P<0.001$; 28.5% *vs.* 12.1%, $P<0.001$; 24.9% *vs.* 17.6%, $P=0.005$, respectively)

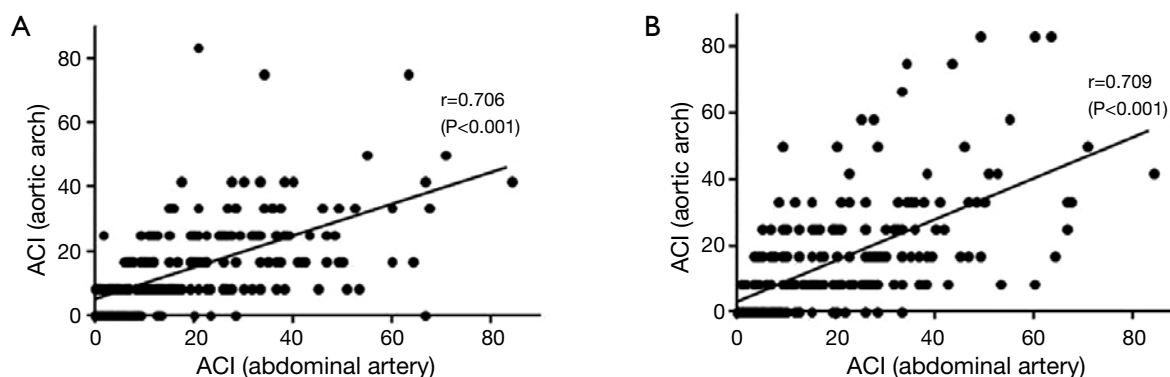


Figure 1 Correlation of ACI in the chest CT with that in the abdominal artery. ACI in both the aortic arch (A) and thoracic artery (B) correlated strongly with that previously established for the abdominal artery. (ACI in aortic arch; $r=0.709$, $P<0.001$; ACI in thoracic artery; $r=0.706$, $P<0.001$). ACI, aortic calcification index; CT, computed tomography.

and far greater proportion of patients with cardiovascular disease (55% vs. 19%, $P<0.001$). Additionally, the AA group had a lower overall value for FEV₁ (1.58 vs. 1.90 liters, $P=0.012$) and FEV₁/FVC (49.2% vs. 53.9%, $P=0.035$) than the non-AA group. Gender, body mass index, co-morbidities except for cardiovascular disease, FEV₁ % predicted, and proportions of patients who were classified according to GOLD guideline were similar for both groups.

In contrast, however, age correlated negatively with body mass index ($r=-0.184$, $P=0.005$), FVC ($r=-0.427$, $P<0.001$), FEV₁ ($r=-0.341$, $P<0.001$) and FEV₁/FVC ($r=-0.138$, $P=0.036$), although greater age correlated positively with aortic calcification ($P<0.001$). Smoking status was also risk factor in both COPD and AA, and it correlated with aortic calcification as well as the FEV₁ % predicted and LAA (data not shown). Accordingly, our univariate analysis detected several characteristics of COPD shared with AA, but the influence of age differed notably between these two groups of patients.

Comparison of subjects with equivalent age

Based on our results, age was one of the most important factors contributing to AA in all patients with COPD. Accordingly, we next examined the clinical characteristics in individuals from both groups of comparable ages.

The ages yielding a 95% confidence interval (CI) in patients with AA was 75.8 to 80.1 years (range, 62–88 years). Therefore, we selected subjects of 76–80 years; 15 patients in AA group (78.5±1.1 years) and 41 patients in non-AA group (78.1±1.3 years) and compared data for the two groups (Table 2). As a result, Goddard scores and ACI in aortic arch

and thoracic artery were higher in the AA group than in the non-AA group (Goddard score; 11.2 vs. 7.2, $P=0.045$: ACI in aortic arch; 30.0% vs. 15.2%, $P=0.001$: ACI in thoracic artery; 36.1% vs. 14.0%, $P<0.001$). However, FEV₁ was not significantly different (1.54 vs. 1.70 L, $P=0.287$; % predicted, 75.3% vs. 83.0%, $P=0.292$) in these two groups. In the multivariate analysis among those three significant parameters (data not shown), on the other hand, the two factors that were independently associated with the existence of AA were ACI in the thoracic artery [odds ratio (OR), 1.87; 95% CI, 1.08 to 3.25; $P=0.026$] and LAA (OR, 1.14; 95% CI, 1.01 to 1.28; $P=0.033$). However, ACI in aortic arch did not prove to be statistically significant (OR, 0.98; 95% CI, 0.51 to 1.86; $P=0.943$).

From those results, we plotted patients' data according to ACI in the thoracic artery and Goddard scores, followed by calculating AIC to determine the most appropriate cut-off level (Figure 2). As a result, the smallest AIC value for the most appropriate cut-off levels of ACI in thoracic artery and Goddard scores were 25.0% and 9 (AIC = -9.14 and -5.31), respectively. Of 28 patients with Goddard score ≤9 and ACI ≤25.0%, only one patient had AA (3.6%), constituting a significantly lower prevalence in patients with low scores, i.e., Goddard score >9 or ACI >25.0% (50.0%, $P<0.001$).

Finally, to determine whether patients with COPD have a higher risk of AA than controls who are matched in age (76.8±4.5 years) and smoking status (packs/year, 87.3±22.7), we performed CT screening for 27 participants without COPD (Table 2). However, we did not detect AA in any of the latter participants (0%). Although the number of our control subjects was small, clearly the prevalence of AA in patients with COPD reached a statistically significant

Table 2 Subject characteristics and clinical information

Clinical variable	All COPD patients		Subjects with 76-80 years		P value	Control (N=27)
	AA group (N=33)	Non-AA group (N=198)	AA group (N=15)	Non-AA group (N=41)		
Age, year (SD)	77.9±6.0	72.5±8.9	78.5±1.1	78.1±1.3	0.270	76.8±4.5
Male, gender n [%]	30 [91]	188 [95]	15 [100]	40 [98]	1.0	26 [96]
Body mass index	22.5±3.2	22.9±3.1	22.0±3.2	22.7±2.9	0.296	23.1±3.4
Smoking status						
Current smoker, n [%]	5 [15]	27 [14]	1 [7]	3 [7]	1.0	2 [7]
Smoking history	77.4±36.3	63.8±33.7	87.7±39.8	67.1±33.2	0.100	87.3±22.7
Duration of disease since diagnosis, year	6.3±4.8	4.9±3.8	6.2±4.6	6.1±3.9	0.900	
Comorbidities, n [%]						
Hypertension	26 [79]	123 [62]	13 [87]	29 [70]	0.307	15 [56]
Hyperlipidemia	15 [45]	53 [27]	5 [33]	13 [32]	1.0	5 [19]
Diabetes mellitus	7 [21]	35 [18]	2 [13]	8 [20]	0.713	7 [26]
Hyperuricemia	5 [15]	21 [11]	2 [13]	6 [15]	1.0	4 [15]
Cardiovascular disease	18 [55]	38 [19]	9 [60]	11 [27]	0.030	3 [11]
Cerebrovascular disease	1 [3]	15 [8]	0	4 [10]	1.0	1 [4]
Spirometry						
FVC (liters)	3.22±0.79	3.48±0.80	3.32±0.61	3.27±0.65	0.723	2.94±0.52
FEV ₁ (liters)	1.58±0.57	1.90±0.68	1.54±0.61	1.70±0.56	0.287	2.26±0.41
FEV ₁ /FVC [%]	49.2±12.5	53.9±12.3	45.8±13.7	51.6±12.7	0.144	76.9±7.0
FEV ₁ % predicted	79.5±27.5	84.5±25.6	75.3±29.1	83.0±26.7	0.292	108.7±20.0
GOLD stage, n [%]						
I	16 [48]	120 [61]	6 [40]	25 [61]	0.227	
II	10 [30]	50 [26]	6 [40]	10 [24]	0.321	
III	6 [18]	24 [12]	2 [13]	6 [15]	1.0	
IV	1 [3]	4 [2]	1 [7]	0	0.268	
Time of acute exacerbation	0.55±1.48	0.15±0.59	0.33±0.79	0.27±0.63	0.936	
LAA (Goddard classification)	10.8±6.2	7.1±5.8	11.2±6.6	7.2±6.0	0.045	
Aortic wall calcification score [%]						
Aortic arch	26.0±17.4	12.2±12.2	30.0±16.0	15.2±12.5	0.001	
Thoracic artery	28.5±19.6	12.1±15.3	36.1±22.7	14.0±13.2	<0.001	
Abdominal artery	24.9±16.7	17.6±17.0	30.7±18.9	22.0±13.9	0.180	

Plus-minus values are means ± SD. SD, standard deviation; COPD, chronic obstructive pulmonary disease; AA, aortic aneurysm; FVC, forced vital capacity; FEV₁, forced expiratory volume in 1 second; LAA, low attenuation area.

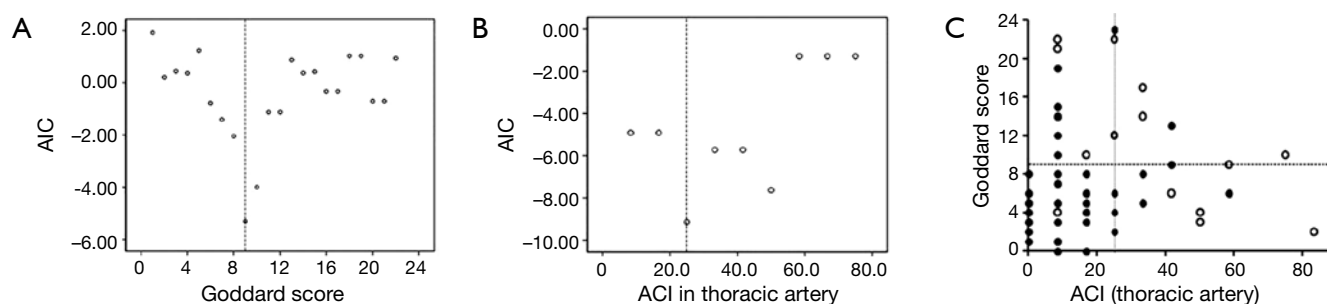


Figure 2 Relationship between ACI and Goddard score in patients 76-80 years-old [with (◐) or without (◑) an aortic aneurysm]. The Goddard score of nine (A) and ACI in the thoracic artery of 25.0% (B) were determined by AIC analysis (AIC = -5.31 and -9.14; respectively) to identify the most appropriate cut-off levels for discriminating between AA and non-AA groups. Broken lines indicate cut off levels of Goddard score (9) and ACI in the thoracic artery (25.0%). Of 28 patients with a Goddard score ≤ 9 and ACI $\leq 25.0\%$, only one patient had AA (3.6%), which indicated a significantly lower prevalence than in patients with Goddard score >9 or ACI $>25.0\%$ (50.0%, $P < 0.001$). ACI, aortic calcification index; AIC, Akaike's information criterion; AA, aortic aneurysm.

higher level than in our control group without COPD ($P = 0.002$).

Discussion

In our prospective CT evaluation, we demonstrated for the first time the prevalence of AA and the specific characteristics of patients with AA among those who are afflicted with COPD. We found that (I) 33 of 231 COPD patients (14.3%) newly or previously diagnosed with AA represented a greater general prevalence of AA than previously reported (1-2%) [19]; (II) The age of 95% CI in the AA group was 75.8 to 80.1 years, and the prevalence of AA in patients of those ages was 26.8% (15 in 56 patients); (III) Comparison between those with COPD and separated into AA and non-AA groups of equivalent age indicated that LAA and ACI values evaluated by chest CT were higher in the AA group than those of the non-AA group, but FEV₁ was not significantly different. Accordingly, our data indicate that COPD patients over 75 years of age have a high prevalence of AA and that severe lung destruction as well as aortic wall calcification is a risk factor for the acquisition of AA in these patients. Our data suggest that abdominal screening in addition to the routine COPD workup is a valuable asset in detecting AA early in the disease course of such patients and in averting AA-related adverse events.

AA involves the progressive dilatation of the aorta leading to a likelihood of tearing and high mortality rate typically associated with advanced age and atherosclerosis (19). Currently, the development of imaging mass spectrometry

has elucidated the pathogenesis of AA. Tanaka *et al.* described adventitial stenosis and intimal hyperplasia of the vaso vasorum (VV) with the accumulation of abnormal lipid molecules in the AA sac and demonstrated that, in this state, the aortic wall of the AA sac was ischemic and hypoxic (20). That is an important risk factor for AA such as aging and smoking affect VV circulation ultimately causing the progression of AA (19,20). The systemic inflammation and hypoxic condition in COPD may also promote the contribution of abnormal VV circulation to AA.

Additionally, COPD shares these risk factors. Patients with AA had a higher prevalence of airway obstruction than age-matched control or patients with coronary artery disease (21).

In an UPLIFT trial, furthermore, AA rupture was one of the common causes of death in spite of the fact that AA was not detected as a major co-morbidity (10). Our study also demonstrated that COPD patients, especially those who are over 75 years old, are at a higher risk of AA development than those without COPD or other cardiovascular co-morbidities. That is, these data suggest that a high degree of under-recognition of AA is likely in patients with COPD. Meanwhile, some epidemiologic studies suggest that diabetes is independently associated with a decreased rate of AA (22,23), but the proportion of patients with diabetes was not different between AA and non-AA group in our population. Whether this point is characteristic of patients with COPD remains unclear, we should re-evaluate it prospectively in multiple centers.

Here, ACI evaluation in chest CTs appeared to be a useful indicator for predicting the presence of AA in COPD patients. Most individuals aged >60 years have progressively enlarging

deposits of calcium mineral in their major arteries (24). This vascular calcification reduces aortic and arterial elastance, which impairs cardiovascular hemodynamics; therefore ACI has been described as a valuable predictor of coronary heart disease (25,26). Methods for ACI evaluation have been reported, and those scores are independent factors for judgments on cardiovascular events (15,16,27). We assessed the aortic calcification in thoracic artery using ACI and confirmed its strong correlation with those scores previously reported (15,16). Accordingly, our data suggest that chest CT provides a good gauge of aortic calcification and cardiovascular risk.

This study had some limitations. First, the subjects in this study were located at a single center, and their number was smaller than in epidemiological studies. That is, we could not evaluate the interaction of LDL-C levels and statins, and the impact of the hypertensive medication such as beta-blockers and Losartan. However, our data were evaluated with state-of-the-art statistics and in correlation with previously established methods. Second, we did not assess the cost-effectiveness for detecting AA early in COPD patients. Because the incidence of AA is comparatively lower than other for cardiovascular diseases, the cost-effectiveness and indications for use should be evaluated. Finally, we considered that systemic inflammation in COPD could relate to the pathogenesis of AA, but we did not assess the systemic inflammatory markers (28). In addition, since our AA group included patients whose AA was previously diagnosed, there was a possibility that it caused a selection bias, and so the population was not representative from patients with COPD population and the prevalence was overestimated. Accordingly, our data including these points should be re-evaluated prospectively in multiple centers.

Conclusions

Our analysis revealed that the prevalence of AA is high in patients with COPD, suggesting a high degree of under-recognition of AA. Especially in patients with severe lung destruction and aortic calcification verifiable by chest CT, its prevalence is high and abdominal CT would be beneficial for detecting AA.

Acknowledgements

The authors thank Dr. Yasutaka Kawamura, M.D., Ph.D., Department of Radiology, Kameda Medical Center, for academic advice about the existence of AA. We also thank

Phyllis Minick for excellent assistance in the review of English.

Authors' contributions: KA had full access to all the data in the study and takes full responsibility for the integrity of the data and the accuracy of the data analysis. KA and KN contributed to the concept and design of the study, acquisition of data, interpretation of data, and drafting and finalizing of the manuscript. AM and TK contributed to the concept and design of the study, and acquisition of data. DT contributed to the statistical analysis and interpretation of data. All authors read and approved the final manuscript.

Disclosure: The authors declare no conflict of interest.

References

1. Global Initiative for Chronic Obstructive Lung Disease (GOLD). Global strategy for the diagnosis, management, and prevention of chronic obstructive pulmonary disease (updated 2011). Bethesda, MD: National Heart, Lung and Blood Institute, World Health Organization, 2011.
2. Curkendall SM, DeLuise C, Jones JK, et al. Cardiovascular disease in patients with chronic obstructive pulmonary disease, Saskatchewan Canada cardiovascular disease in COPD patients. *Ann Epidemiol* 2006;16:63-70.
3. Huiart L, Ernst P, Suissa S. Cardiovascular morbidity and mortality in COPD. *Chest* 2005;128:2640-6.
4. Soriano JB, Visick GT, Muellerova H, et al. Patterns of comorbidities in newly diagnosed COPD and asthma in primary care. *Chest* 2005;128:2099-107.
5. Finkelstein J, Cha E, Scharf SM. Chronic obstructive pulmonary disease as an independent risk factor for cardiovascular morbidity. *Int J Chron Obstruct Pulmon Dis* 2009;4:337-49.
6. Mannino DM, Thorn D, Swensen A, et al. Prevalence and outcomes of diabetes, hypertension and cardiovascular disease in COPD. *Eur Respir J* 2008;32:962-9.
7. Miller J, Edwards LD, Agustí A, et al. Comorbidity, systemic inflammation and outcomes in the ECLIPSE cohort. *Respir Med* 2013;107:1376-84.
8. Lindholt JS, Heickendorff L, Antonsen S, et al. Natural history of abdominal aortic aneurysm with and without coexisting chronic obstructive pulmonary disease. *J Vasc Surg* 1998;28:226-33.
9. Cronenwett JL, Murphy TF, Zelenock GB, et al. Actuarial analysis of variables associated with rupture of small abdominal aortic aneurysms. *Surgery* 1985;98:472-83.
10. Celli B, Decramer M, Kesten S, et al. Mortality in the 4-year trial of tiotropium (UPLIFT) in patients with

- chronic obstructive pulmonary disease. *Am J Respir Crit Care Med* 2009;180:948-55.
11. Sharp DS. Reference values for lung function in the Japanese: recording of normal lung function from 11 institutes in Japan. *Jpn J Thoracic Dis* 1993;31:421-7.
 12. Goddard PR, Nicholson EM, Laszlo G, et al. Computed tomography in pulmonary emphysema. *Clin Radiol* 1982;33:379-87.
 13. Kent KC, Zwolak RM, Egorova NN, et al. Analysis of risk factors for abdominal aortic aneurysm in a cohort of more than 3 million individuals. *J Vasc Surg* 2010;52:539-48.
 14. Hirsch AT, Haskal ZJ, Hertzler NR, et al. ACC/AHA 2005 Practice Guidelines for the management of patients with peripheral arterial disease (lower extremity, renal, mesenteric, and abdominal aortic): a collaborative report from the American Association for Vascular Surgery/Society for Vascular Surgery, Society for Cardiovascular Angiography and Interventions, Society for Vascular Medicine and Biology, Society of Interventional Radiology, and the ACC/AHA Task Force on Practice Guidelines (Writing Committee to Develop Guidelines for the Management of Patients With Peripheral Arterial Disease): endorsed by the American Association of Cardiovascular and Pulmonary Rehabilitation; National Heart, Lung, and Blood Institute; Society for Vascular Nursing; TransAtlantic Inter-Society Consensus; and Vascular Disease Foundation. *Circulation* 2006;113:e463-654.
 15. Ohya M, Otani H, Kimura K, et al. Improved assessment of aortic calcification in Japanese patients undergoing maintenance hemodialysis. *Intern Med* 2010;49:2071-5.
 16. Yukawa S, Sonobe M, Tone Y, et al. Prevention of aortic calcification in patients on hemodialysis by long-term administration of vitamin E. *J Nutr Sci Vitaminol (Tokyo)* 1992;Spec No:187-90.
 17. Akaike H. A new look at statistical model identification. *IEEE Transactions on Automatic Control* 1974;19:716-23.
 18. Wagenmakers EJ, Farrell S. AIC model selection using Akaike weights. *Psychon Bull Rev* 2004;11:192-6.
 19. Lindsay ME, Dietz HC. Lessons on the pathogenesis of aneurysm from heritable conditions. *Nature* 2011;473:308-16.
 20. Tanaka H, Zaima N, Sasaki T, et al. Adventitial vasa vasorum arteriosclerosis in abdominal aortic aneurysm. *PLoS One* 2013;8:e57398.
 21. Sakamaki F, Oya H, Nagaya N, et al. Higher prevalence of obstructive airway disease in patients with thoracic or abdominal aortic aneurysm. *J Vasc Surg* 2002;36:35-40.
 22. Shantikumar S, Ajjan R, Porter KE, et al. Diabetes and the abdominal aortic aneurysm. *Eur J Vasc Endovasc Surg* 2010;39:200-7.
 23. Torsney E, Pirianov G, Cockerill GW. Diabetes as a negative risk factor for abdominal aortic aneurysm - does the disease aetiology or the treatment provide the mechanism of protection? *Curr Vasc Pharmacol* 2013;11:293-8.
 24. Allison MA, Criqui MH, Wright CM. Patterns and risk factors for systemic calcified atherosclerosis. *Arterioscler Thromb Vasc Biol* 2004;24:331-6.
 25. Greenland P, Bonow RO, Brundage BH, et al. ACCF/AHA 2007 clinical expert consensus document on coronary artery calcium scoring by computed tomography in global cardiovascular risk assessment and in evaluation of patients with chest pain: a report of the American College of Cardiology Foundation Clinical Expert Consensus Task Force (ACCF/AHA Writing Committee to Update the 2000 Expert Consensus Document on Electron Beam Computed Tomography). *Circulation* 2007;115:402-26.
 26. Demer LL, Tintut Y. Vascular calcification: pathobiology of a multifaceted disease. *Circulation* 2008;117:2938-48.
 27. Martino F, Di Loreto P, Giacomini D, et al. Abdominal aortic calcification is an independent predictor of cardiovascular events in peritoneal dialysis patients. *Ther Apher Dial* 2013;17:448-53.
 28. Eagan TM, Ueland T, Wagner PD, et al. Systemic inflammatory markers in COPD: results from the Bergen COPD Cohort Study. *Eur Respir J* 2010;35:540-8.

Cite this article as: Ando K, Kaneko N, Doi T, Aoshima M, Takahashi K. Prevalence and risk factors of aortic aneurysm in patients with chronic obstructive pulmonary disease. *J Thorac Dis* 2014;6(10):1388-1395. doi: 10.3978/j.issn.2072-1439.2014.10.01

Analysis of the molecular and clinicopathologic features of surgically resected lung adenocarcinoma in patients under 40 years old

Ting Ye^{1,2}, Yunjian Pan^{1,2}, Rui Wang^{1,2}, Haichuan Hu^{1,2}, Yang Zhang^{1,2}, Hang Li^{1,2}, Lei Wang^{1,2}, Yihua Sun^{1,2}, Haiquan Chen^{1,2}

¹Department of Thoracic Surgery, Shanghai Cancer Center, ²Department of Oncology, Shanghai Medical College, Fudan University, Shanghai 200032, China

Correspondence to: Dr. Haiquan Chen, MD. Department of Thoracic Surgery, Shanghai Cancer Center, Fudan University, 270 Dong'an Road, Shanghai 200032, China. Email: hqchen1@yahoo.com; Dr. Yihua Sun, MD. Department of Thoracic Surgery, Shanghai Cancer Center, Fudan University, 270 Dong'an Road, Shanghai 200032, China. Email: sun_yihua76@hotmail.com.

Introduction: The youthful lung cancer may constitute an entity with distinct clinicopathologic characteristics and a controversial prognosis compared with the older counterpart. Whether the youthful lung cancer has the exclusively distinct molecular features has not been well investigated.

Methods: Thirty-six resected lung adenocarcinomas from young patients under 40 years old were analyzed concurrently for mutations in EGFR, KRAS, HER2, BRAF, AKT1, ALK, RET, TP53 and LKB1 and enrolled as the younger group. Their molecular and clinicopathologic characteristics were compared with those of 87 adenocarcinoma cases from patients above 40 years old which were collected as the older group.

Results: The comparable overall survival (OS) ($P=0.942$), more early adenocarcinomas ($P=0.033$), more wedge resections ($P<0.001$) and fewer smokers ($P=0.004$) were seen in the younger group, when compared with the clinicopathologic characteristics in the older group. Nineteen EGFR mutations (52.8%), 3 KRAS mutations (8.3%), 2 EML4-ALK fusions (5.6%) and 1 KIF5b-RET fusion (2.8%) were identified in the younger group. The difference of oncogenic mutations between the two groups was statistically insignificant ($P=0.396$). Twenty-six TP53 mutations (72.2%) and 4 LKB1 mutations (11.1%) were found in the younger group. When compared with the old patients, young patients showed a higher prevalence of TP53 mutations ($P<0.001$) and a comparable prevalence of LKB1 mutations ($P=0.951$).

Conclusions: The youthful lung cancer unequivocally presented the distinct clinicopathologic characteristics including more early adenocarcinomas and fewer smokers. It showed the similar oncogenic characteristics and higher prevalence of TP53 mutations compared with the older counterpart.

Keywords: The youthful lung cancer; clinicopathologic characteristic; oncogene; tumor suppressor gene; mutation analysis

Submitted May 25, 2014. Accepted for publication Aug 14, 2014.

doi: 10.3978/j.issn.2072-1439.2014.08.50

View this article at: <http://dx.doi.org/10.3978/j.issn.2072-1439.2014.08.50>

Introduction

Lung cancer, one of the most frequent malignancies in the world, is rapidly becoming the main cause of cancer-related death nowadays (1). During the past decade, its incidence has been quickly increasing and age at diagnosis keeps decreasing (2,3). Many studies have suggested that lung cancer in young patients may constitute an entity

with distinct clinicopathologic characteristics, which is common in non-smoker and female patients, and presents a predominance of adenocarcinoma, the advanced stage at diagnosis and thus a generally poor prognosis (4,5). However, it is still controversial whether younger patients with lung cancer have better or worse outcomes compared with the older counterparts (6-8).

Recent advances in translational research has enabled the

classification of non-small cell lung cancer (NSCLC) into various molecular subsets defined by the so-called “driver mutations”, each with distinct clinicopathologic features as well as potential opportunities for targeted therapies (9). With the development of molecular targeted agents, currently about 15% of NSCLC patients benefit from the more personalized treatment protocols based on the genetic background of the tumor (10). For example, EGFR tyrosine kinase inhibitors (TKIs) such as Gefitinib and Erlotinib have been developed, and a subset of patients show significant therapeutic responses to this treatment, which was subsequently revealed to be associated with a mutation (11). In 2007, some patients who had ALK rearrangements were found to have similar remarkable responses to crizotinib, an ALK inhibitor (12). Other well-identified driver mutations in NSCLC include mutations in KRAS, HER2, BRAF, MEK, ERK and AKT1, as well as ALK and RET fusions, for which there are some novel oral TKIs in development (9,13,14). Noticeably, these oncogenes are frequently found in lung adenocarcinoma. On the other hand, mutations in tumor suppressor genes including TP53 and LKB1, which are also frequently seen in lung cancer, have been revealed to contribute to the pathogenesis of NSCLC as well (15-17). However, whether the youthful lung cancer has the exclusively distinct molecular features has not been well investigated.

Given the huge disease burden on public health due to the lung cancer in young patients, identifying its molecular and clinicopathologic features and thus making an appropriate treatment strategy is urgently necessary. In this study, we performed a comprehensive analysis of mutations in oncogenes and tumor suppressor genes in 36 Chinese young patients who were under 40 years old (including 40) from a single institution with surgically resected specimens. Moreover, we investigated the potential factors accounting for the early onset of lung cancer through comparing the molecular and clinicopathologic features with those of the older patients.

Materials and methods

Specimen collection

From October 2007 to November 2012, we consecutively collected lung tumor specimens resected with curative intent at Department of Thoracic Surgery in Fudan University Shanghai Cancer Center. Samples were snap-frozen in liquid nitrogen at the time of resection and stored

at -80°C until use. All cases were reviewed by pathologists for confirmation of tumor histology and tumor content. Subjects eligible in this study had to meet the following criteria: pathologically confirmed lung adenocarcinoma and sufficient tissue for comprehensive mutational analyses. This research was approved by the Institutional Review Board of Fudan University, Shanghai Cancer Center. Written informed consent was obtained from all patients.

Mutation analyses

RNA was extracted as per standard protocol after frozen tumor specimens were dissected into TRIzol (Invitrogen). Total RNA samples were reverse transcribed into single-stranded cDNA. EGFR (exons 18-22), KRAS (exons 2-3), HER2 (exons 18-21), BRAF (exons 11-15), AKT1 (exon 2), TP53 (exons 1-11) and LKB1 (exons 1-10) were amplified by reverse transcriptase polymerase chain reaction (rtPCR) using cDNA and directly sequenced. We examined the ALK and RET fusions using the rtPCR plus quantitative real-time PCR strategy, with validation using immunohistochemistry and fluorescent *in situ* hybridization (FISH) assays, which have been recently described (18,19). All PCR products were directly sequenced in forward and reverse directions. All mutations were verified by analysis of an independent PCR isolate.

Clinicopathologic variables

Clinicopathologic variables collected for analyses included gender, age at diagnosis, pathologic tumor-node-metastasis (pTNM) stage, tumor differentiation, family history, smoking status and histologic subtypes of adenocarcinoma according to the new IASLC/ATS/ERS multidisciplinary classification of lung adenocarcinoma (20). pTNM stages were evaluated in accordance with the seventh edition of the lung cancer staging classification system (21). Patients under 40 years old (including 40) were defined as the younger group and patients above 40 years old were defined as the older group.

Follow-up

The follow-up period was 4 months after surgery. The enhanced chest computed tomography (CT) scan and abdominal ultrasonography were performed every 4 months, while brain magnetic resonance imaging (MRI) and bone scanning were required every 6-8 months. If tumor

recurrence or metastasis was suspected, the pathological evaluation was conducted if possible. The follow-up methods included the outpatient clinic registration and telephone contact.

Statistical analysis

The Pearson's chi-squared test and Fisher's exact test were used to analyze the mutational status and clinicopathologic features between the two groups. Overall survival (OS) was measured from the date of operation until the date of death from lung cancer or the date last seen alive. Those who died from other causes were censored at the date of death. The survival curves of OS were estimated by the Kaplan-Meier method. Differences in survival between the two groups were assessed by the log-rank test. All the statistical analyses were conducted in the SPSS 16.0 for Windows (SPSS Inc., Chicago, IL, USA). P values were two tailed for all the tests. $P < 0.05$ was considered statistically significant.

Results

From October 2007 to November 2012, we consecutively collected a total of 2,676 resected lung cancer specimens. Corresponding clinical and pathological materials were procured as a database. According to the criteria, 36 lung adenocarcinoma cases were enrolled in the younger group. Besides, 87 adenocarcinoma cases in which patients were older than 40 years old were consecutively collected as the older group during January 2008 to June 2010.

Clinicopathologic characteristics in the younger group and comparison with the older counterparts

In the younger group, there were 15 male and 21 female patients. Seven smokers and 29 non-smokers were identified. The mean age was 34.53 ± 4.63 years old. Three patients had a family history of lung cancer and 7 patients had a family history of other malignancies. Surgical resections including 27 lobectomies, 8 wedge resections and 1 pneumonectomy were carried out for the younger patients. Final pathological results showed 3 adenocarcinomas *in situ* (AIS), 3 minimal invasive adenocarcinomas (MIA) and 30 invasive adenocarcinomas (invasive AD). And 18 IAs, 3 IBs, 1 IIA, 1 IIB, 12 IIAs and 1 IV were finally identified. When compared with these clinicopathologic characteristics in the older group, more early adenocarcinomas ($P=0.033$), more wedge resections ($P < 0.001$) and fewer smokers ($P=0.004$) were seen (Table 1).

Table 1 Clinicopathologic characteristics of subjects in the two groups

Parameters	The younger group (N=36)	The older group (N=87)	P value
Age (yr) [range]	34.53 ± 4.63 [22-40]	59.25 ± 9.20 [42-79]	0.000
Gender			0.173
Male	15	48	
Female	21	39	
Surgical resection			0.000
Lobectomy	27	86	
Wedge resection	8	1	
Pneumonectomy	1	0	
Pathological subtype			0.033
AIS*	3	1	
MIA [§]	3	2	
Invasive AD**	30	84	
Differentiation			0.171
Well	7	26	
Moderate	15	41	
Poor	14	20	
pTNM stage			0.423
IA	18	29	
IB	3	9	
IIA	1	10	
IIB	1	6	
IIIA	12	31	
IV	1	2	
Family history of cancer			0.912
Lung cancer	3	6	
Other malignancies	7	15	
None	26	66	
Smoking status			0.004
Smoker	7	41	
Non-smoker	29	46	

*, adenocarcinoma *in situ*; [§], minimal invasive adenocarcinoma;

** , invasive adenocarcinoma; AIS, adenocarcinomas *in situ*; MIA, minimal invasive adenocarcinomas; AD, adenocarcinomas.

Molecular characteristics in the younger group and comparison with those in the older group

Nineteen EGFR mutations (52.8%), 3 KRAS mutations (8.3%), 2 EML4-ALK fusions (5.6%) and 1 KIF5b-RET

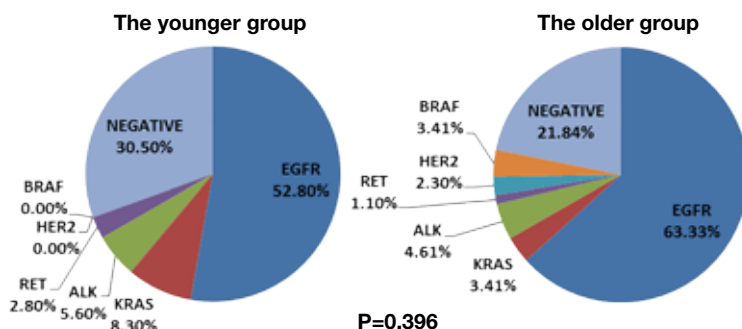


Figure 1 Oncogenic mutation analysis between the younger group and the older group.

Subcategories	The younger group (%)	The older group (%)	P value
EGFR mutations	19	55	0.133
E19	14 (73.7)	27 (49.1)	
E20	1 (5.3)	2 (3.6)	
E21	4 (21.0)	26 (47.3)	

fusion (2.8%) were identified in the younger group, while 55 EGFR mutations (63.2%), 3 KRAS mutations (3.4%), 4 EML4-ALK fusion (4.6%), 1 CCDC6-RET fusion (1.1%), 2 HER2 mutation (2.3%) and 3 BRAF mutations (3.4%) were found in the older group. The difference of oncogenic mutations between the two groups was statistically insignificant ($P=0.396$) (Figure 1). Among the 19 EGFR mutations in the younger group, there were 14 exon 19 deletions, 1 exon 20 insertions and 4 exon 21 missense mutations. The difference of EGFR mutation between the two groups was also insignificant ($P=0.133$) (Table 2).

In addition, we evaluated mutations in tumor suppressor genes between the two groups. We found 26 TP53 mutations (72.2%) and 4 LKB1 mutations (11.1%) in young patients. When compared with these old patients, young patients showed a higher prevalence of TP53 mutations ($P<0.001$) and a comparable prevalence of LKB1 mutations ($P=0.951$) (Figures 2 and 3).

OS between the two groups

In the younger group, the median follow-up time was 14.15 ± 11.77 months (range, 1-48.2 months), and the mean survival time was 40.39 ± 3.94 months (95% CI: 32.66-48.11).

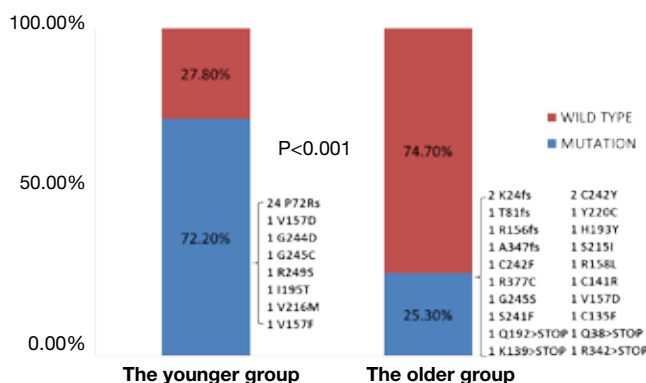


Figure 2 Mutational analysis of TP53 gene between the younger group and the older group.

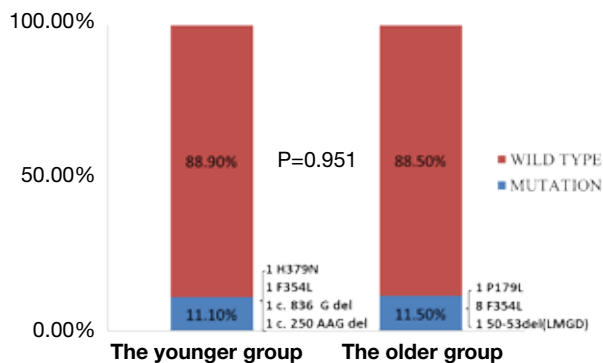


Figure 3 Mutational analysis of LKB1 gene between the younger group and the older group.

In the older group, the median follow-up time was 31.20 ± 1.21 months (range, 0.60-56.50 months), and the mean survival time was 45.57 ± 2.44 months (95% CI: 40.79-50.35). There was no difference in the OS time between the two groups ($P=0.942$) (Figure 4).

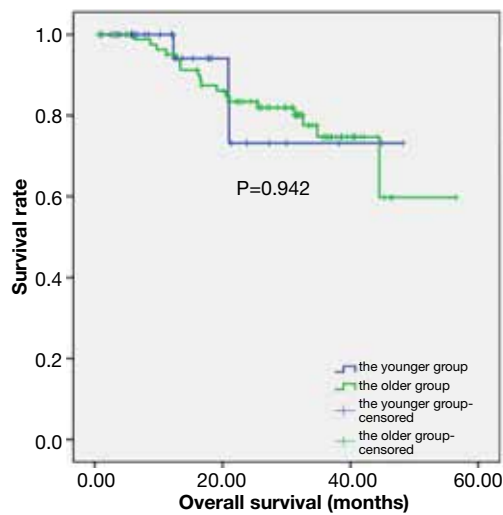


Figure 4 Comparison of the overall survival (OS) between the younger group and the older group.

Discussion

Lung cancer in young patients always attracts more attentions from the public because lung cancer is still the leading cause of cancer-related deaths worldwide (1) and young people are the backbone of the society. Though lung cancer usually affects patients in their 60s and 70s (4), age at diagnosis of lung cancer patients is keeping decreasing these years. Many studies have suggested that lung cancer in the young had its distinct clinicopathologic characteristics with different gender distribution, stage at diagnosis, pathological features and prognosis (4,5). However, the reported data are frequently discordant (6,7). Moreover, the molecular pathologic features of the youthful lung cancer have not been well investigated till now (22,23). In this study, we found that the youthful lung cancer had more early adenocarcinomas and fewer smoker patients (*Table 1*). And younger patients possessed the similar profiles of major oncogenic mutations in comparison with the older patients (*Figure 1*). Moreover, younger patients had a higher prevalence of TP53 mutations (72.2%) and a comparable prevalence of LKB1 mutations (11.1%) (*Figures 2 and 3*).

In the younger group, clinicopathologic features including gender distribution, differentiation of cancer cells, pTNM staging and family history of cancer were comparable with those in the older group, except that more AIS and MIA were seen and thus more wedge resections were performed, which were different from previous reports that younger patients always presented the more advanced stage at diagnosis (3,4,6,7). The discrepancies

could be possibly explained that all patients in this study were candidates for surgical resections, and patients with advanced stage were not included. Moreover, the squamous cell carcinoma, which is always associated with tobacco use, was not enrolled because the prevalence of squamous cell carcinoma is low in the young and its molecular characteristics are still unclear.

Regarding the oncogenic characteristics, EGFR mutations were both predominant in the two groups (52.8% and 63.2%, respectively), followed by KRAS mutations, ALK and RET fusions. As a result, most young patients could benefit from the targeted therapies if indicated. On the other hand, in regard to mutations in tumor suppressor genes, the prevalence of TP53 mutations was 72.2% in the young patients, which is much higher than the rate in the older group. And it was also higher than the previous reports (24,25). Particularly, among the 26 TP53 point mutations, there were 24 P72R polymorphisms. And 5 P72Rs respectively coexisted with the missense mutations in TP53 (1 G244D, 1 G245C, 1 V157F, 1 I195T and 1 V216M, respectively). The P72R polymorphism has been associated with earlier age at first diagnosis of cancer, especially in germline TP53 mutation carriers, partly due to its modifier effect (15,26). Additionally, it has been suggested that familial susceptibility and Mendelian inheritance may produce the early onset of lung cancer (27-29). In this case, it may explain the early onset of the lung cancer in young patients. However, this needs further evaluations. Moreover, two deletions (c.836 G del; c.250 AAG del) and two point mutations (H379N; F354L) were found in LKB1 mutations. The prevalence of LKB1 mutations was comparable between the two groups, which indicated that LKB1 mutations were not particularly common in the youthful lung cancer.

Currently, there is no consensus about the specific cutoff age defining the youthful lung cancer, which could be resulted from different results on clinicopathologic patterns and prognosis of previously reported studies. Forty, forty-five and fifty are the three most common ages which are used to separate the young patients from the old ones (4-8). In this analysis, we selected patients who were under 40 years old (including 40) as the younger group. This age cut-off seems to be more reasonable, since the median age of patients with newly diagnosed NSCLC at presentation is 71 years (4). Surely, this issue is open to question.

OS time in the younger group was similar to that in the older group, although several studies suggested that younger patients with lung cancer had a better outcome than their

older counterparts (4,6,7). In this study, all patients were candidates for surgical resection and the distribution of the pathological TNM stages was comparable between the two groups. Accordingly, younger patients with lung cancer could achieve a better prognosis if early detected and properly treated.

There were only two studies evaluating the molecular characteristics of lung adenocarcinoma in young patients aged 40 or younger before (22,23). In 2012, Nagashima and his colleagues analyzed EGFR, KRAS mutations and EML4-ALK fusion in twelve patients. They used direct sequencing for detecting EGFR mutation and performed FISH assay for detection of EML4-ALK fusion, however, their sample size was too small (22). Moreover, Kim and his colleagues also investigated EGFR mutation and ALK positivity in 31 young patients and 261 older patients with age >50 years last year. They did not find a statistical difference of the rate of EGFR mutation and ALK positivity between the two groups. However, they used the immunohistochemistry (IHC) assay for detection of EGFR mutation and ALK rearrangement in some small biopsy samples, which made their results less powerful (23). Furthermore, neither of them detected mutations in tumor suppressor genes. In this study, we firstly applied the standard methods for mutational detection in the surgically resected specimens and did the comprehensive analysis not only for major known oncogenic mutations, but also for mutations in tumor suppressor genes. We found a high prevalence of TP53 mutations and a comparable frequency of LKB1 mutations.

Though this study highlighted some impressive findings, several limitations in this study were worth noting. First, the sample size in this study was not enough big. If more young patients were available, our results would be more attractive. Moreover, patients with advanced disease were not enrolled since they could not provide enough tissues for comprehensive mutation evaluations. Thus the selection bias might influence our results. Furthermore, if the follow-up period was enough long, the survival analysis would be more powerful. However, most would agree that this study has really provided a brand new idea for the molecular and clinicopathologic features in the youthful lung cancer.

Conclusions

In conclusion, the youthful lung cancer unequivocally presented the distinct clinicopathologic characteristics including more early adenocarcinomas and fewer smoker

patients. It showed the similar oncogenic characteristics compared with the older counterpart. Additionally, the prevalence of TP53 mutations was higher in the young patients, which may provide some insights on further investigations in the youthful lung cancer.

Acknowledgements

Funding: Project supported by Hospital Fund of Shanghai Cancer Center, Fudan University (Grant No. YJ201207) and the National Science Foundation for Young Scholars of China (Grant No.81302008).

Disclosure: The authors declare no conflict of interest.

References

1. Siegel R, Naishadham D, Jemal A. Cancer statistics, 2013. *CA Cancer J Clin* 2013;63:11-30.
2. Levi F, Bosetti C, Fernandez E, et al. Trends in lung cancer among young European women: the rising epidemic in France and Spain. *Int J Cancer* 2007;121:462-5.
3. Green LS, Fortoul TI, Ponciano G, et al. Bronchogenic cancer in patients under 40 years old. The experience of a Latin American country. *Chest* 1993;104:1477-81.
4. Subramanian J, Morgensztern D, Goodgame B, et al. Distinctive characteristics of non-small cell lung cancer (NSCLC) in the young: a surveillance, epidemiology, and end results (SEER) analysis. *J Thorac Oncol* 2010;5:23-8.
5. Antkowiak JG, Regal AM, Takita H. Bronchogenic carcinoma in patients under age 40. *Ann Thorac Surg* 1989;47:391-3.
6. Radzikowska E, Roszkowski K, Głaz P. Lung cancer in patients under 50 years old. *Lung Cancer* 2001;33:203-11.
7. Ramalingam S, Pawlish K, Gadgeel S, et al. Lung cancer in young patients: analysis of a Surveillance, Epidemiology, and End Results database. *J Clin Oncol* 1998;16:651-7.
8. Sekine I, Nishiwaki Y, Yokose T, et al. Young lung cancer patients in Japan: different characteristics between the sexes. *Ann Thorac Surg* 1999;67:1451-5.
9. Heist RS, Engelman JA. SnapShot: non-small cell lung cancer. *Cancer Cell* 2012;21:448.e2.
10. Cufer T, Ovaricek T, O'Brien ME. Systemic therapy of advanced non-small cell lung cancer: major-developments of the last 5-years. *Eur J Cancer* 2013;49:1216-25.
11. Kobayashi K, Hagiwara K. Epidermal growth factor receptor (EGFR) mutation and personalized therapy in advanced nonsmall cell lung cancer (NSCLC). *Target Oncol* 2013;8:27-33.

12. Soda M, Choi YL, Enomoto M, et al. Identification of the transforming EML4-ALK fusion gene in non-small-cell lung cancer. *Nature* 2007;448:561-6.
13. Goldman JW, Garon EB. Targeting MEK for the treatment of non-small-cell lung cancer. *J Thorac Oncol* 2012;7:S377-8.
14. Guo Y, Du J, Kwiatkowski DJ. Molecular dissection of AKT activation in lung cancer cell lines. *Mol Cancer Res* 2013;11:282-93.
15. Olivier M, Hollstein M, Hainaut P. TP53 mutations in human cancers: origins, consequences, and clinical use. *Cold Spring Harb Perspect Biol* 2010;2:a001008.
16. Ji H, Ramsey MR, Hayes DN, et al. LKB1 modulates lung cancer differentiation and metastasis. *Nature* 2007;448:807-10.
17. Gao Y, Xiao Q, Ma H, et al. LKB1 inhibits lung cancer progression through lysyl oxidase and extracellular matrix remodeling. *Proc Natl Acad Sci U S A* 2010;107:18892-7.
18. Wang R, Pan Y, Li C, et al. The use of quantitative real-time reverse transcriptase PCR for 5' and 3' portions of ALK transcripts to detect ALK rearrangements in lung cancers. *Clin Cancer Res* 2012;18:4725-32.
19. Wang R, Hu H, Pan Y, et al. RET fusions define a unique molecular and clinicopathologic subtype of non-small-cell lung cancer. *J Clin Oncol* 2012;30:4352-9.
20. Travis WD, Brambilla E, Noguchi M, et al. International association for the study of lung cancer/american thoracic society/european respiratory society international multidisciplinary classification of lung adenocarcinoma. *J Thorac Oncol* 2011;6:244-85.
21. Detterbeck FC, Boffa DJ, Tanoue LT. The new lung cancer staging system. *Chest* 2009;136:260-71.
22. Nagashima O, Ohashi R, Yoshioka Y, et al. High prevalence of gene abnormalities in young patients with lung cancer. *J Thorac Dis* 2013;5:27-30.
23. Kim L, Kim KH, Yoon YH, et al. Clinicopathologic and molecular characteristics of lung adenocarcinoma arising in young patients. *J Korean Med Sci* 2012;27:1027-36.
24. Skaug V, Ryberg D, Kure EH, et al. p53 mutations in defined structural and functional domains are related to poor clinical outcome in non-small cell lung cancer patients. *Clin Cancer Res* 2000;6:1031-7.
25. Ahrendt SA, Chow JT, Yang SC, et al. Alcohol consumption and cigarette smoking increase the frequency of p53 mutations in non-small cell lung cancer. *Cancer Res* 2000;60:3155-9.
26. Bougeard G, Baert-Desurmont S, Tournier I, et al. Impact of the MDM2 SNP309 and p53 Arg72Pro polymorphism on age of tumour onset in Li-Fraumeni syndrome. *J Med Genet* 2006;43:531-3.
27. Sellers TA, Bailey-Wilson JE, Elston RC, et al. Evidence for mendelian inheritance in the pathogenesis of lung cancer. *J Natl Cancer Inst* 1990;82:1272-9.
28. Coté ML, Kardia SL, Wenzlaff AS, et al. Risk of lung cancer among white and black relatives of individuals with early-onset lung cancer. *JAMA* 2005;293:3036-42.
29. Kharazmi E, Fallah M, Sundquist K, et al. Familial risk of early and late onset cancer: nationwide prospective cohort study. *BMJ* 2012;345:e8076.

Cite this article as: Ye T, Pan Y, Wang R, Hu H, Zhang Y, Li H, Wang L, Sun Y, Chen H. Analysis of the molecular and clinicopathologic features of surgically resected lung adenocarcinoma in patients under 40 years old. *J Thorac Dis* 2014;6(10):1396-1402. doi: 10.3978/j.issn.2072-1439.2014.08.50

Differences in distribution and drug sensitivity of pathogens in lower respiratory tract infections between general wards and RICU

Ruoxi He, Bailing Luo, Chengping Hu, Ying Li, Ruichao Niu

Department of Respiratory Medicine, Xiangya Hospital, Central South University, Changsha 410008, China

Correspondence to: Ruichao Niu, MD. Department of Respiratory Medicine, Xiangya Hospital, Central South University, 87th Xiangya Road, Changsha 410008, China. Email: nrc226@163.com.

Background: Lower respiratory tract infections (LRTIs) are common among patients in hospitals worldwide, especially in patients over the age of 60. This study investigates the differences in distribution and drug sensitivity of pathogens in LRTIs.

Methods: The clinical and laboratory data of 4,762 LRTI patients in the general ward and respiratory intensive care unit (RICU) of Xiangya Hospital (Changsha) were retrospectively analyzed.

Results: The infection rate of Gram-negative bacteria was significantly higher than that of Gram-positive bacteria in both the general ward and RICU ($P < 0.05$). The incidence of Gram-negative bacteria infection was significantly higher in the RICU than in the general ward ($P < 0.05$), whereas the incidence of Gram-positive bacteria infection is less in the RICU than in the general ward ($P < 0.05$). In the general ward, the incidence of Gram-negative bacteria infection significantly increased ($P < 0.05$) over time, whereas the incidence of Gram-positive bacteria infection significantly decreased from 1996 to 2011 ($P < 0.05$). In the RICU, the incidence of Gram-positive bacteria infection decreased, while Gram-negative bacteria infections increased without statistical significance ($P > 0.05$). *Staphylococcus pneumoniae* and *Staphylococcus aureus* were found to be the predominant Gram-positive strains in the general ward (34.70-41.18%) and RICU (41.66-54.87%), respectively ($P > 0.05$). *Pseudomonas aeruginosa* and *Acinetobacter baumannii* were the predominant gram negative strains in the general ward (19.17-21.09%) and RICU (29.60-33.88%), respectively ($P > 0.05$). *Streptococcus pneumoniae* is sensitive to most antibiotics with a sensitivity of more than 70%. *Staphylococcus aureus* is highly sensitive to vancomycin (100%), linezolid (100%), chloramphenicol (74.36-82.19%), doxycycline (69.57-77.33%), and sulfamethoprim (67.83-72.46%); however, its sensitivity to other antibiotics is low and decreased each year. Sensitivity of *Pseudomonas aeruginosa* to most β -lactam, aminoglycoside, and quinolone group antibiotics decreased each year.

Conclusions: The distribution and drug sensitivity of LRTI pathogens exhibit a high divergence between the general ward and RICU. *Streptococcus pneumoniae* may not be the predominant pathogen in LRTIs in some areas of China.

Keywords: Drug sensitivity; lower respiratory tract infections (LRTIs); respiratory intensive care unit (RICU); general ward; antibiotics

Submitted Jun 11, 2014. Accepted for publication Aug 18, 2014.

doi: 10.3978/j.issn.2072-1439.2014.09.22

View this article at: <http://dx.doi.org/10.3978/j.issn.2072-1439.2014.09.22>

Introduction

Lower respiratory tract infections (LRTIs) are common among patients in hospitals worldwide. LRTIs are associated with high overall mortality and account for 3% to 5% of deaths in adults, especially in patients over the age of 60 (1).

Pneumonia is also the leading cause of death in children less than 5 years old (2). LRTIs are also the main cause of death in infants from infectious disease in America (3). LRTIs are classified as either community or hospital acquired. Hospital-acquired pneumonia (HAP) has an attributable

mortality rate of about 33% to 50% (4). LRTIs are usually treated with antibiotics, and management of LRTIs is made difficult by antibiotic resistance.

At present, therapy for community-acquired LRTIs is often empirical. Inappropriate antibiotics therapy, overuse of antibiotics, and misuse of antibiotics often occur, which may predispose patients to increased resistance to a class of antibiotics and may increase hospital mortality rate for patients in respiratory intensive care unit (RICUs) (5,6). Additionally, bacteria are constantly evolving and developing antibiotic-resistance. Therefore, effective selection and administration of antibiotics become a new challenge to clinicians. The knowledge of likely prevalent strains along with their resistance patterns will improve the management of LRTI patients. In China, over-the-counter antibiotics can be obtained easily. This antibiotic policy may increase the chance of bacteria developing drug resistance. Thus, a systemic investigation of the changes in various bacterial strains and their resistance to antibiotics in LRTI patients over a long period of time will benefit disease management.

Hospitalized LRTI patients are placed in the respiratory general ward or the RICU depending on their condition. However, a study comparing the bacterial strains and their resistance to antibiotics in general wards and RICUs is currently unavailable. In this study, we analyzed bacterial strains isolated from the sputum or endotracheal aspiration samples from patients hospitalized in the general ward and RICU from January, 1996 to December, 2011 and further analyzed the antibiotic resistance of predominant strains of bacteria.

Methodology

Subjects

A total of 4,762 positive sputum or endotracheal aspiration samples collected from hospitalized patients who were diagnosed with LRTI at the Department of Pneumology, Xiangya Hospital, Central South University (Changsha) from January 1996 to December 2011 are included in this study. The diagnoses were based on the diagnostic criteria of community-acquired pneumonia (CAP) and HAP, established by the third national pulmonary infection and ILD conference in 1998 (7).

Sputum collection

The second sputum in the morning of the second day after

admission was carefully collected into a sterile container by forcing a deep cough after brushing teeth, rinsing the mouth twice using sterile water, and discarding the first sputum. The sputum was collected for 3 continuous days and sent for bacterial culture within 2 hours of collection. In order to reduce the chance of contamination with resident flora in the oral cavity and nasopharynx, samples were excluded from this study if the sample had more than 10 squamous epithelial cells and less than 25 polymorphonuclear leukocytes or their ratio is higher than 1:2.5 under low magnification microscope in smear examination. The bronchial secretions obtained by bronchofibroscope endotracheal aspiration or a protected specimen brush were sent for bacterial culture within 10 minutes.

Pathogen diagnosis and drug-susceptibility test

Samples were inoculated on blood agar plate using the streak plate technique and incubated for 24-48 hours at 37 °C. The pathogen was identified as the following: (I) the predominant bacterium in three morning sputum cultures was the same; (II) the concentration of pathogen from bronchofibroscope endotracheal aspiration and protected brush sample was no less than 10⁵ CFU/mL (half quantitative); and (III) the pathogens were confirmed by a standard method routinely used in the clinical laboratory. All isolated bacterial strains were tested for drug susceptibility using the Kirby-Bauer method. The double-disc synergy method was used for drug susceptibility assay of extended-spectrum β -lactamases (ESBLs). Results were interpreted according to National Committee for Clinical Laboratory Standards (NCCLS) breakpoints.

Statistic analysis

Data were presented as percentages. All data were statistically analyzed using SPSS 13.0. χ^2 test or Fisher test was used to compare differences between groups. A P<0.05 was considered statistically significant.

Results

Distribution and changes in pathogen

From January 1996 to December 2011, 4,762 positive bacterial strains were isolated, of which 2,685 strains were isolated from the general ward and 2,077 strains from RICU. We divided these 16 years into four periods for analysis: 1996-1999, 2000-2003, 2004-2007 and 2008-2011.

Table 1 Distribution of 4,762 bacteria isolated from 1996 to 2011

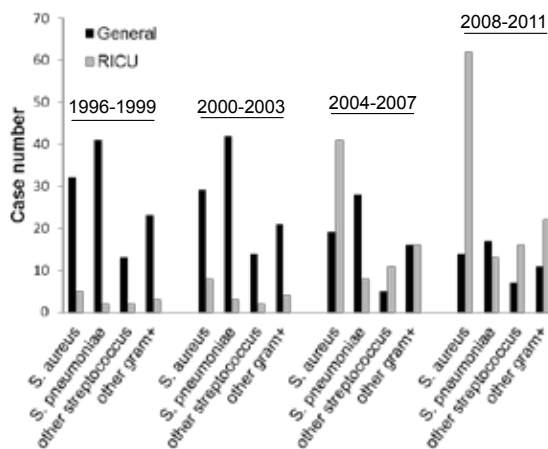
Strain	1996-1999		2000-2003		2004-2007		2008-2011	
	Quantity	Percentage (%)						
G ⁺ bacteria	121	15.14	123	13.73	144	11.33	162	9.02
G ⁻ bacteria	678	84.86	773	86.27	1,127	88.67	1,634	90.98
Total	799	100.00	896	100.00	1,271	100.00	1,796	100.00

Table 2 Distribution of bacteria isolated from general wards from 1996 to 2011

Strain	1996-1999		2000-2003		2004-2007		2008-2011	
	Quantity	Percentage (%)						
G ⁺ bacteria	109	16.47	106	14.87	68	12.62	49	6.36
G ⁻ bacteria	553	83.53	607	85.13	471	87.38	722	93.64
Total	662	100.00	713	100.00	539	100.00	771	100.00

Table 3 Distribution of bacteria isolated from respiratory intensive care unit (RICU) from 1996.01 to 2011.12

Strain	1996-1999		2000-2003		2004-2007		2008-2011	
	Quantity	Percentage (%)						
G ⁺ bacteria	12	8.76	17	9.29	76	10.38	113	11.02
G ⁻ bacteria	125	91.24	166	90.71	656	89.62	912	88.98
Total	137	100.00	183	100.00	732	100.00	1,025	100.00

**Figure 1** Distribution of specific Gram-positive bacteria in general wards and respiratory intensive care unit (RICU) from 1996 to 2011.

Distribution and changes in Gram-positive bacteria

During the four periods, the incidence of Gram-positive bacteria infection is lower than Gram-negative bacteria infection ($P < 0.05$). The combined proportion of gram positive bacteria isolated from patients in the general ward

and RICU decreased ($P < 0.05$) (Table 1). The proportion of gram positive bacteria decreased in the general ward ($P < 0.05$) (Table 2). In contrast, the proportion of gram positive bacteria increased in the RICU (8.76%, 9.29%, 10.38%, and 11.02%) without statistical significance ($P > 0.05$) (Table 3). Among these isolated gram positive bacteria, *Streptococcus pneumoniae* is the most common bacterial strain in patients in the general ward throughout the four periods, while the second most common bacterial strain is *Staphylococcus aureus* ($P > 0.05$) (Figure 1). In the RICU, *S. aureus* is the most common gram positive bacterium isolated from patients throughout those four periods with a tendency of increase each period ($P > 0.05$) (Figure 1).

Distribution and changes in Gram-negative bacteria during the four periods

During the four periods, Gram-negative bacteria remained the major pathogen of hospital-acquired LRTIs ($P < 0.05$). The combined proportion of gram negative bacteria isolated from patients in both the general ward and RICU increased ($P < 0.05$) (Table 1). The proportion of gram negative bacteria increased in the general ward ($P < 0.05$)

Table 4 Distribution of specific Gram-negative bacteria in general wards from 1996 to 2011

Strain	1996-1999		2000-2003		2004-2007		2008-2011	
	Quantity	Percentage (%)						
<i>Pseudomonas aeruginosa</i>	106	19.17	128	21.09	95	20.17	148	20.50
<i>Acinetobacter baumannii</i>	99	17.90	115	18.95	81	17.19	116	16.07
<i>Klebsiella pneumoniae</i>	83	15.01	85	14.00	76	16.14	82	11.36
<i>Haemophilus parainfluenzae</i>	89	16.09	104	17.13	85	18.05	122	16.89
<i>Eschericia coli</i>	56	10.13	55	9.06	49	10.40	58	8.03
<i>Haemophilus influenzae</i>	61	11.03	59	9.72	48	10.19	69	9.56
Other Gram-negative bacteria	59	10.67	61	10.05	37	7.86	127	17.59
Total	553	100.00	607	100.00	471	100.00	722	100.00

Table 5 Distribution of specific Gram-negative bacteria in RICU from 1996 to 2011

Strain	1996-1999		2000-2003		2004-2007		2008-2011	
	Quantity	Percentage (%)						
<i>Pseudomonas aeruginosa</i>	31	24.80	47	28.31	171	26.07	230	25.22
<i>Acinetobacter baumannii</i>	37	29.60	51	30.72	211	32.16	309	33.88
<i>Klebsiella pneumoniae</i>	12	9.60	19	11.45	66	10.06	67	7.35
<i>Haemophilus parainfluenzae</i>	7	5.60	10	6.02	26	3.96	39	4.27
<i>Eschericia coli</i>	11	8.80	19	11.45	54	8.23	67	7.35
<i>Haemophilus influenzae</i>	4	3.20	5	3.01	13	1.98	17	1.86
Other Gram-negative bacteria	23	18.40	15	9.04	115	17.54	183	20.07
Total	125	100.00	166	100.00	656	100.00	912	100.00

(Table 2), but decreased in the RICU without statistical significance ($P>0.05$) (Table 3). In the general ward, *Pseudomonas aeruginosa* was the most common pathogen throughout the four periods. *Acinetobacter baumannii* was the second most common bacterium, followed by *Haemophilus parainfluenzae*, *Klebsiella pneumoniae*, *Haemophilus influenzae*, and *Escherichia coli* ($P<0.05$) (Table 4). In the RICU, *Acinetobacter baumannii* is the most common bacterium isolated from patients throughout those four periods with a

tendency of increase each period, followed by *P. aeruginosa*, *K. pneumoniae*, *E. coli*, *H. parainfluenzae*, and *H. influenzae* ($P>0.05$) (Table 5).

Comparison of pathogens involved in LRTIs between the general ward and RICU

Gram-negative bacteria are the main pathogens of LRTI in both the RICU and general ward, while the total infection

Table 6 Changes in drug-susceptibility of major Gram-positive bacteria to routine antibacterials (%)

Antibacterials	Staphylococcus aureus				Streptococcus pneumoniae			
	1996-1999	2000-2003	2004-2007	2008-2011	1996-1999	2000-2003	2004-2007	2008-2011
Meropenem	48.14	43.05	36.79	19.38	85.82	90.69	83.26	84.42
Imipenem	72.35	65.67	41.18	23.31	96.03	84.22	89.65	87.14
Cefepime	67.27	58.41	33.84	17.95	84.36	79.28	81.99	81.47
Cefoperazone/sulbactam	69.43	54.34	38.27	20.75	81.62	85.78	80.30	81.04
Ceftazidime	52.29	41.07	29.55	18.41	73.52	82.63	76.97	78.80
Ceftriaxone	56.47	37.36	26.54	11.44	79.22	73.58	81.79	76.54
Cefotaxime	44.02	32.45	15.73	9.98	80.33	79.05	75.29	74.37
Cephazolin	–	–	–	–	69.04	83.22	74.32	77.14
Piperacillin/tazobactam	34.15	35.26	21.39	12.72	82.66	68.35	76.47	73.81
Ampicillin/sulbactam	–	–	–	–	66.28	70.15	69.61	71.13
Mezolicillin	–	–	–	–	64.72	68.51	73.19	75.34
Levofloxacin	52.37	43.21	34.55	21.62	77.06	81.14	78.23	80.11
Chloramphenicol	74.36	82.19	75.34	79.01	87.64	80.77	84.41	83.25
Vancomycin	100.00	100.00	100.00	100.00	100.00	100.00	100.00	100.00
Linezolid	–	–	–	100.00	–	–	–	100.00
Doxycycline	69.57	77.33	74.61	73.53	84.22	88.16	91.35	89.23
Sulfamethoprim	72.46	67.83	70.92	68.45	79.52	75.61	80.44	76.37

–, means no report of this bacterium.

rate was higher in the RICU than in the general ward ($P < 0.05$). The total incidence of Gram-positive bacteria infection was higher in the RICU than in the general ward during the periods of 1996-1999 and 2000-2003 ($P < 0.05$), but there were no significant differences during the period of 2004-2007 ($P > 0.05$). The incidence of Gram-negative bacteria infection was higher in the general ward than in RICU during the period of 2008-2011 ($P < 0.05$). Infections of four major kinds of Gram-positive bacteria exhibited significant differences between the two wards ($P < 0.05$). However, there were no significant differences during the periods of 1996-1999 and 2000-2003 ($P > 0.05$). Incidences of seven main types of Gram-negative bacteria infection were significantly different between the RICU and general ward in four periods ($P < 0.05$).

Drug-susceptibility of major LRTI pathogens to routine antibiotics

Among the gram positive bacteria, *S. pneumoniae* was sensitive to most antibiotics with a sensitivity of more than 70%. As the predominant bacterium in the RICU, *S. aureus* is highly sensitive ($>70\%$) to vancomycin, linezolid,

chloramphenicol, doxycycline, and sulfamethoprim without a tendency of decrease in its antibiotic sensitivity during these 16 years. However, its sensitivity to other antibiotics, such as meropenem, imipenem, cefepime, ceftazidime, ceftriaxone, cefotaxime, piperacillin/tazobactam and levofloxacin was relative low ($<25\%$) and decreased yearly (Table 6).

Among the gram negative bacteria, *P. aeruginosa* and *A. baumannii* had a high infection rate in both the general ward and RICU. *P. aeruginosa* remained highly sensitive to meropenem, ceftazidime, ceftriaxone, cefotaxime, piperacillin/tazobactam, amikacin, moderately sensitive to imipenem, cefepime, levofloxacin, ciprofloxacin, and mildly sensitive ($<30\%$) to other antibacterials. However, its sensitivity decreased progressively (Table 7).

A. baumannii was highly sensitive to amikacin and levofloxacin without a tendency of decrease, but its sensitivity to meropenem, imipenem, cefepime, ceftazidime, ceftriaxone, cefotaxime, piperacillin/tazobactam and ampicillin/sulbactam decreased (Table 7). *S. aureus* was highly sensitive to routinely used antibiotics in this hospital. Therefore, its drug-susceptibility was not analyzed.

Table 7 Changes in drug-susceptibility of major Gram-negative bacteria to routine antibacterials (%)

Antibacterials	Pseudomonas aeruginosa				Acinetobacter baumannii			
	1996-1999	2000-2003	2004-2007	2008-2011	1996-1999	2000-2003	2004-2007	2008-2011
Meropenem	95.16	94.24	93.05	86.36	87.44	88.21	77.35	68.42
Imipenem	88.37	83.41	72.55	64.70	84.29	76.40	65.22	41.38
Cefepime	69.25	63.47	59.32	56.61	75.30	66.57	48.65	34.54
Cefoperazone/sulbactam	87.22	87.16	84.43	84.27	96.13	96.06	92.24	51.41
Ceftazidime	76.55	73.46	74.62	54.28	68.30	80.53	71.35	43.65
Ceftriaxone	60.02	51.66	45.87	26.91	77.15	83.26	71.54	37.49
Cefotaxime	42.23	41.08	40.72	23.61	85.35	87.32	70.67	31.51
Piperacillin/tazobactam	–	–	69.08	32.46	–	–	76.30	44.23
Ampicillin/sulbactam	73.14	37.26	34.72	21.63	92.07	93.11	86.35	38.29
Mezolicillin	–	–	32.56	18.69	–	–	40.64	19.87
Aztreonam	76.25	68.19	67.33	34.35	46.23	48.60	51.45	27.94
Levofloxacin	74.66	60.84	53.76	57.29	68.55	82.30	73.51	77.02
Ciprofloxacin	83.11	51.63	64.32	44.05	76.20	34.74	48.33	–
Amikacin	93.03	90.21	79.18	79.04	87.11	88.06	77.41	83.58
Tobramycin	–	–	–	11.95	–	–	–	15.73
Gentamicin	–	–	–	21.84	–	–	–	22.77

–, means no report of this bacterium.

Discussion

LRTI is a major disease in China, affecting 12% to 16% of hospitalized patients (8). Studies on the distribution and drug sensitivity of LRTI pathogens have been conducted in some areas of China with variable observation periods. However, there is still a lack of a longer period of observation in LRTI patients in southern China, and a comparative analysis between general wards and RICU has not been performed previously. This study analyzed the distribution and drug sensitivity of bacterial strains isolated from 2,685 patients in the general ward and 2,077 patients in the RICU for 16 years. We found that the proportion of gram positive bacteria decreased in the general ward, but increased in the RICU yearly. In contrast, the proportion of gram negative bacteria in the general ward increased, but decreased in the RICU yearly. *S. pneumoniae* was the predominant gram positive bacterium, while *P. aeruginosa* was the predominant gram negative bacterium in the general ward. *S. aureus* was the predominant gram positive bacterium, while *A. baumannii* was the predominant gram negative bacterium in the RICU. Among the gram positive bacteria, *S. pneumoniae* and *S. aureus* were sensitive to most antibiotics though resistance was widely observed. Among the gram negative bacteria, *P. aeruginosa* remained highly to moderately sensitive to most

antibiotics, but its sensitivity decreased progressively. Our findings will benefit disease management in this area and help reform the antibiotic policy worldwide.

S. pneumoniae remains the primary cause of severe CAP and a leading cause of death worldwide. It accounts for two-thirds of bacteremic pneumonias (9) and is the most common cause of pneumonia leading to hospitalization in all age groups (10). In this study, we found that *S. pneumoniae* was the predominant gram positive bacteria and accounts for 34.7-39.6% of bacteria in the general ward and 10.5-17.6% of bacteria in the RICU. However, gram positive bacteria account for a smaller proportion of LRTI bacteria with a decreasing tendency during the investigated 16 years (15% to 9%). In contrast, gram negative bacteria account for a bigger proportion of LRTI bacteria with an increasing tendency during the 16 years when the pathogen distribution was analyzed in hospitalized LRTI patients as a whole (85% to 91%). However, this tendency is not consistent with previous investigations in other areas of China (11,12). Notably, *S. pneumoniae* was sensitive to most antibiotics with a sensitivity of more than 70%. Thus, *S. pneumoniae* is not the major cause of LRTI at this particular hospital.

A novel finding in this study is the difference in distribution between patients in the general ward and RICU.

In the general ward, *S. pneumoniae* was the predominant gram positive bacteria, followed by *S. aureus*, and their combined infection rate was more than 66%. However, infection rates of these bacteria did not change over 16 years. In the RICU, *S. aureus* was the predominant gram positive bacterium with an infection rate of about 50%. However, the infection rate increased during each period. This might be associated with an increase in invasive operations performed in the RICU. As for the infection rate of gram negative bacteria, *P. aeruginosa* was the predominant gram negative bacterium in the general ward with no change in infection rate over 16 years. In the RICU, *A. baumannii* was the predominant bacterium, but the infection rate increased during each period. The difference in distribution of pathogens between the general ward and RICU provides valuable insight for the use of antibiotics in treating patients with LRTIs.

The most common treatment of LRTIs is antibiotics, which have varying adverse effects and effectiveness (13). Our study demonstrated that *S. pneumoniae* was sensitive to most antibiotics without a tendency to decrease in sensitivity, while *S. aureus* was highly sensitive to vancomycin, linezolid, chloramphenicol, doxycycline and sulfamethoprim. However, the sensitivity of *S. aureus* to other antibacterials especially β -lactam antibiotics is low and decreased during each period. This phenomenon may be caused by overuse of broad-spectrum antibiotics. Fortunately, no vancomycin and linezolid resistant strains of *S. aureus* were found until now. Consistent with previous findings in *P. Aeruginosa* (14-16), this strain can easily develop drug resistance. The drug sensitivity of *P. aeruginosa* to most β -lactam, aminoglycoside and quinolone antibacterials decreased. The sensitivity of *A. baumannii* is similar to that of *P. aeruginosa*, showing decreased sensitivity to most β -lactam antibacterials. Since the *A. baumannii* infection rate is increasing, especially in the RICU, there is an urgent need to switch to other kinds of antibiotics. The differences mentioned above indicate that routine antibiotic treatment can achieve satisfactory curative effect on gram positive bacteria in general wards, but poor curative effect in the RICU. In the RICU, vancomycin, linezolid, chloramphenicol, doxycycline and sulfamethoprim should be used as soon as possible to prevent patient conditions from worsening due to bacteria developing resistance to currently administered antibiotics.

Conclusions

In conclusion, the distribution and drug sensitivity of

LRTI pathogens exhibit a characteristic of high divergence between different areas in China and even between the general ward and RICU of the same hospital. The guideline for antibiotic use should match the local pathogen distribution and drug sensitivity. *S. pneumoniae* may not be the major cause of LRTIs in other areas. Moreover, overuse of broad-spectrum antibiotics should be avoided.

Acknowledgements

Ethics: The study was approved by the Review Board of Central South University. Data do not identify subjects.

Funding: This work was supported by the National Key Scientific & Technology Support Program: collaborative innovation of Clinical Research for chronic obstructive pulmonary disease and lung cancer (No. 2013BAI09B09).

Disclosure: The authors declare no conflict of interest.

References

1. Xia W, Chen Y, Mei Y, et al. Changing trend of antimicrobial resistance among pathogens isolated from lower respiratory tract at a university-affiliated hospital of China, 2006-2010. *J Thorac Dis* 2012;4:284-91.
2. Kabra SK, Lodha R, Pandey RM. Antibiotics for community-acquired pneumonia in children. *Cochrane Database Syst Rev* 2010;(3):CD004874.
3. Singleton RJ, Wirsing EA, Haberling DL, et al. Risk factors for lower respiratory tract infection death among infants in the United States, 1999-2004. *Pediatrics* 2009;124:e768-76.
4. Grossman RF, Rotschafer JC, Tan JS. Antimicrobial treatment of lower respiratory tract infections in the hospital setting. *Am J Med* 2005;118 Suppl 7A:29S-38S.
5. Gonzales R, Malone DC, Maselli JH, et al. Excessive antibiotic use for acute respiratory infections in the United States. *Clin Infect Dis* 2001;33:757-62.
6. Dupont H, Mentec H, Sollet JP, et al. Impact of appropriateness of initial antibiotic therapy on the outcome of ventilator-associated pneumonia. *Intensive Care Med* 2001;27:355-62.
7. Chinese Medical Association, Respiratory Disease Branch. Diagnosis and treatment guidelines for community-acquired pneumonia and hospital-acquired pneumonia. *Chin J Tuberc Respir Dis* 1999;22:199-203.
8. Kang Y, Deng R, Wang C, et al. Etiologic diagnosis of lower respiratory tract bacterial infections using sputum samples and quantitative loop-mediated isothermal

- amplification. *PLoS One* 2012;7:e38743.
9. Beers MH, Berkow R. eds. *The Merck Manual of Diagnosis and Therapy*. 17th ed. Whitehouse Station, NJ: Merck Research Laboratories, 1999.
 10. Moberley S, Holden J, Tatham DP, et al. Vaccines for preventing pneumococcal infection in adults. *Cochrane Database Syst Rev* 2013;1:CD000422.
 11. Li S, Shi L. Pathogens Distribution and Drug Resistance in Lower Respiratory Tract Infection in Department of Respiratory Medicine. *Chin J Nosocomiol* 2008;18:719-21.
 12. Li WZ. Analysis on the potency of the commonly used antibiotics for G+ pathogenic bacteria. *Progress in Modern Biomedicine* 2007;7:1701-10.
 13. Bjerre LM, Verheij TJ, Kochen MM. Antibiotics for community acquired pneumonia in adult outpatients. *Cochrane Database Syst Rev* 2009;(4):CD002109.
 14. Langton Hewer SC, Smyth AR. Antibiotic strategies for eradicating *Pseudomonas aeruginosa* in people with cystic fibrosis. *Cochrane Database Syst Rev* 2009;(4):CD004197.
 15. Hsueh PR, Chen WH, Luh KT. Relationships between antimicrobial use and antimicrobial resistance in Gram-negative bacteria causing nosocomial infections from 1991-2003 at a university hospital in Taiwan. *Int J Antimicrob Agents* 2005;26:463-72.
 16. Jaryszak EM, Sampson EM, Antonelli PJ. Biofilm formation by *Pseudomonas aeruginosa* on ossicular reconstruction prostheses. *Am J Otolaryngol* 2009;30:367-70.

Cite this article as: He R, Luo B, Hu C, Li Y, Niu R. Differences in distribution and drug sensitivity of pathogens in lower respiratory tract infections between general wards and RICU. *J Thorac Dis* 2014;6(10):1403-1410. doi: 10.3978/j.issn.2072-1439.2014.09.22

Experimentation with aerosol bonsetan, pirfenidone, treprostinil and sildenafil

Haidong Huang¹, Paul Zarogoulidis², Sofia Lampaki², John Organtzis², Dimitris Petridis³, Konstantinos Porpodis², Antonis Papaiwannou², Vasilis Karageorgiou⁴, Georgia Pitsiou², Ioannis Kioumis², Wolfgang Hohenforst-Schmidt⁵, Qiang Li¹, Kaid Darwiche⁶, Lutz Freitag⁶, Aggeliki Rapti⁷, Konstantinos Zarogoulidis²

¹Department of Respiratory Diseases Shanghai Hospital, II Military University Hospital, Shanghai, China; ²Pulmonary Department-Oncology Unit, "G. Papanikolaou" General Hospital, Aristotle University of Thessaloniki, Thessaloniki, Greece; ³Department of Food Technology, School of Food Technology and Nutrition, Alexander Technological Educational Institute, Thessaloniki, Greece; ⁴Department of Chemical Engineering, Aristotle University of Thessaloniki, Thessaloniki, Greece; ⁵II Medical Department, "Coburg" Regional Hospital, Coburg, Germany; ⁶Department of Interventional Pneumology, "Ruhrlandklinik", West German Lung Center, University Hospital, University Duisburg-Essen, Essen, Germany; ⁷Pulmonary Department, "Sotiria" Hospital of Chest Diseases, Athens, Greece

Correspondence to: Paul Zarogoulidis. Pulmonary Department, "G. Papanikolaou" General Hospital, Aristotle University of Thessaloniki, Thessaloniki, Greece. Email: pzarog@hotmail.com.

Introduction: Pulmonary hypertension (PH) has been identified either as a symptom or a primary entity. Several drugs are already on the market and other are being investigated. Idiopathic pulmonary fibrosis (IPF) is also a disease where several drugs are being investigated.

Materials and methods: Three jet nebulizers and three ultrasound nebulizers were used for our experiments with seven different residual cups and four different loadings. Bonsetan, treprostinil, sildenafil and pirfenidone were modified in order to be produced as aerosol in an effort to identify parameters which influence the droplet size production size.

Results: The four-way ANOVA on droplet size using the jet nebulizers revealed two statistically significant factors, drug ($F=6.326$, $P=0.0007$) and residual cup ($F=4.419$, $P=0.0007$), and their interaction term ($F=5.829$, $P<0.0001$). Drugs bonsetan and pirfenidone produce equally the lowest mean droplet size (2.63 and 2.80 respectively) as compared to other two drug mean sizes. The ANOVA results, concerning the ultrasound nebulizers, revealed only the nebulizers as producing significant effect on droplet size ($F=4.753$, $P=0.037$).

Discussion: Our study indicates the importance of the initial drug design formulation. Moreover, further investigation of the residual cup design is an additional parameter that can assist in the optimal droplet size production, indifferently of the drug formulation.

Keywords: Pulmonary hypertension (PH); interstitial lung fibrosis; aerosol; bonsetan; pirfenidone

Submitted Jul 02, 2014. Accepted for publication Aug 19, 2014.

doi: 10.3978/j.issn.2072-1439.2014.08.38

View this article at: <http://dx.doi.org/10.3978/j.issn.2072-1439.2014.08.38>

Introduction

Inhaled therapies have been used for respiratory diseases and symptom relief since many years and vast experience exists for many products (1-4). Several drugs are also being investigated whether they could be administered as aerosol (5-9). The major obstacle for efficient aerosol deposition are the defense mechanisms of the respiratory

system (10) and the drug design for efficient tissue distribution (11). Moreover; safety concerns for novel methods of drugs as aerosol administration, still remain to be investigated and elicited (8,12-16). Previous research studies have identified several parameters that influence the droplet size production and can be summarized to the following: (I) residual cup loading; (II) initial loading of



Figure 1 Jet-nebulizer.

the residual cup; (III) refilling of the residual cup when the initial filling has been reduced to half (this can be done only once); (IV) residual cup design; (V) inlet design (if used) and (VI) drug formulation (17-20). Currently there is an increasing interest in the investigation for drugs administered as aerosol for pulmonary hypertension (PH) and idiopathic pulmonary fibrosis (IPF). PH is defined as a mean pulmonary arterial pressure (PAP) ≥ 25 mmHg at rest when assessed with right heart catheterization (21). It is a fatal disease caused by vascular proliferation, remodeling and small vessel obstruction. Increased pulmonary vascular resistance (PVR) which is often observed, leads to right-sided heart failure (HF) and death (22). Current guidelines have divided PH in five major categories (23). Currently there are new insights presented for the pathophysiology of the disease and progress in the diagnosis. The diagnosis includes (I) right-heart catheterization; (II) optical coherence tomography and (III) computed tomography. Current treatment strategies for pre-capillary PAH include: (I) lifestyle modification; (II) endothelin receptor antagonists; (III) prostacyclins and (IV) immunosuppressive therapy. Novel agents currently considered are: riociquat, imatinib and Rho-kinase inhibitors. Novel agents for post-capillary PAH include: sildenafil, riociquat and Rho-kinase inhibitors. Previous drugs include: angiotensin-receptor blockers, nitrates, diuretics, angiotensin-converting enzyme inhibitors and β -blockers. Pulmonary artery angioplasty is considered the treatment for chronic thromboembolic PH (24). Currently inhaled treprostinil (Tyvaso) has been approved by the FDA [2009] for patients with PAH with NYHA III. Prostacyclin-2 through cyclooxygenase-2, leads to vasodilation and platelet aggregation (25). Prostacyclin causes vasodilation in both systemic and pulmonary arteries. Moreover; it has antiproliferative activity as observed with

the inhibition of growth of smooth muscle cells. Inhaled prostanoids are usually administered in patients who are not candidates for parenteral treatment, or with declining condition. The major advantage is the delivery of the drug directly to the lungs and therefore less systemic side effects have been observed (4,26,27). Inhaled treprostinil through the TRIUMPH trial provided data where the 6-minute walking test was improved when compared to stable doses of bosentan or sildenafil (28). IPF is a debilitating disease occurring in adults between 60 to 75 years of age (29). The disease is fatal with a median survival of 2-5 years, and progressive pulmonary function occurs. Pirfenidone is indicated for mild to moderate IPF based on phase III trials using forced vital capacity (FVC) $\geq 50\%$, carbon monoxide diffusing capacity (DLCO) $\geq 35\%$ and 6-minute walking test (6MWT) distance of ≥ 150 m (30). Additional drugs that have presented positive results as additional treatment for IPF are N-acetylcysteine (NAC) and nintedanib (BIBF 1120), however; further investigation is necessary (31,32). In the current study we have investigated whether modification of the drugs bosentan, sildenafil, treprostinil and pirfenidone with different nebulizers, residual cups and loadings could be used as a future local administration to the lung parenchyma.

Materials and methods

Drugs

The following drugs were purchased: (I) Tracleer[®] (bosentan) 62.5 mg/tab, Actelion; (II) Revatio[®], (sildenafil) 20 mg/tab, Pfizer; (III) Esbriet[®] (pirfenidone) 276 mg/hard capsule, Intermune UK Ltd.; and (IV) Remodulin[®] (treprostinil) 5 mg/mL solution, United Therapeutics Europe Ltd.

Nebulizers and residual cups

Jet-nebulizers and residual cups

Three nebulizers were chosen from our department for the experiment: Maxineb[®] (6 liters/minute and 35 psi), Sunmist[®] (5-7 liters/minute and 35 psi) and Invacare[®] (4-8 liters-minute and 36 psi). In total seven residual cups were chosen for evaluation, four with a capacity of no more than 6 mLs and two with a capacity no more than 10 mLs. The designs for the large residual cups will be mentioned as A, D and E. The small residual cups will be mentioned as C, F, B and J. The large residual cups were not used with a capacity of more than 8 mLs as explained in the discussion section (*Figure 1*).

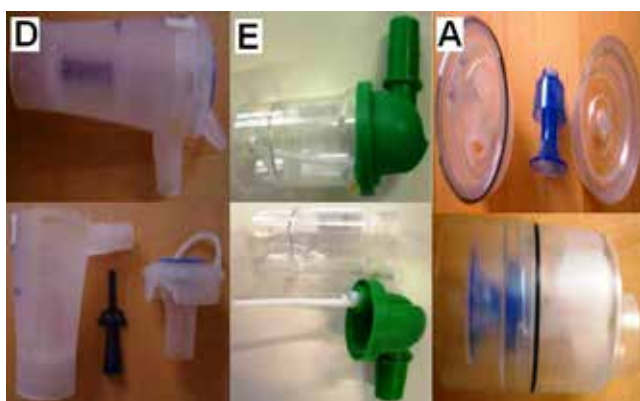


Figure 2 Large residual cups 10 mLs max.



Figure 3 Small residual cups 6 mLs max.



Figure 4 Ultrasound nebulizers.



Figure 5 Mastersizer 2000.

Ultrasound nebulizers

Three new ultrasound nebulizers were chosen from the market based on their cost-effectiveness. The first was Omron® NE-U07, Tokyo, Japan. Compact and weight less than 350 gm, includes 10 mL medication cup. Generates uniform micro millimetre-sized vapor particles. The second was a portable GIMA, Gessate, Italy (Choice Smart Health Care Company Limited, Wan Chai, Hong Kong, No. G2061259328002) with the following operating specifications; particle size: 3-5 μm , frequency: 2.5 MHz, medication cup capacity: 1-6 mLs, sound level at 10 cm: <50 db, operating temperature: min. 10 °C, max. 40 °C and air humidity: min. 10%, max. 95% RH. The third was a portable EASYneb® II, FLAEMNUOVA, Martino, Italy. with the following operating specifications; drug max capacity: 8 mLs, frequency: 2.4 MHz, nebulization capacity (adjustable) 0-0.7 mL/min approximately (tests performed with saline 0.9%), particle size: 2.13 μm mass median aerodynamic diameter (MMAD), sound level at 10 cm: 50 db (A), operating temperature: min. 10 °C, max. 40 °C and air humidity: min. 10%, max. 95% RH (Figures 2-4).

Measurement of droplet size and droplet size distribution

A laser scattering apparatus (Malvern Mastersizer 2000, Malvern, Worcestershire, UK) equipped with a Scirocco dry accessory module (Malvern, Worcestershire, UK) was used for the determination of the mass median diameter of the produced particles. A specific surface area odd 4.3 was used. Light scattering was used instead of a cascade impactor, as (I) a cascade impactor is, by design, limited to the number of size populations it may discriminate, that is the number of filters. In such a case, a limited number of populations can be distinguished. Our light scattering set-up can measure the light scattering intensity at a very large number of angles (that is the equivalent of a cascade impactor filters), so it can construct a particle size distribution plot of a very large number of points; (II) light scattering is non-invasive to all particles. The above, coupled with the application of the very accurate 'Mie theory' used here for transferring the angle-intensity measurements into size-volume data, and the thorough control of our data fitting, give us confidence in the presented results. Our equipment has been previous used in prior publications (5-8,17) (Figure 5).

Milling

The bonsetan, pirfenidone and sildenafil tablets were milled



Figure 6 Milling equipment.



Figure 7 Kern digital scale.

in a planetary ball mill (Frisch, Pulverisette-5) equipped with Agate bowls (500 mL) and 8 balls (20 mm, 20 g) with a rotational speed of approximately 200 rpm which results in an acceleration of about 7.5 g. We initiated our milling at 40 minutes and we acquired a MMAD of 4.4 μm for bonsetan and 3.7 for pirfenidone. The major problem that we encountered was that the sildenafil tablets were

influenced by the heat that was developed during the process and a paste was developed around the walls of the agate bowls (Figure 6). Therefore we had to seek for an alternative method of milling and we used a grinder FALING NUMBER S-12611, Stockholm, Sweden, type 120, 3-phase and 280 rpm, made in Finland. Before proceeding to milling we had measured the weight of the tablets and capsules with a digital scale Kern EG 2200-2NM, Kern & Sohn, GmbH, Balingen, Germany (Figure 7). After milling we collected powder of the same weight from drug and diluted it with 2 mLs in an effort to simulate a future method/compound of administration.

Statistical assessment

MMAD was measured following three different experimental factorial designs:

- (I) Three jet nebulizers in joint with four drugs, seven cup devices with three dosage levels each (2, 4 and 6 mL) were analyzed for potential effects on droplet size by employing a four-factor ANOVA, fixed effects plus their interaction levels, thus totaling $3 \times 4 \times 7 \times 3 = 252$ combined levels;
- (II) The same design was repeated including only the large residual cups (A, D, E) at 8 mL dose level using a three-factor ANOVA and totaling $3 \times 4 \times 3 = 27$ combined levels;
- (III) The droplet size was finally checked for potential effects by applying three ultrasound nebulizers, the same drugs as before and “delivery” constructions (face mask and inlet) at two dose levels (2 and 4 mL). A four-factor ANOVA, fixed effects, was performed making up $3 \times 4 \times 3 \times 2 = 72$ combined levels.

Statistically significant effects and interaction terms were tested graphically using pair-wise comparisons of means together with their 95% confidence intervals. Means whose intervals do not overlap are significantly different.

The major aim is focused on the best combination that provides droplets with the least size.

Results

The four-way ANOVA on droplet size using the jet nebulizers revealed two statistically significant factors, drug ($F=6.326$, $P=0.0007$) and residual cup ($F=4.419$, $P=0.0007$), and their interaction term ($F=5.829$, $P<0.0001$). Drugs tracleer and pirfenidone produce equally the lowest mean droplet size (2.63 and 2.80 respectively) as compared

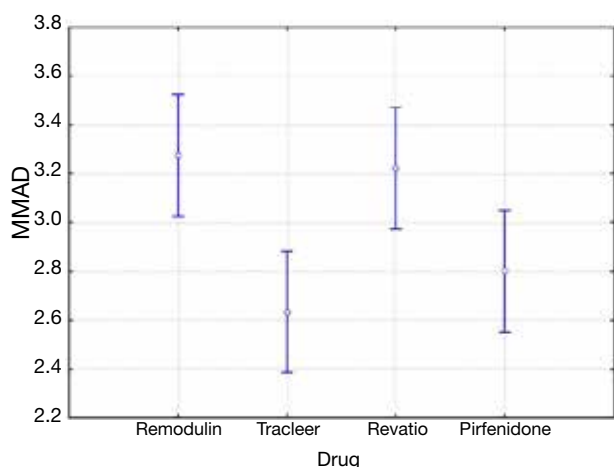


Figure 8 Mean droplet size distribution of four drugs. Vertical bars represent the 95% confidence intervals of the means calculated from the error mean square of ANOVA.

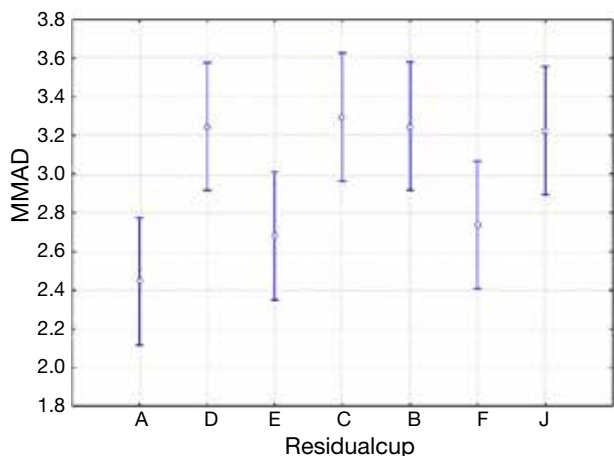


Figure 9 Mean droplet size distribution of seven residual cups. Vertical bars represent the 95% confidence intervals of the means calculated from the error mean square of ANOVA.

to other two drug mean sizes (*Figure 8*). Two groups of different mean droplet size are produced by the residual cups (*Figure 9*). Cups A, E and F are equally the most efficient in small mean droplet size (2.44, 2.68 and 2.74 respectively), while the rest four cups form another group with higher mean sizes, ranging between 3.22 and 3.30. Cup F in joint with drug pirfenidone (*Figure 10*) create the least mean droplet size (1.56), by far lower from all other combined levels and particularly from the combined effect of drug remodulin with cups C, B, and F whose result rises up to 4.1-4.4 μm . The large residual cups (A, D and E), when combined with the four aforesaid

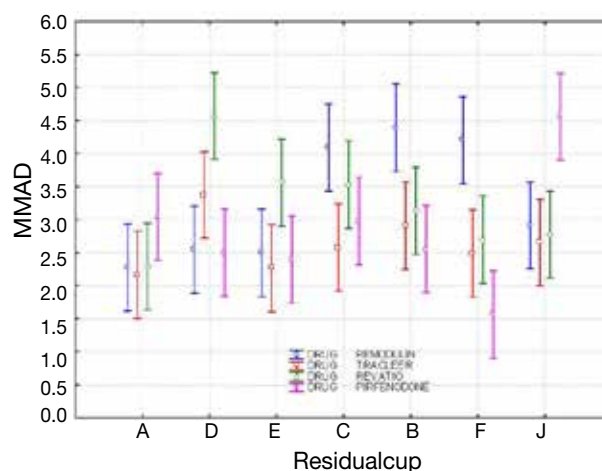


Figure 10 Mean droplet size distribution of the combined levels between drugs and residual cups. Vertical bars represent the 95% confidence intervals of the means calculated from the error mean square of ANOVA.

drugs and the same nebulizers, do not produce statistically significant results at 8 mL dose level ($P > 0.05$ in all factors and interaction terms). The ANOVA results, concerning the ultrasound nebulizers, revealed only the nebulizers as producing significant effect on droplet size ($F = 4.753$, $P = 0.037$). This effect is easily clarified in the *Figure 11* in which the OMRON nebulizer outweighs the others' effect providing a mean droplet size of 2.69 μm . To capitalize, jet nebulizers, although not significant on droplet size, best perform with drugs tracleer and pirfenidone, using cup designs A, E and F, and particularly when combined with cup F and pirfenidone. Loadings greater than 6 mL together with any other factor combined do not exert any significant effect on droplet size. Ultrasound nebulizers produce a unique effect on droplet size, no matter considering any other factor in the study, from which OMRON generates the smallest droplets.

Discussion

Inhalation therapies in order to be efficient they have to bypass the defense mechanisms of the respiratory system. These can be summarized to: (I) beating cilia; (II) macrophages; (III) mucus; (IV) local enzymes; and (V) local transporters (10). Furthermore, an underlying respiratory disease modifies the deposition and absorption of aerosol therapies. Bronchoconstriction which might occur during an exacerbation of asthma or chronic obstructive pulmonary disease (COPD) reduces the distribution and deposition of an aerosol therapy (33,34). The production of mucus

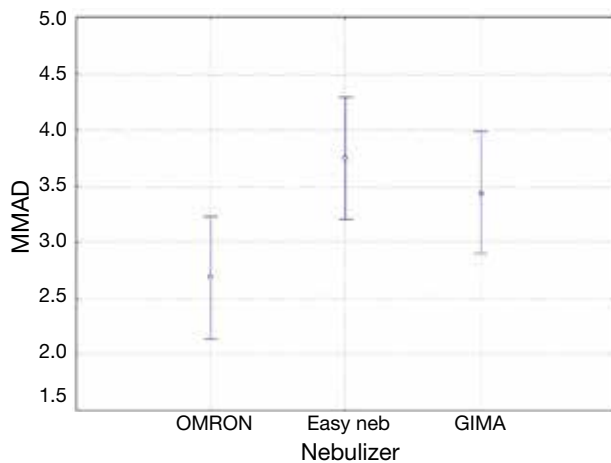


Figure 11 Mean droplet size distribution of three ultrasound nebulizers. Vertical bars represent the 95% confidence intervals of the means calculated from the error mean square of ANOVA.

also reduces the absorption of an aerosol therapy since a concentration of the drug is enclosed within the mucus. Local enzymes and transporters are parameters that their interaction with the aerosol drugs has not been fully investigated. It has been presented that there are different enzymes and transporters at different locations of the respiratory system which modify the absorption of a drug locally (35). Moreover, the aerosol mist has to be composed of droplets of MMAD of $<5 \mu\text{m}$. The third important factor for an efficient aerosol therapy is the drug design. There are two major delivery systems for local absorption; the passive and active transportation. The passive transportation is based on the principals of the drug formulation molecules and interaction with the local enzymes and transporters. The active transportation is based on an antigen-antibody connection of the drug molecules and local tissue (11). Active transportation tends to be usually less expensive in production, however, in several situations less effective. Cost-effective design is another parameter that has to be included in drug design development. Previous investigation of aerosol production systems have indicated that jet-nebulizers and ultrasound nebulizers are easy to use in the everyday practice, however, jet-nebulizers are currently cheaper than ultrasound nebulizers. Moreover, it has been observed that several drugs are more efficiently delivered with one system versus the other, meaning that we should choose the aerosol production system based also on the drug that we want to deliver (20). The production of aerosol regarding the jet-nebulizers is also influenced by the residual cup design,

initial filling, time of nebulisation and drug. Moreover; it has been observed that reduction of the produced droplet size can be achieved with the usage of inlets design (17). Temperature increase from the piezoelectric crystal results in a higher concentration effect of the drug solution, than in the jet-nebulizers (36). However, the combination of temperature and drug concentration cause a shift in the tension and viscosity and consequently change the droplet size distribution (37). The nebulization time also plays a role in the viscosity, surface tension, saturated vapour pressure and finally to the droplet size distribution. Increase of the concentration in the produced aerosol is mostly observed in the ultrasound nebulizers than the jet-nebulizers (38). The variations of the viscosity are also time dependent (low the first 2 minutes, higher after the 4 minutes) and temperature dependent in ultrasound nebulizers. An increase in the mean droplet size range has been also observed when adding buffer (39). The increasing drug concentration is also a factor inducing bronchoconstriction (40). In conclusion the major factors affecting the produced mist are: (I) temperature; (II) viscosity; (III) drug formulations (salts, buffer) and (IV) time of nebulization.

PAH is a complex disease characterized by increased PVR which eventually leads to right-sided HF and death (41). Current recommendations for patients with NYHA II, III, IV symptoms indicate first-line monotherapy with agents targeting the following pathways: endothelin, prostacyclin and nitric oxide. Sequential combination of agents is indicated when there is no evidence of clinical improvement with one specific-PAH agent (42). However, again there are patients who do not present improvement even after a combination treatment (43). Combination treatment has been proposed in advanced stage disease for initial treatment (42). The concept for combination treatment has the advantage of targeting simultaneously different pathological pathways (43). Most studies have investigated the sequential addition of agents and very few initiation of a combination treatment (44). Currently pharmacogenomics are investigated for targeted treatment of PAH as a future treatment (45). Possibly in the future we could target the disease with a combination of aerosol treatment. Treatment for IPF is based on the updated recommendations of 2013 (29). Several agents have been presented and discussed such as, corticosteroids, NAC, interferon-gamma-1b, azathioprine, anticoagulant therapy, oxygen therapy, lung transplantation and pirfenidone (46). Combination of treatments has been also been proposed (46-58). Additionally, “weak no” has been indicated for treatment of PAH due to IPF according to the last updated

recommendations (29). IPF despite current treatment efforts still remains a fatal disease with a median survival between 2-5 years. Currently we investigated whether inhaled pirfenidone could be redesigned to be delivered as aerosol. Major obstacle for IPF is firstly the safety of aerosol administration, because several drugs tend to induce exacerbation of an underlying disease and secondly the efficiency. Production and deposition of a drug does not necessarily mean that the formulation will be distributed from the site of administration to the blood circulation, in specific in patients with IPF since the parenchyma is destroyed. Further investigation has to be investigated probably in a 3D model of lung parenchyma simulating IPF disease.

Conclusions

In our study we investigated drug solutions close to a possible future treatment and we observed that the dilution as it was done it could be a possible method of administration for all drugs. Large concentrations >8 mLs were not necessary as in our previous studies and it is only matter of how much concentration of the drug we want to deliver. Again it was observed that residual cup design plays an important role in the production of the aerosol and the drug formulation. Certainly we need additional local therapies for PH and IPF, local administration has possible advantages, however, future experiments have to present data for the safety of this administration method to the lung.

Acknowledgements

The authors Paul Zarogoulidis, Konstantinos Zarogoulidis and Georgia Pitsiou would like to thank the Special Product Manager Irimi Kefalidou for the provided information regarding treprostinil.

Disclosure: The authors declare no conflict of interest.

References

- Răjnovăanu RM, Antoniu S, Ulmeanu R. Combined long-acting bronchodilator single therapy for COPD. *Expert Opin Pharmacother* 2014;15:139-42.
- Gregersen TL, Ulrik CS. Safety of bronchodilators and corticosteroids for asthma during pregnancy: what we know and what we need to do better. *J Asthma Allergy* 2013;6:117-25.
- Poms A, Kingman M. Inhaled treprostinil for the treatment of pulmonary arterial hypertension. *Crit Care Nurse* 2011;31:e1-10.
- Channick RN, Voswinckel R, Rubin LJ. Inhaled treprostinil: a therapeutic review. *Drug Des Devel Ther* 2012;6:19-28.
- Zarogoulidis P, Darwiche K, Huang H, et al. Time recall; future concept of chronomodulating chemotherapy for cancer. *Curr Pharm Biotechnol* 2013;14:632-42.
- Zarogoulidis P, Darwiche K, Krauss L, et al. Inhaled cisplatin deposition and distribution in lymph nodes in stage II lung cancer patients. *Future Oncol* 2013;9:1307-13.
- Zaric B, Stojic V, Tepavac A, et al. Adjuvant chemotherapy and radiotherapy in the treatment of non-small cell lung cancer (NSCLC). *J Thorac Dis* 2013;5 Suppl 4:S371-7.
- Zarogoulidis K, Boutsikou E, Zarogoulidis P, et al. The role of second-line chemotherapy in small cell lung cancer: a retrospective analysis. *Onco Targets Ther* 2013;6:1493-500.
- Zarogoulidis P, Petridis D, Ritzoulis C, et al. Further experimentation of inhaled; LANTUS, ACTRAPID and HUMULIN with today's production systems. *Int J Pharm* 2013;458:39-47.
- Zarogoulidis P, Darwiche K, Yarmus L, et al. Defense mechanisms of the respiratory system and aerosol production systems. *Med Chem* 2014;10:123-36.
- Bae YH. Interview with Dr You Han Bae: ligand-mediated versus 'passive' targeting approaches in nanoparticle oncology research. *Ther Deliv* 2012;3:933-6.
- Darwiche K, Zarogoulidis P, Karamanos NK, et al. Efficacy versus safety concerns for aerosol chemotherapy in non-small-cell lung cancer: a future dilemma for micro-oncology. *Future Oncol* 2013;9:505-25.
- Zarogoulidis P, Giraleli C, Karamanos NK. Inhaled chemotherapy in lung cancer: safety concerns of nanocomplexes delivered. *Ther Deliv* 2012;3:1021-3.
- Zarogoulidis P, Eleftheriadou E, Sapardanis I, et al. Feasibility and effectiveness of inhaled carboplatin in NSCLC patients. *Invest New Drugs* 2012;30:1628-40.
- Zarogoulidis P, Kontakiotis T, Zarogoulidis K. Inhaled gene therapy in lung cancer: "as for the future, our task is not to foresee it, but to enable it". *Ther Deliv* 2012;3:919-21.
- Zarogoulidis P, Karamanos NK, Porpodis K, et al. Vectors for inhaled gene therapy in lung cancer. Application for nano oncology and safety of bio nanotechnology. *Int J Mol Sci* 2012;13:10828-62.
- Boukovinas I, Tsakiridis K, Zarogoulidis P, et al. Neo-adjuvant chemotherapy in early stage non-small cell lung cancer. *J Thorac Dis* 2013;5 Suppl 4:S446-8.

18. Ferron GA, Kerrebijn KF, Weber J. Properties of aerosols produced with three nebulizers. *Am Rev Respir Dis* 1976;114:899-908.
19. Kendrick AH, Smith EC, Wilson RS. Selecting and using nebuliser equipment. *Thorax* 1997;52 Suppl 2:S92-101.
20. Laube BL, Janssens HM, de Jongh FH, et al. What the pulmonary specialist should know about the new inhalation therapies. *Eur Respir J* 2011;37:1308-31.
21. Badesch DB, Champion HC, Sanchez MA, et al. Diagnosis and assessment of pulmonary arterial hypertension. *J Am Coll Cardiol* 2009;54:S55-66.
22. Humbert M, Morrell NW, Archer SL, et al. Cellular and molecular pathobiology of pulmonary arterial hypertension. *J Am Coll Cardiol* 2004;43:13S-24S.
23. Simonneau G, Robbins IM, Beghetti M, et al. Updated clinical classification of pulmonary hypertension. *J Am Coll Cardiol* 2009;54:S43-54.
24. Fukumoto Y, Shimokawa H. Recent progress in the management of pulmonary hypertension. *Circ J* 2011;75:1801-10.
25. Vane J, Corin RE. Prostacyclin: a vascular mediator. *Eur J Vasc Endovasc Surg* 2003;26:571-8.
26. Hohenforst-Schmidt W, Hornig J, Friedel N, et al. Successful management of an inadvertent excessive treprostinil overdose. *Drug Des Devel Ther* 2013;7:161-5.
27. Channick RN, Olschewski H, Seeger W, et al. Safety and efficacy of inhaled treprostinil as add-on therapy to bosentan in pulmonary arterial hypertension. *J Am Coll Cardiol* 2006;48:1433-7.
28. Benza RL, Seeger W, McLaughlin VV, et al. Long-term effects of inhaled treprostinil in patients with pulmonary arterial hypertension: the Treprostinil Sodium Inhalation Used in the Management of Pulmonary Arterial Hypertension (TRIUMPH) study open-label extension. *J Heart Lung Transplant* 2011;30:1327-33.
29. Travis WD, Costabel U, Hansell DM, et al. An official American Thoracic Society/European Respiratory Society statement: Update of the international multidisciplinary classification of the idiopathic interstitial pneumonias. *Am J Respir Crit Care Med* 2013;188:733-48.
30. Noble PW, Albera C, Bradford WZ, et al. Pirfenidone in patients with idiopathic pulmonary fibrosis (CAPACITY): two randomised trials. *Lancet* 2011;377:1760-9.
31. Richeldi L, Costabel U, Selman M, et al. Efficacy of a tyrosine kinase inhibitor in idiopathic pulmonary fibrosis. *N Engl J Med* 2011;365:1079-87.
32. Idiopathic Pulmonary Fibrosis Clinical Research Network, Raghu G, Anstrom KJ, et al. Prednisone, azathioprine, and N-acetylcysteine for pulmonary fibrosis. *N Engl J Med* 2012;366:1968-77.
33. Barnes N, Calverley PM, Kaplan A, et al. Chronic obstructive pulmonary disease and exacerbations: clinician insights from the global Hidden Depths of COPD survey. *Curr Med Res Opin* 2014;30:667-84.
34. Patel M, Pilcher J, Pritchard A, et al. Efficacy and safety of maintenance and reliever combination budesonide-formoterol inhaler in patients with asthma at risk of severe exacerbations: a randomised controlled trial. *Lancet Respir Med* 2013;1:32-42.
35. Bosquillon C. Drug transporters in the lung--do they play a role in the biopharmaceutics of inhaled drugs? *J Pharm Sci* 2010;99:2240-55.
36. Niven RW, Ip AY, Mittelman S, et al. Some factors associated with the ultrasonic nebulization of proteins. *Pharm Res* 1995;12:53-9.
37. Finlay WH, eds. The mechanisms of inhaled pharmaceutical aerosols. London: Academic Press, 2001.
38. O'Callaghan C, Barry PW. The science of nebulised drug delivery. *Thorax* 1997;52 Suppl 2:S31-44.
39. Steckel H, Eskandar F. Factors affecting aerosol performance during nebulization with jet and ultrasonic nebulizers. *Eur J Pharm Sci* 2003;19:443-55.
40. Hickey AJ, eds. Pharmaceutical inhalation aerosol technology. New York: Marcer Decker, 1992.
41. Humbert M, Sitbon O, Simonneau G. Treatment of pulmonary arterial hypertension. *N Engl J Med* 2004;351:1425-36.
42. Task Force for Diagnosis and Treatment of Pulmonary Hypertension of European Society of Cardiology (ESC), European Respiratory Society (ERS), International Society of Heart and Lung Transplantation (ISHLT), et al. Guidelines for the diagnosis and treatment of pulmonary hypertension. *Eur Respir J* 2009;34:1219-63.
43. Hoepfer MM, Faulenbach C, Golpon H, et al. Combination therapy with bosentan and sildenafil in idiopathic pulmonary arterial hypertension. *Eur Respir J* 2004;24:1007-10.
44. Kemp K, Savale L, O'Callaghan DS, et al. Usefulness of first-line combination therapy with epoprostenol and bosentan in pulmonary arterial hypertension: an observational study. *J Heart Lung Transplant* 2012;31:150-8.
45. Said SI, Hamidi SA. Pharmacogenomics in pulmonary arterial hypertension: Toward a mechanistic, target-based approach to therapy. *Pulm Circ* 2011;1:383-8.
46. Behr J, Richeldi L. Recommendations on treatment for

- IPF. *Respir Res* 2013;14 Suppl 1:S6.
47. Hohenforst-Schmidt W, Zarogoulidis P, Linsmeier B, et al. Enhancement of aerosol cisplatin chemotherapy with gene therapy expressing abc10 protein in respiratory system. *J Cancer* 2014;5:344-50.
 48. Angelis N, Porpodis K, Zarogoulidis P, et al. Airway inflammation in chronic obstructive pulmonary disease. *J Thorac Dis* 2014;6 Suppl 1:S167-72.
 49. Papaiwannou A, Zarogoulidis P, Porpodis K, et al. Asthma-chronic obstructive pulmonary disease overlap syndrome (ACOS): current literature review. *J Thorac Dis* 2014;6 Suppl 1:S146-51.
 50. Walter RF, Zarogoulidis P, Mairinger FD, et al. Cell viability of fibroblasts to pifenidone and sirolimus: a future concept for drug eluting stents. *Int J Pharm* 2014;466:38-43.
 51. Zarogoulidis P, Darwiche K, Tsakiridis K, et al. Learning from the Cardiologists and Developing Eluting Stents Targeting the Mtor Pathway for Pulmonary Application; A Future Concept for Tracheal Stenosis. *J Mol Genet Med* 2013;7:65.
 52. Zarogoulidis P, Porpodis K, Kioumis I, et al. Experimentation with inhaled bronchodilators and corticosteroids. *Int J Pharm* 2014;461:411-8.
 53. Zarogoulidis P, Kioumis I, Porpodis K, et al. Clinical experimentation with aerosol antibiotics: current and future methods of administration. *Drug Des Devel Ther* 2013;7:1115-34.
 54. Zarogoulidis P, Petridis D, Ritzoulis C, et al. Internal mouthpiece designs as a future perspective for enhanced aerosol deposition. Comparative results for aerosol chemotherapy and aerosol antibiotics. *Int J Pharm* 2013;456:325-31.
 55. Zarogoulidis P, Darwiche K, Walter R, et al. Research spotlight: sirolimus-coated stents for airway tracheal stenosis: a future 3D model concept with today's knowledge. *Ther Deliv* 2013;4:1093-7.
 56. Zarogoulidis P, Kioumis I, Ritzoulis C, et al. New insights in the production of aerosol antibiotics. Evaluation of the optimal aerosol production system for ampicillin-sulbactam, meropenem, ceftazidime, cefepime and piperacillin-tazobactam. *Int J Pharm* 2013;455:182-8.
 57. Zarogoulidis P, Hohenforst-Schmidt W, Darwiche K, et al. 2-diethylaminoethyl-dextran methyl methacrylate copolymer nonviral vector: still a long way toward the safety of aerosol gene therapy. *Gene Ther* 2013;20:1022-8.
 58. Zarogoulidis P, Petridis D, Ritzoulis C, et al. Establishing the optimal nebulization system for paclitaxel, docetaxel, cisplatin, carboplatin and gemcitabine: back to drawing the residual cup. *Int J Pharm* 2013;453:480-7.

Cite this article as: Huang H, Zarogoulidis P, Lampaki S, Organtzis J, Petridis D, Porpodis K, Papaiwannou A, Karageorgiou V, Pitsiou G, Kioumis I, Hohenforst-Schmidt W, Li Q, Darwiche K, Freitag L, Rapti A, Zarogoulidis K. Experimentation with aerosol bonsetan, pifenidone, treprostinil and sildenafil. *J Thorac Dis* 2014;6(10):1411-1419. doi: 10.3978/j.issn.2072-1439.2014.08.38

Factors affecting tumor recurrence after curative surgery for NSCLC: impacts of lymphovascular invasion on early tumor recurrence

Chanyeong Park¹, In Jae Lee¹, Seung Hun Jang², Jae Woong Lee³

¹Department of Radiology, ²Department of Internal Medicine, ³Department of Thoracic Surgery, Hallym University College of Medicine, Chuncheon, Republic of Korea

Correspondence to: In Jae Lee, MD, PhD. Department of Radiology, Hallym University Sacred Heart Hospital, 22 Gwanpyeong-ro, 170 beon-gil, Dongan-gu, Anyang-city, Gyeonggi-do, 431-796, Republic of Korea. Email: ijlee2003@medimail.or.kr.

Background: Although surgery is potentially curative treatment for non-small cell lung cancer (NSCLC), the risk of postoperative disease recurrence is still high. This study was conducted to assess the factors associated with postoperative tumor recurrence in patients who underwent curative surgery for NSCLC.

Methods: One hundred seventy-one patients who underwent curative surgery for NSCLC were included in this study. Clinicopathological factors of histologic type, pathologic TNM stage, T stage, N stage, lymphovascular invasion (LVI), perineural invasion (PNI), surgical procedure, adjuvant chemotherapy and adjuvant radiotherapy were investigated. Gender, age, and clinicopathologic factors were included in univariate and multivariate analyses using the Kaplan-Meier method and Cox proportional hazards model, respectively. Mann-Whitney U and Kruskal-Wallis tests were used to investigate the significance of differences in recurrence-free interval (RFI) according to clinicopathological factors.

Results: Median RFI was 20 months. Univariate and multivariate analyses for overall recurrence identified T stage, N stage, and LVI as significant factors ($P=0.045$, 0.044 , and <0.001 , respectively). Pathologic stage ($P=0.005$) was the only factor that was significantly associated with locoregional recurrence. T stage ($P=0.040$) and LVI ($P<0.001$) were significantly associated with distant recurrence. The difference in 2-year freedom from recurrence between LVI positive and negative groups was significant (14.9% vs. 44.6%, $P<0.001$). LVI was the only factor that was significantly associated with a shortened mean RFI ($P<0.001$).

Conclusions: LVI had a significant effect on both overall and distant recurrence rates as well as on early tumor recurrence after curative surgery for NSCLC.

Keywords: Thorax; lung; surgery; pathology; metastases

Submitted Jul 02, 2014. Accepted for publication Sep 09, 2014.

doi: 10.3978/j.issn.2072-1439.2014.09.31

View this article at: <http://dx.doi.org/10.3978/j.issn.2072-1439.2014.09.31>

Introduction

Non-small cell lung cancer (NSCLC) is one of the leading causes of cancer-related deaths worldwide (1). Though surgery is a potentially curative treatment for NSCLC up to stage IIIA disease, the risk of postoperative disease recurrence has been reported to be as high as 52% (2). Postoperative follow-up examinations are periodically performed to detect postoperative recurrence early, so that adequate treatment can be offered to improve survival rate.

Because radiographic imaging is widely used for follow-up and there are numerous guidelines that have been published regarding the management of lung cancer (3), there should be an effort to avoid unnecessary medical treatment and reduce radiation exposure by adjusting follow-up plans. Although the TNM staging system for NSCLC is used to evaluate the extent of disease and guide management for patients (4), meticulous assessment of possible prognostic factors other than TNM stage is important for this reason.

The purpose of this study was to identify factors that associated with recurrence and recurrence-free interval (RFI) after curative surgery for NSCLC.

Material and methods

Patient population

This study was approved by the institutional review board of our institution, and informed consent was waived due to the retrospective nature of the study. Between August 1999 and May 2013, a total of 218 patients underwent curative surgery for lung cancer at our institution, which is an urban tertiary care hospital.

Forty-six of 218 patients were excluded from the study for the following reasons: 26 underwent neoadjuvant therapy, 13 died or transferred to other hospital before the initial follow-up CT scan was obtained, image data or medical records were missing for five patients, one patient had surgically confirmed SCLC, one patient had history of both pancreatic and pulmonary adenocarcinoma with recurred adenocarcinoma of unspecified origin, and one 13-year-old patient was excluded by institutional review board because of absence of his parent's permission.

The remaining 171 patients were included in this study. This patient population comprised 111 men and 60 women with a mean age of 63 years [median age: 64 years (range, 37-79 years)]. Median RFI was 20 months (range, 1-102 months). Other patient characteristics are summarized in *Table 1*.

Pathologic analysis

Three pathologists interpreted lung tumor specimens during the study period. Hematoxylin and eosin stains were performed on all surgical specimens. Other pathologic studies, such as immunostains, were performed at the discretion of the pathologists. Lymphovascular invasion (LVI) was reported when tumor cells or emboli was identified in lymphatic or blood vessel lumens. Tumor involvement of epineurium was defined as perineural invasion (PNI) (5). Patients with unknown LVI or PNI status were grouped into the negative category (6). Postoperative pathologic reports from electronic medical records were reviewed. Data such as histologic type, pathologic TNM staging (pathologic staging), LVI, and PNI were collected. All postoperative pathologic staging for NSCLC at our institution has been performed according to

the new TNM classification system of the American Joint Committee on Cancer (AJCC), 7th edition, since February 2010. Cases prior to this date were reevaluated according to the new TNM classification system by a radiologist with 4 years of experience of chest CT interpretation. Pathologic specimens of recurred lesions were obtained by bronchoscopic biopsy, core needle biopsy, and fine needle aspiration. Other lesions without pathologic confirmation were diagnosed by image analysis. RFI was defined as the time from the day of surgery to the date of the last normal follow-up for patients without recurrence, and to the date of first detection of a recurred lesion for patients with recurrence (7). For lesions that were not possible to distinguish between recurrence and second primary lung cancer, we considered the lesion to be recurred cancer, because it is often impractical to clarify disease recurrence from second primary lung cancer (7).

Image analysis

All CT scans were obtained using a 16-, 64- or 256-slice multidetector CT scanner (MX 8000 IDT, Phillips Medical System, Netherlands; Brilliance 64, Phillips Medical Systems, Israel; Somatom Definition Flash, Siemens Healthcare, Germany, respectively). All PET-CT scans were obtained using a large-bore, time-of-flight PET-CT scanner (Philips Gemini TF, Philips Healthcare, Andover, MA, USA). Routine follow-up chest CT for surveillance of recurrence was performed 3, 6, 12, 18, and 24 months after surgery, and then annually. Additional chest radiography, CT, or PET-CT scanning was performed depending on the clinical situation. CT and PET-CT scan data were collected from a picture archiving and communication system (PACS; Infinitt Healthcare Co. Ltd., Seoul, Korea). Consensus review of preoperative and follow-up CT and PET-CT images were performed by two radiologists, one with 16 years and the other with 4 years of experience in chest radiology.

In patients without pathologic confirmation, recurrence was presumed when there was any newly identified or enlarging soft tissue lesion or lymph node enlargement with more than one of the following: intense FDG uptake on PET-CT scans taken within a month of detection, either persistence or aggravation on the next follow-up study. Lymph node enlargement was defined when the short axis diameter was greater than 1 cm on CT scans.

In this study, recurrence was classified as locoregional or distant recurrence. Locoregional recurrence was defined

Table 1 Demographic features of 171 patients underwent curative surgery for NSCLC	
Factors	Number of cases (%)
Age	
<40	3 (1.8)
40-49	9 (5.3)
50-59	44 (25.7)
60-69	63 (36.8)
≥70	52 (30.4)
Gender	
Male	111 (64.9)
Female	60 (35.1)
Histology	
Adenoca	108 (63.2)
SqCC	53 (31.0)
Large cell neuroendocrine ca	4 (2.3)
Large cell undifferentiated ca	3 (1.8)
Adenosquamous cell ca	1 (0.6)
Pleomorphic ca	1 (0.6)
Mucoepidermoid ca	1 (0.6)
Pathologic stage	
IA	63 (36.8)
IB	49 (28.7)
IIA	19 (11.1)
IIB	17 (9.9)
IIIA	23 (13.5)
T stage	
T1a	43 (25.1)
T1b	28 (16.4)
T2a	67 (39.2)
T2b	9 (5.3)
T3	21 (12.3)
T4	3 (1.8)
N stage	
N0	133 (77.8)
N1	20 (11.7)
N2	18 (10.5)
LVI	
Negative	125 (73.1)
Positive	21 (12.3)
Unknown	25 (14.6)

Table 1 (Continued)

Table 1 (Continued)	
Factors	Number of cases (%)
PNI	
Negative	140 (81.9)
Positive	6 (3.5)
Unknown	25 (14.6)
Surgical procedures	
Pneumonectomy	17 (9.9)
Others	
Lobectomy	92 (53.8)
VATS lobectomy	38 (22.2)
Bilobectomy	13 (7.6)
Wedge resection	6 (3.5)
Sleeve lobectomy	4 (2.3)
VATS wedge resection	1 (0.6)
Adjuvant CTx	
Yes	118 (69.0)
No	53 (31.0)
Adjuvant RTx	
Yes	158 (92.4)
No	13 (7.6)

Numbers in parentheses are percentages. Adenoca, adenocarcinoma; SqCC, squamous cell carcinoma; ca, carcinoma; LVI, lymphovascular invasion; PNI, perineural invasion; CTx, chemotherapy; RTx, radiotherapy.

when disease recurred at the surgical resection margin or regional lymph nodes (ipsilateral hilar and/or mediastinum) (3,6). The location of locoregional recurrence was subclassified into stump, endobronchial, regional lymph node, and pleural invasion directly from recurrent mass. Pleural seeding and recurrence in the remaining ipsilateral or contralateral lung were regarded as distant metastasis (8). The location of distant recurrence was subclassified into ipsilateral and contralateral lung, distant lymph node, ipsilateral pleura incontinuous to surgical margin, contralateral pleura, and distant organ. When locoregional and distant recurrences were concurrently identified (concurrent cases), the two were counted separately.

Statistical analysis

Several clinicopathologic parameters were evaluated in this study: histologic type, pathologic stage, T stage, N stage, LVI, PNI, surgical procedure, adjuvant chemotherapy,

Table 2 Differences of mean RFI according to clinicopathologic factors

Factors	Mean RFI (months)	P value
Histologic type		0.470
Adenoca	29.81	
SqCC	27.06	
Others	27.10	
Pathologic stage		0.393
IA	28.38	
IB	28.10	
IIA	37.05	
IIB	32.53	
IIIA	21.83	
T stage		0.126
T1a	21.47	
T1b	27.50	
T2a	27.67	
T2b	39.33	
T3	22.00	
T4	29.33	
N stage		0.271
N0	28.55	
N1	36.30	
N2	22.28	
PNI		0.201
Negative	29.28	
Positive	15.50	
LVI		<0.001
Negative	31.43	
Positive	10.29	
Surgical procedure		0.057
Pneumonectomy	21.53	
Others	29.60	
Adjuvant CTx		0.185
Yes	24.49	
No	30.73	
Adjuvant RTx		0.921
Yes	31.62	
No	28.56	

RFI, recurrence-free interval; Adenoca, adenocarcinoma; SqCC, squamous cell carcinoma; PNI, perineural invasion; LVI, lymphovascular invasion; CTx, chemotherapy; RTx, radiotherapy.

and adjuvant radiotherapy. Surgical procedure, adjuvant chemotherapy and adjuvant radiotherapy were dichotomous: pneumonectomy or others, received or not. Because the clinicopathologic parameters did not show a normal distribution, the Mann-Whitney U test and Kruskal-Wallis test were applied to each clinicopathologic factor to investigate the significance of differences in mean RFI according to the factor.

Univariate and multivariate analyses were performed to examine factors affecting recurrence using the Kaplan-Meier method and Cox proportional hazards model, respectively. Log-rank test was used for univariate analysis of recurrence differences. Clinicopathologic parameters were included in univariate analysis. Gender, age, histologic type, and factors with $P \leq 0.1$ on univariate analysis (pathologic stage, T stage, N stage, LVI, and adjuvant chemotherapy) were included in multivariate analysis of overall, locoregional, and distant recurrences. Fisher's exact test was performed to identify preferred initial recurrence location on recurrent cases with LVI, compared with recurrent cases without LVI.

We also performed Kaplan-Meier analysis of the relationship between LVI and distant recurrence with stratification according to pathologic stage to identify whether pathologic stage was a confounding factor. Association between LVI and pathologic stage was evaluated by linear association.

All statistical analyses were performed using SPSS version 19.0 (IBM-SPSS, Chicago, IL, USA). All differences with $P < 0.05$ on two-tailed tests were considered to be statistically significant.

Results

Among 171 patients, 53 (31.0%) had recurrent lesions, which were diagnosed by pathologic confirmation in 11 patients and imaging data in the remaining 42 patients. There were no significant differences in mean RFI according to clinicopathologic factors except for LVI ($P < 0.001$), which was associated with 3-fold increase in mean RFI (31.43 *vs.* 10.29 months). Surgical procedure showed borderline significance ($P = 0.057$). Differences in mean RFI according to clinicopathologic factors are summarized in *Table 2*.

Univariate analysis revealed the following factors that were significantly associated with recurrence rate: pathologic stage ($P = 0.003$), T stage ($P = 0.012$), N stage ($P = 0.016$), LVI ($P < 0.001$), pneumonectomy ($P < 0.001$), and adjuvant chemotherapy ($P = 0.011$) (*Figure 1*). Histologic

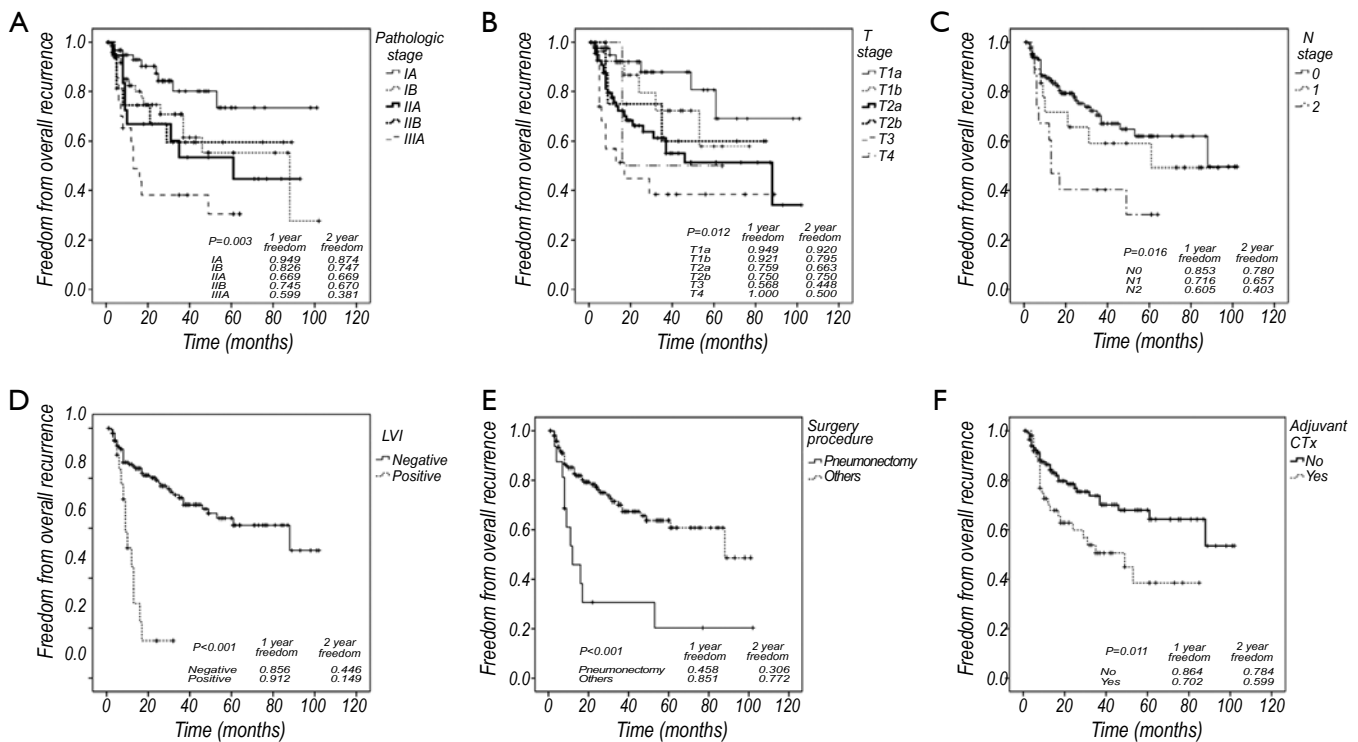


Figure 1 Univariate analyses for overall recurrence according to clinicopathologic factors in all patients (n=171). The RFI was statistically significant according to pathologic stage (A), T stage (B), N stage (C), LVI (D), surgery procedure (E), and adjuvant chemotherapy (F) ($P=0.003$, 0.012 , 0.016 , <0.001 , and 0.011 , respectively). Two-year recurrence-free rate remarkably decreased compared with 1-year recurrence-free rate on LVI positive group. RFI, recurrence-free interval.

type and PNI did not show statistical significance ($P=0.514$ and 0.701 , respectively). Patients with LVI had a lower 2-year recurrence-free rate than patients without LVI by one-third (44.6% vs. 14.9% , *Figure 2*). There was an approximately 2-fold difference in 2-year recurrence-free rate between the highest and lowest tiers of other significant factors on univariate studies (pathologic stage IA vs. IIIA, 0.874 vs. 0.381 ; T stage T1a vs. T4, 0.920 vs. 0.500 ; N stage N0 vs. N2, 0.780 vs. 0.403 ; pneumonectomy vs. others, 0.306 vs. 0.772 ; received adjuvant chemotherapy vs. not, 0.599 vs. 0.784).

Multivariate analysis of overall recurrence revealed that T stage ($P=0.045$), N stage ($P=0.044$), and LVI [$P<0.001$, hazards ratio (HR): 4.76 , 95% confidence interval: 2.08 - 10.90] were independent predictors of overall recurrence. Pathologic stage ($P=0.068$) showed borderline significance. Gender, age, histologic type, surgical procedure, adjuvant chemotherapy were not statistically significant ($P=0.562$, 0.603 , 0.739 , 0.124 , and 0.748 respectively). Among these, there was a substantial decrease in the statistical support

for an association between surgical procedure and RFI compared to the univariate analysis. On multivariate analysis of locoregional recurrence, only pathologic stage ($P=0.005$) was significant. Histologic type, and surgical procedure ($P=0.081$ and 0.079 , respectively) showed borderline significance. Gender, age, T stage, N stage, LVI, and adjuvant chemotherapy did not show statistical significance ($P=0.386$, 0.110 , 0.351 , 0.549 , and 0.813 , respectively). LVI and T stage were demonstrated to be the significant factors affecting distant recurrence ($P<0.001$, $P=0.040$, respectively). Gender, age, histologic type, N stage, surgical procedure, and adjuvant chemotherapy did not show statistical significance ($P=0.192$, 0.877 , 0.273 , 0.686 , 0.375 , and 0.748 , respectively). Pathologic stage could not be included in this analysis because it did not converge. Results of multivariate analyses are summarized in *Table 3*.

On the analysis with Fisher's exact test, there was no preferred initial recurrence location that showed statistical significance on LVI positive cases.

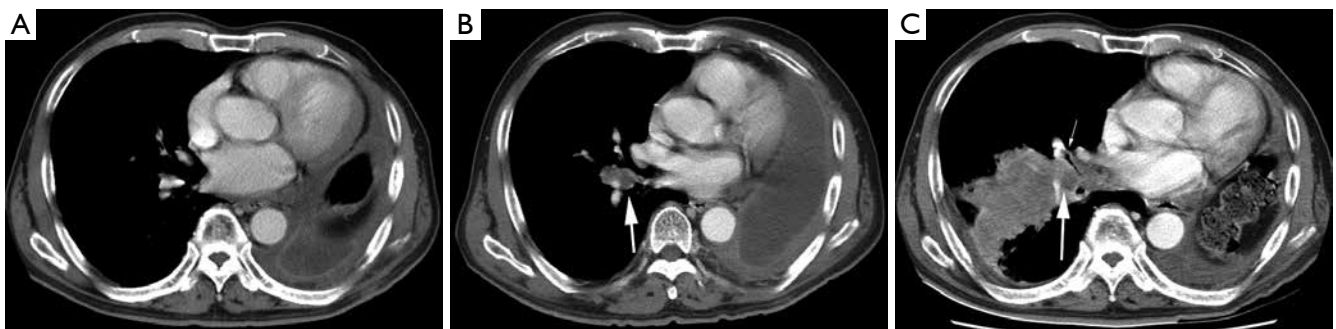


Figure 2 Recurred squamous cell carcinoma in a 69-year-old man. Patient underwent left pneumonectomy with lymph node dissection. Pathologic stage was IIA and LVI was pathologically confirmed. (A) Mediastinal window of enhanced CT scan obtained at the level of RML bronchus 3 months after the surgery shows no evidence of recurrence; (B) follow-up CT scan obtained at similar level 8 months after the surgery shows lymph node recurrence in right interlobar area (arrow); (C) follow-up CT scan 12 months after the surgery revealed aggravated lymph node metastasis (big arrow) with right middle lobar bronchus narrowing (small arrow) and right lower lobe obstructive pneumonitis.

Table 3 Multivariate analyses for overall, locoregional and distant recurrence in all patients (n=171)

Factors	Overall recurrence		Locoregional recurrence		Distant recurrence	
	Hazard ratio	P value	Hazard ratio	P value	Hazard ratio	P value
Gender		0.562		0.386		0.192
Age		0.603		0.110		0.877
Histologic type		0.739		0.081		0.273
Pathologic stage		0.068		0.005		(-)
IA			1			
IB			2.15 (0.63-7.40)			
IIA			1.81 (0.40-8.19)			
IIB			3.21 (0.65-15.85)			
IIIA			8.97 (2.67-30.18)			
T stage		0.045		0.351		0.040
T1a	1				1	
T1b	1.82 (0.58-5.73)				7.93 (0.88-71.57)	
T2a	2.63 (0.63-11.00)				11.38 (1.51-85.70)	
T2b	0.73 (0.07-7.41)				8.49 (0.77-94.03)	
T3	1.97 (0.31-12.63)				7.21 (0.81-64.48)	
T4	0.03 (0.00-1.09)				5.58 (0.33-94.55)	
N stage		0.044		0.549		0.686
N0	1					
N1	0.25 (0.04-1.58)					
N2	0.03 (0.00-0.44)					
LVI		<0.001		0.566		<0.001
Negative	1				1	
Positive	4.76 (2.08-10.90)				7.18 (2.74-18.81)	
Surgical procedure		0.124		0.079		0.375
Adjuvant CTx		0.748		0.813		0.748

Numbers in parentheses are 95% CIs. Adenoca, adenocarcinoma; SqCC, squamous cell carcinoma; LVI, lymphovascular invasion; Pn, pneumonectomy; CTx, chemotherapy.

Discussion

There are some reports that radiation therapy in patients with early stage recurrence can increase survival rate (2,9,10). Considering that the postoperative recurrence rate for NSCLC has been reported to be as high as 52% (2), early detection of recurrence is critical to allow effective local treatment. Pathologic staging is known as the most powerful prognostic factor for lung cancer (11). According to the retrospective study of Sawada *et al.*, the combination of T stage, N stage, and LVI was correlated with the risk of recurrence (4). Another study identified pneumonectomy as a significant variable, although the authors attributed this to technical advancement (12). In the current study, we evaluated these parameters as independent factors that could be associated with NSCLC recurrence.

T stage, N stage, and LVI had a significant impact on the overall recurrence rate in multivariate analysis, consistent with previous studies (4,11,12). Surgical procedure was a significant factor in univariate analysis of overall recurrence and showed borderline significance on the Mann-Whitney U test. That was probably due to confounding effects of other clinicopathologic factors, as there was a substantial decrease in significance in multivariate analysis of overall recurrence. However, further evaluation is warranted considering the results of a previous study (12).

One of the reasons why the risk of local recurrence is poorly defined is that the definition of locoregional recurrence varies widely among studies. Martini and colleagues defined local recurrence as evidence of tumor within the same lung or at the bronchial stump, and regional recurrence as clinically or radiologically manifest disease in the mediastinum or in the supraclavicular lymph nodes (13). Kelsey *et al.* (7) and Higgins *et al.* (6) defined it as disease recurrence at the surgical resection margin, ipsilateral hilum, or mediastinum. This definition was adopted for practical reasons as it includes typical radiation fields in a postoperative setting (7). Although the temporal relation between locoregional and distant recurrence is uncertain in concurrent cases, it can be assumed that locoregional recurrence occurred first, and might be the cause of the distant recurrence (7). Therefore, we counted locoregional recurrence and concurrent distant recurrence separately, despite the fact that local treatment such as surgery or radiation therapy cannot be used in such cases. In the study of Jang and colleagues (8), the locoregional pattern differed significantly according to histologic type.

Its borderline significance in multivariate analysis of locoregional recurrence in this study ($P=0.081$) may be consistent with the results of the previous study.

Vessel invasion has already been demonstrated to be a prognostic pathological marker for survival in breast, colorectal, and head and neck cancers (14). Although LVI is not included in the TNM staging system currently used, several recent studies reported LVI as an adverse prognostic factor for NSCLC recurrence (4-6,14,15). Higgins *et al.* reported LVI as an adverse prognostic factor for the development of distant recurrence in their study of the patients with NSCLC stage IA to IIIB (6). In the current study, we demonstrated that LVI had a significant association with high distant recurrence rate ($P<0.001$) in contrast to other pathological factors. This result is consistent with the previous study of Higgins and colleagues (6).

In this study, the result of distant recurrence include T stage as a significant independent factor, which is in agreement with the study of Hung *et al.* (16), which concludes that T stage increases the risk of distant metastasis on stage I NSCLC. However, further study with NSCLC of advanced stages is warranted as this study targets all operable stages.

The retrospective study of Al-Alao and colleagues of 457 patients with stage I and II NSCLC identified lymphatic vessel invasion, excluding intratumoral vascular invasion, as a significant predictor of early tumor recurrence (14). Univariate analysis revealed a significant difference in 5-year disease-free survival according to the presence or absence of LVI. Shiono *et al.* studied 547 patients with stage II to IV NSCLC and reported LVI as an independent significant factor for earlier recurrence by demonstrating a significant difference in postoperative recurrence survival on univariate analysis (17). We included all operable stages of NSCLC in our study and defined LVI as tumor cells or emboli in at least one lymphatic or blood vessel. We found a 3-fold difference between the 2-year recurrence-free survival of the LVI positive and negative groups, which was statistically significant (44.6% vs. 14.9%, $P<0.001$). This finding is consistent with that of previous studies (14,17). Considering this result and identification of LVI as a significant prognostic factor for overall recurrence in multivariate analysis, the significantly shorter mean RFI of the LVI positive group than that of the LVI negative group on the Mann-Whitney U test was expected. The lack of significance of other factors that were significant in multivariate analysis of overall recurrence (pathologic stage,

T stage, and N stage) indicates that LVI may be one of the factors explaining the high incidence of recurrence within 2 years in NSCLC patients treated by curative surgery (3,18). Therefore, detection of LVI may form the basis for adjuvant therapy (14) and meticulous radiologic follow-up during the early postoperative period in patients with any operable stage of primary NSCLC.

In our study, there was no significantly preferred initial recurrence location on LVI positive cases. This is probably because lymphatics and blood vessels might be reservoir of viable tumor cells and common route for tumor spread.

The limitations of this study are as follows. As immunohistochemical stainings were not performed in all cases, the underestimation of LVI and PNI was inevitable. However, the definitions of LVI and PNI were identical to several previous studies (5,7,14,15). Because this retrospective study was carried out on a relatively small group of patients within a single institution, statistical power to make universal conclusions is lacking (14). Pathologic stage could not be included in multivariate analysis of distant recurrence. That was due to the small number of patients although sufficient patients were analyzed to be able to demonstrate a relationship between LVI and high distant recurrence rate. However, pathologic stage did not appear to be a confounding factor; Kaplan-Meier analysis of the association between LVI and distant recurrence stratified according to pathologic stage was highly significant ($P<0.001$) and was not significantly associated with distant recurrence ($P=0.215$). Further studies with larger numbers of patients are warranted. Additionally, more than half of the cases were stage I cases, indicating that our findings may not be widely generalized. Absence of survival analysis was also a limitation of this study, although it is known that the prognosis of patients with NSCLC recurrence after surgery is poor (19).

In conclusion, T and N stages were significantly related to overall recurrence, and pathologic TNM staging showed borderline significance for overall recurrence, consistent with previous studies (4,11,12). LVI was associated with both high overall and distant recurrence rates, as well as early tumor recurrence after curative surgery for NSCLC. Meticulous radiologic follow-up might be helpful for LVI positive cases.

Acknowledgements

Disclosure: The authors declare no conflict of interest.

References

1. Yamazaki K, Sugio K, Yamanaka T, et al. Prognostic factors in non-small cell lung cancer patients with postoperative recurrence following third-generation chemotherapy. *Anticancer Res* 2010;30:1311-5.
2. Zimmermann FB, Molls M, Jeremic B. Treatment of recurrent disease in lung cancer. *Semin Surg Oncol* 2003;21:122-7.
3. Colice GL, Rubins J, Unger M, et al. Follow-up and surveillance of the lung cancer patient following curative-intent therapy. *Chest* 2003;123:272S-83S.
4. Sawada S, Yamashita N, Suehisa H, et al. Risk factors for recurrence after lung cancer resection as estimated using the survival tree method. *Chest* 2013;144:1238-44.
5. Yilmaz A, Duyar SS, Cakir E, et al. Clinical impact of visceral pleural, lymphovascular and perineural invasion in completely resected non-small cell lung cancer. *Eur J Cardiothorac Surg* 2011;40:664-70.
6. Higgins KA, Chino JP, Ready N, et al. Lymphovascular invasion in non-small-cell lung cancer: implications for staging and adjuvant therapy. *J Thorac Oncol* 2012;7:1141-7.
7. Kelsey CR, Marks LB, Hollis D, et al. Local recurrence after surgery for early stage lung cancer: an 11-year experience with 975 patients. *Cancer* 2009;115:5218-27.
8. Jang KM, Lee KS, Shim YM, et al. The rates and CT patterns of locoregional recurrence after resection surgery of lung cancer: correlation with histopathology and tumor staging. *J Thorac Imaging* 2003;18:225-30.
9. Jeremic B, Shibamoto Y, Milicic B, et al. External beam radiation therapy alone for loco-regional recurrence of non-small-cell lung cancer after complete resection. *Lung Cancer* 1999;23:135-42.
10. Kagami Y, Nishio M, Narimatsu N, et al. Radiotherapy for locoregional recurrent tumors after resection of non-small cell lung cancer. *Lung Cancer* 1998;20:31-5.
11. Hashizume S, Nagayasu T, Hayashi T, et al. Accuracy and prognostic impact of a vessel invasion grading system for stage IA non-small cell lung cancer. *Lung Cancer* 2009;65:363-70.
12. Ichinose Y, Kato H, Koike T, et al. Overall survival and local recurrence of 406 completely resected stage IIIa-N2 non-small cell lung cancer patients: questionnaire survey of the Japan Clinical Oncology Group to plan for clinical trials. *Lung Cancer* 2001;34:29-36.
13. Martini N, Bains MS, Burt ME, et al. Incidence of local recurrence and second primary tumors in resected stage I lung cancer. *J Thorac Cardiovasc Surg* 1995;109:120-9.

14. Al-Alao BS, Gately K, Nicholson S, et al. Prognostic impact of vascular and lymphovascular invasion in early lung cancer. *Asian Cardiovasc Thorac Ann* 2014;22:55-64.
15. Yanagawa N, Shiono S, Abiko M, et al. Prognostic impact and initial recurrence site of lymphovascular and visceral pleural invasion in surgically resected stage I non-small-cell lung carcinoma. *Eur J Cardiothorac Surg* 2013;44:e200-6.
16. Hung JJ, Jeng WJ, Hsu WH, et al. Predictors of death, local recurrence, and distant metastasis in completely resected pathological stage-I non-small-cell lung cancer. *J Thorac Oncol* 2012;7:1115-23.
17. Shiono S, Kanauchi N, Yanagawa N, et al. Stage II-IV lung cancer cases with lymphovascular invasion relapse within 2 years after surgery. *Gen Thorac Cardiovasc Surg* 2014;62:112-8.
18. Bogot NR, Quint LE. Imaging of recurrent lung cancer. *Cancer Imaging* 2004;4:61-7.
19. Saisho S, Yasuda K, Maeda A, et al. Post-recurrence survival of patients with non-small-cell lung cancer after curative resection with or without induction/ adjuvant chemotherapy. *Interact Cardiovasc Thorac Surg* 2013;16:166-72.

Cite this article as: Park C, Lee IJ, Jang SH, Lee JW. Factors affecting tumor recurrence after curative surgery for NSCLC: impacts of lymphovascular invasion on early tumor recurrence. *J Thorac Dis* 2014;6(10):1420-1428. doi: 10.3978/j.issn.2072-1439.2014.09.31

The role of red blood cell distribution width in mortality and cardiovascular risk among patients with coronary artery diseases: a systematic review and meta-analysis

Chang Su^{1*}, Li-Zhen Liao^{2*}, Yan Song³, Zhi-Wei Xu³, Wei-Yi Mei⁴

¹Department of Hematology, the First Affiliated Hospital, Sun Yat-sen University, Guangzhou 510080, China; ²Department of Health, Guangdong Pharmaceutical University, Guangzhou Higher Education Mega Center, Guangzhou 510080, China; ³Department of Pathophysiology, Zhongshan Medical College, Sun Yat-sen University, Guangzhou 510080, China; ⁴Department of Cardiology, Huangpu Division of the First Affiliated Hospital, Sun Yat-Sen University, Guangzhou 510080, China

*These authors contributed equally to this work.

Correspondence to: Wei-Yi Mei, Ph.D. Department of Cardiology, Huangpu Division of the First Affiliated Hospital, Sun Yat-Sen University, Guangzhou 510080, China. Email: mwy_medicine@163.com; Zhi-Wei Xu, Ph.D. Department of Pathophysiology, Zhongshan Medical College, Sun Yat-sen University, 74 Zhongshan Second Road, Guangzhou 510080, China. Email: xuzhiwei19810115@163.com.

Background: Red cell distribution width (RDW) might be a novel biomarker that reflects multiple physiological impairments related to atherosclerosis and coronary artery diseases (CAD). We conducted this systematic review and meta-analysis to evaluate the association of RDW between all-cause mortality and fatal/non-fatal cardiovascular disease (CVD) events in CAD patients.

Methods: Relevant studies were searched and identified in the MEDLINE and EMBASE databases. English-language prospective studies that reported risk estimates for RDW and mortality/CVD events were included. Data were extracted regarding the characteristics and clinical outcomes, and a quality assessment was conducted. Results were extracted for the highest versus lowest RDW level, and meta-analyses were carried out using random effects models.

Results: We identified 22 studies enrolling 80,216 participants. The study duration ranged between 1 month and 23 years. Of the 15 studies that were included in the meta-analysis, higher RDW indicated a significant increased risk for all-cause mortality in CAD patients: pooled risk ratio (RR) 2.20 (95% CI, 1.42-3.39; $P < 0.0004$). The results for fatal, non-fatal and fatal/non-fatal events were: pooled RR 1.80 (95% CI, 1.35-2.41; $P < 0.0001$), RR 1.86 (95% CI, 1.50-2.31; $P < 0.00001$) and RR 2.13 (95% CI, 1.20-3.77; $P = 0.01$). Heterogeneity was moderately present; however, sensitivity analyses for follow-up duration, CAD subtype, or RDW as dichotomous values showed similar results.

Conclusions: The meta-analysis indicates that higher RDW levels are associated with increased risk of mortality and CVD events in patients with established CAD.

Keywords: Red cell distribution width (RDW); coronary artery diseases (CAD); mortality; cardiovascular (CV); meta-analysis

Submitted Jul 27, 2014. Accepted for publication Aug 14, 2014.

doi: 10.3978/j.issn.2072-1439.2014.09.10

View this article at: <http://dx.doi.org/10.3978/j.issn.2072-1439.2014.09.10>

Brief summary

The red cell distribution width (RDW) is a quantitative measure of the size variation of circulating erythrocytes. Of note, RDW might be a novel biomarker that reflects multiple physiological impairments related to atherosclerosis and coronary artery disease. However, conflicting findings have been reported on the association of RDW with risk of subsequent cardiovascular (CV) events. We therefore conducted this systematic review and meta-analysis to synthesize all available evidence of prospective studies on this interesting issue.

Introduction

RDW is a quantitative measure of the size variation of circulating erythrocytes with higher values reflecting greater heterogeneity in cell sizes (1). RDW is routinely reported to physicians in clinical practice as part of the automated complete blood count (CBC), which mainly served as an auxiliary index in the differential diagnosis of microcytic anemia (2).

In addition to its traditionally known role, RDW is of interest for its potential impact on cardiovascular disease (CVD) and mortality risk in general population (3-5). A previous meta-analysis and prospective studies have showed that higher RDW, even within the normal reference range, was strongly associated with increased risk of death and CVD risk in community-dwelling adults (3-5). Of note, RDW significantly improved mortality risk prediction beyond established risk factors, as assessed by several indices of model calibration and discrimination. Although the exact mechanisms are unclear, this association is provocative because it is independent of numerous factors, including nutritional status, anemia, inflammation, and others comorbidity diseases. Hence, it is possible that RDW is a novel biomarker that reflects multiple physiological impairments related to atherosclerosis and coronary artery diseases (CAD).

However, conflicting findings have been reported on the association of RDW with risk of subsequent CVD events during prospective follow-up of individuals with established CAD (3-5). With implications for drug development and secondary prevention, the pathogenesis of first and subsequent CVD events may not be precisely equivalent. We therefore conducted this systematic review and meta-analysis to synthesize all available evidence of prospective studies that report the association of RDW in relation to all-cause mortality and fatal/non-fatal CVD events in patients with prior CAD.

Methods

A prospective protocol of objectives, literature-search strategies, inclusion and exclusion criteria, outcome measurements, and methods of statistical analysis was prepared a priori according to the Preferred Reporting Items for Systematic Reviews and Meta-Analyses (PRISMA) Statement and the Meta-analysis of Observational Studies in epidemiology (MOOSE) guideline (6,7).

Search strategy

Study data were obtained through the following ways: searching on PubMed (1948 to January 2013), EMBASE (1948 to January 2013) and Cochrane Library database included terms “red blood cell distribution width”, “mortality” and “CV events” and their corresponding index words using the special features in titles and/or abstracts. Only human studies were included. To identify further potentially relevant studies missed by the electronic database search, reference lists of identified trials and review reports were manually screened and searches are based on English language only. In addition, we verified the search strategy by hand-searching the reference lists of primary studies, review articles, and clinical guidelines. Email-alerts with newly published articles from MEDLINE were checked until October 1, 2013.

Inclusion and exclusion criteria

Inclusion criteria were the following: (I) serum or plasma RDW was the determinant; (II) outcomes: all-cause mortality, fatal and/or non-fatal CV events such as CV death, myocardial infarction (MI), stroke, heart failure (HF) and readmission; (III) paper type: original prospective quantitative cohort study (i.e., no review, commentary, case reports, editorial); (IV) study performed in participants ≥ 18 years. We excluded studies that did not report any of the outcomes mentioned above. The titles and abstracts of studies identified by the search strategy were independently screened by two reviewers (L.Z.L. and C.S.). Differences between authors were resolved by consensus or by consultation of an additional reviewer (X.Z.W.).

Quality assessment and data extraction

A quality checklist was developed to determine the quality of the eligible studies based on the PRISMA Statement and the MOOSE guideline in combination with a previously

Table 1 Quality checklist based on the PRISMA Statement and the MOOSE guideline

Selection bias
Is the study population clearly described in terms of age, gender, and setting?
Is the percentage of eligible subjects who participated in the study mentioned?
Are participants in the study similar to eligible non-participants, in terms of age, gender, and important disease characteristics?
Were reasons for loss to follow-up presented and assessed during the study for possible systematic attrition? (subjects that did not finish the study)
Information bias
Is a clear description provided of the measurement method?
Are clear definitions of each outcome variable provided?
Statistical analyses
Are statistical analyses adequate to answer the research question?
Were multivariable analyses performed? If yes, continue with question 9
Was it clearly described which variables were included in the (multivariable) model(s)?
Final question
Were there any other important flaws in the design or analyses of the study? If yes, study not included
PRISMA, Preferred Reporting Items for Systematic Reviews and Meta-Analyses; MOOSE, Meta-analysis of Observational Studies in epidemiology.

published quality checklist for observational studies (6-8) (see *Table 1*). Studies were scored based on nine quality criteria on a binary scale; including description of characteristics of the study population, assessment of exposure and outcome, confounding and potential flaws. The quality of each study was independently assessed by Y.S and W.Y.M and scores were compared for each item of the checklist. The scores were summed and quality was considered poor [0-4], moderate [5-6], or good [7-9]. Studies with potential flaws or rated as poor quality were not included.

Of the eligible studies, information including first author, years of follow-up, country of origin, name of the study, number of participants, participants' characteristics, determination of outcome, RDW concentrations and category, and outcome measures were recorded. When the report did not contain sufficient details to adjudicate the validity of the study, or outcome data were missing, attempts were made to contact the authors by email and in writing.

Data synthesis and statistical methods

Results reported as count data were presented for all-cause mortality, fatal CVD events and non-fatal CVD events: adjusted hazard ratio (HR), odd ratio (OR) or regression

coefficients (β) and 95% confidence interval (CI). We extracted the results of the highest versus lowest RDW concentrations and used the lowest RDW category as the reference. If the study reported more than one estimate, only the result of the largest RDW difference was included. We transformed risk estimates by taking their natural logarithms and calculated the standard errors as follows: $(\ln \text{upper limit} - \ln \text{HR})/1.96$. We weighted the natural logarithm of the risk estimates by generic inverse variance to account for the sample size and distribution of the included studies (9).

We used Review Manager 5.2 (The Cochrane Collaboration, Oxford, United Kingdom) to analyze the collected data. The results of the included studies were pooled and meta-analyses were carried out using fixed or random-effects models. Statistical heterogeneity between studies was assessed using the chi-square test with significance set at $P < 0.10$ and heterogeneity was quantified using the I^2 statistic. I^2 values represent the proportion of total variation attributable to heterogeneity rather than chance whereby 0% is no observed heterogeneity and 100% maximal heterogeneity.

Potential publication bias was evaluated by visual inspection of a funnel plot. A priori sensitivity analyses were defined to evaluate the stability of the pooled estimates and to examine changes in results after excluding specific

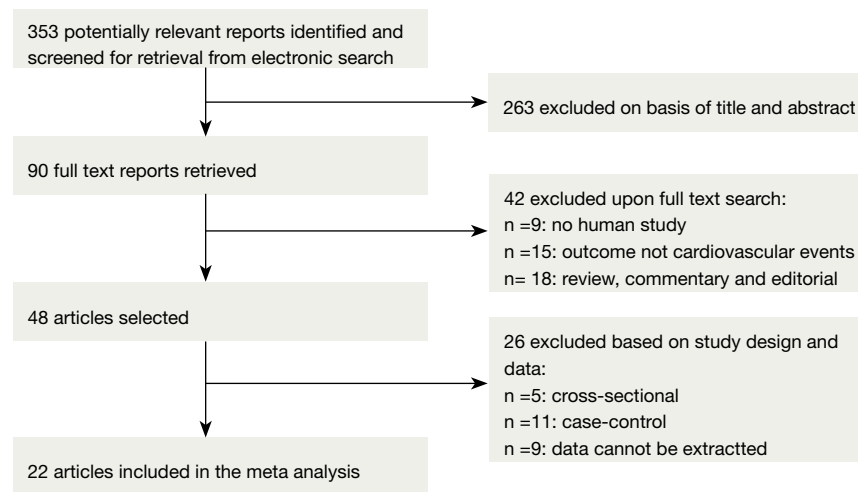


Figure 1 Flow diagram of the study selection process.

studies. The subgroup analyses were preplanned for: length of follow-up >4 years, subtype of CAD [acute coronary syndrome (ACS), coronary artery bypass grafting (CABG) and percutaneous coronary intervention (PCI)] and RDW as dichotomous values. The authors had full access to the data and take responsibility for its integrity. All authors have read and agreed to the manuscript as written.

Results

Search results

The systematic literature search yielded 353 potentially relevant articles. *Figure 1* shows the flow diagram for the identification process. Briefly, 263 articles were excluded based on title and abstract. The remaining 90 studies were identified in full-text; 42 studies were excluded for study type and outcome. Then, another 26 studies were excluded based on study design (n=5 cross-sectional, n=11 case-control, n=9 data cannot be extracted). The hand search did not result in any additional articles. The email alerts yielded in two additional studies. Twenty-two studies were eligible for quality assessment and ranked according to their sum scores (see *Table 1*), of which 20 studies were graded as “good” and 2 as “moderate” quality. Agreement between the two reviewers was 97% for study selection and 96% for quality assessment of trials.

Study characteristics

Table 2 represents the main characteristics and results of the

included studies on mortality and CVD events. Of the 22 studies (10-30), 15 investigated the relation between RDW and all-cause mortality, four and eight investigated fatal and non-fatal CVD events, respectively. Six studies investigated the relation between RDW and fatal and/or non-fatal CVD events. The total number of participants was 80,216. The population sizes of the studies, all published between 2007 and 2014, varied between 100 and 29,526. The mean study duration ranged between 1 month and 23 years. Overall, 22 different cohorts were used of which one included only men (12). Ten cohorts were conducted in Asia, six in the United States and four in Europe; mean age ranged between 55.6 and 66.6 years. Risk estimates (HRs/ORs), regression coefficients, and 95% CI were reported in 15 studies for RDW levels (highest *vs.* lowest) or dichotomous cut-off values of RDW, which were include in the subsequent meta-analysis. Additionally, risk estimates of RDW were reported as a continuous variable in seven studies.

RDW and all-cause mortality

Of the 15 studies that were included in the meta-analysis, all studies reported positive associations between high RDW concentrations and all-cause mortality, except one studies reported negative association (16). In the meta-analysis, the summary estimates for the highest compared with lowest category of baseline RDW indicated a significant increased risk for all-cause mortality in CAD patients: pooled risk ratio (RR) 2.20 (95% CI, 1.42-3.39; $P < 0.0004$) (*Figure 2*). Heterogeneity was relatively high present ($I^2 = 93\%$).

Table 2 Characteristics of studies included in the systemic review and meta-analysis

Study year	Follow-up/year	Country	Type of CAD	Patients	Mean age/year	Male (%)	Measurement outcomes	RDW levels	Results HR (95% CI)	Adjustments	Quality scores
Bekler 2014 (10)	1.5	Turkey	NSTE-ACS	237	61.1±11.9	75.5	CV death	14.1	1.55 (1.16-2.06)	Na	6/moderate
Benedetto 2013 (11)	11.8±4.1	Italy, United Kingdom	Isolated CABG	8,340	64.4±12.6	80.2	All-cause late death after discharge	12.9-13.4-14	2.91 (1.05-4.81)	Age; BMI <18.5 and >30 kg/m ² , GFR; chronic lung disease; diabetes, extracardiac arteriopathy; LV function	9/good
Cavusoglu 2010 (12)	2	US	CAG patients	389	65.6±10.0	100	All-cause mortality	14.4	2.69 (1.5-4.84)	Elderly status, high hs-CRP, presence of anemia, impaired LV function	8/good
Dabbah 2010 (13)	2.25	Israel	Patients with AMI	1,709	61.2±12.6	78.2	All-cause mortality; readmission	12.8-13.2-13.7-14.3	2.8 (1.6-4.7)	Age, gender, previous infarction, heart failure, history of diabetes, hypertension, smoking status, serum creatinine, anterior location of infarction, ST-elevation infarction, Killip class at admission, thrombolytic therapy, primary angioplasty, medical therapy, LVEF, baseline HB, and MCV	9/good
Tsuboi 2013 (14)	3.9	Japan	Stable CAD	560	66.6±10.2	80	All-cause mortality	12.1-13.1-14.2	2.66 (1.14-6.94)	Na	8/good
Lee 2013 (15)	1	Korea	AMI	5,196	64.5±11.9	67.3	MACE defined as death, non-fatal MI	12.6-13.1-13.9	6.18 (2.1-18.21)	Sex, age, HB, BMI, prior coronary heart disease, hypertension, diabetes mellitus, serum creatinine, total cholesterol, PCI, antiplatelet agents, β-blockers, and ACEI/arbs	9/good
Nabais 2009 (16)	0.5	Portugal	Patients with ACS	1,796	64.0±13.0	77.9	Death or MI	12.8-13.6	1.35 (0.86-2.11)	Age, renal failure, LVEF, Killip class, systolic blood pressure, heart rate, history of PCI	9/good
Ephrem 2013 (17)	3.8	US	NSTE-ACS patients	543	65.0±3.0	56	Readmission	16.3	1.35 (1.02-1.79)	Age, sex, race, type of insurance, creatinine, heart failure, hypertension, diabetes, and length of stay	9/good
Poludasu 2009 (18)	3.1±4.4	USA	PCI pts	859	62.2±10.4	49.4	Mortality	13.3-15.7	0.97 (0.33-2.87)	Na	7/good

Table 2 (continued)

Study year	Follow-up/year	Country	Type of CAD	Patients	Mean age/year	Male (%)	Measurement outcomes	RDW levels	Results HR (95% CI)	Adjustments	Quality scores
Tonelli 2008 (19)	4.96	CARE study	Hyperlipidemia and MI	4,111	58.6±9.3	59.7	MACE (death, MI, stroke, HF)	12.6-13.4-13.8	1.78 (1.28-2.47)	Age; sex; race; smoking status; diabetic status; use of failure, hypaceis, aspirin, and pravastatin; GFR; proteinuria on dipstick urinalysis; systolic and diastolic blood pressure; HB; waist to hip circumference ratio; LVEF; fasting glucose; LDL-C; HDL-C; total cholesterol; and MCV.	9/good
Wang (20)	2011 1 mon	Chinese	ACS	1,654	64.9±11.9	58.1	Cardiac death, HF, recurrent infarction	12.1-12.8-13.3	2.116 (1.427-2.137)	Age, gender, history of hypertension and diabetes, smoking status, BNP, LVEF, BMI, AMI on presentation, serum creatinine, peak CPK, number of diseased vessels, Troponin-I, hs-CRP, HB and medical therapy.	8/good
Isik (21)	2012 0.5	Turkey	STEMI patients with primary PCI	100	61.3±12.8	77	Cardiovascular mortality	14	mid-term mortality 5.89 (1.63-21.24)	Age, sex, HB, hypertension, previous CAD, basal CK-MB, hs-CRP and d hyperten	7/good
Warwick 2013 (22)	5.8	UK	Isolated CABG patients	8,615	64.9±9.0	80.4	In-hospital mortality and long-term survival	13.5-14.2-15.3	1.05 (1.02-1.07)	Age; sex; race; smoking status; diabetic status; use of β-blockers, aceis, aspirin, and pravastatin; GFR; proteinuria on dipstick urinalysis; systolic and diastolic blood pressure; HB; serum phosphate; waist to hip circumference ratio; LVEF; serum triglyceride; LDL-C; HDL-C; total cholesterol; and MCV	9/good
Anderson 2007 (23)	4.9±3.1	IHC study	Suspected CAD	29,526	61.1±14.7	62	All-cause mortality	12.6-13.3-14	3.0 (2.3-3.9)	Na	8/good
Uyarel 2011 (24)	1.8±1.3	Turkey	Primary PCI for STEMI	2,506	55.6±11.8	82.8	Mace	14.8	1.831 (1.034-3.24)	Sex, age, time to reperfusion, DM, hypertension, smoking habit, GFR, multivessel disease, unsuccessful procedure, anterior MI, admission anemia, transfusion	9/good
Azab (25)	2011 4	USA	NSTEMI	619	64.5±11.9	67.4	All-cause mortality	>14	1.104 (1.004-1.214) per 1 unit	Appropriate GRACE score, HB, serum glucose, LDL, LVEF, use of statin, use of aspirin, use of clopidogrel, prior CABG, prior coronary angioplasty and in-hospital bypass surgery	8/good

Table 2 (continued)

Table 2 (continued)

Study year	Follow-up/year	Country	Type of CAD	Patients	Mean age/year	Male (%)	Measurement outcomes	RDW levels	Results HR (95% CI)	Adjustments	Quality scores	
Ren (26)	2013	1	Chinese	Stable angina	1,442	59.8±5.4	62.1	Mortality/ACS	11.7-12.5-13.1	1.544 (1.058-3.216) per quintiles	Age, gender, history of hypertension, diabetes or arrhythmia, the smoking status, BMI, blood pressure, the levels of serum creatinine, glucose, lipids, ALT, AST, hs-CRP and HB, number of diseased vessels, BNP level, the white blood cell count, an LVEF	9/good
Yao (27)	2014	2.41	Chinese	CAD DES-PCI	2,169	60.2±10.9	67.7	MACE	12.27-13-13.5	1.37 (1.15-1.62)	Age, gender, DM, hypertension, peripheral vascular disease, number of vessels, multivessel disease, prior MI, GFR, LVEF, number of stents implanted, total stent length, and stent diameter	8/good
Osadnik (28)	2013	2.5	Poland	Stable CAD/PCI	2,550	63.9±9.5	70.5	Mortality	13.1-13.6-14.1	1.23 (1.13-1.35) per 1%	Age, sex, heart failure, atrial fibrillation, hypertension, previous MI and PCI, previous CABG, previous stroke, diabetes, lipid abnormalities, obesity, CKD, smoking, NYHA class, heart rate, blood pressure, LVEF, number and type(s) of stent implanted, number of PCI vessels, HB, MCV	8/good
Arbel (29)	2014	3	Israel	CAG pts	3,222	65.6±11.8	72.3	MACE (death, MI, stroke)	13.5	1.12 (1.07-1.18) per 1%	Age, gender and anemia status in addition to conventional cardiovascular risk factors, cardiovascular medications, metabolic variables, inflammatory variables, ACS status	9/good
Patel (30)	2009	2.4±1.0	USA	Suspected CAD	2,584	63.0±11.0	66	All cause death	14.5	1.29 (1.19-1.38) per 1%	Na	7/good
Lappé (30)	2011	8.4±15.2	USA	CAD	1,489	65.5±11.3	74.4	Mortality	13.2	1.37 (1.29-1.46) per quintile	Age, gender, diabetes, hypertension, dyslipidemia, smoking, family history of early CAD, and other risk factors: smoking, family history, hyperlipidemia	8/good

AMI, acute myocardial infarction; ACS, acute coronary syndrome; CAD, coronary artery disease; PCI, percutaneous coronary intervention; MACE, major adverse cardiovascular events; HF, heart failure; CABG, coronary artery bypass grafting; BMI, body mass index; CRP, C-reactive protein; LVEF, left ventricular ejection fraction; NYHA, New York Heart Association; MCV, mean corpuscular volume; HB, hemoglobin; ACEI, angiotensin converting enzyme inhibitor; ARB, angiotensin receptor blocker; LDL-C, low-density lipoprotein cholesterol; HDL-C, high-density lipoprotein cholesterol; BNP, brain natriuretic peptide; CK-MB, creatine kinase-MB; GFR, glomerular filtration rate.

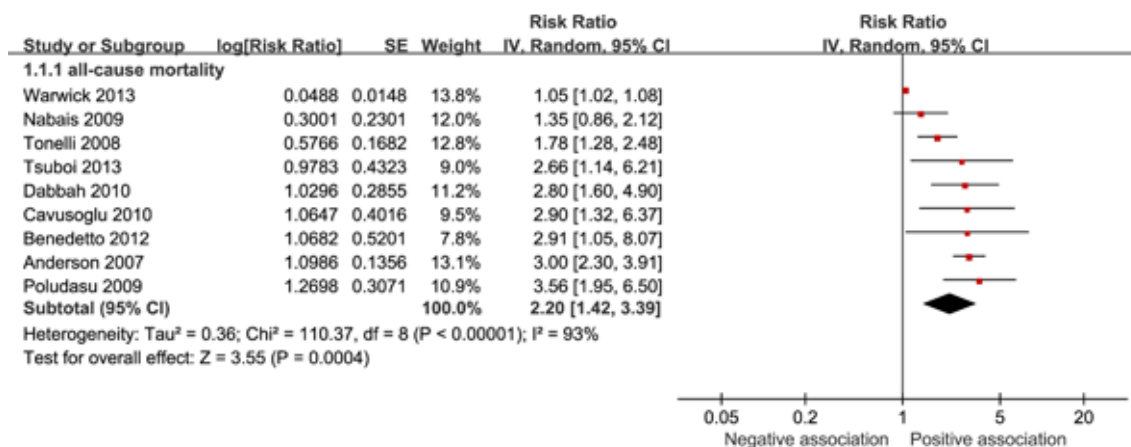


Figure 2 Pooled relative risk of RDW and all-cause mortality of the included studies. Risk ratios (RRs) are shown with 95% CIs. RDW, red cell distribution width.

RDW and fatal/non-fatal CVD events

Four studies investigated excess RDW level and fatal CVD events specifically (10,20,21,26). Eight studies (10,13,16,17,20,21,26,27) investigated high RDW and non-fatal CVD events and three studies (14,15,19,24) reported the association between RDW and fatal/non-fatal CVD events. All studies reported positive associations between high RDW concentrations and fatal CVD events. For non-fatal CVD events, six studies reported positive associations and in two studies (16,17) higher RDW was not significantly associated with non-fatal CVD events. One study reported cardiac events for HF and stroke separately. In the meta-analysis, the pooled estimates for the highest compared with lowest category of baseline RDW indicated a significant increased risk for fatal CVD events: pooled RR 1.80 (95% CI, 1.35-2.41; $P < 0.0001$), with a moderate heterogeneity ($I^2 = 44\%$). The pooled estimate for non-fatal CVD events resulted in a slightly higher association: RR 1.86 (95% CI, 1.50-2.31; $P < 0.00001$), with a low heterogeneity ($I^2 = 28\%$). The pooled estimate for the overall fatal/non-fatal CVD events resulted in a higher association: RR 2.13 (95% CI, 1.20-3.77; $P = 0.01$; $I^2 = 66\%$) (see *Figure 3*).

Publication bias and sensitivity analysis

The funnel plot (*Figure 4*) for studies of RDW and all-cause mortality shows reasonable symmetry at the top of the funnel plot and a little asymmetry at the bottom, which suggest some evidence of publication bias for smaller studies.

The findings were similar whether fixed or random-effects models were used. However, sensitivity analyses for follow-up duration >4 years only marginally changed the results (*Figure 5*). The inclusion of studies with ACS patients attenuated the results; nonetheless, the estimate was still significant: RR 1.91 (95% CI, 0.93-3.89; $P = 0.08$; $I^2 = 75\%$). The inclusion of studies with PCI patients resulted in a more pronounced estimate and negligible heterogeneity: HR 3.23 (95% CI, 1.98-5.27; $P < 0.0001$; $I^2 = 0\%$). No sensitivity analyses were performed for fatal CVD events, because of too few studies.

Discussion

Our study provides the first systematic review and meta-analysis of prospective studies of RDW and total mortality, fatal and non-fatal CVD events in populations with established CAD. The meta-analysis indicates a significant increased risk for RDW excess and all-cause mortality and CVD events that range from 80% to 120%.

Our systematic review and subsequent meta-analysis has several strengths. This first systematic review gives a broad overview of all prospective studies on RDW in relation to all-cause mortality and fatal/non-fatal CVD events, and provides insight in its associated risks. The systematic review and meta-analysis were performed according to the PRISMA Statement and the MOOSE guideline and included a quality assessment—an important component to evaluate the methodological quality (31,32). The quality assessment allowed us to distinguish between poor, moderate and good quality studies and to the selection of

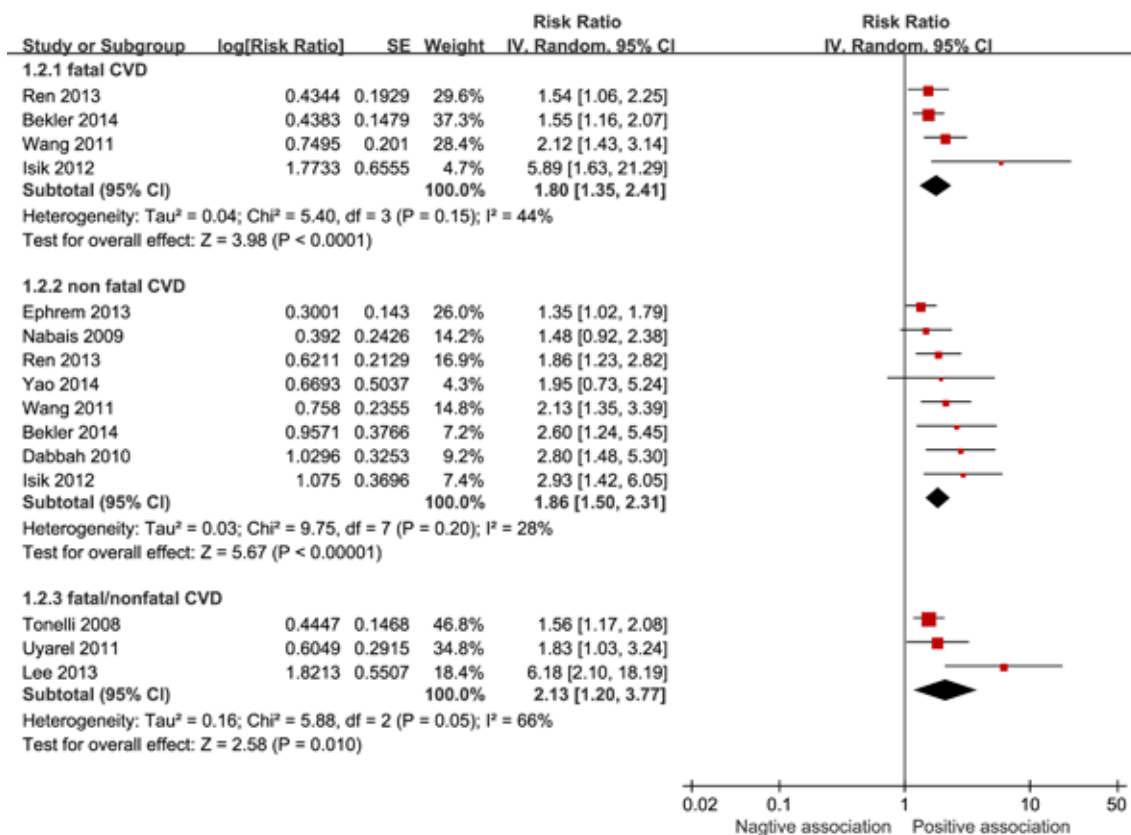


Figure 3 Pooled relative risk of red cell distribution width (RDW) and fatal cardiovascular (CV) events, non-fatal CV events and fatal/non-fatal CV events of the included studies. Risk ratios (RRs) are shown with 95% CIs.

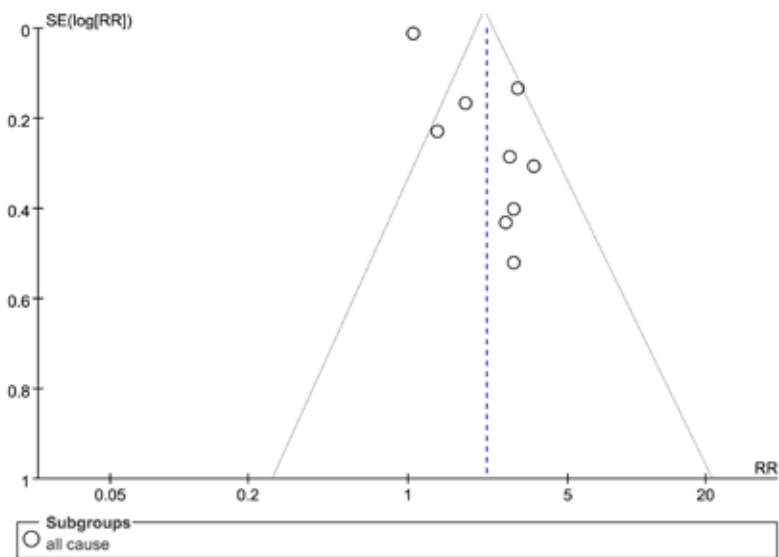


Figure 4 Funnel plot for red cell distribution width (RDW) and all-cause mortality. Each square indicates one study with its standard error indicating the weight of the study and its relative risk. The dotted lines represent 95% CI to visualize the symmetry around the pooled estimate.

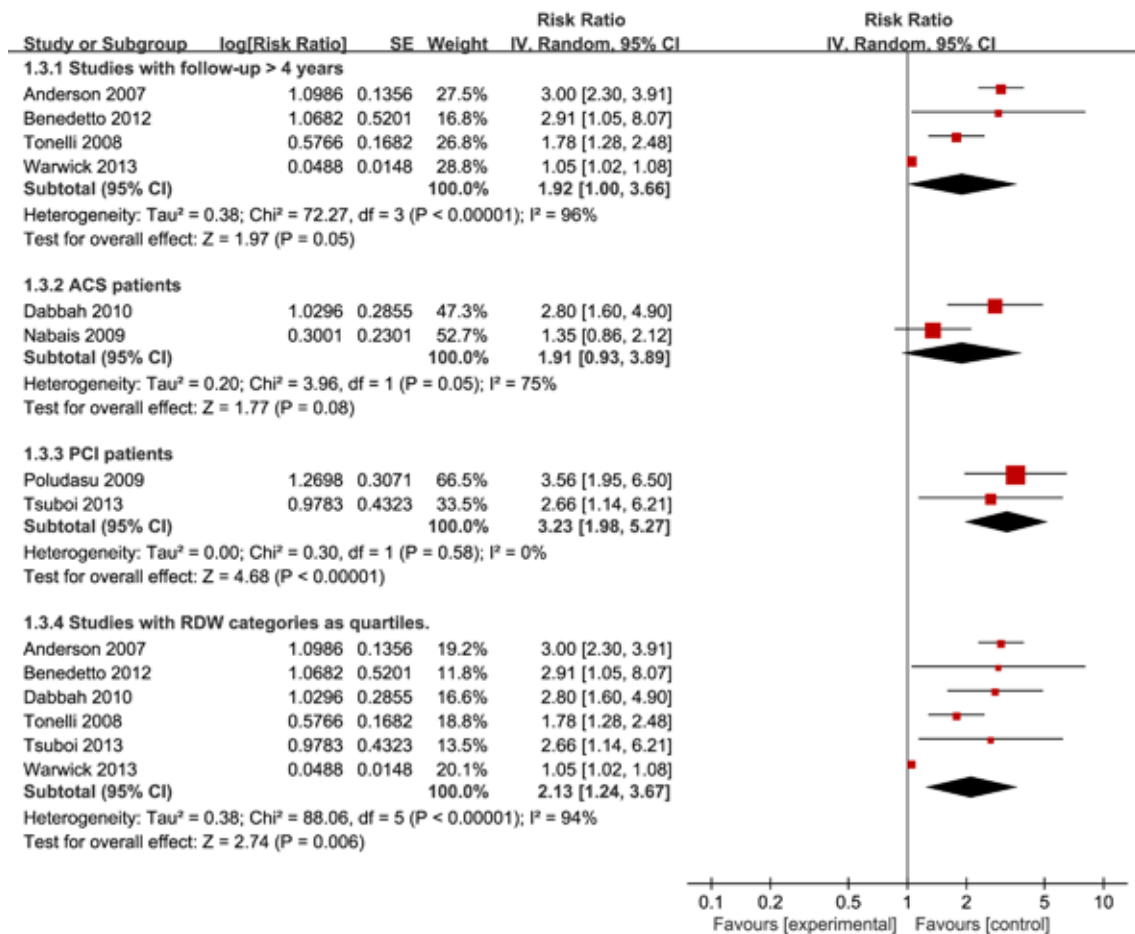


Figure 5 Forest plots of red cell distribution width (RDW) and all-cause mortality of the included studies: studies with follow-up >4 years; B, ACS patients; percutaneous coronary intervention (PCI) patients; studies with RDW categories as quartiles. Risk ratios (RRs) are shown with 95% CIs.

only moderate and good quality studies. This resulted in studies with multivariable adjusted risk estimates and a large number of included CVD cases >80,000. Moreover, the present analysis included only prospective cohort studies and most follow-ups lasted more than 23 years (30), which limits the problem of reverse causation bias.

The meta-analysis of observational studies might be influenced by heterogeneity. The variance between the included studies could partly be due to differences in study populations, RDW assays, outcome definitions, and adjustment for confounders. The use of random-effects models in our analyses adjusts in part for these variances between studies (9). Subgroup analyses were performed to test the stability of the pooled estimates. The positive association between higher RDW concentrations and CVD events was consistent given the similar pooled risk estimates

for total mortality, fatal and non-fatal CVD events in both fixed and random models. This suggests that higher RDW level might be involved in pathological processes that lead to CVD. Of note, the inclusion of studies with PCI patients resulted in a higher HR, which might indicate that PCI patients are more prone to RDW excess and thereby have a higher risk of developing a secondary CVD event.

However, it should be noted that the results of our meta-analysis could not identify whether RDW is a causal factor for CVD. The studies in the meta-analysis used different approaches to define RDW categories. This might have affected our results, although we took into account the result of quartile 4 versus quartile 1 when available and used this approach consistently for all included studies. Sensitivity analyses for RDW and total mortality based on RDW quartiles resulted in a similar estimate than

studies that used dichotomous cut-off values: pooled RR 2.13 (95% CI, 1.24-3.67). RDW cut-off values reflect a smaller difference in RDW concentration between RDW groups compared with RDW quartiles. However, pooling studies that reported cut-off values still showed a significant RR, which suggests that moderate elevations in RDW concentrations could play a role in the development of mortality risk of CAD patients.

Visual inspection of the funnel plot illustrates that studies with a smaller standard error at the top of the funnel plot were more symmetrically distributed than studies with a larger standard error at the bottom of the funnel plot (9). This suggests possible publication bias favoring smaller studies with significant results, which implies that the pooled estimate could be an overestimation of the true association; however, the power to detect publication bias is low given the limited number of studies. In addition, negative studies are less likely to be published and not all endpoints of the included studies were adjudicated and definitions of end points could be different between studies.

Based on the available prospective studies and the absence of randomized controlled trials, this meta-analysis highlights a risk factor for subsequent mortality and CVD events in populations with established CAD. Randomized controlled trials in these persons are therefore warranted to determine whether RDW-modifying therapies could result in less CVD events. It should be noted that lack of a gold standard to measure RDW hampers clinical decision making and treatment for subjects with high RDW concentrations. Nonetheless, more awareness should be given to individuals with a high RDW concentration in CAD populations.

Conclusions

Our meta-analysis supports that higher RDW concentrations are associated with increased risk of subsequent mortality risk and CVD events in established CAD patients. Despite the possibility of some publication bias, the results provide evidence for positive associations considering the quality, direction and magnitude of the associations of the included studies. Future studies should focus on RDW-modifying therapies to give more insight into the underlying mechanisms that might lead to CVD events.

Acknowledgements

This study was supported by National Natural Science

Foundation of China (No.81102709), Technology Planning Project of Guangdong Province in China (2010B031600068 and 2011B031800137), Doctor's Research Fund of Science Education Ministry of China (No.20110171120056). This manuscript has been read and approved by all the authors, the requirements for authorship have been met, everyone who qualifies for authorship has been listed as an author and each author believes that the manuscript represents honest work.

Disclosure: The authors declare no conflict of interest.

References

1. Lippi G, Plebani M. Red blood cell distribution width (RDW) and human pathology. One size fits all. *Clin Chem Lab Med* 2014;52:1247-9.
2. Viswanath D, Hegde R, Murthy V, et al. Red cell distribution width in the diagnosis of iron deficiency anemia. *Indian J Pediatr* 2001;68:1117-9.
3. Patel KV, Ferrucci L, Ershler WB, et al. Red blood cell distribution width and the risk of death in middle-aged and older adults. *Arch Intern Med* 2009;169:515-23.
4. Perlstein TS, Weuve J, Pfeffer MA, et al. Red blood cell distribution width and mortality risk in a community-based prospective cohort. *Arch Intern Med* 2009;169:588-94.
5. Chen PC, Sung FC, Chien KL, et al. Red blood cell distribution width and risk of cardiovascular events and mortality in a community cohort in Taiwan. *Am J Epidemiol* 2010;171:214-20.
6. Liberati A, Altman DG, Tetzlaff J, et al. The PRISMA statement for reporting systematic reviews and meta-analyses of studies that evaluate healthcare interventions: explanation and elaboration. *BMJ* 2009;339:b2700.
7. Stroup DF, Berlin JA, Morton SC, et al. Meta-analysis of observational studies in epidemiology: a proposal for reporting. Meta-analysis Of Observational Studies in Epidemiology (MOOSE) group. *JAMA* 2000;283:2008-12.
8. Stang A. Critical evaluation of the Newcastle-Ottawa scale for the assessment of the quality of nonrandomized studies in meta-analyses. *Eur J Epidemiol* 2010;25:603-5.
9. Reeves BC, Deeks JJ, Higgins JP, et al. Chapter 13: Including non-randomized studies. In: Higgins JPT, Green S. eds. *Cochrane Handbook for Systematic Reviews of Interventions*. Version 5.0.1. Vol. 5. Chichester: The Cochrane Collaboration; 2008.
10. Bekler A, Gazi E, Tenekecioglu E, et al. Assessment of the relationship between red cell distribution width and

- fragmented QRS in patients with non-ST elevated acute coronary syndrome. *Med Sci Monit* 2014;20:413-9.
11. Benedetto U, Angeloni E, Melina G, et al. Red blood cell distribution width predicts mortality after coronary artery bypass grafting. *Int J Cardiol* 2013;165:369-71.
 12. Cavusoglu E, Chopra V, Gupta A, et al. Relation between red blood cell distribution width (RDW) and all-cause mortality at two years in an unselected population referred for coronary angiography. *Int J Cardiol* 2010;141:141-6.
 13. Dabbah S, Hammerman H, Markiewicz W, et al. Relation between red cell distribution width and clinical outcomes after acute myocardial infarction. *Am J Cardiol* 2010;105:312-7.
 14. Tsuboi S, Miyauchi K, Kasai T, et al. Impact of red blood cell distribution width on long-term mortality in diabetic patients after percutaneous coronary intervention. *Circ J* 2013;77:456-61.
 15. Lee JH, Yang DH, Jang SY, et al. Incremental predictive value of red cell distribution width for 12-month clinical outcome after acute myocardial infarction. *Clin Cardiol* 2013;36:336-41.
 16. Nabais S, Losa N, Gaspar A, et al. Association between red blood cell distribution width and outcomes at six months in patients with acute coronary syndromes. *Rev Port Cardiol* 2009;28:905-24.
 17. Ephrem G. Red blood cell distribution width is a predictor of readmission in cardiac patients. *Clin Cardiol* 2013;36:293-9.
 18. Poludasu S, Marmur JD, Weedon J, et al. Red cell distribution width (RDW) as a predictor of long-term mortality in patients undergoing percutaneous coronary intervention. *Thromb Haemost* 2009;102:581-7.
 19. Tonelli M, Sacks F, Arnold M, et al. Relation Between Red Blood Cell Distribution Width and Cardiovascular Event Rate in People With Coronary Disease. *Circulation* 2008;117:163-168.
 20. Wang YL, Hua Q, Bai CR, et al. Relationship between red cell distribution width and short-term outcomes in acute coronary syndrome in a Chinese population. *Intern Med* 2011;50:2941-5.
 21. Isik T, Kurt M, Ayhan E, et al. The impact of admission red cell distribution width on the development of poor myocardial perfusion after primary percutaneous intervention. *Atherosclerosis* 2012;224:143-9.
 22. Warwick R, Mediratta N, Shaw M, et al. Red cell distribution width and coronary artery bypass surgery. *Eur J Cardiothorac Surg* 2013;43:1165-9.
 23. Anderson JL, Ronnow BS, Horne BD, et al. Usefulness of a complete blood count-derived risk score to predict incident mortality in patients with suspected cardiovascular disease. *Am J Cardiol* 2007;99:169-74.
 24. Uyarel H, Ergelen M, Cicek G, et al. Red cell distribution width as a novel prognostic marker in patients undergoing primary angioplasty for acute myocardial infarction. *Coron Artery Dis* 2011;22:138-44.
 25. Azab B, Torbey E, Hatoum H, et al. Usefulness of red cell distribution width in predicting all-cause long-term mortality after non-ST-elevation myocardial infarction. *Cardiology* 2011;119:72-80.
 26. Ren H, Hua Q, Quan M, et al. Relationship between the red cell distribution width and the one-year outcomes in Chinese patients with stable angina pectoris. *Intern Med* 2013;52:1769-74.
 27. Yao HM, Sun TW, Zhang XJ, et al. Red blood cell distribution width and long-term outcome in patients undergoing percutaneous coronary intervention in the drug-eluting stenting era: a two-year cohort study. *PLoS One* 2014;9:e94887.
 28. Osadnik T, Strzelczyk J, Hawranek M, et al. Red cell distribution width is associated with long-term prognosis in patients with stable coronary artery disease. *BMC Cardiovasc Disord* 2013;13:113.
 29. Arbel Y, Birati EY, Finkelstein A, et al. Red blood cell distribution width and 3-year outcome in patients undergoing cardiac catheterization. *J Thromb Thrombolysis* 2014;37:469-74.
 30. Lappé JM, Horne BD, Shah SH, et al. Red cell distribution width, C-reactive protein, the complete blood count, and mortality in patients with coronary disease and a normal comparison population. *Clin Chim Acta* 2011;412:2094-9.
 31. Moher D, Liberati A, Tetzlaff J, et al. Preferred reporting items for systematic reviews and meta-analyses: the PRISMA statement. *PLoS Med* 2009;6:e1000097.
 32. Stroup DF, Berlin JA, Morton SC, et al. Meta-analysis of observational studies in epidemiology: a proposal for reporting. Meta-analysis Of Observational Studies in Epidemiology (MOOSE) group. *JAMA* 2000;283:2008-12.

Cite this article as: Su C, Liao LZ, Song Y, Xu ZW, Mei WY. The role of red blood cell distribution width in mortality and cardiovascular risk among patients with coronary artery diseases: a systematic review and meta-analysis. *J Thorac Dis* 2014;6(10):1429-1440. doi: 10.3978/j.issn.2072-1439.2014.09.10

Correlations between brachial endothelial function and cardiovascular risk factors: a survey of 2,511 Chinese subjects

Ping-Ting Yang¹, Hong Yuan², Ya-Qin Wang¹, Xia Cao¹, Liu-Xin Wu¹, Zhi-Heng Chen¹

¹Department of Healthy Management Center, ²The Center of Clinical Pharmacology, The Third Xiangya Hospital, Central South University, Changsha 410013, China

Correspondence to: Dr. Zhi-Heng Chen. Department of Health Management Center, The Third Xiangya Hospital, Central South University, Changsha 410013, China. Email: 873127193@qq.com.

Objective: We examined the relationship of several cardiovascular risk factors (CVRF) to brachial artery flow-mediated dilatation (FMD) in Chinese subjects.

Methods: This was a cross-sectional study. In 2,511 Chinese adults (age 46.86±9.52 years, 1,891 men and 620 women) recruited from people who underwent health screening at The Third Xiangya Hospital, patients' CVRF [age, body mass index (BMI), waist circumference (WC), blood pressure (BP), cholesterol parameters, creatinine (Cr), uric acid (UA), glucose level and smoking] and prevalence of present disease (hypertension, diabetes mellitus, coronary heart disease and hyperlipidemia) were investigated.

Results: Multivariate analysis revealed that FMD negative correlated with age ($\beta=-0.29$, $P<0.001$), gender ($\beta=-0.12$, $P<0.001$), BMI ($\beta=-0.12$, $P=0.001$), WC ($\beta=-0.10$, $P=0.011$), systolic BP (SBP) ($\beta=-0.12$, $P<0.001$), fasting glucose ($\beta=-0.04$, $P=0.009$), total cholesterol (TC) ($\beta=-0.04$, $P=0.014$), smoking ($\beta=-0.05$, $P=0.003$), and baseline brachial artery diameter ($\beta=-0.35$, $P<0.001$). FMD decreased with increasing age in both genders. In women, FMD was higher than men and age-related decline in FMD was steepest after age 40; FMD was similar in men above 55 years old.

Conclusions: In Chinese subjects, FMD may be a usefully marker of CVRF. Age, gender, BMI, WC, SBP, fasting glucose, TC, smoking, and baseline brachial artery diameter were independent variables related to the impairment of FMD. The influence of CVRF on endothelial function is more in women than men.

Keywords: Endothelial function; brachial artery flow-mediated dilatation (FMD); cardiovascular risk factors (CVRF)

Submitted Jul 24, 2014. Accepted for publication Jul 25, 2014.

doi: 10.3978/j.issn.2072-1439.2014.08.04

View this article at: <http://dx.doi.org/10.3978/j.issn.2072-1439.2014.08.04>

Introduction

Vascular endothelial dysfunction is an early change during atherosclerosis, an initial step in the development of arteriosclerosis, and also an important sign of arteriosclerosis (1,2). In addition, the vascular endothelial dysfunction is also an independent predictor of cardiovascular events and all-cause mortality (3,4). In clinical practice, brachial artery flow-mediated dilatation (FMD) is used to reflect endothelial function, which can be evaluated by a noninvasive ultrasound technique (5). Compared with the ultrasound machine, this new device enables the automatic and rapid tracking of FMD over time in a reliable and repeatable way, avoiding the inaccuracy due to manual positioning.

The cardiovascular risk factors (CVRF) refer to the factors that may increase the occurrence and progression of cardiovascular diseases (CVD). Previous studies have demonstrated that FMD is associated with CVRF including smoking, body mass index (BMI), age, blood pressure (BP), blood glucose, and blood lipids. However, the conclusions remain controversial. Some investigators believed that such correlations were not statistically significant or even did not exist (6,7), while others argued that FMD was only associated with one or few of these risk factors (8,9). Such diversities may be explained by the differences in subjects, methodologies, sample sizes, measurement methods of FMD, and inclusion of vascular baseline diameters in

multivariate analyses. In addition, racial differences have been found in FMD (10). While FMD has been found to be different between Asian populations and European populations, all the previous studies were conducted among European or Japanese population. Data from Chinese populations are still rare. Therefore, this study was designed to explore the potential correlations between FMD and CVRF and summarize their features.

Subjects and method

Study population

We retrospectively analyzed the clinical data of 2,511 participants who had undergone a health examination at The Third Xiangya Hospital of Central South University from March 1, 2013 to March 31, 2014. All participants received a general health questionnaire survey, anthropometric measurement, and routine blood sample tests. The questionnaire covered demographic background and medical history. Anthropometric measurements included height, weight, waist circumference (WC) and BP; both height and weight were measured with light clothing without shoes. BMI was calculated as body weight (kg) divided by the square of body height (m). BP was measured on the right upper arm in the sitting position after a 10-15-minute rest between 7 and 9 AM using a validated digital automatic BP monitor. Informed consent was obtained from all of the participants prior to entering the study. The study was conducted with the adherence to the Declaration of Helsinki and with the approval of the Ethics Guidelines Committee of the Central South University.

Measurements of laboratory

Blood samples were drawn after overnight fasting (>8 hours) for laboratory tests. All lab tests were conducted by certified experimental specialists using standard protocols at the hospital's Department of Laboratory. The biochemical tests included assessments of fasting glucose, total cholesterol (TC), triglycerides (TG), low-density lipoprotein cholesterol (LDL-C), and high-density lipoprotein cholesterol (HDL-C), creatinine (Cr) and uric acid (UA).

Measurements of FMD

We measured FMD according to the international guidelines (11) using a vascular ultrasound system equipped with an edge-tracking system for 2D imaging and pulsed

Doppler flow velocimeter for automatic measurement (UNEXEF18G; UNEX Co. Ltd., Nagoya, Japan). Participants were measured between 8 and 12 AM by trained and experienced ultrasound doctors. In brief, the diameter of the brachial artery at rest was measured in the cubital region, and subsequently, the cuff was inflated to 50 mmHg above systolic BP (SBP) for 5 min and deflated. The diameter at the same point of the artery was monitored continuously, and the maximum dilatation from 45-60 s after deflation was recorded. This method has been validated previously (12).

FMD was calculated from the following equation: FMD (%) = (maximum diameter - diameter at rest) × 100 / diameter at rest.

CVRF and CVD definition

Hyperlipidemia was defined in accordance with the criteria set forth in the guidelines for dyslipidemia control in Chinese adults (2007 edition) (13). Total blood lipid level was defined as hyperlipidemia if TC, TG, or LDL-C were high (TC ≥ 6.22 mmol/L, TG ≥ 2.26 mmol/L, LDL-C ≥ 4.14 mmol/L).

Smoking status was defined as non-smoker, occasional smoker or regular smoker. The term non-smoker included patients who quit smoking >1 month before admission. The term occasional smoker included patients who smoking ≥ 4 times a week but less than one cigarette Average per day. The term regular smoker included patients who smoking >1 cigarette per day and last over 6 months.

Hypertension was diagnosed previously or newly, based on the 2010 Chinese guidelines for the management of hypertension (14).

Coronary artery disease. We included in the study patients with a history of acute coronary syndrome and/or confirmed by coronary angiography atherosclerosis of coronary vessels.

Diabetes mellitus. Patients with diabetes mellitus previously or newly diagnosed during hospitalization were taken into consideration.

Statistical analysis

Continuous variables were presented as mean ± standard deviation (SD). Categorical variables were compared by means of χ^2 test. Clinical and characteristics between sexes of the study population were compared with the *t*-test. Two-sided *P* < 0.05 was considered statistically significant.

Table 1 Demographics and clinical characteristics of the subjects (mean \pm SD)

Variables	Total (n=2,511)	Male (n=1,891)	Female (n=620)	P value
Age (year)	46.86 \pm 9.52	46.43 \pm 8.98	48.15 \pm 10.91	<0.001
BMI (kg/m ²)	25.16 \pm 3.18	25.75 \pm 2.97	23.33 \pm 3.13	<0.001
WC (cm)	85.95 \pm 9.29	88.60 \pm 8.02	77.88 \pm 8.19	<0.001
SBP (mmHg)	125.83 \pm 16.60	126.67 \pm 15.24	123.26 \pm 19.98	<0.001
DBP (mmHg)	80.15 \pm 11.77	81.50 \pm 11.53	76.02 \pm 11.54	<0.001
Fasting glucose (mmol/L)	5.40 \pm 1.48	5.48 \pm 1.57	5.18 \pm 1.13	<0.001
TC (mmol/L)	5.08 \pm 0.99	5.07 \pm 0.98	5.11 \pm 1.05	0.456
TG (mmol/L)	2.07 \pm 1.76	2.31 \pm 1.91	1.34 \pm 0.80	<0.001
LDL-C (mmol/L)	2.70 \pm 0.87	2.68 \pm 0.86	2.76 \pm 0.92	0.08
HDL-C (mmol/L)	1.47 \pm 0.37	1.37 \pm 0.32	1.75 \pm 0.38	<0.001
Cr (μ mol/L)	72.83 \pm 15.93	78.33 \pm 13.13	56.07 \pm 11.35	<0.001
UA (μ mol/L)	324.71 \pm 89.24	353.58 \pm 76.97	236.68 \pm 62.45	<0.001
Hypertension, n (%)	554 (22.06)	413 (21.84)	141 (22.74)	0.638
Diabetes mellitus, n (%)	231 (9.20)	189 (9.99)	42 (6.77)	0.016
Hyperlipidaemia, n (%)	872 (34.72)	746 (39.45)	126 (20.32)	<0.001
CVD, n (%)	58 (2.31)	40 (2.11)	18 (2.90)	0.257
Smoking, n (%)				
Non-smoker	1,514 (60.29)	908 (48.02)	606 (97.74)	<0.001
Occasional smoker	221 (8.80)	212 (11.21)	9 (1.45)	<0.001
Regular smoker	776 (30.90)	771 (40.77)	5 (0.80)	<0.001
FMD (%)	6.80 \pm 2.49	6.65 \pm 2.43	7.23 \pm 2.860	<0.001
Baseline brachial artery diameter, mm	4.12 \pm 0.62	4.33 \pm 0.52	3.52 \pm 0.49	<0.001

Note: SD, standard deviation; BMI, body mass index; WC, waist circumference; BP, blood pressure; SBP, systolic blood pressure; DBP, diastolic blood pressure; TC, total cholesterol; TG, triglyceride; LDL-C, low-density lipoprotein cholesterol; HDL-C, high-density lipoprotein cholesterol; Cr, creatinine; UA, uric acid; CVD, cardiovascular disease; FMD, flow-mediated dilatation. $P < 0.05$ is considered statistically significant.

One-way analysis of variance (ANOVA) followed by a post-hoc Student-Newman-Keul's test was used to determine the differences among multiple groups. Relations between variables were determined by Spearman correlation coefficient analysis. Multivariate regression analyses were performed to identify factors associated with FMD in risk factors and laboratory data. All data analyses were performed using SPSS statistical software, version 20.0 (SPSS Inc., Chicago, IL, USA).

Results

Baseline data

Table 1 summarizes the baseline data of the subjects.

A total of 2,511 subjects [1,891 men (75.31%) and 620 women (24.69%)] aged 20-86 years (mean: 46.86 \pm 9.52 years) were enrolled in this study. Among them there were 554 hypertensive patients (22.06%), 231 diabetic patients (9.2%), 872 patients with hyperlipidemia (34.72%), 58 patients with coronary heart disease (2.31%), 221 occasional smokers (8.8%), and 776 frequent smokers (30.9%). Except for TC and LDL-C, the other indicators showed significant differences between men and women. The average FMD value was 6.80 \pm 2.49%. Women had significantly higher FMD value than men (7.23 \pm 2.86% *vs.* 6.65 \pm 2.43%, $P < 0.001$). Meanwhile, the baseline vascular diameter was significantly smaller in women than in men (3.52 \pm 0.49 *vs.* 4.33 \pm 0.52 mm, $P < 0.001$).

Table 2 Univariate correlations between FMD and clinical characteristics in the overall population and in different gender

Variables	All population (n=2,511)		Male (n=1,891)		Female (n=620)	
	r	P value	r	P value	r	P value
Age (year)	-0.413	<0.001	-0.361	<0.001	-0.584	<0.001
BMI (kg/m ²)	-0.164	<0.001	-0.093	<0.001	-0.304	<0.001
WC (cm)	-0.184	<0.001	-0.108	<0.001	-0.376	<0.001
SBP (mmHg)	-0.303	<0.001	-0.221	<0.001	-0.462	<0.001
DBP (mmHg)	-0.223	<0.001	-0.171	<0.001	-0.320	<0.001
Fasting glucose (mmol/L)	-0.189	<0.001	-0.160	<0.001	-0.239	<0.001
TC (mmol/L)	-0.104	<0.001	-0.052	0.023	-0.247	<0.001
TG (mmol/L)	-0.139	<0.001	-0.062	0.007	-0.272	<0.001
LDL-C (mmol/L)	-0.063	0.001	-0.006	0.0797	-0.230	<0.001
HDL-C (mmol/L)	0.042	0.035	-0.028	0.217	0.079	0.048
Cr (μmol/L)	-0.055	0.006	0.038	0.098	-0.069	0.085
UA (μmol/L)	-0.102	<0.001	-0.015	0.511	-0.213	<0.001
Baseline brachial artery diameter, mm	-0.336	<0.001	-0.311	<0.001	-0.421	<0.001

Coefficients (r) and P values were calculated with the spearman correlation analysis for continuous variables. BMI, body mass index; WC, waist circumference; SBP, systolic blood pressure; DBP, diastolic blood pressure; TC, total cholesterol; TG, triglyceride; LDL-C, low-density lipoprotein cholesterol; HDL-C, high-density lipoprotein cholesterol; Cr, creatinine; UA, uric acid; FMD, flow-mediated dilatation. P<0.05 is considered statistically significant.

Associations between FMD and CVRF

Analysis of the associations between FMD and the reported CVRF showed that FMD was significantly correlated with age ($r=-0.413$, $P<0.001$), BMI ($r=-0.164$, $P<0.001$), WC ($r=-0.184$, $P<0.001$), SBP ($r=-0.303$, $P<0.001$), DBP ($r=-0.223$, $P<0.001$), fasting glucose ($r=-0.189$, $P<0.001$), TC ($r=-0.104$, $P<0.001$), TG ($r=-0.139$, $P<0.001$), LDL-C ($r=-0.063$, $P=0.001$), HDL-C ($r=0.042$, $P=0.035$), Cr ($r=-0.055$, $P=0.006$), UA ($r=-0.102$, $P<0.001$), and baseline brachial artery diameter ($r=-0.336$, $P<0.001$) (Table 2). Multivariate linear regression analysis showed that the following CVRF were entered into the stepwise regression equation: age ($t=-16.068$, $P<0.001$), gender ($t=-5.090$, $P<0.001$), BMI ($t=3.408$, $P<0.001$), WC ($t=-2.554$, $P<0.001$), SBP ($t=-6.498$, $P<0.001$), fasting glucose ($t=-2.610$, $P=0.009$), TC ($t=-2.467$, $P=0.014$), smoking ($t=-2.943$, $P=0.003$), and baseline brachial artery diameter ($t=-15.946$, $P<0.001$) (Table 3).

Relationship between FMD and gender

Analysis on the relationship between FMD and gender showed that: in men, age, BMI, WC, SBP, DBP, fasting

glucose, TC, TG, and baseline brachial artery diameter were significantly correlated with FMD (all $P<0.001$); in women, age, BMI, WC, SBP, DBP, fasting glucose, TC, TG, LDL-c, HDL-c, UA, and baseline brachial artery diameter were significantly correlated with FMD (all $P<0.001$). The major five CVRF were defined as hypertension, diabetes, hyperlipidemia, coronary heart disease, and smoking. The subjects were grouped based on the number of their major CVRF (Figure 1). FMD gradually decreased with the increase of the number of major CVRF. Among subjects without any major cardiovascular risk factor, the FMD values were higher in women than in men; among subjects with one or more major CVRF, the FMD values were lower in women than in men. The differences between women and men increased along with the increase of the number of major CVRF.

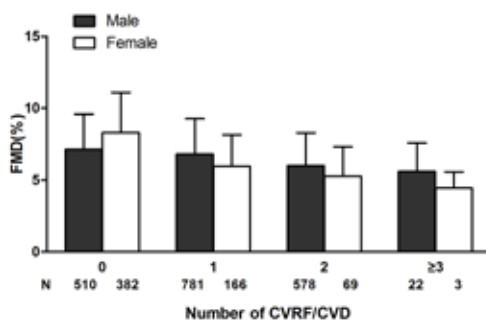
Relationship between FMD and age

The 20-86-year-old subjects were grouped according to their ages (ten 5-year groups) (Figure 2). The potential relationship between FMD and age was evaluated in subjects with different

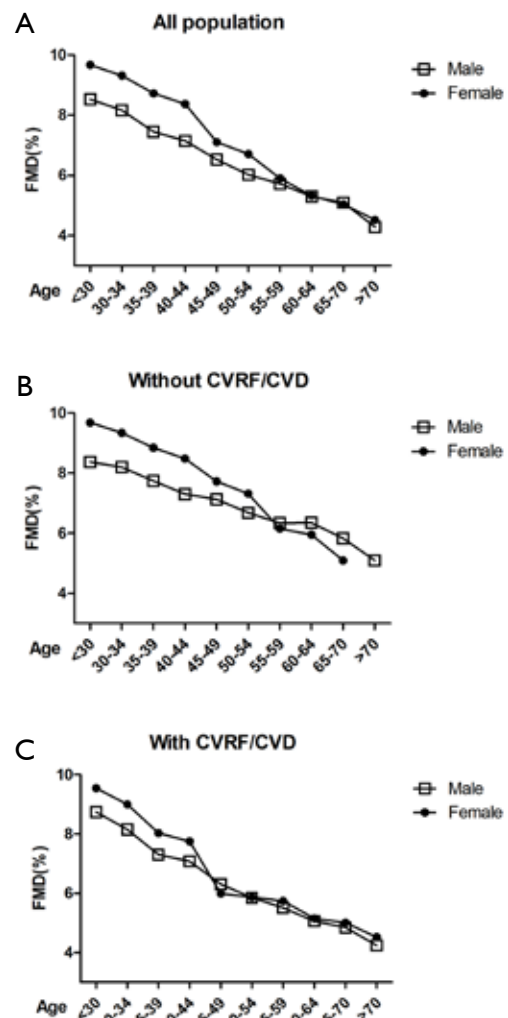
Table 3 Multivariate analysis of the relation between flow-mediated vasodilation and variables

Variables	β	T value	P value
Age (year)	-0.298	-16.068	<0.001
Gender	-0.122	-5.090	<0.001
BMI (kg/m ²)	-0.125	-3.408	0.001
WC (cm)	-0.100	-2.554	0.011
SBP (mmHg)	-0.124	-6.498	<0.001
Fasting glucose (mmol/L)	-0.046	-2.610	0.009
TC (mmol/L)	-0.043	-2.467	0.014
Smoking	-0.056	-2.943	0.003
Baseline brachial artery diameter (mm)	-0.354	-15.946	<0.001

BMI, body mass index; WC, waist circumference; SBP, systolic blood pressure; TC, total cholesterol.

**Figure 1** Illustration of FMD, flow-mediated dilatation depending on number of coexisting risk factors/diseases; 0, no risk factors/diseases; 1, have one risk factors/diseases; 2, have two risk factors/diseases; ≥3, have more than three factors/diseases. FMD, flow-mediated dilatation; CVRF, cardiovascular risk factors; CVD, cardiovascular disease.

number of major CVRF. Among all subjects, the FMD was significantly higher in women than in men in the 20 to 55 age groups. It significantly declined in the 40-45 age group in women; however, it showed no significant difference between women and men in the 55 and over age groups. Among subjects without major CVRF, the FMD values were significantly higher in women than in men in the 55 and under age groups, similar in the 55-59 age group, and significantly lower in the 60 and over age groups. Among subjects with major CVRF, the FMD values were higher in women than in men in the 45 and under age groups but showed no significant differences in the 45 and over age groups.

**Figure 2** (A) Line graphs show FMD in all subjects classified into 10 groups based on 5-year of age; (B) line graphs show FMD in men and women classified into 10 groups based on 5-year of age in the no risk group; (C) line graphs show FMD in men and women classified into 10 groups based on 5-year of age in the cardiovascular risk factor and cardiovascular disease groups. CVRF, cardiovascular risk factors; CVD, cardiovascular disease; FMD, flow-mediated dilatation.

Discussion

It is well known that the CVRF can bring damage to vascular endothelium (15). As the biggest endocrine organ in human body, vascular endothelium maintains the normal systolic and diastolic conditions of blood vessels by secreting NO, endothelin-1, prostacyclin, bradykinin, and other factors. A decreased secretion of NO

by vascular endothelium is manifested as endothelium-dependent diastolic dysfunction (16). In our current study, we determined the NO secretion to reflect the changes in vascular diastolic function, or by measuring the FMD value to reflect the endothelial dysfunction. In addition, we explored the potential relationships between the decline of FMD and the major CVRF.

We found that, among the various CVRF, age, gender, BMI, waist, SBP, fasting glucose, TC, smoking, and baseline brachial artery diameter are independent predictors of FMD. The relationships between FMD and CVRF have been reported in many literatures. Among them 18 studies are listed in *Table 4*. The included variables include age, sex, SBP, EPO, BMI, DBP, FPG, TC, HDL-c, Cr, UA, hsCRP, insulin, smoking, alcohol use, hypertension, dyslipidemia, diabetes mellitus, hyperuricemia, baseline brachial artery diameter, metabolic syndrome (MetS), and Framingham risk score. Multivariate analyses resulted in different conclusions. Schnabel *et al.* (22) believed FMD was associated with age, sex, BMI, SBP, DBP, TC, HDL-c, TG, C-reactive protein, hypertension, hypertension treatment, and dyslipidemia, whereas Philpott *et al.* (8) argued FMD was only associated with SBP. Although Mizia-Stec *et al.* (6) agreed FMD was associated with CVRF, he insisted that such correlations were limited among populations at high risk of CVD. Among these studies, disputes existed even in a single indicator. Maruhashi *et al.* (19) believed UA was an independent risk factor of impaired endothelial function in postmenopausal women, while Oikonen *et al.* (7) argued that UA was not correlated with the endothelial function. Thus, there is no definite conclusion on the associations between FMD and CVRF. As shown in our current study, FMD was correlated with the traditional CVRF including BP, blood sugar, blood lipid, obesity, and smoking, in particular the baseline brachial artery diameter; however, it was not correlated with Cr and UA. In our study, we further listed hyperlipidemia, hypertension, diabetes, coronary heart disease, and smoking as the five major risk factors. Grouping based on the number of risk factors showed that the FMD value declined along with the increase of the number of risk factors. Therefore, we can conclude that these CVRF can bring damage to vascular endothelium and then cause the decreased vasodilation capacity, resulting in the decline of FMD value.

FMD has shown certain racial differences (10). In their study on 5,000 German subjects aged 55.5 ± 10.9 years, Schnabel *et al.* (22) found that the baseline FMD value was $8.08 \pm 4.88\%$ among all the subjects, $6.53 \pm 3.73\%$ in men,

$9.69 \pm 5.39\%$ in women; meanwhile, the baseline brachial artery diameter was 4.32 ± 0.82 mm in all the subjects, 4.89 ± 0.59 mm in men, and 3.74 ± 0.59 mm in women. Oikonen *et al.* (7) studied 1,985 Finnish subjects aged 30–45 years and found that the FMD value was $7.64 \pm 3.79\%$ in men and $9.88 \pm 4.84\%$ in women. Maruhashi *et al.* (18) studied 5,314 Japanese subjects aged 46 ± 13 years and found the average FMD value was $6.16 \pm 3.26\%$ and the brachial artery diameter was 4.01 ± 0.60 mm. In our current study, we found that, among the 2,511 Chinese subjects, the average FMD value was 6.80 ± 2.49 mm and the brachial artery diameter was 4.12 ± 0.62 mm. Thus, the FMD value is higher in the Caucasian populations than in East Asian populations but is basically the same between Chinese and Japanese. This can be explained both by the differences in the diastolic function and baseline brachial artery diameter among different populations and by the different measurement methods. Therefore, it is necessary to carry out studies on the CVRF that may affect the vascular endothelial dysfunction among different races and populations.

In our current study, women had higher FMD values than men, which was consistent with the previous study (29,30), suggesting the endothelial function is better in women than in men. However, further multivariate analysis showed that the difference in FMD between women and men might be due to the different baseline brachial artery diameter, which was smaller in women than in men; as a result, the vascular dilatation function differs between men and women. In our current study, we also explored the impacts of CVRF on FMD in men or women. Along with the increase of the number of CVRF, the FMD values declined in both men and women. Among subjects without any major cardiovascular risk factor, the FMD values were higher in women than in men; among subjects with one or more major CVRF, the FMD values were lower in women than in men; furthermore, the difference of the FMD values between women and men was even larger in subjects with more major CVRF. Obviously, these major CVRF have larger impacts on women. After the subjects were grouped according to age, comparisons of the FMD values among subjects with different age and gender showed that the vascular endothelial function dramatically declined in the 40 and over age groups; however, the differences in the FMD values between women and men were not statistically different in the 55 and over age groups. We then further divided our subjects into two groups: subjects with major CVRF and those without major CVRF. In subjects with major CVRF, the FMD value dramatically decreased in

Table 4 Summary of cross-sectional studies on relationship between FMD, flow-mediated dilatation and cardiovascular risk factors

No.	Author, year	Population	Age (years)	Country/ ethnic/race	Indicators included in the multivariate analysis index for analysis	Multivariate analysis	Key findings
1	Mizia-Stec <i>et al.</i> , 2014 (6)	617 subjects (men: 349; women: 268)	Mean age: 50.1±14.9	Polish	CVD, hyperlipidaemia, age, valve heart disease, Brachial artery diameter	Yes	FMD is related to the number of traditional CVRF/CVD. The value of FMD assessment in high risk patients is limited
2	Tilling <i>et al.</i> , 2013 (17)	317 subjects (men: 134; women: 183; premenopausal: 33)	Mean age: 55±6.8	British	Age, sex, SBP, Hb, EPO, BMI, DBP, FPG, TC, HDL, hsCRP	Yes	FMD was independently negatively correlated with age, male sex and SBP
3	Maruhashi <i>et al.</i> , 2013 (18)	5,314 subjects (men: 4,135; women: 1,179)	Aged 17-86, mean age: 46±13	Japanese	Age, sex, BMI, SBP, DBP, dyslipidemia, diabetes mellitus, smoking, baseline brachial artery diameter	Yes	FMD was correlated with age, sex, BMI, SBP, diabetes mellitus, smoking, and baseline brachial artery diameter
4	Maruhashi <i>et al.</i> , 2013 (19)	749 women (368 premenopausal and 381 postmenopausal)	Aged 30-74, mean age: 50.2±10.6	Japanese	UA, age, HDL, FPG, smoking	Yes	UA was a significantly independent risk factor for endothelial dysfunction in postmenopausal women, but not in premenopausal women
5	Oikonen <i>et al.</i> , 2012 (7)	1,985 young adults (men: 923; women: 1,062)	Aged 30-45, women (37.9±4.9), men (37.6±5.0)	Finnish	BMI, GFR, SBP, TC, TG, Cr, UA, adiponectin, insulin, FPG, CRP, alcohol use	Yes	No associations were found between UA and FMD
6	Lunder <i>et al.</i> , 2012 (20)	100 healthy men	Aged 30-50, mean age: 41.9±6.4	Slovenian	Age, BMI, SBP, DBP, HR, TC, HDL, FPG	Yes	FMD was associated with HR and HDL
7	Kawano <i>et al.</i> , 2012 (12)	181 T2DM patients (men: 108; women: 73)	Mean age: 64±10	Japanese	Age, duration of diabetes, smoking, WC, SBP, HbA1c, TC, Cr, statin, ACEI/ARB	Yes	FMD was associated with age, smoking, SBP, HbA1c and TC
8	Tomiyama <i>et al.</i> , 2011 (21)	2,732 healthy men	Mean age: 49±8	Japanese	Hyperuricemia, Mets	No	Mild hyperuricemia may be a significant independent risk factor for endothelial dysfunction in subjects without Mets, whereas only severe hyperuricemia appeared to exacerbate endothelial dysfunction in similar subjects with Mets

Table 4 (continued)

Table 4 (continued)		Indicators included in the multivariate analysis index for analysis				Multivariate analysis	Key findings
No.	Author, year	Population	Age (years)	Country/ethnic/race	Indicators included in the multivariate analysis index for analysis	Multivariate analysis	Key findings
9	Schnabel et al., 2011 (22)	5,000 subjects (men: 2,540; women: 2,460)	Aged 34-74, mean age: 55.5±10.9	German	Age, sex, BMI, current smoking, SBP, DBP, HR, height, TC, HDL, TG, FPG, CRP, diabetes, hypertension, hypertension treatment, dyslipidemia, CVD	Yes	FMD was associated with age, sex, BMI, SBP, DBP, TC, HDL, TG, CRP, hypertension, hypertension treatment and dyslipidemia
10	Hamburg et al., 2011 (23)	7,031 subjects (men: 3,234; women: 3,797)	Aged 19-88, mean age: 48±13	White	Age, sex, SBP, DBP, HR, BMI, TC, HDL, diabetes, current smoker, lipid-lowering medication, CVD	Yes	FMD was associated with age, sex, SBP and BMI
11	Philpott et al., 2009 (8)	1,477 men without CVD	Mean age: 49.4±9.9	Canadians	Age, SBP, FPG, BMI, LDL, HDL, current smoking, CRP	Yes	The only CVRF independently associated with FMD was SBP
12	Patel et al., 2009 (24)	185 consecutive women	Mean age: 51±1	Multi-Ethnic (White, black, Asian, Hispanic)	Age, BMI, CVD, current smoking, hypertension, diabetes, hypercholesterolemia, anti-hypertensive medication, lipid-lowering medication	Yes	FMD was associated with age, BMI and current smoking
13	Yeboah et al., 2008 (25)	2,338 elderly	Aged 72-98, mean age: 78.3±4.2	Multi-ethnic	Age, SBP, DBP, BMI, TC, LDL, HDL, TC, waist/hip ratio, Cr, number of CVRF, cigarette smoking	Yes	FMD was associated with age, HDL, waist/hip ratio, TC, number of CVRF
14	Tomiyama et al., 2008 (26)	819 subjects free of CVD (men: 611; women: 208)	Mean age: 45±10	Japanese	Age, gender, BMI, smoking, SBP, DBP, TC, HDL, TG, FPG	Yes	FMD was negative correlation with age, gender and smoking habit. In subjects ≥50 years of age, the FMD in men with one CVRF, excluding smoking, was similar to that in men with no CVRF. CVRF did not attenuate FMD in women

Table 4 (continued)

Table 4 (continued)

No.	Author, year	Population	Age (years)	Country/ ethnic/race	Indicators included in the multivariate analysis index for analysis	Multivariate analysis	Key findings
15	Suzuki <i>et al.</i> , 2008 (27)	819 subjects (men: 352; women: 467)	Mean age: 66.5±8.8	17% African- American, 66% Hispanic, 15% white	WC, TC, HDL, FPG, SBP	No	FMD was associated with WC, FPG and SBP
16	Gardin <i>et al.</i> , 2008 (10)	205 subjects (105 adult MA (42 men and 63 women) and 100 NHW (59 men and 41 women)	MA (age 46±14) and NHW (age 50±11)	MA NHW	Age, brachial artery diameter, BMI, SBP, LDL, HDL, TC, FPG, current smoking, urine albumin	Yes	MA men (BMI, SBP, urine albumin); MA women (BMI, urine albumin), NHW men (BMI, HDL), NHW women (age, BMI)
17	Yan <i>et al.</i> , 2005 (9)	1,578 men	Mean age: 49.37±9.92	Canadian	Age, SBP, DBP, BMI, FPG, TC, TG, HDL, LDL, FRS	Yes	FMD was associated with SBP and DBP
18	Rodriguez <i>et al.</i> , 2005 (28)	579 subjects (men: 237; women: 342)	Mean age: 66±9	Multi-ethnic (white, black, and Hispanic)	Age, gender, BMI, FPG, hypertensive status	Yes	After adjustment for age, gender, BMI, and hypertensive status, a higher FPG was significantly associated with a lower FMD

CVD, cardiovascular disease; CVRF, cardiovascular risk factors; SBP, systolic blood pressure; Hb, haemoglobin concentration; EPO, erythropoietin; BMI, body mass index; DBP, diastolic blood pressure; FPG, fasting plasma glucose; TC, total cholesterol; HDL, high density lipoprotein cholesterol; hsCRP, high-sensitivity C-reactive protein; UA, uric acid; GFR, glomerular filtration rate; Cr, creatinine; CRP, C-reactive protein; TG, triglycerides; HR, heart rate; WC, waist circumference; HbA1c, glycosylated hemoglobin; MetS, Metabolic syndrome; LDL, low density lipoprotein cholesterol; MA, Mexican-American; NHW, non-Hispanic Whites; FRS, Framingham risk score.

the 40 and over age groups; however, the differences in the FMD values between women and men were not statistically different in the 45 and over age groups. In subjects without major CVRF, the changes in the FMD value were basically consistent with the general populations. In women, the age-related endothelial dysfunction is associated with the decline of female hormones. Among them the estrogen level begins to fall in the 40-45 age group; during the perimenopause stage (45-55 years), the female hormone levels further decline. Thus, among women without major CVRF, the vascular endothelium is no longer protected by estrogen, and the FMD value, which reflects the vascular endothelial function, is no longer different between women and men. In contrast, in women with major CVRF, the decline of FMD value arrives early and becomes similar as that in men after the age of 45 years, suggesting that the protective effect of estrogen on endothelial dysfunction is offset by the CVRF. This is consistent with the previous reports. However, we divided the subjects on a 5-year basis, which was different from the 10-year grouping in other studies. Therefore, while Tomiyama *et al.* (26) and Maruhashi *et al.* (18) proposed that the cut-off age for the same FMD value between women and men was 50 years, we, on the basis of a smaller age interval, found it would be 55 years.

However, our study had some limitations. First, the sample size of women in our study was relatively small because our subjects were recruited from individuals who had received health check-ups and there were far more males receiving vascular disease screening in China mainly due to the income levels and the awareness about health and disease. Second, due to the lack of follow-up data, we were not able to elucidate the impacts of CVRF on FMD. Further follow-up of these subjects will be included in our future studies.

Conclusions

To conclude, FMD measurement is one of the useful methods for assessing the arterial endothelial function, which is correlated with multiple CVRF. FMD has shown certain racial differences. Our study, for the first time, explored the correlations of FMD with CVRF and its age- and gender-related specificities in a large Chinese population. We hope the findings of this study may shed a light on similar research on the endothelial dysfunction and cardiovascular events in Chinese populations and provide evidences for the establishing the FMD threshold values that suit the Chinese populations.

Acknowledgements

Funding: Supported by Foundation of Hunan Provincial Science & Technology Department (2014SK3062); Supported by Key Projects in the National Science & Technology Pillar Program during the Twelfth Five-year Plan of China (2013BAI04B01).

Disclosure: The authors declare no conflict of interest.

References

1. Stoner L, Erickson ML, Young JM, et al. There's more to flow-mediated dilation than nitric oxide. *J Atheroscler Thromb* 2012;19:589-600.
2. Ruggiero D, Paolillo S, Ratta GD, et al. Endothelial function as a marker of pre-clinical atherosclerosis: assessment techniques and clinical implications. *Monaldi Arch Chest Dis* 2013;80:106-10.
3. Xu Y, Arora RC, Hiebert BM, et al. Non-invasive endothelial function testing and the risk of adverse outcomes: a systematic review and meta-analysis. *Eur Heart J Cardiovasc Imaging* 2014;15:736-46.
4. Kaźmierski M, Michalewska-Włodarczyk A, Krzych LJ. Intima-media thickness and flow-mediated dilatation in the diagnosis of coronary artery disease in perimenopausal women. *Pol Arch Med Wewn* 2010;120:181-8.
5. Charakida M, de Groot E, Loukogeorgakis SP, et al. Variability and reproducibility of flow-mediated dilatation in a multicentre clinical trial. *Eur Heart J* 2013;34:3501-7.
6. Mizia-Stec K, Wieczorek J, Orszulak M, et al. Flow-mediated dilatation (FMD) and prevalence of cardiovascular risk factors: the value of FMD assessment in high risk patients is limited. *Kardiol Pol* 2014;72:254-61.
7. Oikonen M, Wendelin-Saarenhovi M, Lyytikäinen LP, et al. Associations between serum uric acid and markers of subclinical atherosclerosis in young adults. The cardiovascular risk in Young Finns study. *Atherosclerosis* 2012;223:497-503.
8. Philpott AC, Lonn E, Title LM, et al. Comparison of new measures of vascular function to flow mediated dilatation as a measure of cardiovascular risk factors. *Am J Cardiol* 2009;103:1610-5.
9. Yan RT, Anderson TJ, Charbonneau F, et al. Relationship between carotid artery intima-media thickness and brachial artery flow-mediated dilation in middle-aged healthy men. *J Am Coll Cardiol* 2005;45:1980-6.
10. Gardin JM, Allebban Z, Wong ND, et al. Endothelial

- function and urine albumin levels among asymptomatic Mexican-Americans and non-Hispanic whites. *Cardiovasc Ultrasound* 2008;6:43.
11. Corretti MC, Anderson TJ, Benjamin EJ, et al. Guidelines for the ultrasound assessment of endothelial-dependent flow-mediated vasodilation of the brachial artery: a report of the International Brachial Artery Reactivity Task Force. *J Am Coll Cardiol* 2002;39:257-65.
 12. Kawano N, Emoto M, Mori K, et al. Association of endothelial and vascular smooth muscle dysfunction with cardiovascular risk factors, vascular complications, and subclinical carotid atherosclerosis in type 2 diabetic patients. *J Atheroscler Thromb* 2012;19:276-84.
 13. Joint Committee for Developing Chinese guidelines on Prevention and Treatment of Dyslipidemia in Adults. Chinese guidelines on prevention and treatment of dyslipidemia in adults. *Zhonghua Xin Xue Guan Bing Za Zhi* 2007;35:390-419.
 14. Liu LS, Writing Group of Chinese Guidelines for the Management of H. 2010 Chinese guidelines for the management of hypertension. *Zhonghua Xin Xue Guan Bing Za Zhi* 2011;39:579-615.
 15. Lerman A, Zeiher AM. Endothelial function: cardiac events. *Circulation* 2005;111:363-8.
 16. Wilkinson IB, Franklin SS, Cockcroft JR. Nitric oxide and the regulation of large artery stiffness: from physiology to pharmacology. *Hypertension* 2004;44:112-6.
 17. Tilling L, Hunt J, Jiang B, et al. Endothelial function does not relate to haemoglobin or serum erythropoietin concentrations and these do not explain the gender difference in endothelial function in healthy middle-aged men and women. *Eur J Clin Invest* 2013;43:225-30.
 18. Maruhashi T, Soga J, Fujimura N, et al. Relationship between flow-mediated vasodilation and cardiovascular risk factors in a large community-based study. *Heart* 2013;99:1837-42.
 19. Maruhashi T, Nakashima A, Soga J, et al. Hyperuricemia is independently associated with endothelial dysfunction in postmenopausal women but not in premenopausal women. *BMJ Open* 2013;3:e003659.
 20. Lunder M, Janic M, Kejzar N, et al. Associations among different functional and structural arterial wall properties and their relations to traditional cardiovascular risk factors in healthy subjects: a cross-sectional study. *BMC Cardiovasc Disord* 2012;12:29.
 21. Tomiyama H, Higashi Y, Takase B, et al. Relationships among hyperuricemia, metabolic syndrome, and endothelial function. *Am J Hypertens* 2011;24:770-4.
 22. Schnabel RB, Schulz A, Wild PS, et al. Noninvasive vascular function measurement in the community: cross-sectional relations and comparison of methods. *Circ Cardiovasc Imaging* 2011;4:371-80.
 23. Hamburg NM, Palmisano J, Larson MG, et al. Relation of brachial and digital measures of vascular function in the community: the Framingham heart study. *Hypertension* 2011;57:390-6.
 24. Patel AR, Hui H, Kuvin JT, et al. Modestly overweight women have vascular endothelial dysfunction. *Clin Cardiol* 2009;32:269-73.
 25. Yeboah J, Burke GL, Crouse JR, et al. Relationship between brachial flow-mediated dilation and carotid intima-media thickness in an elderly cohort: the Cardiovascular Health Study. *Atherosclerosis* 2008;197:840-5.
 26. Tomiyama H, Matsumoto C, Yamada J, et al. The relationships of cardiovascular disease risk factors to flow-mediated dilatation in Japanese subjects free of cardiovascular disease. *Hypertens Res* 2008;31:2019-25.
 27. Suzuki T, Hirata K, Elkind MS, et al. Metabolic syndrome, endothelial dysfunction, and risk of cardiovascular events: the Northern Manhattan Study (NOMAS). *Am Heart J* 2008;156:405-10.
 28. Rodriguez CJ, Miyake Y, Grahame-Clarke C, et al. Relation of plasma glucose and endothelial function in a population-based multiethnic sample of subjects without diabetes mellitus. *Am J Cardiol* 2005;96:1273-7.
 29. Skaug EA, Aspenes ST, Oldervoll L, et al. Age and gender differences of endothelial function in 4739 healthy adults: the HUNT3 Fitness Study. *Eur J Prev Cardiol* 2013;20:531-40.
 30. Virdis A, Taddei S. Endothelial aging and gender. *Maturitas* 2012;71:326-30.

Cite this article as: Yang PT, Yuan H, Wang YQ, Cao X, Wu LX, Chen ZH. Correlations between brachial endothelial function and cardiovascular risk factors: a survey of 2,511 Chinese subjects. *J Thorac Dis* 2014;6(10):1441-1451. doi: 10.3978/j.issn.2072-1439.2014.08.04

Analysis on minimally invasive diagnosis and treatment of 49 cases with solitary nodular ground-glass opacity

Hu Zhang¹, Jing Duan², Zhi-Jun Li², Zheng-Fu He², Zhou-Miao Chen², Yong Xu², Wei-Wen Ye², Ou Wu³

¹Department of Thoracic Surgery, ²Department of Anesthesiology, Sir Run Run Shaw Hospital Affiliated with Medical College of Zhejiang University, Hangzhou 310016, China; ³Department for Chronic and Noncommunicable Disease Control and Prevention, Hangzhou center for disease control and prevention, Hangzhou 310021, China

Correspondence to: Jing Duan. Department of Anesthesiology, Sir Run Run Shaw Hospital Affiliated with Medical College of Zhejiang University, Hangzhou 310016, China. Email: 654710199@qq.com.

Objective: This study is designed to investigate the treatment approach and prognosis of pulmonary ground-glass-like shadow, especially solitary nodular ground-glass opacity (SNGGO).

Methods: Forty-nine cases of SNGGO that persisted after anti-inflammatory treatment in our hospital were retrospectively studied. These patients received thoracoscopic surgery due to indefinite diagnosis and a tendency of canceration (some cases were followed up for 1-24 months before surgery). Intraoperative rapid frozen section was performed for pathological diagnosis, and surgery method was chosen according to pathological results and the health status of the patients.

Results: Forty-three cases showed malignancy, among which 36 cases received thoracoscopic total resection of the lung cancer and seven received simple wedge resection or pulmonary segment resection due to poor lung function; two cases were atypical adenomatous hyperplasia (AAH) and received wedge resection; and four cases were benign and received lesion resection only. Intraoperative frozen section results were in line with postoperative pathological analysis. No lymph node metastasis was detected in any malignant cases as indicated by lymph node dissection or sampling. All malignant cases were staged Ia by postoperative pathological analysis. Neither recurrence nor metastasis occurred during the 1-30 months' follow-up.

Conclusions: SNGGO that persists after anti-inflammatory treatment tend to be adenocarcinoma, which can hardly be diagnosed in the early stage through non-invasive examination. If there's no contraindication for surgery, video-assisted thoracoscopy (VATS)-guided resection of the lesion plus intraoperative rapid frozen section should be performed to synchronize diagnosis and treatment, which could achieve satisfactory prognosis.

Keywords: Nodular ground-glass opacity; video-assisted thoracoscopy (VATS)

Submitted Apr 21, 2014. Accepted for publication Oct 08, 2014.

doi: 10.3978/j.issn.2072-1439.2014.10.09

View this article at: <http://dx.doi.org/10.3978/j.issn.2072-1439.2014.10.09>

Introduction

In recent years, with the improvement of people's health awareness and the development of imaging technology as well as the application of lung cancer screening, pulmonary ground-glass opacity (GGO), especially solitary nodular ground-glass opacity (SNGGO), has attracted more and more attention from clinicians due to its difficulty in diagnosis through non-invasive examination. In literature, GGO is used to describe a finding on high-resolution CT

(HRCT) of the lung in which "hazy increased attenuation of the lung with preservation of bronchial and vascular margins" is seen. It could be caused by partial filling of air spaces, interstitial thickening, partial collapse of alveoli, normal expiration, or increased capillary blood volume. It may be associated with an air bronchogram. The literature further pointed out that GGO should not be confused with "consolidation", in which bronchovascular margins are obscured. Moreover, GGO has the characteristics of small

size (usually <20 mm in diameter), low density, and atypical morphology at the same time (1). This study is designed to investigate the treatment approach and prognosis of SNGGO. Forty-nine cases of SNGGO admitted by our hospital from June 2011 to February 2014 were retrospectively reviewed, and the experiences in treating the 49 cases are reported here in reference with literatures.

Patients and methods

Patients

We retrospectively studied patients with pulmonary nodules who met the following criteria: (I) HRCT showed the lesions were GGO; (II) lesion of ≥ 5 mm in diameter; (III) GGO proportion of $\geq 50\%$; and (IV) the lesion persisted or continued growing after 2 weeks' anti-inflammatory treatment.

Surgical procedure

After adequate preoperative preparation, patients received surgical treatment. For those with small or deeply located lesion, methylene blue tattooing or hookwire positioning was performed before surgery. Double-lumen endotracheal intubation and intravenous general anesthesia were performed and three incisions were made: a 3 cm incision in the 3rd or 4th intercostal space at the anterior axillary line as the primary operating hole; a 1 cm incision in the 7th or 8th intercostal space at the middle axillary line as the observation hole; and a 1 cm incision in the 7th or 8th intercostal space at the infrascapular line as the auxiliary operating hole. After that, a wedge resection was made by Endo-GIA stapler, and the specimens were put in the endobag and removed from the main port. The GGO were resected from the specimens, marked with suture, and diagnosed by intraoperative frozen section. If the GGO was benign, the chest was closed. If it was malignant, lobectomy plus lymph node dissection was performed; for those who cannot tolerate, lung segment resection or pulmonary wedge resection was performed.

Statistical analyses

SPSS13.0 software is used to analyze the data. Chi-square test is adopted to evaluate the correlation between malignancy and patient age, gender, lesion size and location. $P < 0.05$ is recognized as the level of significance.

Results

General information

Among patients admitted by our hospital from June 2011 to February 2014, 49 met the inclusion criteria and were included for further analysis in this study. The 49 cases included 12 male and 37 female patients aged 53.54 ± 12.57 years. Of these patients, 23 showed no symptom and the GGO were detected during physical checkup; the other 26 patients were hospitalized due to varying degrees of cough, chest pain, chest discomfort or other symptoms. After 2 weeks' anti-inflammatory treatment, the lesions persisted or continued growing. The size of the GGO in this study ranged from 5×7 to 15×18 mm. Specifically, 20 cases was <10 mm in diameter, other 29 cases was 10-20 mm, and none of them was >20 mm. Seventeen lesions were located in the upper right lung, 3 in middle right, 7 in lower right, 12 in upper left, and 10 in lower left (Figure 1A-E). None of the patients had pathological diagnosis before the surgery.

Surgical treatment

Intraoperative frozen section showed 43 cases of malignancy (87.75%), among which 36 cases received VATS lobectomy and seven received simple wedge resection or pulmonary segment resection due to poor lung function. No metastasis was detected during lymph node dissection or sampling. For six non-malignant cases, two cases were atypical adenomatous hyperplasia (AAH) (4.09%), and four cases were benign and received lesion resection only. No operative deaths occurred. Four patients had pulmonary infection after surgery but were all cured after proper treatment.

Postoperative pathological diagnosis

Postoperative pathological analysis results were in agreement with intraoperative frozen section results. For details, 43 cases were primary adenocarcinoma or micro-infiltrating adenocarcinoma; two cases were AAH of alveolar epithelia; one case was hyaline nodules; one case was chronic inflammation of lung tissue combined with focal vasodilation, hemorrhage and interstitial fibrosis; one case was normal lung tissue; and one case was focal angiogenesis and epithelial hyperplasia. Postoperative pathological staging for 43 malignant cases were all Ia.

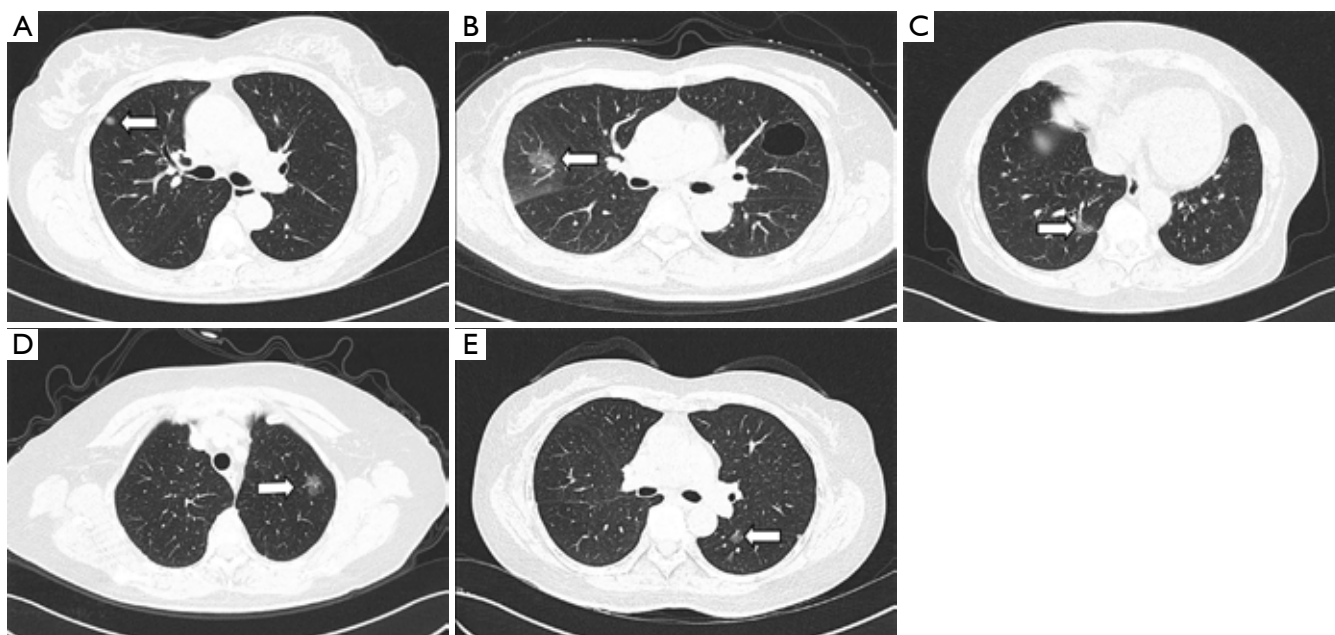


Figure 1 Representative SNGGO in patients. (A) SNGGO in right upper lobar (white arrow), female, 56 years, adenocarcinoma *in situ*; (B) SNGGO in right middle lobar (white arrow), male, 61 years, adenocarcinoma; (C) SNGGO in right lower lobar (white arrow), male, 63 years, adenocarcinoma; (D) SNGGO in left upper lobar (white arrow), male, 54 years, adenocarcinoma; (E) SNGGO in left lower lobar (white arrow), female, 50 years, adenocarcinoma. SNGGO, solitary nodular ground-glass opacity.

Postoperative outcome

The patients were followed up for 1 to 30 months with a median follow-up time of 19 months. Neither recurrence nor metastasis was detected during the follow-up period.

Correlation analyses

Correlation between malignancy and patient age, gender, lesion size and location was analyzed by chi square test and the results were shown in *Table 1*. No correlation was found between malignancy and patient age, gender, lesion size or location.

Discussion

Pulmonary GGO is one of the hot spots in clinical research of lung in recent years. Pulmonary GGO can be clouding or nodular, solitary or multiple. SNGGO is often found in lung cancer screening. Due to its high rate of malignancy and difficulty in diagnosis, it was much more studied by radiologists in the initial stage (2-5). According to whether there is a solid component within the composition, lesions are divided into pure GGO (pGGO)

and mixed GGO (mGGO). In this study, most of the cases are pGGO. Because only three cases of GGO containing solid component were adenocarcinoma, the proportion of the cases was very small, and the analysis results had no statistical significance, the further discussion was not performed. In the future, when this type cases are adequate, the analysis of this type cases will be performed separately.

Currently there is still no non-invasive method that can accurately diagnose SNGGO. As reported by Infante *et al.* (6), PET has low sensitivity for nodular GGO (25%), therefore is not considered as a routine diagnostic method. As for invasive diagnostic methods, there are mainly two types:

- (I) CT-guided lung biopsy: for nodular GGO that persists after antibiotic treatment, CT-guided lung biopsy can identify patients that require surgical resection. As reported by Kim *et al.* (7), this method has few complications and has a positive predictive value of 97% and a negative predictive value of 75%, so it is commonly used for the identification of nodular GGO. As reported by Godoy *et al.* (8), CT-guided lung biopsy has an overall diagnostic rate of only 64.6%, and the rate is even lower for lesions

Table 1 Correlation between malignancy and patient age, gender, and lesion size and location

Characteristics	SNGGO (n=49)	Malignant (n=43)	P value
Age (years)			0.814
≥60	20	19	
<60	29	24	
Gender			0.081
Men	12	9	
Women	37	34	
Size (mm)			0.662
≥10	29	27	
<10	20	16	
Location			0.115
Right upper lobar	17	16	
Right middle lobar	3	2	
Right lower lobar	7	6	
Left upper lobar	12	11	
Left lower lobar	10	8	

SNGGO, solitary nodular ground-glass opacity.

with a diameter ≤ 10 mm and GGO $>50\%$, which is about 35.2%. It was reported that for patients diagnosed with adenocarcinoma in biopsy, treatment with radiofrequency ablation achieved nearly 100% 1-, 3-, and 5-year survival (9). This outcome is comparable to that of surgical resection, but only in the context of clear diagnosis. A negative biopsy result cannot rule out the possibility of malignancies; missed diagnosis and misdiagnosis are common.

- (II) VATS-guided wedge resection: intraoperative rapid frozen section can be made for clear diagnosis, so that diagnosis and treatment of GGO can be performed simultaneously. All malignant cases in this study were adenocarcinoma. It has been reported that for GGO diagnosed as adenocarcinoma, minimally invasive wedge resection is superior to lobectomy because the former can better reserve lung function (10). Limited resection (e.g., a wedge resection or segmentectomy) can greatly reserve pulmonary function, reduce trauma, achieve quick recovery, reduce complications, especially in patients with poor pulmonary function, as well as reduce economic burden for patients at the same time. However, limited excision also has some limitations:

extrusion could cause metastasis in the process of palpation or resection, and inadequate resection margin may lead to recurrence. Therefore, regular follow-up for imaging examination and treatment is highly recommended. Based on our experience, we propose that for patients with tolerability in lung function, especially young patients, lobectomy shall be recommended. However, there's currently no solid evidence to support this idea, and long-term follow-up of large number of cases needs to be conducted. For GGO near the hilum and larger than 10 mm in diameter, lobectomy is considered if lung function permits (11). But if the diameter of the lesion is 5-10 mm, we suggest regular review of the case, and if the solid component is more than 50%, lobectomy is recommended. For GGO hard to be found during surgical procedure, the patient's HRCT was pored over by the surgeon in order to locate the lesion, and the lung tissue containing GGO according to the corresponding position of the CT image was resected for frozen section analysis. In some cases, multiple wedge resections were needed and continuous frozen section analysis was performed by surgeon and pathologist collaboratively until the lesion was found.

Some scholars suggested that the size of GGO lesion is of significance in the diagnosis of malignancy (12). In the current study, the size of the 49 cases of GGO ranged from 5×7 to 15×18 mm. Sixteen of the 20 cases that had a lesion of 5-10 mm in diameter were malignant, accounting for 80%; and 27 of the 29 cases that had a lesion of 10-20 mm in diameter were malignant, accounting for 93%. It seems that bigger lesion size indicates higher rate of malignancy, but exact probability analysis showed no significant correlation between the two ($P=0.662$), which is in accordance with the results reported by Li *et al.* (13). Therefore, cautions shall be taken when taking lesion size into diagnostic consideration. For lesions less than 5 mm in diameter, we recommend continuous follow-up for these cases. If the lesion has no change, HRCT should be taken every three months for the 1st year and every 6 months after 1 year. If expansion of the lesion or obvious solid component is observed, surgical resection is recommended.

As for the location of the lesion, although in the current study, it seems that GGO tends to occur in the upper lobe of the lung, it doesn't help identify the nature of the lesion either ($P=0.115$).

In this study, all malignancies were adenocarcinoma.

Nine of the 12 male patients (75%) and 34 of the 37 female patients (92%) were malignant. Female seems to have a higher rate of malignancy than male, but chi-square test showed no significant difference between them ($P=0.08$). The negative result may be due to the insufficient number of patients in this study.

Two cases of AAH of alveolar epithelium in this study had a >10 mm lesion, and received lung segment resection. World Health Organization has suggested that AAH is a putative precursor to lung adenocarcinoma, the initial stage in the process of adenoma—bronchioloalveolar carcinoma (BAC) (BAC, currently renamed as adenocarcinoma *in situ* or AIS)—invasive adenocarcinoma. As for whether non-cancerous solitary AAH should be surgically resected, no consensus has been reached at present. But if the patient has high risks of lung cancer, minimally invasive surgery might be worthy.

Generally speaking, nodules stable for over 2 years or calcified need no further treatment. However, there're cases where the nodule has been stable for over 2 years but turned out to be malignant when surgically resected. When nodular GGO is found in lung CT scan, imaging features including the density, size of the lesion and existence of solid components should be carefully analyzed. Lung CT scan showing lobulation, speculation, vascular convergence, etc. should be actively examined and treated. Specialty Committee of Lung Cancer has suggested in *Clinical Guidelines for the Diagnosis and Treatment of Lung Cancer* that "solitary nodular lesions of the lung should receive thoracoscopic resection of the tumor or thoracotomy for tumor resection plus intraoperative frozen section, so as to perform diagnosis and treatment simultaneously" (14). Some Chinese experts suggested that for micro lesion of the lung that persisted after 2 weeks of anti-inflammatory therapy or 1 month of anti-tuberculosis therapy, minimally invasive surgery should be performed for definitive diagnosis and complete recovery (15).

Conclusions

In summary, according to the results of our research, SNGGO has high tendency of canceration. Prognoses after surgical resection in patients with malignant SNGGO nodules are favorable. Neither local recurrence nor metastases occurred irrespective of nodule number, size, surgical method, presence of size change before surgical removal, or histopathological diagnosis. VATS-guided resection of tumor plus intraoperative frozen section

with preservation of lung volume and adequate follow-up imaging studies are recommended for both diagnosis and treatment. Since the number of cases is limited and the follow-up time is relatively short in this study, long-term prognosis of SNGGO requires further investigation.

Acknowledgements

This work was supported by grants from the National Natural Science Foundation of China (81102200/H2610).

Disclosure: The authors declare no conflict of interest.

References

- Collins J, Stern EJ. Ground-glass opacity at CT: the ABCs. *AJR Am J Roentgenol* 1997;169:355-67.
- Kim HY, Shim YM, Lee KS, et al. Persistent pulmonary nodular ground-glass opacity at thin-section CT: histopathologic comparisons. *Radiology* 2007;245:267-75.
- Nakata M, Saeki H, Takata I, et al. Focal ground-glass opacity detected by low-dose helical CT. *Chest* 2002;121:1464-7.
- Henschke CI, Yankelevitz DF, Mirtcheva R, et al. CT screening for lung cancer: frequency and significance of part-solid and nonsolid nodules. *AJR Am J Roentgenol* 2002;178:1053-7.
- Lee HJ, Goo JM, Lee CH, et al. Nodular ground-glass opacities on thin-section CT: size change during follow-up and pathological results. *Korean J Radiol* 2007;8:22-31.
- Infante M, Lutman RF, Imparato S, et al. Differential diagnosis and management of focal ground-glass opacities. *Eur Respir J* 2009;33:821-7.
- Kim TJ, Lee JH, Lee CT, et al. Diagnostic accuracy of CT-guided core biopsy of ground-glass opacity pulmonary lesions. *AJR Am J Roentgenol* 2008;190:234-9.
- Godoy MC, Naidich DP. Subsolid pulmonary nodules and the spectrum of peripheral adenocarcinomas of the lung: recommended interim guidelines for assessment and management. *Radiology* 2009;253:606-22.
- Kodama H, Yamakado K, Hasegawa T, et al. Radiofrequency ablation for ground-glass opacity-dominant lung adenocarcinoma. *J Vasc Interv Radiol* 2014;25:333-9.
- Lee HY, Lee KS. Ground-glass opacity nodules: histopathology, imaging evaluation, and clinical implications. *J Thorac Imaging* 2011;26:106-18.
- Park JH, Lee KS, Kim JH, et al. Malignant pure pulmonary ground-glass opacity nodules: prognostic

- implications. *Korean J Radiol* 2009;10:12-20.
12. Lin JH, Jiang HW, Wang WH. Study of the histological and radiologic characteristics of pulmonary focal ground-glass opacity. *Radiol Practice* 2006;21:667-9.
 13. Li F, Sone S, Abe H, et al. Malignant versus benign nodules at CT screening for lung cancer: comparison of thin-section CT findings. *Radiology* 2004;233:793-8.
 14. Alzahouri K, Velten M, Arveux P, et al. Management of SPN in France. Pathways for definitive diagnosis of solitary pulmonary nodule: a multicentre study in 18 French districts. *BMC Cancer* 2008;8:93.
 15. Gossot D, de Kerviler E, Paladines G, et al. Thoracoscopic approach in pulmonary nodules: a prospective evaluation of a series of 120 patients. *Rev Mal Respir* 1997;14:287-93.

Cite this article as: Zhang H, Duan J, Li ZJ, He ZF, Chen ZM, Xu Y, Ye WW, Wu O. Analysis on minimally invasive diagnosis and treatment of 49 cases with solitary nodular ground-glass opacity. *J Thorac Dis* 2014;6(10):1452-1457. doi: 10.3978/j.issn.2072-1439.2014.10.09

Hypoxia induces cardiac fibroblast proliferation and phenotypic switch: a role for caveolae and caveolin-1/PTEN mediated pathway

Yao Gao*, Ming Chu*, Jian Hong, Jingping Shang, Di Xu

Department of Geriatrics, First Affiliated Hospital with Nanjing Medical University, Nanjing 210029, China

*These authors contributed equally to this work.

Correspondence to: Di Xu. Department of Geriatrics, First Affiliated Hospital with Nanjing Medical University, Nanjing 210029, China.

Email: xudi1964@gmail.com.

Background: Cardiac fibrosis following myocardial infarction (MI) results in heart failure. Caveolin-1, the main structural protein of caveolae, regulates signal transduction pathways controlling cell proliferation and apoptosis. Meanwhile, low phosphatase and tensin homolog (PTEN) activity enhances the PI3K/Akt signal pathway to induce cell proliferation. But whether caveolin-1 and PTEN activation regulates cardiac fibroblast proliferation and contributes to cardiac fibrosis from ischemic injury is incompletely understood. This study investigates whether hypoxia inducing cardiac fibroblast proliferation and phenotypic switch is caveolin-dependent.

Methods: We used *in vitro* and *in vivo* models of ischemic injury, immunohistochemical staining, and cell proliferation assays to address this hypothesis.

Results: We found that MI induced collagen deposition and cardiac dysfunction. After MI, mice displayed reduced caveolin-1 and PTEN expression and increased α -smooth muscle actin (α -SMA) expression in the infarct zone. Qualitative and quantitative analyses indicated that caveolin-1 expression was lowest at 7 days after MI, accompanied by increased collagen deposition and attenuated cardiac function. We cultured cardiac fibroblasts of mice were in hypoxia or normoxia conditions for 12, 24 and 48 hours. At all the time points, caveolin-1 and PTEN expression were gradually reduced, whereas, α -SMA was gradually increased. We also observed that cell viability was increased at 12 and 24 h after hypoxia then lightly decreased at 48 h. Additionally, disruption of caveolae with methyl- β -cyclodextrin (M β CD) enhanced p-Akt and α -SMA expression and fibroblast proliferation and phenotypic switch.

Conclusions: These findings suggest a key role for caveolae, perhaps through the caveolin-1/PTEN signaling pathway, in cardiac fibroblast proliferation and phenotypic switch under hypoxia.

Keywords: Caveolin-1; phosphatase and tensin homolog (PTEN); cardiac fibroblast; hypoxia

Submitted Jul 16, 2014. Accepted for publication Aug 05, 2014.

doi: 10.3978/j.issn.2072-1439.2014.08.31

View this article at: <http://dx.doi.org/10.3978/j.issn.2072-1439.2014.08.31>

Introduction

Coronary artery disease and ischemic cardiomyopathy represent the leading cause of heart failure and continue to grow at exponential rates (1). After myocardial infarction (MI), myocardial cells die, cardiac fibroblasts proliferate, and results in pathologic fibrosis. Cardiac fibroblasts constitute more than 90% of the non-myocytes and play an essential role in the physiology of the heart. Cardiac fibroblasts produce extracellular matrix proteins

and synthesize angiogenic and cardioprotective factors. Although cardiac fibroblasts are known to be resistant to apoptosis and to remain metabolically active in situations compromising cell survival, the underlying mechanisms are unknown (2). Cardiac fibrosis is an important contributor to the development of cardiac dysfunction in diverse pathological conditions, such as ischemia, and is typically characterized by uncontrolled proliferation of fibroblasts and excessive deposition of extracellular matrix proteins in the myocardium (3-5).

Caveolae are plasmalemmal invaginations enriched in cholesterol, glycosphingolipids, and lipid-anchored proteins relative to the bulk of the plasma membrane, and caveolae biogenesis and function depend on two distinct caveolar components: caveolins and cavins (6-9). The caveolin gene family consists of three distinct genes: namely, caveolin-1, caveolin-2, and caveolin-3 (10-14). Caveolin-1 is a cholesterol-binding and integral membrane protein that regulates a variety of cellular processes, including integrin turnover and signal transduction pathways controlling cell proliferation and apoptosis (14-17). Caveolin-3 appears to be muscle specific and is expressed in cardiac, skeletal, and smooth muscle cells, whereas caveolin-1 and caveolin-2 are usually coexpressed and are particularly abundant in endothelial cells, fibroblasts, smooth muscle cells, adipocytes, and epithelial cells (12-14,18,19). Caveolin-1 has recently been found to be involved in the pathogenesis of ischemic injury (14,20-22). Cavins are also structural components of caveolae and has four isoforms.

Phosphatase and tensin homolog (PTEN) is a dual lipid/protein phosphatase that negatively regulates proliferation by repressing the integrin/PI3K/Akt pathway (15,23-30). In the cytoplasm, PTEN inhibits PI3K signaling by transforming PIP3 into PIP2 (31). Activated Akt positively regulates cell growth or activity, but negatively regulates cell autophagy and apoptosis. At low levels of PTEN in cytoplasm, PIP3 accumulates, and both Akt and phosphoinositide-dependent kinase-1 (PDK1), which contain a PH domain, binds to membrane-bound PIP3. Once bound to the membrane, PDK1 and the mammalian target of rapamycin1 (mTOR1) activate Akt through phosphorylation at various sites (32). Amino acid sequence analysis of PTEN indicates that PTEN contains the caveolin-1 consensus binding sequence OXOXXXXO corresponding to amino acids 271-278 (FHFVWNTF), where O represents the aromatic amino acid phenylalanine (F) (15,33). This suggests a relationship between caveolin-1 expression and PTEN function. However, it is unknown that whether caveolin-1 and PTEN, together, modulate cardiac fibroblast proliferation and phenotypic switch under hypoxia.

Materials and methods

Animal Model of acute MI and left ventricular function assay

Male C57BL/6 mice (Nanjing medical university laboratory animal center, Nanjing, China) were subjected to permanent ligation of left anterior descending coronary artery (LAD)

to induce MI (n=10) (34). Sham-operated mice were used as controls. Sham-operated group (n=6). Mice underwent echocardiography at 7, 14 and 28 days, after surgery. Trans-thoracic echocardiography was performed with a 14 MHz il3L linear probe (Vivid 7 Ultrasound Machine, GE Medical). Data of heart function was measured according to modified recommendations by the American Society of Echocardiography. A mean value of 3 measurements was examined at day 7, 14 and 28. Hearts were also harvested at day 7, 14 and 28 for Masson trichrome staining, immunohistochemical staining and western blot analysis (n=6-10/group).

Cell culture

We obtained neonatal cardiac fibroblasts from the heart of 1-3-day-old C57BL/6 mice (Nanjing medical university laboratory animal center, Nanjing, China). After digestion of the hearts with Type-2 Collagenase (Gibco, New York, USA), cells were pelleted and seeded in 10-cm FALCON polystyrene dishes (Corning, NY, USA), and incubated for 120 min in media containing High glucose Dulbecco's modified Eagle's medium (DMEM, GIBCO, Inc., USA), with 10% fetal calf serum (PAA, Dartmouth, MA), and antibiotics at 37 °C and 5% CO₂. After 2 hours, the medium was removed to eliminate cardiomyocytes that did not attach to the non-coated plates, and replaced with fresh medium. Cardiac fibroblasts were allowed to grow until confluence, then trypsinized, and passaged twice before use. For induction of cellular hypoxia, cells were replaced by DMEM without glucose (GIBCO, Inc., USA) and incubated at 37 °C with 5% CO₂, 1% O₂ and 94% N₂ in a GENbag anaer (bioMerieux® sa, Marcy l'Etoile, France) for 6, 12, 24, and 48 h. At these culture conditions, cardiac fibroblasts experienced varying levels of hypoxia in the presence or absence of methyl-β-cyclodextrin (MβCD, 2 mM) (Sigma, Inc., Germany), which binds cholesterol and disrupts caveolae.

Immunohistochemical staining

Immunohistochemistry was performed as described previously (35). The following primary antibodies were used for immunohistochemical staining: anti-caveolin-1-IgG (HuaAnBiotech, Inc., Hangzhou, China), anti-PTEN-IgG (Epitomics, Inc., California, USA), anti-α-SMA-Ig-G (Epitomics, Inc., California, USA).

The signal was enhanced by avidin-biotin-peroxidase complex

(VectastainABCkit, Vector Laboratories, Burlingame, CA, USA), followed by visualization of the reaction with 3, 3'-diaminobenzidine tetrahydrochloride (DAB) solution (Peroxidase Substrate Kit, Vector Laboratories, Burlingame, CA, USA). Controls were incubated with PBS in place of the primary antibody and no positive staining was observed (36).

Western blot analysis

Cells were collected in cold buffer containing 20 mM Tris (pH 7.5), 150 mM NaCl, 1 mM EDTA, 1 mM EGTA, 1% Triton X-100, 2.5 mM sodium pyrophosphate, 1 mM β -glycerophosphate, 1 mM Na_3VO_4 , 1 g/mL leupeptin, 1 mM PMSF, and centrifuged at 11,000 rpm for 20 min. The protein extracts (10 g/lane) were electrophoresed on a 12% Tris HCl gel from Bio-Rad and transferred to a nitrocellulose membrane, which was stained by naphthol blue-black to confirm equal protein loading. The membranes were incubated in 5% skim milk for 2 h and then incubated with the following primary antibodies: caveolin-1 antibody (HuaAnBiotech, Inc., Hangzhou, China), PTEN antibody, phospho-Akt (pS129) antibody (Epitomics, Inc., California, USA), Akt (S473) antibody (Epitomics, Inc., California, USA), α -SMA antibody (Epitomics, Inc., California, USA), and Gapdh antibody (HuaAnBiotech, Inc., Hangzhou, China), and, followed by incubation with horseradish peroxidase-conjugated goat anti-rabbit IgG and anti-mouse IgG secondary antibody and detection using Supersignal West picostable peroxide solution (Pierce, Rockford, IL) (37). Western blot was also performed as described above for examination of caveolin-1 expression from heart protein extracts.

Cell proliferation and viability assays

Cell proliferation was quantified using a colorimetric method based on the metabolic reduction of 3-(4, 5-dimethylthiazol-2-yl)-2, 5-diphenyltetrazolium bromide (MTT) dye to formazan, as described earlier (38). Briefly, cardiac fibroblasts were plated onto 96-multiwell plates at 8,000 cells/well. The next day, cells cultured under hypoxic conditions after 12, 24, or 48 hours were rinsed with PBS, and MTT was added. Four hours later, DMSO was added, and cells were incubated 15 minutes at 37 °C. Samples were measured at 570 nm.

Statistical analysis

Statistics were performed using GraphPad Prism software

(GraphPad Software, Inc., CA, USA). All data was analyzed by SPSS 17.0 software (SPSS Inc, Chicago, Illinois, 2008). All experiments were repeated with at least three batches of cardiac fibroblasts and in all repetitions qualitatively similar data were obtained. Data were tested for significance using ANOVA or *t*-test, as appropriate. Results with $P < 0.05$ were considered statistically significant.

Results

Collagen deposition increased and cardiac function attenuated following MI

To evaluate the process of cardiac fibrosis from ischemic injury, we induced myocardial infarction in a mouse model. Myocardial fibrosis was determined by qualitative evaluation of collagen deposition using Masson Trichrome Staining. Red staining indicated viable myocardium while blue staining indicated fibrosis due to infarction damage (*Figure 1*). We observed that the collagen fibers were disorganized in early MI, dominated by non-fibrillar collagen deposition, while in late MI, cross-linking matrix formed mature scar. Collagen deposition was found to be significantly increased at day 14 and 28 post-MI compared to day 7 (*Figure 1*). After MI, the mice also displayed cardiac dysfunction. The echocardiographic data from surviving mice after MI are shown in *Table 1*. LV contractile function (EF, FS) were significantly attenuated following MI. Interestingly, MI for 14, 28 days increased LV dimension and function as shown from LVIDd, LVISd, EF and FS compared with the day 7 group (all $P < 0.05$). These results demonstrate that MI causes an increase in collagen deposition, as well as cardiac dysfunction. During the progression of cardiac fibrosis at day 14 and 28, increased collagen deposition and replacement fibrosis improved cardiac function.

Down regulation of caveolin-1 and α -SMA expression increased after MI

To evaluate the role of caveolin-1 in cardiac fibrosis, we measured caveolin-1 expression after MI in mouse models. We investigated the expression of caveolin-1 by Western blot in whole hearts. We have found that caveolin-1 levels in the infarct area were decreased post-MI. Compared to the 7 days post-MI, the protein expression of caveolin-1 at day 14 and 28 after MI were increased (*Figure 2A*). Western blotting assays confirmed a significant decrease in caveolin-1 protein at 7 days

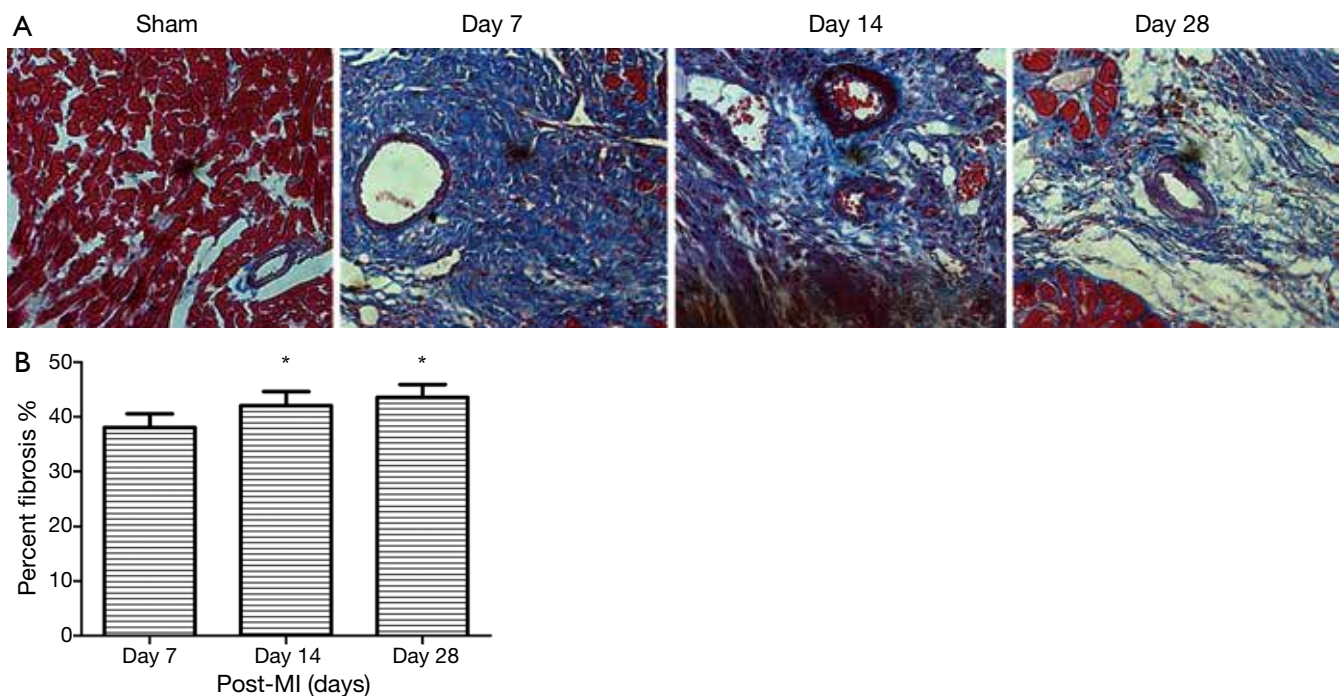


Figure 1 Myocardial fibrosis was determined by qualitative evaluation of collagen deposition using Masson Trichrome Staining in hearts from male C57BL/6 mice post-surgery groups and sham operated group (A). Red staining indicated viable myocardium, while blue staining indicated fibrosis. Original magnification: 400 \times . Percent of myocardial fibrosis in mice following myocardial infarction (B), *, $P < 0.05$.

Table 1 Echocardiography in surviving male C57BL/6 mice after MI. LV contractile function (EF, FS) were significantly attenuated following MI. Interestingly, at 14 and 28 days after MI, there is increased LV dimension and function as shown from LVIDd, LVISd, EF and FS compared with day 7 group

Variable	Sham	Day 7	Day 14	Day 28
IVSd (mm)	0.82 \pm 0.08 (n=6)	0.58 \pm 0.07 (n=10)	0.62 \pm 0.16 (n=8)	0.52 \pm 0.08 (n=6)
LVPWd (mm)	0.90 \pm 0.10 (n=6)	1.10 \pm 0.12 (n=10)	1.00 \pm 0.12 (n=8)	0.90 \pm 0.20 (n=6)
LVIDs (mm)	1.90 \pm 0.22 (n=6)	3.96 \pm 0.30 (n=10)*	3.72 \pm 0.37 (n=8)#	3.78 \pm 0.33 (n=6)#
LVIDd (mm)	3.20 \pm 0.32 (n=6)	4.88 \pm 0.38 (n=10)*	4.68 \pm 0.30 (n=8)#	4.68 \pm 0.32 (n=6)#
EF (%)	77.98 \pm 1.40 (n=6)	44.37 \pm 1.97 (n=10)*	47.93 \pm 2.31 (n=8)#	46.12 \pm 2.55 (n=6)#
FS (%)	40.62 \pm 1.29 (n=6)	18.63 \pm 0.92 (n=10)*	20.46 \pm 1.17 (n=8)#	19.53 \pm 1.83 (n=6)#

LVIDd, Left Ventricular Internal Diastolic diameter; LVISd, Left Ventricular Internal Systolic diameter; EF, Ejection Fraction; FS, Fractional Shortening. (*: vs. Sham, $P < 0.05$; #: vs. day 7, $P < 0.05$).

post MI (Figure 2B,C). And α -SMA was used as a marker of myofibroblasts, which indicated cardiac fibroblast phenotypic switch. The protein expression of α -SMA post-MI was increased compared to the sham operated control group. Furthermore, the expression of α -SMA protein at 7 days post-MI was greater than at 14 and 28 days post-MI (Figure 2D). Taken together, after myocardial infarction, both caveolin-1 and α -SMA protein expression peaks at 7 days post-MI and all these changes appeared in the

infarct zone. This result indicates that caveolin-1 may inhibit cardiac fibroblasts from transforming to myofibroblasts.

PTEN protein expression decreased in cardiac fibrosis following MI

We also demonstrated by immunohistochemical staining that membrane PTEN levels were decreased post-MI. Compared to 7 days post-MI, the protein expression of

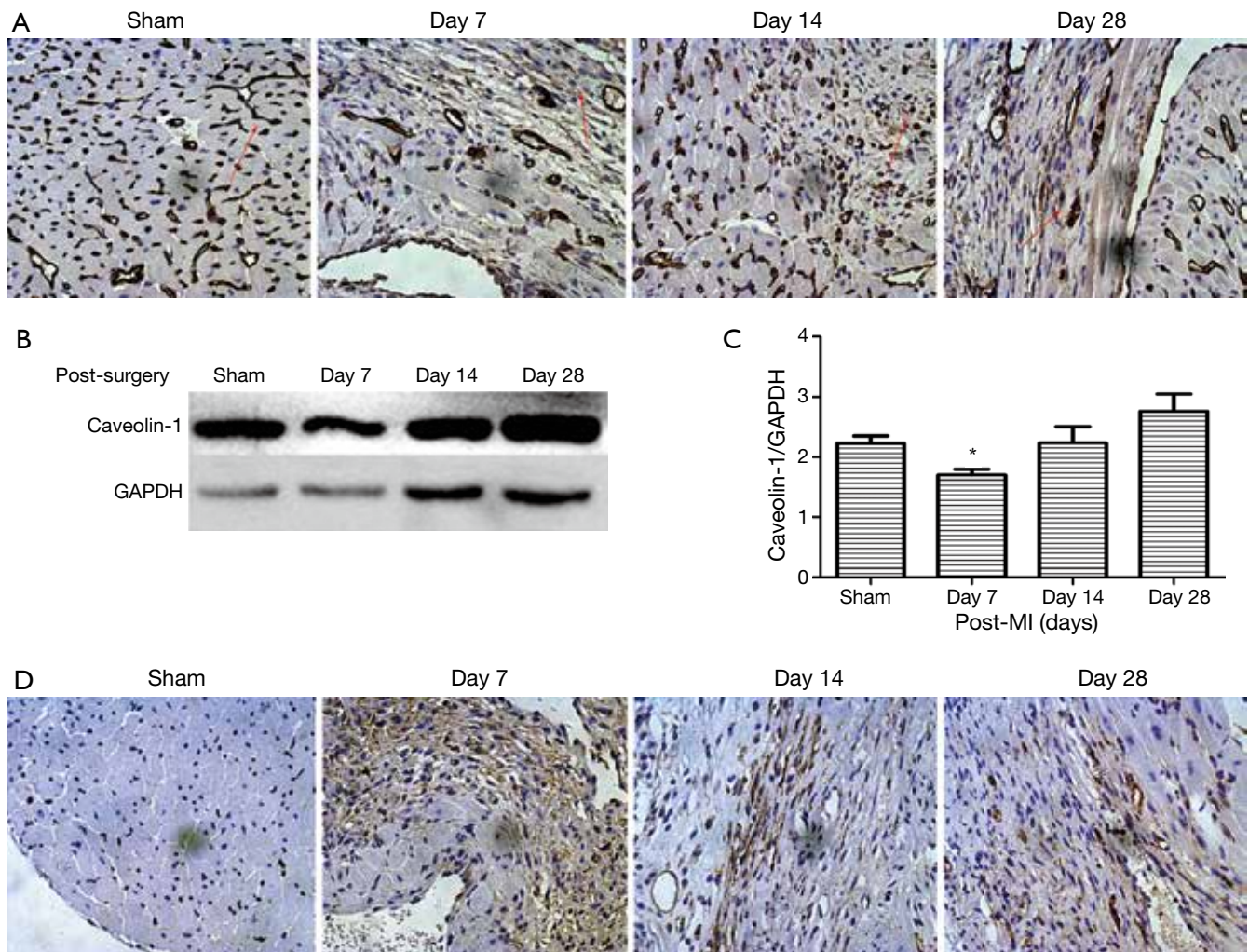


Figure 2 Immunohistochemical staining and western blotting of caveolin-1 (A-C) and α -SMA (D) expression in hearts from male C57BL/6 mice in the sham operated group and at 7, 14 and 28 days after MI. (A) Immunohistochemical staining of caveolin-1 expression; (B,C) western blotting of caveolin-1 expression, *, $P < 0.05$; (D) immunohistochemical staining of α -SMA. Original magnification: 400 \times .

membrane PTEN at 14 days after MI was decreased (Figure 3). Previous studies have found that membrane PTEN activity inhibits the integrin/PI3K/Akt signal pathway. Therefore, reduced PTEN expression enhances the PI3K/Akt signal pathway to promote myocardial fibrosis.

Hypoxia promotes cardiac fibroblasts proliferation and increases α -SMA expression

To explore whether cardiac fibroblasts displayed proliferation under hypoxia, we used the MTT assay, a colorimetric determination of cell viability after hypoxia *in vitro*. Cell viability was increased at 12, 24, and 48 hours after hypoxia compared with the untreated group, and

peaked at 24 hours after hypoxia (Figure 4). The data demonstrated that hypoxia could promote cardiac fibroblasts proliferation. We also observed that α -SMA, which is the marker of myofibroblasts, was gradually increased with increased hypoxia treatment time and was significantly increased at 24 and 48 hours $P = 0.0017$ (Figure 5). Overall, these results indicate that under hypoxia stimulus, fibroblasts will proliferate and switch their phenotype to myofibroblasts (α -SMA positive cells).

Caveolin-1 and PTEN protein expression was reduced in fibroblasts under hypoxia in vitro

Pathological cardiac fibrosis can develop from a number

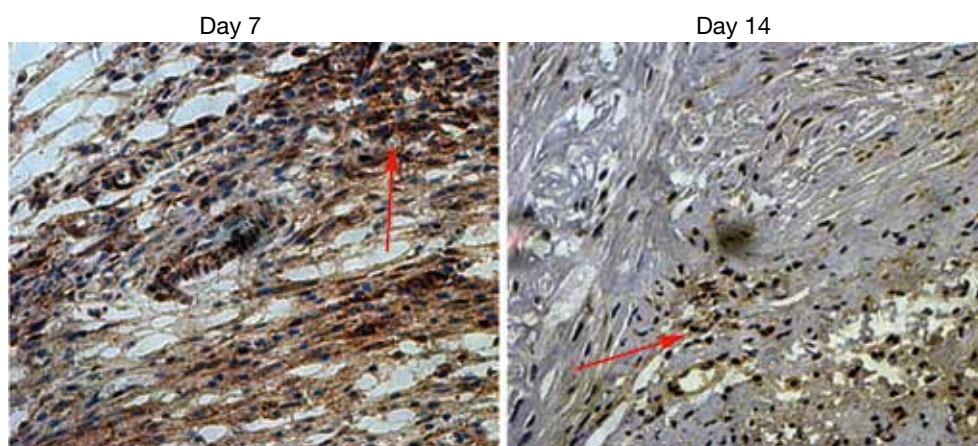


Figure 3 Immunohistochemical staining PTEN expression in hearts from male C57BL/6 mice at 7 and 14 days post-MI groups. PTEN protein expression was decreased at 14 days post-MI compared to 7 days post-MI. Original magnification: 400 \times . PTEN, phosphatase and tensin homolog.

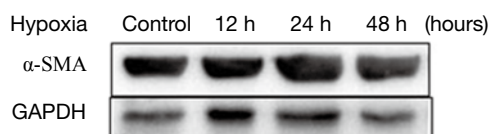
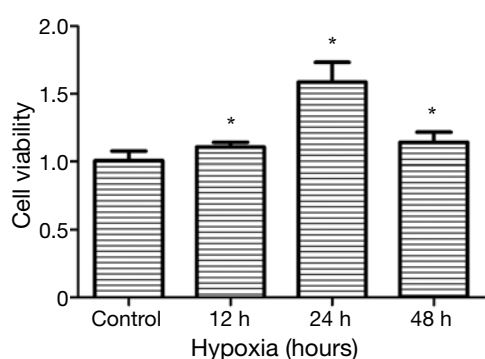


Figure 4 MTT cell proliferation assay of cardiac fibroblasts under hypoxia 12, 24 and 48 hours. *, $P < 0.05$. Data are representative of three separate experiments.

of stimuli, including ischemia, inflammation, pressure overload and volume overload (39,40). A common feature of all these stimuli is tissue hypoxia, either directly or indirectly, because of increases in oxygen consumption by infiltrating inflammatory cells and activated resident cells. Prolonged local tissue hypoxia can lead to aberrant ventricular remodeling and cardiac fibrosis (40-43). *In vivo* experiments, we have verified that both caveolin-1 and PTEN protein expression are decreased in the infarct zone post-MI. To further investigate that result, we performed

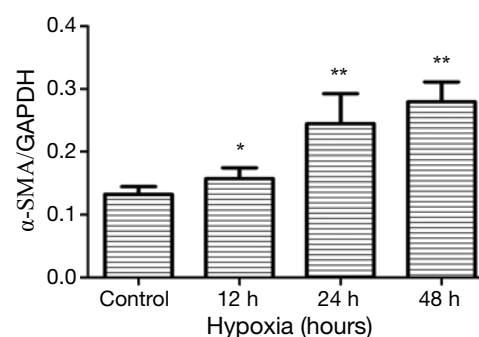


Figure 5 Expression of α -smooth muscle actin (α -SMA) in cardiac fibroblasts under normoxia and hypoxia conditions. Cardiac fibroblasts of hypoxia groups were exposed to GENbag anaer for 12, 24, and 48 hours. Hypoxia versus normoxia, *, $P < 0.05$; **, $P < 0.005$. Data are representative of three separate experiments.

hypoxia experiments *in vitro*. We analyzed caveolin-1, PTEN, and p-AKT expression in myofibroblasts derived from cardiac fibroblasts after culturing in hypoxia or normoxia conditions by western analysis. The protein expression of caveolin-1 and PTEN were gradually decreased and the expression of p-Akt was significantly increased after 12, 24 and 48 hours in hypoxia conditions (Figure 6).

Disruption of caveolae with methyl- β -cyclodextrin (M β CD) enhanced p-Akt and α -SMA expression and fibroblast proliferation

M β CD depletes cholesterol and disrupts caveolae (44).

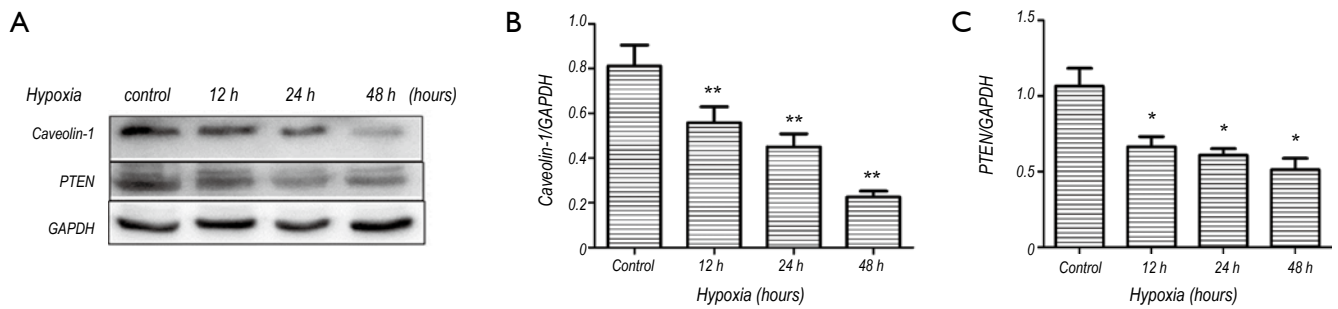


Figure 6 Expression of caveolin-1 and PTEN in cardiac fibroblasts of normoxia and hypoxia groups. Cardiac fibroblasts of hypoxia groups were exposed to GENbag anaer for 12, 24 and 48 hours. Hypoxia versus normoxia, * $P < 0.05$, ** $P < 0.005$. (A) Western blotting; (B) expression of Caveolin-1, $P = 0.0019 < 0.005$; (C) expression of PTEN, $P = 0.006 < 0.05$. Data are representative of three separate experiments. PTEN, phosphatase and tensin homolog.

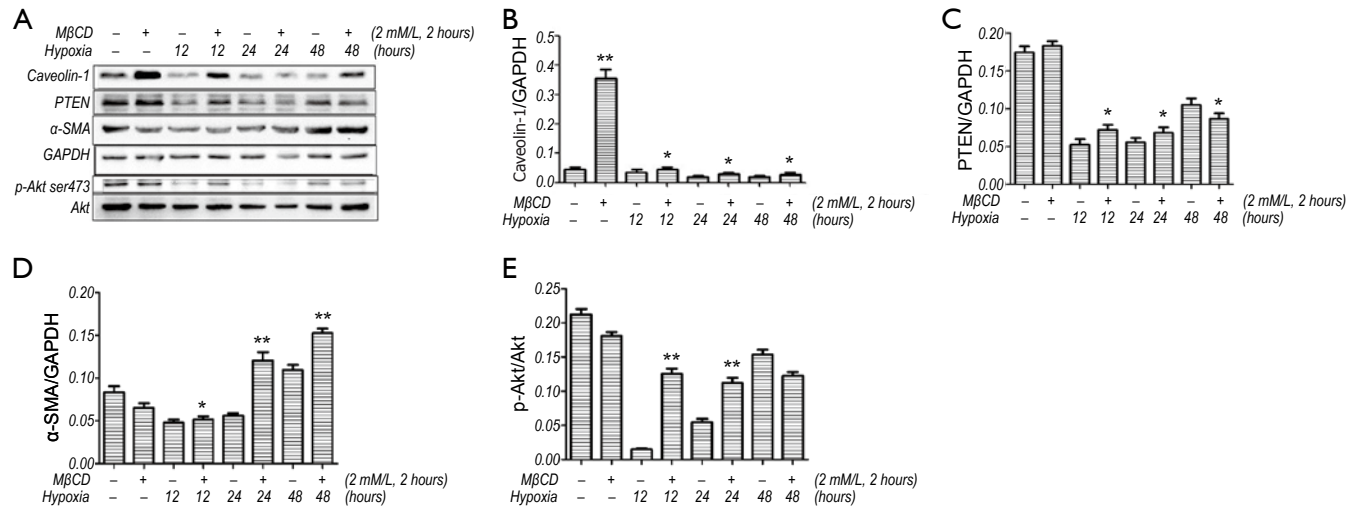


Figure 7 Expression of Caveolin-1, PTEN, α -SMA and p-Akt in cardiac fibroblasts in the presence and absence of M β CD (2 Mm/L 2 hours) and under hypoxic conditions. Cardiac fibroblasts of hypoxia groups were incubated in 2 Mm/L doses of M β CD 2 hours before exposure to GENbag anaer for 12, 24 and 48 hours. *, $P < 0.05$; **, $P < 0.005$. (A) Western blotting; (B) expression of Caveolin-1; (C) expression of PTEN; (D) expression of α -SMA; (E) expression of p-Akt. Data are representative of three separate experiments. PTEN, phosphatase and tensin homolog; α -SMA, α -smooth muscle actin.

To further study that the mechanism of caveolae on caveolin-1/PTEN mediated signal pathway, we incubated cardiac fibroblasts with a 2 mM/L dose of M β CD for 2 hours before treatment with GENbag anaer. The p-Akt and α -SMA expression and cell viability increased after exposure to M β CD compared to cells not treated with M β CD after exposure to the same hypoxia conditions (Figure 7). We also showed that expression of caveolin-1 was higher in the M β CD treated groups. Therefore the caveolin-1/PTEN mediated signal pathway was dependent on caveolae formation. The MTT assay also demonstrated that cardiac fibroblasts displayed significant proliferation

after exposure to hypoxia for 12, 24 and 48 hours in the presence of M β CD than in the untreated group (Figure 8). Over all, disruption of caveolae with M β CD leads to increased cardiac fibroblasts proliferation and conversion to myofibroblasts.

Discussion

Ischemia caused by coronary artery disease and MI leads to aberrant ventricular remodeling and cardiac fibrosis (40). Cardiac fibroblasts play a pivotal role in the development of cardiac fibrosis. We showed that ischemic injury induced

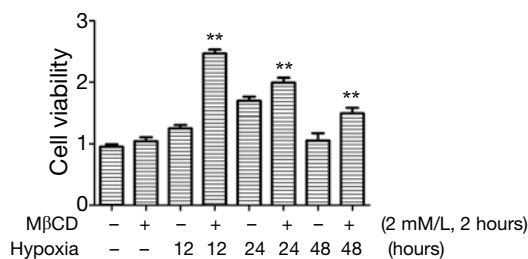


Figure 8 MTT cell proliferation assay of cardiac fibroblasts in absence or presence of MβCD after 12, 24 and 48 hours in hypoxic conditions. **, P<0.001. Data are representative of three separate experiments.

phenotypic differentiation of cardiac fibroblasts into myofibroblasts which secreted more cardiac extracellular matrix (41,45-47). We also found that caveolin-1 protein expression was transiently down-regulated after MI, concomitant with inhibition of PTEN expression and therefore activation of the Integrin/PI3K/Akt signal pathway in cardiac fibroblasts. *In vivo* experiments found that hypoxia induced proliferation and phenotypic differentiation of cardiac fibroblasts. Furthermore, caveolin-1 and PTEN protein expression in cardiac fibroblast were gradually decreased under hypoxia conditions, accompanied by increased α -SMA expression. Interestingly, disruption of caveolae with MβCD also enhanced PI3K/Akt signal pathway and caused increased cardiac fibroblast proliferation and phenotypic differentiation. These results suggest that ischemic injury leads to enhanced fibrosis of the heart and caveolae play a key role in cardiac fibroblast proliferation and phenotypic switch under hypoxia, possibly mediated by the caveolin-1/PTEN signaling pathway to activate PI3K/Akt expression.

Following acute MI, cardiac fibroblasts in the heart become activated and rapidly proliferate (48). Our study showed that collagen deposition by Masson trichrome staining and myofibroblasts by immunohistochemical staining gradually increased after permanent ligation of LAD at 7, 14 and 28 days after MI. MI injury induces cardiac fibroblasts to undergo a phenotypic switch to myofibroblasts which are central players in the profibrotic post-MI repair process (7,16,35). A trend toward increased α -SMA expression indicative of the transformation of fibroblasts to myofibroblasts was observed in the present study in infarcted regions, and is consistent with previous reports (9). We also found that systolic heart function at later stages after MI was improved than at earlier timepoints following MI. This result indicates that local collagen

deposition may be beneficial for improvement of systolic cardiac function during heart remodeling.

Considerable data indicate that PTEN colocalizes with caveolin-1 at the plasma membrane as an Integrin/PTEN/caveolin-1 complex (15). We also found that caveolin-1 and PTEN expression in cardiac fibroblasts is significantly reduced during myofibroblast proliferation and collagen deposition in the formation of a mature scar after MI. Meanwhile *in vitro*, ischemic injury induced cardiac fibroblast differentiation and proliferation, and exhibited a similar decrease in caveolin-1 and PTEN protein levels. Here we provide several evidences that caveolae and the caveolin-1/PTEN signaling pathway are involved in the progression of cardiac fibrosis resulting from ischemic injury. First, low caveolin-1 expression in cardiac fibroblast peaked concurrently with augmented α -SMA levels in mouse models after MI. Immunohistochemical staining results indicates that myofibroblasts are a key component of the infarct zone and display low caveolin-1 expression at 7 days after MI, while caveolin-1 expression gradually returns to almost normal levels by 28 days post-MI, accompanied with lower α -SMA levels. Recent studies indicate that the extracellular matrix modulates fibroblast phenotype and function in the infarcted myocardium (49). Therefore, with the progress of collagen deposition, increased caveolin-1 expression results in inhibition of myofibroblast proliferation. Secondly, both *in vivo* and *in vitro* experiments revealed a decline in caveolin-1 and PTEN protein levels after hypoxia and leads to increases in cardiac fibroblast proliferation. Lastly, *in vitro* disruption of caveolae with MβCD enhanced cardiac fibroblast proliferation and phenotypic differentiation in hypoxia conditions. This result demonstrates that signal pathways such as PTEN/PI3K/Akt and caveolin-1, which control cardiac fibroblast proliferation and phenotypic differentiation, are dependent on caveolae formation.

Numerous studies have revealed that caveolae, highly enriched in cholesterol and sphingolipids, play a pivotal role in regulating cell signaling (6,7). Membrane rafts and caveolae concentrate membrane proteins and other components involved in transport and signal transduction (10,11). Caveolins are the main structural and functional components of caveolae, cholesterol homeostasis, and cell signaling, and caveolin-1 is an essential constituent of adipocyte caveolae (50). Other studies have been confirmed that cholesterol can be depleted by MβCD treatment and therefore disrupt caveolae formation (51). Here we demonstrated that caveolin-1 and PTEN protein

expression increased in cardiac fibroblasts groups exposed to M β CD compared to untreated controls. In addition, the protein levels of α -SMA and p-Akt both increased in cardiac fibroblasts treated with M β CD compared to the untreated groups under hypoxic conditions. Meanwhile, the MTT assay demonstrated that cardiac fibroblasts displayed greater proliferation after exposure to hypoxia for 12, 24 and 48 hours in the presence of M β CD (2 mM and 2 hours). Taken together, cholesterol depletion by M β CD induced disruption of caveolae up-regulated the activation of the PI3K/Akt pathway, thereby causing increased α -SMA and p-Akt protein expression and cell proliferation. We also have unexpectedly found that caveolin-1 and PTEN expression of fibroblasts in M β CD group was greater than in the untreated group. Recent studies suggests that down-regulation of caveolin-1 may enhance increased atrial fibrosis in atrial fibrillation patients (52). Therefore, cardiac fibroblasts proliferation and phenotypic differentiation may be resulting from disruption of the caveolin-1/PTEN complex, while increases in caveolin-1 and PTEN levels may be a feedback effect of enhanced fibrosis. Further studies will be needed to further explore how caveolin-1 and PTEN pathways modulate fibrosis from ischemic injury.

Acknowledgements

The present study was supported by Grants from Six Big Talent Peak of Jiangsu Province.

Disclosure: The authors declare no conflict of interest.

References

1. Lavine KJ, Kovacs A, Weinheimer C, et al. Repetitive myocardial ischemia promotes coronary growth in the adult mammalian heart. *J Am Heart Assoc* 2013;2:e000343.
2. Mayorga M, Bahi N, Ballester M, et al. Bcl-2 is a key factor for cardiac fibroblast resistance to programmed cell death. *J Biol Chem* 2004;279:34882-9.
3. Wang L, Yuan T, Du G, et al. The impact of 1,25-dihydroxyvitamin D3 on the expression of connective tissue growth factor and transforming growth factor- β 1 in the myocardium of rats with diabetes. *Diabetes Res Clin Pract* 2014;104:226-33.
4. Dean RG, Balding LC, Candido R, et al. Connective tissue growth factor and cardiac fibrosis after myocardial infarction. *J Histochem Cytochem* 2005;53:1245-56.
5. Gaspard GJ, MacLean J, Rioux D, et al. A novel β -adrenergic response element regulates both basal and agonist-induced expression of cyclin-dependent kinase 1 gene in cardiac fibroblasts. *Am J Physiol Cell Physiol* 2014;306:C540-50.
6. Ogata T, Naito D, Nakanishi N, et al. MURC/Cavin-4 facilitates recruitment of ERK to caveolae and concentric cardiac hypertrophy induced by alpha1-adrenergic receptors. *Proc Natl Acad Sci U S A* 2014;111:3811-6.
7. Parton RG, Simons K. The multiple faces of caveolae. *Nat Rev Mol Cell Biol* 2007;8:185-94.
8. Hansen CG, Nichols BJ. Exploring the caves: cavins, caveolins and caveolae. *Trends Cell Biol* 2010;20:177-86.
9. Briand N, Dugail I, Le Lay S. Cavin proteins: New players in the caveolae field. *Biochimie* 2011;93:71-7.
10. Glenney JR Jr, Soppet D. Sequence and expression of caveolin, a protein component of caveolae plasma membrane domains phosphorylated on tyrosine in Rous sarcoma virus-transformed fibroblasts. *Proc Natl Acad Sci U S A* 1992;89:10517-21.
11. Rothberg KG, Heuser JE, Donzell WC, et al. Caveolin, a protein component of caveolae membrane coats. *Cell* 1992;68:673-82.
12. Scherer PE, Okamoto T, Chun M, et al. Identification, sequence, and expression of caveolin-2 defines a caveolin gene family. *Proc Natl Acad Sci U S A* 1996;93:131-5.
13. Tang Z, Scherer PE, Okamoto T, et al. Molecular cloning of caveolin-3, a novel member of the caveolin gene family expressed predominantly in muscle. *J Biol Chem* 1996;271:2255-61.
14. Jasmin JF, Rengo G, Lymperopoulos A, et al. Caveolin-1 deficiency exacerbates cardiac dysfunction and reduces survival in mice with myocardial infarction. *Am J Physiol Heart Circ Physiol* 2011;300:H1274-81.
15. Xia H, Khalil W, Kahm J, et al. Pathologic caveolin-1 regulation of PTEN in idiopathic pulmonary fibrosis. *Am J Pathol* 2010;176:2626-37.
16. Shi F, Sottile J. Caveolin-1-dependent beta 1 integrin endocytosis is a critical regulator of fibronectin turnover. *J Cell Sci* 2008;121:2360-71.
17. Li L, Ren CH, Tahir SA, et al. Caveolin-1 maintains activated Akt in prostate cancer cells through scaffolding domain binding site interactions with and inhibition of serine/threonine protein phosphatases PP1 and PP2A. *Mol Cell Biol* 2003;23:9389-404.
18. Scherer PE, Lewis RY, Volonte D, et al. Cell-type and tissue-specific expression of caveolin-2. Caveolins 1 and 2 co-localize and form a stable hetero-oligomeric complex in vivo. *J Biol Chem* 1997;272:29337-46.
19. Song KS, Li Shengwen, Okamoto T, et al. Co-purification

- and direct interaction of Ras with caveolin, an integral membrane protein of caveolae microdomains. Detergent-free purification of caveolae microdomains. *J Biol Chem* 1996;271:9690-7.
20. Jasmin JF, Malhotra S, Singh Dhallu M, et al. Caveolin-1 deficiency increases cerebral ischemic injury. *Circ Res* 2007;100:721-9.
 21. Mahmoudi M, Willgoss D, Cuttle L, et al. In vivo and in vitro models demonstrate a role for caveolin-1 in the pathogenesis of ischaemic acute renal failure. *J Pathol* 2003;200:396-405.
 22. Ratajczak P, Damy T, Heymes C, et al. Caveolin-1 and -3 dissociations from caveolae to cytosol in the heart during aging and after myocardial infarction in rat. *Cardiovasc Res* 2003;57:358-69.
 23. Yamada KM, Araki M. Tumor suppressor PTEN: modulator of cell signaling, growth, migration and apoptosis. *J Cell Sci* 2001;114:2375-82.
 24. Georgescu MM, Kirsch KH, Akagi T, et al. The tumor-suppressor activity of PTEN is regulated by its carboxyl-terminal region. *Proc Natl Acad Sci U S A* 1999;96:10182-7.
 25. Stambolic V, Tsao MS, Macpherson D, et al. High incidence of breast and endometrial neoplasia resembling human Cowden syndrome in pten^{+/-} mice. *Cancer Res* 2000;60:3605-11.
 26. Lee JO, Yang H, Georgescu MM, et al. Crystal structure of the PTEN tumor suppressor: implications for its phosphoinositide phosphatase activity and membrane association. *Cell* 1999;99:323-34.
 27. Tamura M, Gu J, Danen EH, et al. PTEN interactions with focal adhesion kinase and suppression of the extracellular matrix-dependent phosphatidylinositol 3-kinase/Akt cell survival pathway. *J Biol Chem* 1999;274:20693-703.
 28. Stambolic V, Suzuki A, de la Pompa JL, et al. Negative regulation of PKB/Akt-dependent cell survival by the tumor suppressor PTEN. *Cell* 1998;95:29-39.
 29. Lu Y, Yu Q, Liu JH, et al. Src family protein-tyrosine kinases alter the function of PTEN to regulate phosphatidylinositol 3-kinase/AKT cascades. *J Biol Chem* 2003;278:40057-66.
 30. Li DM, Sun H. TEP1, encoded by a candidate tumor suppressor locus, is a novel protein tyrosine phosphatase regulated by transforming growth factor beta. *Cancer Res* 1997;57:2124-9.
 31. Denley A, Gymnopoulos M, Kang S, et al. Requirement of phosphatidylinositol(3,4,5)trisphosphate in phosphatidylinositol 3-kinase-induced oncogenic transformation. *Mol Cancer Res* 2009;7:1132-8.
 32. Degtyarev M, De Mazière A, Orr C, et al. Akt inhibition promotes autophagy and sensitizes PTEN-null tumors to lysosomotropic agents. *J Cell Biol* 2008;183:101-16.
 33. Couet J, Li S, Okamoto T, et al. Identification of peptide and protein ligands for the caveolin-scaffolding domain. Implications for the interaction of caveolin with caveolae-associated proteins. *J Biol Chem* 1997;272:6525-33.
 34. Wu W, Hu Y, Li J, et al. Silencing of Pellino1 improves postinfarct cardiac dysfunction and attenuates left ventricular remodeling in mice. *Cardiovasc Res* 2014;102:46-55.
 35. Savin S, Cvejic D, Isic T, et al. Thyroid peroxidase and galectin-3 immunostaining in differentiated thyroid carcinoma with clinicopathologic correlation. *Hum Pathol* 2008;39:1656-63.
 36. Janković J, Paskaš S, Marečko I, et al. Caveolin-1 expression in thyroid neoplasia spectrum: comparison of two commercial antibodies. *Dis Markers* 2012;33:321-31.
 37. Crisostomo PR, Wang Y, Markel TA, et al. Human mesenchymal stem cells stimulated by TNF-alpha, LPS, or hypoxia produce growth factors by an NF kappa B- but not JNK-dependent mechanism. *Am J Physiol Cell Physiol* 2008;294:C675-82.
 38. Ryhänen T, Mannermaa E, Oksala N, et al. Radicolol but not geldanamycin evokes oxidative stress response and efflux protein inhibition in ARPE-19 human retinal pigment epithelial cells. *Eur J Pharmacol* 2008;584:229-36.
 39. Swynghedauw B. Molecular mechanisms of myocardial remodeling. *Physiol Rev* 1999;79:215-62.
 40. Watson CJ, Collier P, Tea I, et al. Hypoxia-induced epigenetic modifications are associated with cardiac tissue fibrosis and the development of a myofibroblast-like phenotype. *Hum Mol Genet* 2014;23:2176-88.
 41. van den Borne SW, Diez J, Blankesteijn WM, et al. Myocardial remodeling after infarction: the role of myofibroblasts. *Nat Rev Cardiol* 2010;7:30-7.
 42. Barallobre-Barreiro J, Didangelos A, Schoendube FA, et al. Proteomics analysis of cardiac extracellular matrix remodeling in a porcine model of ischemia/reperfusion injury. *Circulation* 2012;125:789-802.
 43. Opie LH, Commerford PJ, Gersh BJ, et al. Controversies in ventricular remodelling. *Lancet* 2006;367:356-67.
 44. Kim S, Han J, Lee DH, et al. Cholesterol, a Major Component of Caveolae, Down-regulates Matrix Metalloproteinase-1 Expression through ERK/JNK Pathway in Cultured Human Dermal Fibroblasts. *Ann*

- Dermatol 2010;22:379-88.
45. Porter KE, Turner NA. Cardiac fibroblasts: At the heart of myocardial remodeling. *Pharmacology & therapeutics* 2009;123:255-78.
 46. Turner NA, Porter KE. Function and fate of myofibroblasts after myocardial infarction. *Fibrogenesis Tissue Repair* 2013;6:5.
 47. Sedgwick B, Riches K, Bageghni SA, et al. Investigating inherent functional differences between human cardiac fibroblasts cultured from nondiabetic and Type 2 diabetic donors. *Cardiovasc Pathol* 2014;23:204-10.
 48. Deb A, Ubil E. Cardiac fibroblast in development and wound healing. *J Mol Cell Cardiol* 2014;70:47-55.
 49. Dobaczewski M, de Haan JJ, Frangogiannis NG. The extracellular matrix modulates fibroblast phenotype and function in the infarcted myocardium. *J Cardiovasc Transl Res* 2012;5:837-47.
 50. Boscher C, Nabi IR. CAVEOLIN-1: Role in Cell Signaling. *Adv Exp Med Biol* 2012;729:29-50.
 51. Schönfelder U, Radestock A, Elsner P, et al. Cyclodextrin-induced apoptosis in human keratinocytes is caspase-8 dependent and accompanied by mitochondrial cytochrome c release. *Exp Dermatol* 2006;15:883-90.
 52. Yi SL, Liu XJ, Zhong JQ, et al. Role of caveolin-1 in atrial fibrillation as an anti-fibrotic signaling molecule in human atrial fibroblasts. *PLoS One* 2014;9:e85144.

Cite this article as: Gao Y, Chu M, Hong J, Shang J, Xu D. Hypoxia induces cardiac fibroblast proliferation and phenotypic switch: a role for caveolae and caveolin-1/PTEN mediated pathway. *J Thorac Dis* 2014;6(10):1458-1468. doi: 10.3978/j.issn.2072-1439.2014.08.31

The association of lipopolysaccharide and inflammatory factors with hepatopulmonary syndrome and their changes after orthotopic liver transplantation

Huimin Yi^{1*}, Yuling An^{2*}, Haijin Lv², Xuxia Wei², Xiaomeng Yi², Genshu Wang¹, Yang Yang¹, Guihua Chen¹, Shuhong Yi¹

¹Liver Transplantation Center, ²SICU, The Third Affiliated Hospital of Sun Yat-sen University, Guangzhou 510630, China

*These authors contributed equally to the manuscript.

Correspondence to: Pro. Shuhong Yi. Liver Transplantation Center, The Third Affiliated Hospital of Sun Yat-sen University, Guangzhou 510630, China. Email: yishuhong@163.com.

Background: The level of lipopolysaccharides (LPS) and inflammatory factors were higher in end stage liver disease patient than in normal person for the damage of intestinal mucosal barrier function. Hepatopulmonary syndrome (HPS) was a common pulmonary complication in end stage liver disease. But the association of LPS and inflammatory factors such as toll like receptor 2 (TLR2), TNF- α and ET-1 with the development of HPS was undefined.

Methods: Thirty-one HPS patients were researched (26 patients were performed liver transplantation, five were not). Ten healthy volunteers were recruited as negative control. Blood was collected from the 26 HPS patients before and 3, 7, 14, 21 and 28 days after orthotopic liver transplantation (OLT), and from five HPS patients without OLT and ten healthy volunteers once to detect TLR2 mRNA and iNOS mRNA in peripheral blood monocytes and plasma LPS, TNF- α and ET-1 level. Their levels before and after OLT were compared.

Results: TLR2 mRNA, iNOS mRNA, LPS, TNF- α and ET-1 before OLT in HPS patients were $336,594.1 \pm 366,901.1$, $63,982.2 \pm 74,127.5$ copies/ugRNA, 4.3 ± 3.3 , 90.1 ± 76.0 and 319.9 ± 124.4 ng/L, respectively. They were $10,338.3 \pm 3,814.6$, $19,168.5 \pm 2,417.4$ copies/ugRNA, 0.94 ± 0.69 , 2.7 ± 0.1 and 84.2 ± 10.6 ng/L in normal control group. They were significantly higher in HPS patients than those in control group ($P < 0.05$). After OLT, liver function improved to normal. Also TLR2 mRNA, TNF- α and ET-1 decreased in HPS patients after OLT compared with those before OLT. And PaO₂ and PaO₂/FiO₂ improved greatly with intrapulmonary shunt decreased to normal after OLT.

Conclusions: Lipopolysaccharides at the end stage of liver disease with the release of series of inflammatory factors may be associated with the development of HPS.

Keywords: Hepatopulmonary syndrome (HPS); orthotopic liver transplantation (OLT); toll-like receptor (TLR); inducible nitric oxide synthase (iNOS); tissue necrosis factor alpha (TNF- α); mechanism

Submitted Aug 10, 2014. Accepted for publication Sep 28, 2014.

doi: 10.3978/j.issn.2072-1439.2014.10.05

View this article at: <http://dx.doi.org/10.3978/j.issn.2072-1439.2014.10.05>

Introduction

Hepatopulmonary syndrome (HPS) is a relatively common and severe pulmonary vascular complication of advanced liver cirrhosis and/or portal hypertension (PH), occurring in 10-30% of patients with cirrhosis (1). It is characterized by pulmonary microvascular dilatation and remodeling, resulting in impaired oxygenation in the absence of marked intrinsic cardiopulmonary disease (2,3). Medical therapy for severe HPS has generally been ineffective. Orthotopic liver transplantation (OLT) is the only successful treatment and typically results in complete resolution of the gas exchange impairment (4-8). However, the pathogenesis of HPS is unknown. Inflammation might play a role in its pathogenesis and development (9). The objectives of our study were to investigate the role of lipopolysaccharide (LPS), toll-like receptor 2 (TLR2), inducible nitric oxide synthase (iNOS), tissue necrosis factor alpha (TNF- α) and endothelin-1 (ET-1) in HPS and the change in the levels of these factors after OLT.

Materials and methods

Patient selection

From March 2004 to January 2006, 279 patients with end-stage liver disease received OLT in the Liver Transplantation Center of Sun Yat-sen University. During this period, 31 patients with HPS were evaluated in our center and were included in this analysis. Among these 31 HPS patients, 26 underwent OLT and the other five patients did not undergo OLT due to either late timing or expectation of a poor outcome. Written informed consent was obtained from each patient included in the study. The study protocol was approved by the institution's Human Research Committee and the Medical Ethics Committee of The Third Affiliated Hospital of Sun Yat-sen University. Ten other healthy volunteers were selected as the healthy control group.

Diagnostic criteria for HPS

HPS was diagnosed by: (I) evidence of chronic liver disease with clinical manifestations of PH (varices, ascites, splenomegaly); (II) abnormal arterial oxygenation ($\text{PaO}_2 \leq 70$ mmHg) while breathing room air; and (III) "positive" $^{99\text{m}}\text{Tc}$ -MAA lung and brain perfusion scans suggesting intrapulmonary vascular dilatation (abnormal pulmonary

shunt $>7\%$), or positive contrast echocardiography. Non-HPS patients were those with end-stage liver disease without hypoxemia ($\text{PaO}_2 \geq 70$ mmHg) (10).

$^{99\text{m}}\text{Tc}$ -MAA lung perfusion scan

Every patient with $\text{PaO}_2 \leq 70$ mmHg underwent a $^{99\text{m}}\text{Tc}$ -MAA lung and brain perfusion scan to specifically quantify the degree of intrapulmonary vascular dilatation (11). Twenty minutes after injection (standing) of 2 mCi of $^{99\text{m}}\text{Tc}$ -MAA with 90% of particles between 10 and 90 μm (Dupont Pulmolite, Billerica, MA, USA), quantitative brain imaging was performed in the supine position.

Brain uptake or shunt fraction (assuming a constant 13% blood flow to the brain) was obtained by the following calculation: brain uptake (%) = $(\text{GMT brain}/0.13)/(\text{GMT brain}/0.13 + \text{GMT lung})$. GMT is the geometric mean count of $^{99\text{m}}\text{Tc}$ -MAA in the brain and lung. An abnormal intrapulmonary shunt was defined as greater than 7%. The severity of liver disease was described by the Child-Turcotte-Pugh (CTP) classification (A, B, or C) and the Model for End-stage Liver Disease (MELD) score. These variables were assessed within one week of the PaO_2 measurements.

Blood sample collection

Fasting venous blood samples from all OLT patients with HPS were collected on the morning before transplantation and on postoperative days 3, 7, 14, 21 and 28. Samples were also taken from HPS patients without OLT once, and from healthy volunteers once for controls. Peripheral blood levels of TLR2 messenger ribonucleic acid (mRNA), iNOS mRNA, LPS, TNF- α and ET-1 were measured. Liver function and arterial blood gas (ABG) was examined periodically.

Experimental procedure

The expression levels of TLR2 mRNA and iNOS mRNA were measured by the fluorogenic quantitative polymerase chain reaction (FQ-PCR). The instrument, reagents and technique for real time fluorogenic quantitative reverse transcription-PCR (RT-PCR) were provided by Da An Gene Co., Ltd. of Sun Yat-Sen University. The following procedure was used: (I) peripheral blood total RNA extraction: total RNA was extracted from 500 μL of EDTA-anticoagulated whole blood cells and stored at -80 $^{\circ}\text{C}$ with ethanol for preservation; (II) primers and probe:

Table 1 Clinical data for end-stage liver disease patients with HPS before OLT

Clinical data	HPS (n=26)
Age (yr)	48.8±10.9
Sex (male:female)	24:2
Child-Turcotte-Pugh score	11.2±1.7
Child-Turcotte-Pugh classification (cases, %)	
A	2 (7.7)
B	1 (3.9)
C	23 (88.5)
PT (seconds)	32.3±15.2
APTT (seconds)	69.3±39.3
FIB (g/L)	1.6±1.1
ALB (g/L)	35.1±5.7
ALT (U/L)	204.8±314.3
TB (μmol/L)	368.2±294.0
PaCO ₂ (mmHg)	33.6±4.5
Etiology of cirrhosis (case, %)	
Hepatitis B	23 (88.5)
Hepatitis C	2 (6.5)
Alcoholic cirrhosis	1 (3.2)

OLT, orthotopic liver transplantation; HPS, hepatopulmonary syndrome; PT, prothrombin time; APTT, activated partial thromboplastin time; FIB, fibrinogen; ALB, albumin; ALT, alanine aminotransferase; TB, total bilirubin; PaCO₂, partial pressure of carbon dioxide in artery.

the primer sequence of TLR2 was the forward primer 5'-CATTCCTCAGGGCTCACAG-3' and the reverse primer 5'-TTGTTGGACAGGTCAAGGCTT-3'; the primer sequence of iNOS was the forward primer 5'-AATGGCTGGTACATGGGCAC-3' and the reverse primer 5'-GACGTCA CAGAAGTCCCGGA-3'; (III) reverse transcription: for reverse transcription, 4 μL of extracted RNA were used with the Qiagen RT-PCR Kit (Qiagen, Venlo, Netherlands) in the Perkin Elmer PE 9700 PCR instrument (Perkin Elmer, Waltham, MA). The reaction was conducted using 4 μL of RT-PCR buffer, 0.4 μL (10 pmol/μL) of forward primers, 0.4 μL (10 pmol/μL) of reverse primers, 0.2 μL (25 mmol/L) of dNTP Mix, 1 μL (10 U/μL) of MMLV, 10 μL of RNase-free water, and 4 μL of total RNA in a final volume of 20 μL. The RT-PCR buffer contains the combination of 50 mmol/L of Tris-HCl (pH 8.0), 50 mmol/L of KCl, 4 mmol/L of MgCl₂, and 10 mmol/L of DTT. Reaction conditions were an

initial incubation at 37 °C for one hour, followed by 95 °C for 3 min; (IV) positive control cDNA template preparation and quantitative polymerase chain reaction (Q-PCR): for Q-PCR, 5 μL of the RT-PCR cDNA products were used in the Perkin Elmer PE9700 PCR instrument. Reverse and positive control cDNA were in a mixture as follows: 10 μL of 5× SYBR Green 1 buffer, 1 μL (10 pmol/μL) of forward primers, 1 μL (10 pmol/μL) of reverse primers, 0.5 μL (25 mmol/L) of dNTPs, 1.5 μL (2 U/μL) of Taq DNA Polymerase, 5 μL of cDNA, 31 μL of RNase-free water up to a final volume of 50 μL. Initial reactions at 94 °C for three min were followed by 40 cycles of 93 °C for 1 min and 55 °C for 1 min, and 72 °C for 1 min. Final results were automatically analyzed by the computer.

LPS was detected by the EDS-99 LPS detection system (Jinshanchuan Co. Ltd., Beijing) through a dynamic turbidimetric method. TNF-α and ET-1 were detected by Elisa methodology.

Statistical analysis

Patient demographic data are described by the mean and standard deviation for quantitative variables and percentages for binomial variables. SPSS 10.0 software was used for statistical analysis. Measurement data were analyzed by a *t*-test and expressed as mean ± standard deviation. *P*<0.05 was considered statistically significant.

Results

Patient characteristics

From March 2004 through January 2006, 31 with end-stage liver disease were diagnosed with HPS. Twenty-eight (90%) were male and three (10%) were female, and the mean age was 48 years (range, 28-69 years). Among the 31 HPS patients, 26 (84%) underwent OLT, and five potential OLT candidates (16%) did not undergo transplantation. All patients met minimal listing criteria for liver transplantation (CTP score ≥7 points). The clinical data of 26 OLT recipients including gender ratios, average age, and etiologies of liver cirrhosis, as well as MELD and CTP scores before OLT were listed in *Table 1*.

Levels of inflammatory factors in HPS and healthy control groups

The expression levels of TLR2 mRNA and iNOS mRNA

Table 2 Levels of TLR2 mRNA, iNOS mRNA, LPS, TNF- α and ET-1 before OLT in HPS and healthy control groups

Inflammatory factors	HPS group	Healthy control group	P value	F value	t value
LPS (ng/L)	4.3 \pm 3.3	0.9 \pm 0.7	0.042	3.417	2.243
TLR2 mRNA	336,594.1 \pm 366,901.1	10,338.3 \pm 3,814.6	0.001	4.822	2.151
iNOS mRNA	63,982.2 \pm 74,172.5	19,168.5 \pm 2,417.4	0.004	4.809	1.462
TNF- α (ng/L)	90.1 \pm 76.0	2.7 \pm 0.1	0.000	4.798	3.05
ET-1 (ng/L)	319.9 \pm 124.4	84.2 \pm 10.6	0.000	8.903	4.582

OLT, orthotopic liver transplantation; HPS, hepatopulmonary syndrome; LPS, lipopolysaccharide; TLR2 mRNA, toll-like receptor 2 messenger ribonucleic acid; iNOS mRNA, inducible nitric oxide synthase messenger ribonucleic acid; TNF- α , tissue necrosis factor alpha; ET-1, endothelin-1.

and the plasma levels of LPS, TNF- α and ET-1 before operation are shown for the HPS and healthy control groups in *Table 2*.

After OLT, liver function improved greatly. The decrease of total bilirubin (TB) is shown in *Figure 1*. In all HPS recipients, the levels of TLR2 mRNA (*Figure 2*), TNF- α (*Figure 3*), and ET-1 (*Figure 4*) decreased 28 days after OLT.

Liver function, oxygenation, and intrapulmonary shunt improved after OLT

PaO₂ and PaO₂/FiO₂ in HPS patients improved to normal within 28 days after OLT with the normalization of liver function (*Table 3*). The intrapulmonary shunt measured by 99mTc-MAA decreased to less than 7% when the PaO₂/FiO₂ recovered to normal.

Discussion

HPS is a common complication in advanced liver disease patients. In our research, we proved that LPS increased in end-stage liver disease and was especially significant in those with HPS. This means that LPS might play a role in the pathogenesis of HPS. We concluded that the increased LPS might come from the intestine because the intestine is the biggest reservoir for intestinal bacteria and endotoxin, and the intestinal barrier is damaged severely in cirrhosis (12). PH and impaired microvascular circulation of the intestinal mucosa are associated with decreased intestinal movement, poor repair of the damaged barrier, and bacterial overgrowth, resulting in bacterial imbalance and dislocation because of increased permeability of the intestinal barrier. In cirrhosis, the incidence of intestinal bacterial dislocation was 48% (13,14). Bacteria and endotoxin from the intestine

were released into the circulation, resulting in endotoxemia and inflammation with the release of various inflammatory cytokines (14).

In our research, we found that the levels of LPS, TLR2 mRNA, iNOS mRNA, TNF- α and ET-1 were significantly higher in the HPS group before OLT than in the healthy control group ($P < 0.05$). Our results demonstrated that LPS and inflammatory cytokines, such as TNF- α , ET-1 and NO, might play a role in the pathogenesis and pathophysiology of HPS through TLR2. TLR2 (15), part of the transmembrane protein TLR family, was expressed by antigen-presenting cells and cells of the innate immune system, including neutrophils, mastocytes, basophils and eosinophilic granulocytes, as well as those exposed to the external environment, such as epithelial and endothelial cells in the lung and the gastrointestinal tract. TLR2 is essential for the recognition of a variety of pathogen-associated molecular patterns (PAMPs) from gram-positive bacteria, including bacterial lipoproteins, LPS, lipomannans and lipoteichoic acids. These highly conserved, soluble, membrane-bound proteins are collectively called pattern-recognition receptors (PRRs), and it is the PAMP/PRR interaction that triggers the innate immune system (16). LPS is a glycolipid constituent of the outer membrane of gram-negative bacteria, bound to LPS-binding proteins (LBP). With CD14 and MD-2, the LPS-LBP complex combines with TLR4/TLR2 and initiates the TLR2 \rightarrow MyD88 \rightarrow IRAK \rightarrow TRAF \rightarrow NIK \rightarrow IKK \rightarrow NF- κ B signaling cascade in cells, similar to the process followed by TLR4 with a similar downstream effect. Finally, NF- κ B is activated and causes the release of IL-12, IFN- γ , TNF- α , IL-1, IL-6, NO, ET-1 (17). ET-1 is released by Kupffer cells in the liver and macrophages in the lungs. Its level increases greatly because of liver dysfunction and collateral

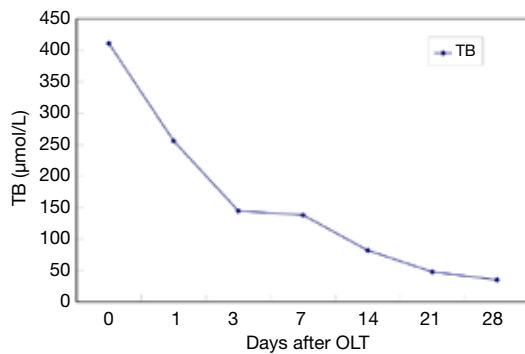


Figure 1 The decrease of TB in HPS patients after OLT. TB, total bilirubin; HPS, hepatopulmonary syndrome; OLT, orthotopic liver transplantation.

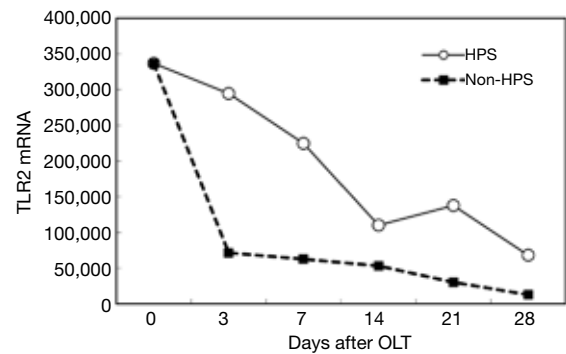


Figure 2 The decrease of TLR2 mRNA expression in HPS patients after OLT. TLR, toll like receptor; HPS, hepatopulmonary syndrome; OLT, orthotopic liver transplantation.

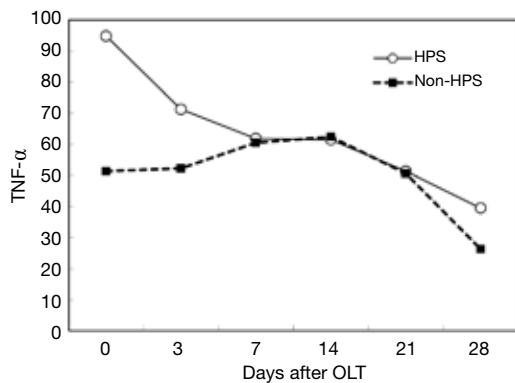


Figure 3 The decrease of plasma TNF-α level in HPS patients after OLT. TNF-α, tissue necrosis factor alpha; HPS, hepatopulmonary syndrome; OLT, orthotopic liver transplantation.

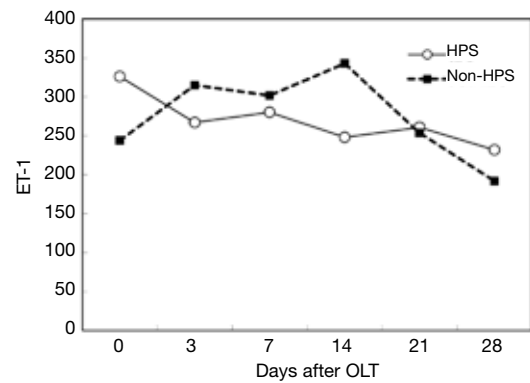


Figure 4 The decrease of plasma ET-1 level in HPS patients after OLT. ET-1, endothelin-1; HPS, hepatopulmonary syndrome; OLT, orthotopic liver transplantation.

Table 3 The levels of PaO₂, PaO₂/FiO₂ and TB in HPS patients after OLT

Variables	Pre-operation			Days after OLT			
	0	1	3	7	14	21	28
PaO ₂	64.47	90.16	82.74	80.89	76.67	78	81.27
PaO ₂ /FiO ₂	287.73	210.49	210.19	222.31	281.78	341.35	382.28
TB	410.94	256	144.72	138.07	81.86	47.63	34.96

OLT, orthotopic liver transplantation; PaO₂, partial pressure of oxygen; PaO₂/FiO₂, the ratio of partial pressure of oxygen to fraction of inspire oxygen; TB, total bilirubin; HPS, hepatopulmonary syndrome.

circulation, and through the ETB receptor, it activates eNOS (18,19), causing accumulation of macrophages in the pulmonary vasculature and overexpression of iNOS and HO-1. The overproduction of NO and carbon monoxide (CO) results in widespread pulmonary vasodilatation at the precapillary and capillary level that leads to a right-to-left shunt, pulmonary V/Q unbalance and hypoxemia.

On the other hand, with the improvement of liver function in HPS patients, TLR2 mRNA, TNF- α and ET-1 decrease, and then, hypoxemia is relieved gradually. In our study, the decrease of these inflammatory factors did not reach statistical significance at 28 days after OLT; however, longer observation might be needed. LPS and iNOS mRNA decreased early after OLT, but they increased again later. HPS patients are extremely prone to the complication of pneumonia. We hypothesized that a later increase in LPS and iNOS mRNA might be associated with subsequent infection in some HPS patients.

Our research demonstrated that LPS might upregulated TLR2 mRNA expression and activation of the downstream inflammatory factor production in cirrhosis before OLT. The overproduction of inflammatory factors might play an important role in the pathogenesis and pathophysiology of HPS. We supposed that LPS came from the intestine because of a damaged intestinal barrier in cirrhosis. After OLT, the liver and intestinal function recovered, and the intestinal barrier was repaired; thus, the levels of inflammatory factors decreased as the hypoxemia of HPS was relieved gradually and completely.

There were limitations in our research in that we could not prove that the origin of LPS was from the intestine. Nor did we detect the expression level of TLR4, which was predominantly activated by LPS. Further research is needed to clarify the function of immune cells and how they work through LPS and TLR activation in HPS.

Conclusions

Above all, LPS and inflammatory factors increased at the end stage of liver disease before OLT, but decreased after OLT with the recovery of liver function. Oxygenation of lungs also got better and the HPS was cured. Our results showed LPS with the release of series of inflammatory factors may be associated with the pathogenesis and development of HPS.

Acknowledgements

Disclosure: The authors declare no conflict of interest.

References

1. Grace JA, Angus PW. Hepatopulmonary syndrome: update on recent advances in pathophysiology, investigation, and treatment. *J Gastroenterol Hepatol* 2013;28:213-9.
2. Agarwal PD, Hughes PJ, Runo JR, et al. The clinical significance of intrapulmonary vascular dilations in liver transplant candidates. *Clin Transplant* 2013;27:148-53.
3. Zhang J, Luo B, Tang L, et al. Pulmonary angiogenesis in a rat model of hepatopulmonary syndrome. *Gastroenterology* 2009;136:1070-80.
4. Yi HM, Chen GH, An YL, et al. Effect of orthotopic liver transplantation on hepatopulmonary syndrome: 5 years of postoperative follow-up and survival analysis. *Organ Transplantation* 2012;03:145-50.
5. Yi HM, Wang GS, Yi SH, et al. Prospective evaluation of postoperative outcome after liver transplantation in hepatopulmonary syndrome patients. *Chin Med J (Engl)* 2009;122:2598-602.
6. Houlihan DD, Holt A, Elliot C, et al. Review article: liver transplantation for the pulmonary disorders of portal hypertension. *Aliment Pharmacol Ther* 2013;37:183-94.
7. Saigal S, Choudhary N, Saraf N, et al. Excellent outcome of living donor liver transplantation in patients with hepatopulmonary syndrome: a single centre experience. *Clin Transplant* 2013;27:530-4.
8. Gupta S, Castel H, Rao RV, et al. Improved survival after liver transplantation in patients with hepatopulmonary syndrome. *Am J Transplant* 2010;10:354-63.
9. Liu L, Liu N, Zhao Z, et al. TNF- α neutralization improves experimental hepatopulmonary syndrome in rats. *Liver Int* 2012;32:1018-26.
10. Perkins JD. Diagnosing hepatopulmonary syndrome. *Liver Transpl* 2007;13:1464-5.
11. Abrams GA, Nanda NC, Dubovsky EV, et al. Use of macroaggregated albumin lung perfusion scan to diagnose hepatopulmonary syndrome: a new approach. *Gastroenterology* 1998;114:305-10.
12. Cartin-Ceba R, Swanson KL, Krowka MJ, et al. Pulmonary arteriovenous malformations. *Chest* 2013;144:1033-44.
13. Rodríguez-Roisin R, Krowka MJ. Hepatopulmonary syndrome—a liver-induced lung vascular disorder. *N Engl J Med* 2008;358:2378-87.
14. Sztrymf B, Libert JM, Mougeot C, et al. Cirrhotic rats with bacterial translocation have higher incidence and severity of hepatopulmonary syndrome. *J Gastroenterol Hepatol* 2005;20:1538-44.
15. Riordan SM, Skinner N, Nagree A, et al. Peripheral

- blood mononuclear cell expression of toll-like receptors and relation to cytokine levels in cirrhosis. *Hepatology* 2003;37:1154-64.
16. Paik YH, Schwabe RF, Bataller R, et al. Toll-like receptor 4 mediates inflammatory signaling by bacterial lipopolysaccharide in human hepatic stellate cells. *Hepatology* 2003;37:1043-55.
 17. He H, Genovese KJ, Nisbet DJ, et al. Profile of Toll-like receptor expressions and induction of nitric oxide synthesis by Toll-like receptor agonists in chicken monocytes. *Mol Immunol* 2006;43:783-9.
 18. Showpittapornchai U, Wattanasirichaigoon S, Pradidarcheep W. Predominant vascular dilatation with NOS expression in lung lower lobe of thioacetamide induced-cirrhotic rat. *J Med Assoc Thai* 2012;95 Suppl 12:S99-104.
 19. Fallon MB, Zhang J. The lung in liver disease: old problem, new concepts. *Trans Am Clin Climatol Assoc* 2013;124:250-62.

Cite this article as: Yi H, An Y, Lv H, Wei X, Yi X, Wang G, Yang Y, Chen G, Yi S. The association of lipopolysaccharide and inflammatory factors with hepatopulmonary syndrome and their changes after orthotopic liver transplantation. *J Thorac Dis* 2014;6(10):1469-1475. doi: 10.3978/j.issn.2072-1439.2014.10.05

Nonspecific interstitial pneumonia and usual interstitial pneumonia: comparison of the clinicopathologic features and prognosis

Xia Li¹, Chang Chen², Jinfu Xu¹, Jinming Liu¹, Xianghua Yi³, Xiwen Sun⁴, Jingyun Shi⁴

¹Department of Respiratory Medicine, ²Department of Surgery, Shanghai Pulmonary Hospital, Tongji University School of Medicine, Shanghai 200433, China; ³Department of Pathology, Tongji Hospital, Tongji University School of Medicine, Shanghai 200065, China; ⁴Department of Radiology, Shanghai Pulmonary Hospital, Tongji University School of Medicine, Shanghai 200433, China

Correspondence to: Xia Li. Department of Respiratory Medicine, Shanghai Pulmonary Hospital, Tongji University School of Medicine, 507 Zhengmin Road, Shanghai 200433, China. Email: lixia2309@163.com; Chang Chen. Department of Surgery, Shanghai Pulmonary Hospital, Tongji University School of Medicine, 507 Zhengmin Road, Shanghai 200433, China. Email: changchenc@hotmail.com.

Background: Nonspecific interstitial pneumonia (NSIP) has recently been proposed as a histologic type of idiopathic interstitial pneumonia (IIP), but its broad spectrum of clinicopathologic findings and variable prognosis are poorly understood. It is particularly unclear how NSIP and usual interstitial pneumonia (UIP) are related. The present study investigated the clinicopathologic features and prognosis of NSIP, and its differential diagnosis from UIP.

Methods: The clinicopathologic findings and prognosis in 21 NSIP and 18 UIP patients who underwent surgical or video-assisted thoracoscopic lung biopsy were reviewed.

Results: NSIP was more frequent in women and showed nonspecific clinical manifestations. High-resolution computed tomography (HRCT) demonstrated ground-glass, net-like, and patchy attenuation in both lungs. Semiquantitative HRCT showed a median fibrosis score of 3 (range, 0 to 7) in NSIP patients and 5 (range, 2 to 7) in UIP patients ($P < 0.01$). On histopathologic examination, NSIP cases were heterogeneous and the findings could be categorized into cellular and fibrosing patterns. The mean age of the NSIP and UIP patients was 48 and 60 years, respectively. The frequencies of fibroblast foci, myogelosis, honeycomb lesions, and pulmonary structural destruction in NSIP and UIP patients were 16.7% and 100% ($P < 0.001$), 22.2% and 85.7% ($P < 0.05$), 16.7% and 92.9% ($P < 0.001$), and 27.8% and 100% ($P < 0.05$), respectively. The responses to glucocorticoid treatment and the prognosis were significantly greater in NSIP than those in UIP.

Conclusions: NSIP was difficult to be differentiated from UIP by general clinical manifestations, but HRCT can be helpful for this purpose. Definitive diagnosis depends on the results of surgical lung biopsy.

Keywords: Nonspecific interstitial pneumonia (NSIP); usual interstitial pneumonia (UIP); clinicopathology; diagnosis

Submitted Sep 05, 2014. Accepted for publication Oct 16, 2014.

doi: 10.3978/j.issn.2072-1439.2014.10.16

View this article at: <http://dx.doi.org/10.3978/j.issn.2072-1439.2014.10.16>

Introduction

Idiopathic nonspecific interstitial pneumonia (NSIP) has been recently named as a histological type of idiopathic interstitial pneumonia (IIP). Interstitial pneumonia that cannot be categorized is referred to as NSIP, which includes three subtypes. However, there are questions regarding the

possible similarities between NSIP and usual interstitial pneumonia (UIP). Comparative histopathologic studies about these two conditions have rarely been conducted and reported worldwide (1,2), and the distinctions between them remains unclear. Therefore, in the present study, the clinical, pathologic, and follow-up findings in NSIP and

Table 1 Comparison of clinical characteristics between UIP and NSIP patients

Clinical characteristic	UIP group	NSIP patients
Symptoms and signs		
Exercise-induced dyspnea	18 (100.00)	13 (61.9)
Velcro's sound (inspiratory phase crackle)	17 (94.44)	9 (42.86)
Clubbing	8 (44.44)	3 (14.29)
Respiratory function tests		
Restrictive ventilatory disorder	12 (66.67)	9 (42.86)
Diffusion function reduction	18 (100.00)	11 (52.38)
Mixed ventilatory disorder	6 (33.33)	6 (28.57)
Honeycomb lung on CT/HRCT	15 (83.33)	3 (14.29)

UIP, usual interstitial pneumonia; NSIP, idiopathic nonspecific interstitial pneumonia; HRCT, high-resolution computed tomography.

UIP patients who underwent open surgical or video-assisted thoracoscopic lung biopsy and treatment over a 10-year duration at our institution were reviewed. Furthermore, the differential diagnosis of NSIP and UIP, and the potential mechanisms of NSIP were discussed.

Materials and methods

Patients and setting

The medical records of 121 patients with diffuse lung disease (suspected as IIP) examined and underwent video-assisted thoracoscopic surgery (VATS) or open surgical lung biopsy at Shanghai Pulmonary Hospital (affiliated hospital of Tongji University) between March 1999 and February 2005 were reviewed. In the 121 cases, 21 were diagnosed with UIP, and 29 were diagnosed with NSIP. A total of 18 UIP patients and 21 NSIP patients who had a complete clinical history and were followed up for at least 1 year postoperatively were analyzed.

Patients were diagnosed with UIP or NSIP according to the IIP diagnostic criteria described by the American Thoracic Society (ATS) and European Respiratory Society (ERS) in 2000 and 2002 (1,3). All final diagnoses were made by consensus of pulmonologists, pathologists, and radiologists (clinical-radiologic-pathologic diagnosis). The study was approved by the institutional review board. The requirement for informed consent was waived.

Treatment and follow-up

Glucocorticoids and symptomatic treatment were administered in 39 patients; 11 UIP patients and 5 NSIP patients were also administered azathioprine (4). Chest radiography and high-resolution computed tomography (HRCT) were performed at 1, 3, 6, 9, and 12 months after initiating treatment. Therapeutic success was determined based on clinical symptoms and signs, such as improvement, stabilization, or deterioration. Improvement and stabilization were considered signs of treatment effectiveness. The criteria used to define improvement were as follows: no overt symptoms, improved respiratory function, resolution of lesions on imaging, stable condition, and no evidence of disease recurrence. Stabilization was considered on the basis of the following findings: resolution of symptoms, mild improvement in respiratory function, partial, or no absorption of lesions on imaging, or disease recurrence. The treatment was considered invalid when symptoms did not resolve and lesions showed no absorption on imaging.

Statistical analysis

Data were analyzed using the SPSS 10.0 software package. Data between the patient groups were compared using χ^2 test (chi-square test). Statistical significance was designated at $P < 0.05$.

Results

Patient demographics and clinical findings

The mean patient age in the UIP group was 60 years and ranged from 50-75 years; the group comprised 12 men and 6 women. Thirteen patients had a history of smoking, and 6 patients had previous contact with inorganic or organic dust. Previous exposure ranged from 5-62 months and averaged 21.6 months. In the NSIP group, the mean patient age was 48 years and ranged from 28-70 years; the group included 7 men and 14 women. Eight patients had a history of smoking, and four patients had previous contact with inorganic or organic dust. Previous exposure ranged from 1-24 months and averaged 7.8 months.

The clinical findings in the UIP and NSIP patients are summarized in *Table 1*. Bacterial culture of sputum yielded negative results in all patients. Anti-nuclear antibody and molecular reactions yielded negative results in all patients

Table 2 Comparison of the imaging findings, histopathology, glucocorticoid response, and long-term outcomes between UIP and NSIP patients

	UIP group (%)	NSIP group (%)	P value
Glucocorticoid response			
Effective	7 (38.89)	16 (76.19)	<0.01
Ineffective	11 (61.11)	5 (23.81)	<0.01
Follow-up outcome			
Recovery	0 (0.00)	6 (28.57)	
Survival with disease	12 (66.67)	15 (71.43)	
Death	6 (33.33)	0 (0.00)	
HRCT score (mean fibrosis score)	3	5	<0.05
Histopathology findings			
Moderate/severe interstitial inflammation	8 (44.44)	10 (47.62)	>0.05
Fibroblast foci	18 (100.00)	4 (19.05)	<0.001
Myogelosis	16 (88.89)	4 (19.05)	<0.05
Diffuse collagen deposition	18 (100.00)	14 (66.67)	<0.05
Honeycomb lesion	17 (94.44)	5 (23.81)	<0.05
Alveolar restructuring	18 (100.00)	7 (33.33)	<0.01
Type II alveolar cell proliferation	15 (83.33)	15 (71.43)	>0.05
BOOP lesion	7 (38.89)	9 (42.86)	>0.05
DIP lesion	8 (44.44)	7 (33.33)	>0.05
Alveolar epithelial cell with columnar metaplasia and squamous metaplasia	11 (61.11)	14 (66.67)	>0.05
Bronchiolitis obliterans	9 (50.00)	13 (61.90)	>0.05

UIP, usual interstitial pneumonia; NSIP, idiopathic nonspecific interstitial pneumonia; HRCT, high-resolution computed tomography; BOOP, bronchiolitis obliterans organizing pneumonia; DIP, desquamative interstitial pneumonia.

except one patient in the NSIP group, who had increased O antibody levels. In the UIP patients, the chest radiographs showed asymmetric bilateral reticular shadows in the basal and peripheral lungs, and decreased lung volume. The CT and HRCT showed flake- and net-like shadows, primarily in the basal lungs. In a few patients, ground-glass shadows and severe fibrosis were present and were accompanied

by traction bronchiectasis, bronchiolectasis, or subpleural honeycomb-like lesions.

In the NSIP patients, the chest radiographs showed interstitial diffuse infiltration with net-like and fibrous linear pulmonary opacities. The CT and HRCT images showed varying severities of ground-glass shadows, and net-like and fibrous linear pulmonary opacities, with no honeycomb-like changes. Based on the history of occupational exposure, clinical manifestation, laboratory examination, and histopathology (including polarizer observation), collagen vascular disease, occupational pneumoconiosis, drug-induced interstitial lung disease, and infection were excluded.

Histopathologic examination

An incisional biopsy was performed in 4 patients of the UIP group and 8 patients of the NSIP group; the remainder underwent a VATS lung biopsy. In each procedure, at least three samples were taken from mildly, moderately, and severely diseased tissues, which were ≥ 1.0 cm \times 0.7 cm \times 0.5 cm.

Histopathology in the UIP group

At low magnification, the lesions varied in severity and were distributed erratically. Chronic and acute lesions of interstitial inflammation, fibrosis, and honeycombing were interspersed among the normal lung tissue, and were primarily within the subpleural lung parenchyma. The interstitial inflammation was typically patchy with alveolar septum infiltrates comprising leukomonocytes and plasmacytes accompanied by type II alveolar cell proliferation. Diffuse hyperplastic fibrous tissue with collagen deposition formed the alveolar structure. In the areas of inflammation, fibrosis, and honeycomb changes, foci in a light-blue myxoid stroma background were observed. These foci comprised proliferative fibroblast and myoblast cells were identified as myofibroblast cell foci. The honeycombed lung formed by a cystic fiber chamber was often covered by bronchial epithelial cells and contained mucus. In the fibrotic and honeycomb areas, smooth muscle proliferation was observed, which was patchy and at times with myogelosis. In two cases, mixed diffuse alveolar damage, cell proliferation, and the loss of the alveolar epithelial cells were also present. The lung interstitium also showed fibroblast proliferation and a macrophagocyte mass along with serous effusion from the alveolar space. The incidences of each particular lesion in both patient groups are summarized in *Table 2*.

Histopathology in the NSIP group

All cases showed varying severities of chronic inflammation and interstitial fibrosis. The pathological changes were similar across the tissue samples. On histologic examination, the subtypes were distributed as follows: one case of cellular type, nine cases of mixed type, and eight cases of fibrous type lesions. Inflammatory cell infiltration and fibrous tissue proliferation were observed in the mixed type cases, which primarily comprised lymphocytes and a small number of plasmacytes. In the fibrous type cases, the inflammation was comparatively less, but the collagen deposition was significantly greater. The comparison between the pathologic characteristics in the NSIP and UIP patients is shown in *Table 2*.

Discussion

UIP and NSIP are the most common subtypes of IIP. In 2000 and 2002, the ATS and ERS respectively published reports detailing the diagnosis and treatment of IPF formed by consensus of experts worldwide. These reports described the most updated classification scheme (ATS/ERS classification) for IIP, including UIP, NSIP, and other subtypes (a total of seven subtypes). In 1994, Katzenstein et al. first described NSIP as interstitial pneumonia, which was not fit into other categories. In the new classification system, NSIP also excludes diseases with known causes, and presently includes three subtypes—cellular, fibrous, and mixed, which differ in their respective clinical manifestations, therapeutic options, and prognosis. The current ATS/ERS classification provides specific IIP categories, rather than employing general descriptions, which enables standardized diagnosis, treatment, and studies of IIP, and forms a foundation for domestic and international cooperation in research. However, the ATS/ERS classification requires clinical verification of its rationale and practicality. The ATS/ERS classification fails to address several questions concerning IIP. And the relationship between UIP and NSIP is still unclear. The disease course, treatment outcomes, and prognoses of the fibrous type of NSIP and UIP are quite similar, and techniques are unclear to distinguish them. The ideal pathologic, clinical and radiologic diagnostic criteria for UIP and NSIP require investigation and confirmation in additional cases. Large-scale studies in this field are presently lacking in China (5).

According to the present study, UIP occurred primarily

in men over 50 years of age. More than 50% of the patients were over 60 years of age at the initial examination. This is in stark contrast to the mean onset age (48.2 years of age) in the NSIP patients. UIP occurred more frequently in men, while NSIP occurred more often in women. There were no significant differences in the clinical manifestations between the UIP and NSIP patients. Dry cough and dyspnea were main features in both groups, and inspiratory crackles were detected in most of the patients, which was most apparent at the base of both lungs. Clubbing was observed primarily in UIP patients. There were no significant differences between the UIP and NSIP patients in the respiratory function and laboratory findings. Although laboratory tests cannot diagnose UIP and NSIP, they can detect other diffuse lung diseases.

The chest radiographs were similarly ineffective in the diagnosis of UIP and NSIP; however, CT, especially HRCT, was quite useful diagnostically. On HRCT, the UIP cases showed patchy shadows in the basal regions of both lungs, and very few ground-glass opacities were present. Due to the severe fibrosis, traction bronchiectasis, bronchiolectasis, and subpleural honeycomb changes were observed in all UIP cases. NSIP mainly showed patchy and ground-glass opacities in both lungs. The honeycomb lesions were typically present in advanced cases of fibrous NSIP. HRCT was useful in the differential diagnosis of intractable cases. On HRCT, UIP was characterized by peripheral shadows and honeycomb changes. However, honeycomb changes were rare in NSIP (6), which only occurred late in the disease course (4,7).

The clinical and imaging characteristics were reportedly quite similar between the IIP subtypes; therefore, diagnosis relies on VATS or surgical lung biopsy findings (8). At low magnifications, NSIP showed phase consistency across the different fields, but the most distinctive characteristics were in the varying pathologic lesions, which comprised both acute and chronic features. The fibroblast foci in NSIP were small, and few were observed, with only 19.05% (4/21) of samples showing the foci. Honeycomb changes appeared later in the disease course in the fibrous type. Overall, it was difficult to distinguish mixed and fibrous NSIP, despite their different occurrence of fibroblast foci, honeycombing, myogelosis, diffuse collagen deposition, and alveolar restructuring. Therefore, comprehensive evaluation of these characteristics is necessary for the differential diagnosis (6,9,10).

In a previous study, the glucocorticoid response and prognosis differed between UIP and NSIP (11). We found

that the UIP patients responded poorly to glucocorticoid therapy. Although a few patients experienced intermittent improvement, most received no significant therapeutic benefit even when cytotoxic drugs were added to the regimen. In contrast, the NSIP patients responded favorably to glucocorticoid therapy, and only patients with the fibrous type failed to respond; the glucocorticoid response rates were 38.89% and 76.19% in the two groups, respectively ($P < 0.01$). On follow-up, six UIP patients died of respiratory failure 3 years after therapy, and the NSIP patients had an overall superior quality of life. These findings are consistent with those reported by Travis *et al.* (11), indicating that diagnosis based on the UIP and NSIP classifications have clinical significance. However, the NSIP pathology is clinically nonspecific; therefore, pathologic diagnosis mostly include both clinical and imaging data, namely a clinic-radiologic-pathologic diagnosis. This is a key point of IIP classification and diagnosis; a diagnosis made by clinical physicians, radiologists, or pathologists alone is likely to be biased. By investigating both the clinical history and laboratory examination data, conditions such as collagen vascular disease, tuberculous pulmonary fibrosis, occupational pulmonary fibrosis, eosinophilic pneumonia, and other interstitial lung disease can be excluded. Sampling errors may be a concern according to some studies; however, if the clinical manifestations and imaging features meet the criteria of UIP, then a lack of fibroblasts does not exclude the condition. According to the ATS/ERS classification, surgical lung biopsy (VATS or mini-incision surgical lung biopsy) is recommended in IIP patients without surgical contraindications in order to exclude other similar conditions and definitively diagnose IIP. It enables the implementation of effective therapies and prevents misdiagnosis and inappropriate treatment (12-17).

Conclusions

NSIP was difficult to be differentiated from UIP by general clinical manifestations, but HRCT can be helpful for this purpose. Definitive diagnosis depends on the results of surgical lung.

Acknowledgements

This work was supported by the funding of Shanghai Municipal Health Bureau Project (No. 054Y036).

Authors's contributions: Xia Li designed the overall study, carried out experiments, collected and analyzed data, and

wrote the paper. Chang Chen performed the VATS and the open surgical lung biopsy procedures and collected data for histopathologic examinations. Jinfu Xu and Jinming Liu collected clinic data, and Xianghua Yi collected and analyzed histopathologic data. Xiwen Sun and Jingyun Shi collected and analyzed radiologic data.

Disclosure: The authors declare no conflict of interest.

References

1. Travis WD, King TE, Bateman ED, et al. ATS/ERS consensus statement of idiopathic interstitial pneumonias. *Am J Respir Crit Care Med* 2002;265:277-304.
2. American Thoracic Society; European Respiratory Society. American Thoracic Society/European Respiratory Society International Multidisciplinary Consensus Classification of the Idiopathic Interstitial Pneumonias. This joint statement of the American Thoracic Society (ATS), and the European Respiratory Society (ERS) was adopted by the ATS board of directors, June 2001 and by the ERS Executive Committee, June 2001. *Am J Respir Crit Care Med* 2002;165:277-304.
3. Raghu G, Collard HR, Egan JJ, et al. An official ATS/ERS/JRS/ALAT statement: idiopathic pulmonary fibrosis: evidence-based guidelines for diagnosis and management. *Am J Respir Crit Care Med* 2011;183:788-824.
4. MacDonald SL, Rubens MB, Hansell DM, et al. Nonspecific interstitial pneumonia and usual interstitial pneumonia: comparative appearances at and diagnostic accuracy of thin-section CT. *Radiology* 2001;221:600-5.
5. Honoré PM, Spapen H. Embracing western and Chinese research and clinical knowledge: We take up the translational gauntlet! *J Transl Intern Med* 2013;1:1-2.
6. Kondoh Y, Taniguchi H, Yokoi T, et al. Cyclophosphamide and low-dose prednisolone in idiopathic pulmonary fibrosis and fibrosing nonspecific interstitial pneumonia. *Eur Respir J* 2005;25:528-33.
7. Marten K, Milne D, Antoniou KM, et al. Non-specific interstitial pneumonia in cigarette smokers: a CT study. *Eur Radiol* 2009;19:1679-85.
8. Popescu A, Săftoiu A. Can elastography replace fine needle aspiration? *Endosc Ultrasound* 2014;3:109-17.
9. Riha RL, Duhig EE, Clarke BE, et al. Survival of patients with biopsy-proven usual interstitial pneumonia and nonspecific interstitial pneumonia. *Eur Respir J* 2002;19:1114-8.
10. Travis WD, Hunninghake G, King TE Jr, et al. Idiopathic nonspecific interstitial pneumonia: report of an American

- Thoracic Society project. *Am J Respir Crit Care Med* 2008;177:1338-47.
11. Travis WD, Matsui K, Moss J, et al. Idiopathic nonspecific interstitial pneumonia: prognostic significance of cellular and fibrosing patterns: survival comparison with usual interstitial pneumonia and desquamative interstitial pneumonia. *Am J Surg Pathol* 2000;24:19-33.
 12. Martinez FJ. Idiopathic interstitial pneumonias: usual interstitial pneumonia versus nonspecific interstitial pneumonia. *Proc Am Thorac Soc* 2006;3:81-95.
 13. Swigris JJ, Kuschner WG, Kelsey JL, et al. Idiopathic pulmonary fibrosis: challenges and opportunities for the clinician and investigator. *Chest* 2005;127:275-83.
 14. Fujita J, Ohtsuki Y, Yoshinouchi T, et al. Idiopathic non-specific interstitial pneumonia: as an "autoimmune interstitial pneumonia". *Respir Med* 2005;99:234-40.
 15. Halkos ME, Gal AA, Kerendi F, et al. Role of thoracic surgeons in the diagnosis of idiopathic interstitial lung disease. *Ann Thorac Surg* 2005;79:2172-9.
 16. Monaghan H, Wells AU, Colby TV, et al. Prognostic implications of histologic patterns in multiple surgical lung biopsies from patients with idiopathic interstitial pneumonias. *Chest* 2004;125:522-6.
 17. Drent M, du Bois RM, Poletti V. Recent advances in the diagnosis and management of nonspecific interstitial pneumonia. *Curr Opin Pulm Med* 2003;9:411-7.

Cite this article as: Li X, Chen C, Xu J, Liu J, Yi X, Sun X, Shi J. Nonspecific interstitial pneumonia and usual interstitial pneumonia: comparison of the clinicopathologic features and prognosis. *J Thorac Dis* 2014;6(10):1476-1481. doi: 10.3978/j.issn.2072-1439.2014.10.16

The experience of using Endo GIA™ Radial Reload with Tri-Staple™ Technology for various lung surgery

Toshinari Ema

Department of Thoracic Surgery, Meirikai Central Hospital, 3-2-11 Higashijyuujyou Itabashi-ku, Tokyo 114-0001, Japan

Correspondence to: Toshinari Ema. Department of Thoracic Surgery, Meirikai Central Hospital, 3-2-11 Higashijyuujyou Itabashi-ku, Tokyo 114-0001, Japan. Email: toshinariema09@yahoo.co.jp.

Abstract: Endo GIA™ Radial Reload with Tri-Staple™ Technology (RR) is a device for colorectal surgery. However, with its rounded staple line, Radial Reload is suitable for various lung surgeries. We use the device for lung wedge resection, and cutting bronchus in lung lobectomy. The total number of use counts up to 56 fires, and all fires came out well.

Keywords: Radial Reload; stapler; video-assisted thoracic surgery (VATS)

Submitted Jul 02, 2014. Accepted for publication Aug 18, 2014.

doi: 10.3978/j.issn.2072-1439.2014.09.06

View this article at: <http://dx.doi.org/10.3978/j.issn.2072-1439.2014.09.06>

Introduction

Endo stapler is now dispensable for video-assisted thoracic surgery (VATS) (1). The indication of VATS is spreading, and now various operations are performed with VATS. We always need some consideration to perform operation safely and certainly with the change of operational procedures. Endo GIA™ Radial Reload with Tri-Staple™ Technology (RR) is a very useful for various lung operations including VATS. RR is a device that is first designed for colorectal surgery. The most particular characteristic of the stapler is its rounded stapling line (*Figure 1*). Moreover, the head part of the stapler is designed perpendicular to shaft of the device, therefore, input vector of stapler is turned 90 degrees for its output (*Figure 2*). It is very useful for lung surgery.

Materials and methods

RR is suitable for resection of tumor which exists at periphery of lung. We usually seize a tumor with a device such as PN catch. Then, we mostly use straight type stapler to cut around PN catch with enough surgical margin. During this manipulation, we often experience the difficulties that occur because of the direction of stapler. A straight type stapler's head mobilization is limited and it

makes it difficult to frame an ideal staple line. Therefore, we sometimes make another port to insert a stapler to make a correct staple line. We use RR in this situation. RR is able to be inserted through the same window which PN catch is inserted with parallel direction. This feature makes the first fire to be formed easily as ideal design. Also, its rounded shape enables to resect along the line of PN catch taking enough surgical margin (*Figure 3*). This first fire mobilized the tumor, therefore, the second fire becomes easier to make (*Figures 4,5*). RR is the only stapling device that has this characteristic. The important point is that input vector of stapler is changed perpendicularly, so RR can be inserted parallel to PN catch. Because it is necessary to perceive the tumor by touch in order to assure safety margin, the RR is effective for its rounded shape. RR is also useful for resection of bronchus in lung lobectomy. Right angle shape of RR is suitable for cutting a bronchus. Whereas TA™ is a widely used device for closing bronchus, RR has a merit for its cutting ability (*Figures 6,7*). Because RR has a wider width compared to other types of staplers, we need to release layers of bronchus for longer distance than using others. This manipulation is not so easy and seems like a demerit for cutting bronchus. However, we think that this manipulation leads to define resection of #11 lymph node. When cutting bronchus, it is necessary to check if the device is not holding surrounding tissue, especially

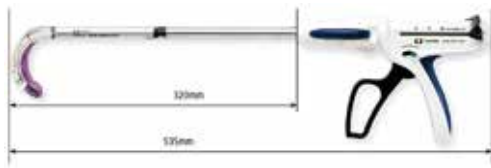


Figure 1 Endo GIA™ Radial Reload with Tri-Staple™ Technology (RR).

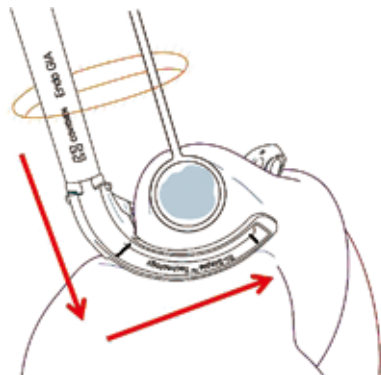


Figure 2 The most particular characteristic of the stapler is its rounded stapling line. Moreover, the head part of the stapler is designed perpendicular to shaft of the device, therefore, input vector of stapler is turned 90 degrees for its output.

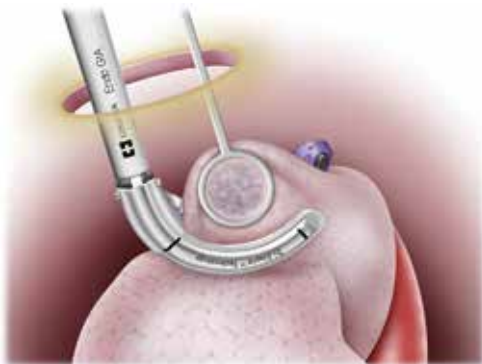


Figure 3 Endo GIA™ Radial Reload with Tri-Staple™ Technology (RR) is able to be inserted through the same window which PN catch is inserted with parallel direction. And its rounded shape enables to resect along the line of PN catch taking enough surgical margin.

pulmonary artery behind it. Unlike its rounded shape, the cutting line of RR for bronchus is almost straight and not curved. Looking at the line, it is clear that we do not have to worry about unwilling effect caused by the shape of stump (Figure 7).

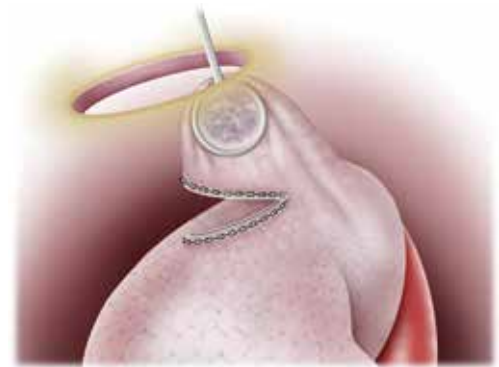


Figure 4 The first fire mobilized the tumor.

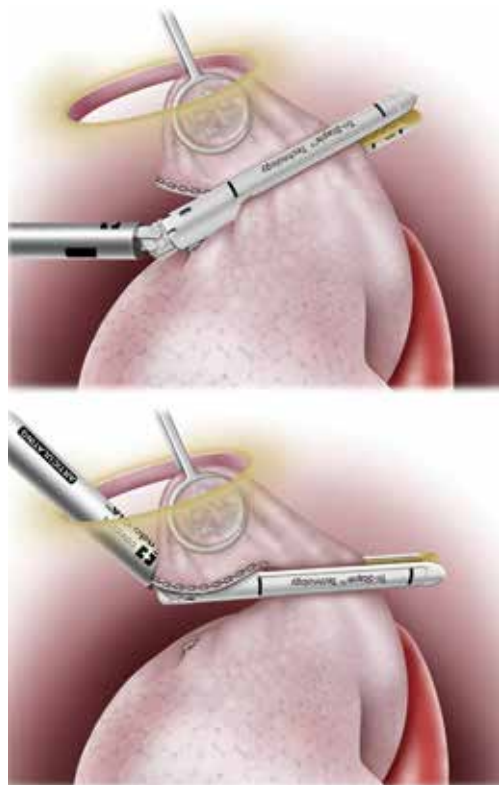


Figure 5 The second fire becomes easier to make.

Results

We used RR for 56 fires in lung surgery. Its breakdown is that 40 for lung wedge resection, and 16 for cutting bronchus (Table 1). There is no complication until now.

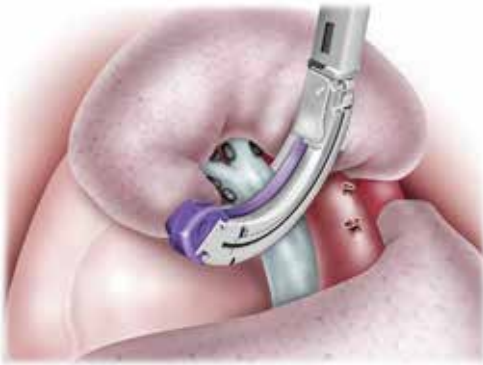


Figure 6 Endo GIA™ Radial Reload with Tri-Staple™ Technology (RR) is also useful for resection of bronchus in lung lobectomy.



Figure 7 Unlike its rounded shape, the cutting line of Endo GIA™ Radial Reload with Tri-Staple™ Technology (RR) for bronchus is almost straight and not curved.

Comments

RR is a device that is very useful for lung surgery especially with VATS. And this real operation's procedure which had ruptured into the right atrium (*Figure 8*).

Acknowledgements

Disclosure: The author declares no conflict of interest.

Table 1 RR for 56 fires in lung surgery	
Types	No. of patients, fires
Disease	
Primary lung cancer	20
Metastatic lung cancer	3
Other	12
Surgery method	
Wedge resection	40
Cut of bronchus	16
Complication	
	0



Figure 8 Endo GIA™ Radial Reload with Tri-Staple™ Technology for various lung surgery (2). Endo GIA™ Radial Reload with Tri-Staple™ Technology (RR) is able to be inserted through the same window which PN catch is inserted with parallel direction. The first fire mobilized the tumor. The second fire with RR. Water sealing test: No air leakage. RR is also useful for resection of bronchus in lung lobectomy. Using RR with cutting lower bronchus. The staple line is not rounded. Water sealing test: No air leakage. Available online: <http://www.asvide.com/articles/309>

References

1. Sugarbaker DJ, Mentzer SJ. Improved technique for hilar vascular stapling. *Ann Thorac Surg* 1992;53:165-6.
2. Ema T. Endo GIA™ Radial Reload with Tri-Staple™ Technology for various lung surgery. *Asvide* 2014;1:296. Available online: <http://www.asvide.com/articles/309>

Cite this article as: Ema T. The experience of using Endo GIA™ Radial Reload with Tri-Staple™ Technology for various lung surgery. *J Thorac Dis* 2014;6(10):1482-1484. doi: 10.3978/j.issn.2072-1439.2014.09.06

Non-intubated complete thoracoscopic bronchial sleeve resection for central lung cancer

Wenlong Shao^{1,2,3}, Kevin Phan⁴, Xiaotong Guo⁵, Jun Liu^{1,2,3}, Qinglong Dong⁶, Jianxing He^{1,2,3}

¹Department of Thoracic Surgery, First Affiliated Hospital of Guangzhou Medical University, Guangzhou 510120, China; ²Department of Surgery, Guangzhou Institute of Respiratory Diseases, Guangzhou 510120, China; ³National Respiratory Disease Clinical Research Center, Guangzhou 510000, China; ⁴The Collaborative Research (CORE) Group, Macquarie University Hospital, New South Wales, Australia; ⁵Department of Thoracic Surgery, Second Affiliated Hospital of Harbin Medical University, Harbin 15000, China; ⁶Department of Anesthesiology, First Affiliated Hospital of Guangzhou Medical University, Guangzhou 510120, China

Correspondence to: Jianxing He, MD, PhD, FACS. Department of Cardiothoracic Surgery, The First Affiliated Hospital of Guangzhou Medical University, No. 151, Yanjiang Rd, Guangzhou 510120, China. Email: drjianxing.he@gmail.com.

Abstract: Bronchial sleeve resection has emerged as an effective thoracoscopic approach for central lung cancer with reduced operation mortality rates, optimal lung function and long-term survival. Endobronchial intubation is a commonly used method of anesthesia for such thoracoscopic procedures, but is associated with increased intubation-related and lung complications. Non-intubated epidural anesthesia represents an alternative approach which may avoid such difficulties, particularly in complicated sleeve resection situations. Here we have described a case of complete endoscopic bronchial sleeve resection of right lower lung cancer under non-intubated epidural anesthesia.

Keywords: Lung cancer; bronchial sleeve resection; non-intubated epidural anesthesia

Submitted Aug 09, 2014. Accepted for publication Aug 11, 2014.

doi: 10.3978/j.issn.2072-1439.2014.08.10

View this article at: <http://dx.doi.org/10.3978/j.issn.2072-1439.2014.08.10>

Introduction

Bronchial sleeve resection of lung tumors has emerged as an effective approach which not only removes the lesion but also avoids pneumonectomy, thereby reducing surgical mortality and maximizing lung function and long-term survival (1). Chen *et al.* reported a video-assisted thoracic surgery (VATS) lobectomy for lung cancer under non-intubated epidural anesthesia, which demonstrated acceptable safety and feasibility (2). However, there are no reports describing bronchial sleeve resection under non-intubated anesthesia. Here, we describe a case of complete endoscopic bronchial sleeve resection of right lower lung cancer under non-intubated epidural anesthesia.

Case report

A 70-year-old man presented with a mass in the right lower lung during physical examination. Lung function tests

showed forced vital capacity (FVC) of 73.1% and forced expiratory volume in 1 s (FEV₁) of 71.5%. Computed tomography (CT) showed a mass at the dorsal segment of the lower right pulmonary lobe (*Figure 1*), measuring approximately 3×4 cm², as a thick-walled eccentric cavity. On November 11, 2013, the patient underwent complete thoracoscopic resection under non-intubated epidural anesthesia. Intramuscular midazolam (0.07 mg/kg) and atropine (0.01 mg/kg) were administered at 30 min before anesthesia. Epidural puncture was performed at the T7-8 intervertebral space, with the epidural catheter tip pointed towards the head and fixed after confirming successful placement. Following epidural injection of 0.375% ropivacaine and a test dose of 2 mL ropivacaine, the patient was observed for 5 min for signs of total spinal anesthesia. If total spinal anesthesia was not achieved, two more injections of 0.375% ropivacaine were administered, totaling 8 mL.

With a mask to supply oxygen and remove nitrogen, 2 µg/mL of intravenous propofol was given via target-

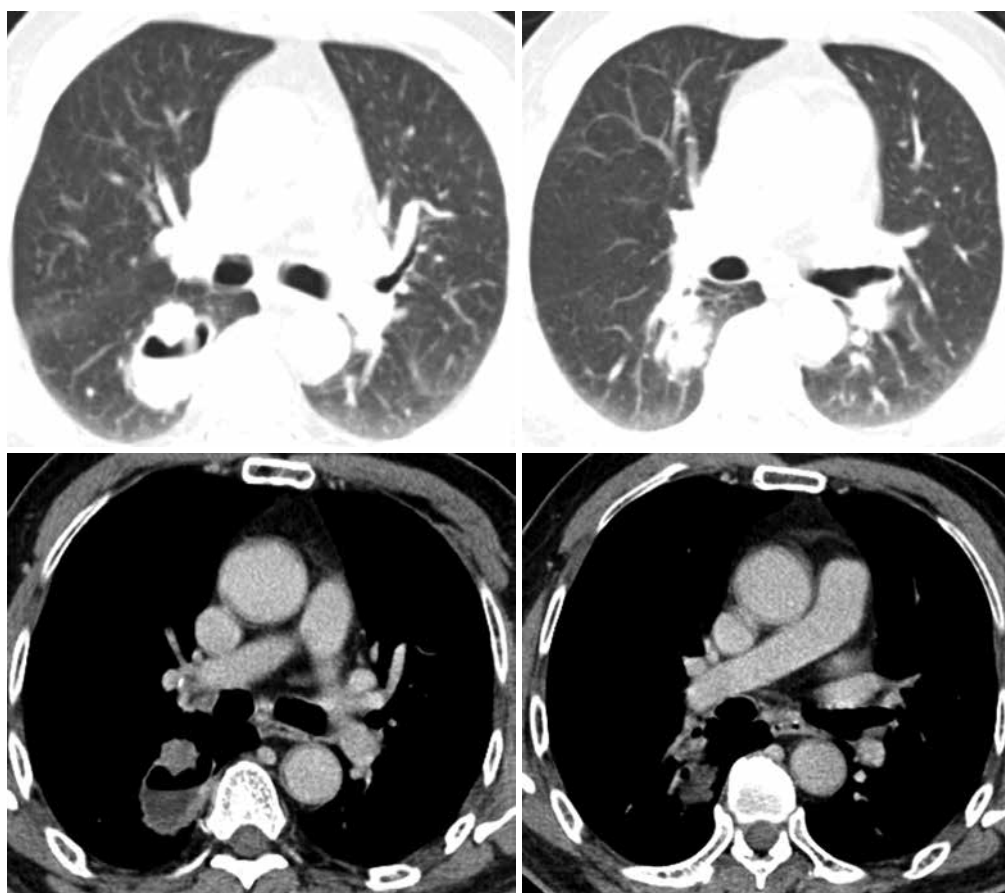


Figure 1 Mass at the dorsal segment of the right lung on computed tomography (CT).

controlled infusion (TCI) in combination with 0.2 µg/kg intravenous infusion of sufentanil. When adequate sedation was achieved, a laryngeal mask airway (LMA) was inserted and the anesthesia machine was connected to provide simultaneous intermittent mandatory ventilation (SIMV). Arterial catheterization was performed at the right internal jugular vein and the radial artery on the non-operative side.

Epidural injection of 4 mL 0.375% ropivacaine was administered at an interval of 60 min. Continuous intravenous infusion of 1.0-1.5 µg/mL propofol was performed via TCI. Continuous infusion of remifentanyl 0.03 µg/kg·min and dexmedetomidine hydrochloride 0.5-1.0 µg/kg·h was administered to maintain sedation. An intraoperative spectrum analyzer was used to monitor the sedative effect, with the bispectral index (BIS) maintained at 40-60. The sedation depth was adjusted according to the monitored parameters. Spontaneous breathing was maintained, with a respiratory rate of 12-20 beats/min.

To suppress the cough reflex caused by lung tissue stretch

during the thoracoscopic operation, the intrathoracic vagus nerve was blocked. Under direct vision in thoracoscopy, 3-5 mL of 0.375% ropivacaine was injected near the vagus nerve inferior to the mediastinal pleura above the azygos arch adjacent to the trachea.

The approach for non-intubated epidural thoracoscopic surgery was the 3-port method. With the patient in a left lateral position, the endoscopic observation port was made in the 7th intercostal space at the anterior axillary line, the working port in the 5th intercostal space at the anterior axillary line, and the auxiliary port in the 7th intercostal space at the posterior axillary line. Using a 30° endoscope, the observation field covered the entire chest cavity. Using the connection between the operated side and the outer atmosphere and a gentle push on the lesion side, an iatrogenic pneumothorax was formed to collapse the right lung. After vagus nerve blockade, exploration of the dorsal side of the right lower lung was performed, where a mass measuring 4×5×5 cm³ was found, with evident pleural

surface indentation. Johnson's endoscopic automatic stapler was initially used to isolate the incomplete fissure, and the right lower pulmonary artery and vein were incised. The right lower lobular bronchus was then similarly transected, sent for frozen biopsy and shown to be "bronchial margin residual cancer". While waiting for the pathological result, systematic lymphadenectomy was performed. To preserve the right and middle lung, bronchial sleeve resection was planned, and the surgery was continued without switching to intubation. The right middle lobe and the bronchi in the middle segment were transected at the root. The frozen pathology showed no residual lesions in the margin of the intermediate segment and the proximal middle bronchus. The right middle lobular bronchus was then joined with the right intermediate bronchus, and was continuously sutured with single 3-0 Prolene suture silk. After anastomosis, a pressurized balloon was applied in conjunction with laryngeal mask ventilation to expand the lungs, and no leakage was observed at the bronchial anastomosis. Upon confirmation of hemostasis, the operation was completed.

Results

The operation time was 165 min, involving 25 min of bronchial anastomosis and 120 mL blood loss. Five groups of a total of 18 lymph nodes were dissected during surgery. Histopathology results were as follows: moderately differentiated squamous cell carcinoma of the right lower lung, stump carcinoma in situ of the lower lobe bronchus, no tumor in the proximal margins of the right middle lobe and intermediate bronchi, and no lymph node metastasis in any dissected group (0/18). The patient did not require assisted breathing postoperatively. He was able to drink and eat at 4 h postoperatively and was mobile at postoperative day 1. At postoperative day 3, the drainage was removed, and no leaks, pulmonary infection, atelectasis, bronchial fistula, or other complications were observed. He was discharged on postoperative day 6. Pulmonary CT at 1 month postoperatively showed no anastomotic strictures (*Figure 2*).

Comment

In the present case, since there was a stump residual tumor in the bronchus after lobular resection, we switched to the sleeve resection technique. Given that the patient was stable and the advantage of reduced operative time required for bronchial anastomosis, the non-intubated anesthetic



Figure 2 Postoperative pulmonary computed tomography (CT) revealed no anastomotic stricture at 1 month after surgery.

approach was undertaken with the hope of avoiding further injury. Therefore, we performed bronchial sleeve resection under non-intubated anesthesia with satisfactory results, demonstrating that non-intubated anesthesia could be successfully used in not only conventional VATS lobectomy but also for complicated bronchial anastomosis.

To avoid perioperative respiratory failure, non-intubated epidural anesthesia is usually performed only in a select group of patients, with estimated operation time within 3 h and have ASA grade I-II, body mass index <25, and good lung function reserves. In such patients, $SPO_2 \geq 90\%$ can be maintained (2-4). In this patient, since we needed to open the airway for bronchial sleeve resection, which stopped the inhalation of oxygen from the nostrils, the inhaled oxygen concentration was reduced and the SPO_2 briefly decreased to 80%. We therefore provided assisted ventilation with a laryngeal mask and balloon to increase the oxygen flow and ventilation, rapidly improving the SPO_2 to a safe range of 90-95%, reversing the hypoxemia while reducing CO_2 reabsorption. After completing bronchial anastomosis, the patient's ventilation recovered immediately, and hypoxemia and hypercapnia improved significantly.

In conclusion, thoracoscopic bronchial resection under non-intubated epidural anesthesia can be performed, allowing successful removal of the tumor while retaining adequate functionality of the lung tissue. The patient recovered rapidly, awakened quickly postoperatively, began to eat and drink and was mobile soon after surgery, with a short hospital stay.

Acknowledgements

Disclosure: The authors declare no conflict of interest.

References

1. Schmid T, Augustin F, Kainz G, et al. Hybrid video-assisted thoracic surgery-robotic minimally invasive right upper lobe sleeve lobectomy. *Ann Thorac Surg* 2011;91:1961-5.
2. Chen JS, Cheng YJ, Hung MH, et al. Nonintubated thoroscopic lobectomy for lung cancer. *Ann Surg* 2011;254:1038-43.
3. Dong Q, Liang L, Li Y, et al. Anesthesia with nontracheal intubation in thoracic surgery. *J Thorac Dis* 2012;4:126-30.
4. Chen KC, Cheng YJ, Hung MH, et al. Nonintubated thoroscopic lung resection: a 3-year experience with 285 cases in a single institution. *J Thorac Dis* 2012;4:347-51.

Cite this article as: Shao W, Phan K, Guo X, Liu J, Dong Q, He J. Non-intubated complete thoroscopic bronchial sleeve resection for central lung cancer. *J Thorac Dis* 2014;6(10):1485-1488. doi: 10.3978/j.issn.2072-1439.2014.08.10

Chinese expert consensus on molecularly targeted therapy for advanced non-small cell lung cancer (2013 edition)

Guoming Wu^{1*}, Caicun Zhou^{2*}, Chunxue Bai³, Guisheng Qian¹

¹Xinqiao Hospital of the Third Military Medical University, Chongqing 400037, China; ²Pulmonary Hospital of Tongji University, Shanghai 200433, China; ³Zhongshan Hospital of Fudan University, Shanghai 200032, China

*These authors contributed equally to this work.

Correspondence to: Chunxue Bai. Pulmonary Hospital of Tongji University, Shanghai 200433, China. Email: bai.chunxue@zs-hospital.sh.cn; Guisheng Qian. Xinqiao Hospital of the Third Military Medical University, Chongqing 400037, China. Email: qiangs1220@163.com.

Submitted Aug 20, 2014. Accepted for publication Sep 09, 2014.

doi: 10.3978/j.issn.2072-1439.2014.09.20

View this article at: <http://dx.doi.org/10.3978/j.issn.2072-1439.2014.09.20>

Lung cancer is one of the most common malignant tumors worldwide, ranking the first of all cancers in terms of mortality. More than 80-85% lung cancers are non-small cell lung cancer (NSCLC), and most of them are in advanced stages at the time of diagnosis (1). Although the role of chemotherapy for NSCLC remains virtually unchanged in recent years, the therapeutic efficacy has reached a plateau. Moreover, toxic and adverse reactions have limited its further clinical applications. Instead, targeted therapy has aroused the widest attention and become one of the most promising therapeutic strategies owing to the reliable therapeutic effect, low toxicity and mild adverse reactions (2). The expert panels from the Respiratory Disease Branch Lung Cancer Study Group of the Chinese Medical Association and the Chinese Alliance Against Lung Cancer have discussed issues related to molecularly targeted treatments for advanced NSCLC and reached consensus on molecularly targeted treatments for advanced NSCLC (2013 edition) in the context of the national conditions in Mainland China.

Detection of lung cancer driver genes

Epidermal growth factor receptor (EGFR) gene mutations

The results of numerous studies have demonstrated that the *EGFR* mutation status is the most important predictive factor for assessing the therapeutic effect of EGFR-tyrosine kinase inhibitors (EGFR-TKIs) for the treatment of advanced NSCLC. Such mutations usually occur within exon 18-21, in which exon 19 deletion and exon 21 L858R

mutation (defined as sensitive mutations) are the most common mutations indicative of the sensitivity to EGFR-TKI treatment. Multiple studies (3,4) have demonstrated that the overall mutation rate in unselected Chinese NSCLC patients is about 30%, about 50% in patients with lung adenocarcinoma, or even as high as 60-70% in non-smoking patients with lung adenocarcinoma. The *EGFR* mutation rate in patients with squamous cell carcinoma is about 10%. It is therefore necessary for clinicians to enhance their awareness about the routine detection of *EGFR* mutations.

The detection of *EGFR* mutations can be performed on surgically resected specimens, histology biopsy specimens and cytology specimens, but whatever specimen is used, it should contain at least 200-400 tumor cells. The use of blood specimens for the detection of *EGFR* mutations has not been well established due to less sensitive as compared with tissue specimens, and therefore is not recommended for routine use for the time being. Quality control (QC) of the specimen to be detected should be under the supervision of experienced pathologists (4).

There are various methods for the detection of *EGFR* mutations at present, including the direct sequencing assay and real-time fluorescence quantitative polymerase chain reaction (FQ-PCR)-based assays such as scorpion amplification refractory mutation system-scorpion assay (ARMS), fragment length analysis and denaturing high performance liquid chromatography. These methods have their respective advantages and disadvantages, and there is no consensus at present about which is more advantageous.

The DNA direct sequencing assay is widely utilized to detect known and unknown mutations, but it has a high requirement on the content (more than 50% and at least 30%) of tumor cells in the specimen. Real-time FQ-PCR-based methods such as ARMS is more sensitive and can detect 1.0-0.1% mutant cells in the specimen, and therefore is more suitable for detecting small specimens that contain a relatively small number of tumor cells. ARMS is the most common method used in clinical practice due to simplicity. However, it can only detect known mutations, the specimen needs to be pre-treated, and the cost is relatively high (4,5).

Anaplastic lymphoma kinase fusion gene

Anaplastic lymphoma kinase (ALK) fusion gene is a newly discovered NSCLC driver gene, where echinoderm microtubule-associated protein-like4 (EML4) and ALK fusion (EML4-ALK) is the most common type. ALK fusion gene is mainly found in non-smoking or light-smoking patients with lung adenocarcinoma, and usually does not co-exist with *EGFR* mutations in the same patient. The occurrence of ALK fusion gene in NSCLC patients is about 5% vs. 25% in NSCLC patients without *EGFR*, *KRAS*, *HER2* or *TP53* mutations. In Mainland China, the positive rate of ALK fusion gene in NSCLC patients with both *EGFR* and *KRAS* wild type lung adenocarcinoma is as high as 30-42% (4). There are mainly three methods to detect ALK fusion gene at present: fluorescence in situ hybridization (FISH), PCR amplification-based techniques and immunohistochemistry (IHC). FISH remains the reference standard for confirming ALK fusion gene at present. But as it is costly and has high technical requirements, it is not applicable to screen ALK positive patients. qRT-PCR is easy to follow with a high sensitivity, but it needs specific reagent kits and instruments and there have been commercially available kits approved by the Chinese Food and Drug Administration (CFDA) for clinical qRT-PCR assays at present. IHC is easy to follow, inexpensive and technically mature. The antibody specificity and sensitivity of high affinity D5F3 (Cell Signaling) and 5A4 (Abcam) have reached 100% and 95-99% respectively. The Ventana ALK fusion protein IHC diagnostic reagent kit has improved the sensitivity without affecting the specificity. Its coincidence rate with FISH is as high as 98.8%, and the reproducibility is as high as 99.7%. It has been approved by the CFDA for the diagnosis of ALK-positive NSCLC patients. The detection method should be selected appropriately according to the histological

specimen type and the laboratory conditions. Specimen QC should be supervised by experienced pathologists. When the reliability of a test method is suspected, another method should be employed for verification (6).

ROS-1 fusion gene

ROS1 is another receptor tyrosine kinase (RTK) gene that forms fusions and a newly discovered NSCLC driver gene as well. The most common type is CD74-ROS-1, occurring in about 1% of NSCLC patients (7), especially in non-smoking or light-smoking young patients with lung adenocarcinoma. It usually does not overlap with other driver genes. ROS-1 fusion gene is very much like ALK fusion gene with respect to the clinical characteristics, suggesting that these two mutation subsets may share the same pathogenic mechanism. There are various methods for detection ROS-1 fusion gene, among which the FISH method is the most commonly used (7).

Conclusions: (I) every possible effort should be made to obtain specimens for the detection of *EGFR* mutations before treatment for NSCLC patients; (II) specimen QC for the detection of *EGFR* mutations should be supervised by experienced pathologists, and an appropriate detection method should be selected, preferably by selecting a highly sensitive method such as ARMS; (III) it is advisable to undertake ALK and ROS-1 fusion gene detection in patients without *EGFR* mutations; (IV) it is advisable to undertake detections of *EGFR* mutations, ALK and ROS-1 fusion genes simultaneously if it is possible.

Epidermal growth factor receptor-tyrosine kinase inhibitors (EGFR-TKIs)

First-line treatment

The IPASS study reported in 2009 was a large-scale, international, multi-center, randomized controlled phase III clinical trial (8), the primary endpoint of which was progression-free survival (PFS). The results of IPASS showed that PFS in patients with *EGFR* mutations who used gefitinib as the first-line treatment was obviously superior to that in patients who used carboplatin + paclitaxel (9.8 vs. 6.4 months; HR =0.48, P<0.001). The objective response rate (ORR) in Gefitinib group was also improved significantly, accompanied with better tolerance and quality of life (QoL), though there was no significant difference in overall survival (OS) between the two groups, probably

because a relatively large proportion of the patients received crossover or other treatments in subsequent periods. IPASS study is of milestone significance in targeted therapy because it opens the door of true individualized therapy for lung cancer.

The WJTOG 3405 study is an open-label, multi-center, randomized controlled phase III clinical trial. It compared the therapeutic effect between gefitinib and cisplatin + docetaxel as the first-line treatment in 177 advanced NSCLC patients with *EGFR* mutations. The results showed that PFS in the two groups was 9.2 and 6.3 months respectively, indicating that the therapeutic effect of gefitinib was obviously superior to that of cisplatin + docetaxel (HR =0.49, $P<0.0001$) (9).

The NEJ 002 study compared the therapeutic effect between gefitinib and carboplatin + paclitaxel as the first-line treatment in 230 advanced NSCLC patients with *EGFR* mutations. The results showed that the therapeutic effect of gefitinib was obviously superior to that of carboplatin + paclitaxel in terms of PFS (10.8 *vs.* 5.4 months; HR =0.30, $P<0.001$) (10).

OPTIMAL is a randomized phase III clinical trial sponsored by the Chinese Thoracic Oncology Group (CTONG). It compared the therapeutic effect between Erlotinib and gemcitabine + carboplatin as the first-line treatment in 165 advanced NSCLC patients with *EGFR* mutations. The results showed that the therapeutic effect of Erlotinib was obviously superior to that of gemcitabine + carboplatin in terms of PFS (13.1 *vs.* 4.6 months; HR =0.16, $P<0.0001$), accompanied with better QoL, though there was no significant difference in OS between the two groups (11). However, the results of subgroup analysis showed that the survival duration was relatively short in patients who only received chemotherapy, with a median OS of 11.7 (n=21) *vs.* 20.6 months in patients who only received EGFR-TKI (n=33) and 30.4 months in patients who first received EGFR-TKI and then chemotherapy (n=94), suggesting that EGFR-TKI makes great contributions to the improvement of survival in patients with *EGFR* mutations (12).

EURTAC is a study equivalent to OPTIMAL conducted in Caucasian population. It compared the therapeutic effect between Erlotinib and chemotherapy as the first-line treatment in 174 NSCLC patients with *EGFR* mutations, using PFS as the primary endpoint of research. The results showed that PFS of the two groups was 9.7 and 5.2 months respectively, suggesting that the therapeutic effect of erlotinib was obviously superior to that of chemotherapy alone (HR =0.37, $P<0.0001$) (13).

A more recent randomized phase III clinical trial (FASTACT-II) showed that PFS in patients receiving double agents chemotherapy in combination with intercalated use of erlotinib as the first-line treatment for 6 cycles followed by erlotinib maintenance therapy was 7.6 *vs.* 6.0 months in patients who received double agents chemotherapy + placebo (HR =0.57, $P<0.0001$), and OS was 18.3 and 15.2 months respectively (HR =0.79, $P=0.0420$). The result of subgroup analysis on the *EGFR* mutation status showed that only patients with *EGFR* mutations rather than patients with wild-type *EGFR* benefited from this mode of treatment (14).

The LUX-LUNG3 study is an international, multi-center, randomized controlled phase III clinical trial, showing that PFS in advanced lung adenocarcinoma patients with *EGFR* mutations who received irreversible inhibitor of the erbB family Afatinib as the first-line treatment was obviously superior to cisplatin + pemetrexed (11.1 *vs.* 6.9 months; HR =0.58, $P=0.001$). In addition, ORR in Afatinib group was also significantly improved (56% *vs.* 23%; $P=0.001$) (15).

LUX-LUNG6 is another randomized controlled phase III clinical trial conducted in Asian population. The results showed that Afatinib as the first-line treatment was also obviously superior to gemcitabine + cisplatin in advanced lung adenocarcinoma patients with *EGFR* mutations in terms of PFS as the primary endpoint of research (11.0 *vs.* 5.6 months; HR =0.28, $P<0.0001$). In addition, ORR in Afatinib group was also significantly improved (66.9% *vs.* 23.0%; $P<0.0001$) (16).

The adverse reactions of EGFR-TKIs are relatively mild, mainly including skin reactions (rash, pruritus, skin dryness and acne) and diarrhea. Adverse reactions occur in more than 50% NSCLC patients who received the first-generation EGFR-TKIs but they are usually mild. Adverse reactions more than grade 3 usually occur in about 2-10% patients, of which interstitial pneumonia is a rare but severe adverse reaction, accounting for about 1%, and needs special attention, because it may lead to death if not treated properly or positively. The occurrence of adverse reactions with the second-generation EGFR-TKI Afatinib is even higher and the symptoms are more severe than the first-generation EGFR-TKIs.

Conclusions: (I) EGFR-TKIs are recommended as the first-line treatment for advanced NSCLC patients with *EGFR* mutations (gefitinib and erlotinib have been approved as the first-line treatment agents in many countries, but only gefitinib has been approved in Mainland China.

Afatinib has been approved as the first-line treatment agent in the United State and Taiwan region of China); (II) the first-line chemotherapy + intercalated use of erlotinib for 6 cycles followed by erlotinib as maintenance therapy can be considered in advanced NSCLC patients with *EGFR* mutations.

Maintenance therapy

The INFORM study conducted in Mainland China compared the therapeutic effect of maintenance therapy between gefitinib and placebo in advanced NSCLC patients, finding that PFS in gefitinib group was significantly longer than that in placebo group (4.8 *vs.* 2.6 months; HR =0.42, $P<0.0001$). Notably, the PFS was more significantly longer in the subgroup of advanced NSCLC patients with *EGFR* mutations using gefitinib than that in placebo group (16.6 *vs.* 2.8 months; HR =0.17), indicating that advanced NSCLC patients, especially those with *EGFR* mutations can benefit from gefitinib maintenance therapy (17). In another phase III study (WJTOG0203), 604 patients with stage IIIb or IV NSCLC were randomly assigned to two groups: one group receiving 3 cycles of standard first-line platinum-doublet chemotherapy followed by gefitinib maintenance therapy, and the other group receiving 6 cycles of platinum-doublet chemotherapy. PFS of the two groups was 4.6 *vs.* 4.3 months ($P<0.001$). Although there was no significant difference in OS between the two groups, OS in gefitinib maintenance therapy group was significantly longer than that in chemotherapy group alone in the adenocarcinoma subgroup (15.4 *vs.* 14.3 months; $P=0.03$) (18).

A meta-analysis on erlotinib maintenance therapy (included SATURN, ATLAS and IFCT-GFPC0502 study) showed that erlotinib was able to prolong PFS and OS of patients with advanced NSCLC who achieved disease control (DC) [partial response (PR)/complete response (CR)/stable disease (SD)] after first-line chemotherapy. All subgroup patients benefited from Erlotinib maintenance therapy, especially female patients, non-smokers and non-squamous cell carcinoma patients, probably because the *EGFR* mutation rate in these patients is relatively high (19). The subgroup analysis of SATURN study showed that PFS in patients with *EGFR* mutations who received Erlotinib maintenance therapy was significantly longer than that in placebo group (HR =0.10, $P<0.0001$) (20,21).

Conclusions: gefitinib or erlotinib maintenance therapy can be considered in advanced NSCLC patients who achieved DC (PR/CR/SD) after first-line chemotherapy.

Second-line and subsequent therapies

A meta-analysis enrolling four phase II/III clinical trials showed that the risk of disease progression in unselected Asian patients with pretreated advanced NSCLC who received Gefitinib was 19% lower than that in those who received Docetaxel, and ORR increased remarkably (117%) (22). The Chinese subgroup analysis of INTEREST study showed that ORR of gefitinib and docetaxel was 21.9% and 9.1% respectively ($P=0.016$), in which the median PFS in adenocarcinoma subgroup was 5.4 months for Gefitinib and 3.9 months for docetaxel (23). A Korean phase III KCSG-LU-0801 study showed that ORR in Asian non-smoking patients with previously treated advanced lung adenocarcinoma who used Gefitinib and Pemetrexed was 58.8% *vs.* 22.4% respectively ($P<0.001$), median PFS was 9.0 *vs.* 3.0 months respectively ($P=0.0006$) (24). BR.21 study showed that OS in unselected previously treated advanced NSCLC who used Erlotinib and Placebo was 6.7 and 4.7 months respectively, and the difference was significantly different (HR =0.70, $P<0.001$) (25). TITAN and HORG study compared the therapeutic effect of erlotinib, pemetrexed and docetaxel, finding that the therapeutic effect of erlotinib was equivalent to that of Pemetrexed or Docetaxel as the standard second-line single chemotherapy agent but had better tolerance (26,27).

ICOGEN, a non-inferiority phase III clinical trial conducted in Mainland China (28), compared the therapeutic effect of icotinib and gefitinib in unselected patients with previously treated advanced NSCLC, and found that PFS of icotinib and Gefitinib was 4.6 and 3.4 months respectively ($P=0.13$), confirming that icotinib was not inferior to gefitinib in unselected patients with pretreated advanced NSCLC.

Studies comparing the therapeutic effect of gefitinib and erlotinib (29,30) and that comparing the therapeutic effect of gefitinib and icotinib (28) suggested that the therapeutic effect of the three *EGFR*-TKIs as second-line treatment agents was similar for advanced NSCLC patients.

TAILOR, an international, multi-center, phase III clinical trial, showed that PFS and OS in advanced NSCLC patients with wild-type *EGFR* who received erlotinib as the second-line treatment were significantly shorter than those who received docetaxel (PFS 2.4 *vs.* 2.9 months, HR =0.71, $P=0.02$; 6-month OS 16.5% *vs.* 27.3%) (31). The DELTA study also demonstrated that PFS and ORR in advanced NSCLC patients with wild-type *EGFR* who received Erlotinib as the second-line treatment were also inferior than those who received docetaxel (PFS 1.3 *vs.* 2.9, $P=0.013$;

ORR 5.6% *vs.* 20.0%, $P=0.003$) (32). The CTONG0806 study showed that PFS in advanced non-squamous NSCLC patients with wild-type EGFR who received Pemetrexed or Gefitinib was 4.8 *vs.* 1.6 months ($P<0.001$), and the disease control rate (DCR) was 61.3% and 32.0% respectively ($P<0.001$) (33). The results of the above three studies all showed that second-line chemotherapy should be the first treatment choice in advanced NSCLC patients with wild-type *EGFR*.

Conclusions: (I) EGFR-TKIs (gefitinib, erlotinib or icotinib) can be used as second- or third-line treatment agents in advanced NSCLC patients, while EGFR-TKIs are preferably recommended in advanced NSCLC patients with *EGFR* mutations; (II) EGFR-TKIs are not preferably recommended as second-line treatment in advanced NSCLC patients with wild-type EGFR.

Treatment of elderly patients and patients with poor performance status

Elderly (>70 years) patients with lung cancer are usually intolerable to platinum-doublet chemotherapy due to relatively poor organ functions and the existence of complications, in whom EGFR-TKIs can be considered as the first-line treatment because of relatively good tolerance. A systematic analysis on three NEJ studies (001,002,003) compared ORR and PFS in elderly patients with advanced NSCLC and *EGFR* mutations who used Gefitinib or chemotherapy, and found that ORR was 73.2% *vs.* 26.5%, and PFS was 14.3 *vs.* 5.7 months, both showing significant differences between the two groups (34). Of the three studies, NEJ002 showed that there was no significant difference in toxicity and QoL between elderly and young patients who used Gefitinib, indicating that the therapeutic effect of Gefitinib as the first-line treatment is relatively good and the toxicity is tolerable in elderly patients with lung cancer of *EGFR* mutations. Another randomized phase III clinical trial TOPICAL in advanced NSCLC patients who received erlotinib or placebo because of being intolerable to first-line chemotherapy showed that the risk of disease progression in erlotinib group was 17% lower than that in placebo group (35).

A pooled analysis on the therapeutic effect of gefitinib or erlotinib and single agent chemotherapy in elderly patients or patients with poor performance status included five studies (330 patients) in EGFR-TKI group and ten studies (1,095 patients) in single agent chemotherapy group. The results showed that ORR was 18% and DCR was 50%

in EGFR-TKI group *vs.* 12% and 36% in single agent chemotherapy group (36).

The WJTOG 0402 study showed that ORR was 20%, DCR was 47%, median PFS was 2.7 months, and median OS was 11.9 months in elderly patients with adenocarcinoma who received Gefitinib as the first-line treatment. The most common toxic reactions included rash, followed by diarrhea, anorexia, hepatic dysfunction and anemia, but all these toxic reactions were relatively mild and could be managed without difficulty. In non-smokers, ORR was 43%, DCR was 57%, median PFS was 7.1 months, and median OS was 13 months, suggesting that both the therapeutic effect and tolerance of Gefitinib as the first-line treatment are relatively good in elderly patients or patients with poor performance status of selected populations (37).

Conclusions: (I) EGFR-TKI (gefitinib or erlotinib) is recommended in elderly NSCLC patients with *EGFR* mutations; (II) EGFR-TKI (gefitinib or erlotinib) can be tried in elderly NSCLC patients or NSCLC patients who are intolerable to chemotherapy or whose *EGFR* mutation status is uncertain, knowing that the *EGFR* mutation rate in Chinese patients is relatively high and there is no other effective treatment at present. At the same time, the therapeutic effect and toxic/adverse reactions should be observed and followed up closely.

Treatment after EGFR-TKI resistance

Disease progression is often observed 9-10 months after initiation of EGFR-TKIs as the first-line treatment in NSCLC patients with *EGFR* mutations, suggesting the occurrence of acquired EGFR-TKI resistance (8-13). A retrospective study enrolled 227 patients with acquired resistance and explored the therapeutic mode in patients who received EGFR-TKI treatment and developed disease progression. The patients were assigned into three clinical failure modes according to the duration of DC, evolution of tumor burden and 6 clinical symptoms: (I) dramatic progression (DC lasting ≥ 3 months with EGFR-TKI treatment, where the tumor burden increases quickly as compared with the previous assessment and the symptom score reaches 2); (II) gradual progression (DC lasting ≥ 6 months with EGFR-TKI treatment, where the tumor burden increases mildly as compared with the previous assessment and the symptom score is ≤ 1); and (III) local progression (DC lasting ≥ 3 months with EGFR-TKI treatment, with solitary extra- or intra-cranial progression and the symptom score is ≤ 1). The results showed that PFS

of the three modes was 9.3, 12.9 and 9.2 months respectively ($P=0.007$), and the median survival was 17.1, 39.4 and 23.1 months respectively ($P<0.0001$). The survival duration of the patients with dramatic progression who continued TKI treatment was shorter than that in those who converted to chemotherapy. It is therefore suggested that EGFR-TKIs should be discontinued and replaced by chemotherapy in patients with dramatic progression. The median OS in gradual progression patients who continued TKI or converted to chemotherapy was 39.4 and 17.8 months respectively ($P=0.02$). It is therefore suggested that TKI treatment should be continued in patients with gradual progression. OS in local progression patients who continued TKI was similar to that in patients who converted to chemotherapy. However, continuation of TKI treatment in combination with local treatment is suggested in local progression patients, given QoL of the patients and limitation of the local-progression focus (38).

In a retrospective study enrolling 78 patients with acquired resistance to EGFR-TKI (including 70 patients with *EGFR* mutations), the results showed that ORR in 34 patients who received chemotherapy + erlotinib was 41% vs. 18% in 44 patients who received chemotherapy alone ($P=0.02$), and PFS was 4.4 vs. 4.2 months ($P=0.34$) (39).

According to the recommendation of the National Comprehensive Cancer Network (NCCN) guidelines (2013 edition), EGFR-TKIs should be continued in NSCLC patients with *EGFR* mutations who are asymptomatic when disease progression with first-line EGFR-TKI treatment, but chemotherapy in combination with EGFR-TKI should be considered in symptomatic patients.

There are few high-level evidence-based medical references about treatment after EGFR-TKI resistance, but a series of related studies is under way or on the way, such as the IMPRESS study concerning the therapeutic mode by comparing TKI + chemotherapy and chemotherapy alone after EGFR-TKI resistance; the ASPIRATION study on continuous use of TKIs after EGFR-TKI resistance; research on TKIs in combination with other drugs; and research on new drugs specific to EGFR-TKI resistance. It is anticipated that these studies could provide more evidence-based medical references.

Conclusions: (I) continuation of the original EGFR-TKI treatment or EGFR-TKIs in combination with chemotherapy is suggested in patients with gradual progression; (II) discontinuation of EGFR-TKIs and conversion to chemotherapy are suggested in patients with dramatic progression; (III) continuation of EGFR-

TKI plus local treatment is suggested in patients with local progression and whose primary lesion is well controlled.

ALK and ROS-1 fusion gene inhibitors

The results of two multi-center clinical trials showed that the ALK inhibitor Crizotinib could offer a remarkable therapeutic effect in advanced NSCLC patients with positive EML4-ALK fusion genes. The A8081001 study showed ORR in Crizotinib group was 60.8%, the median duration of response was 49.1 weeks, and the median PFS was 9.7 months (40). The A8081005 study showed that ORR was 50% in previously treated NSCLC patients with positive *ALK* who received crizotinib, and the median duration of response was 41.9 weeks. Common adverse reactions (occurrence $\geq 25\%$) included visual disorders, nausea, diarrhea, edema and constipation (41).

The phase III clinical trial A8081007 compared the therapeutic effect and safety of crizotinib, pemetrexed or docetaxel in advanced NSCLC patients with positive *ALK* who had a previous history of receiving chemotherapy. Using PFS as the primary end-point, 347 patients with positive *ALK* who had received platinum-based chemotherapy before enrollment were randomly assigned to Crizotinib group and chemotherapy group. The results showed that PFS of the two groups was 7.7 and 3.0 months respectively ($HR=0.49$, $P<0.001$), and ORR was 65% and 20% respectively ($P<0.001$) (42). In January 2013, the CFDA approved the use of Crizotinib in the treatment of local advanced or metastatic NSCLC patients with positive *ALK* in Mainland China.

Shaw *et al.* reported the preliminary therapeutic effect of Crizotinib in the treatment of 13 NSCLC patients with positive *ROS-1*, where ORR was 54% and the 8-week DCR was 85%, showing good tolerance in 2012 ASCO (43). Ou *et al.* reported the therapeutic effect of Crizotinib in 25 assessable patients with advanced NSCLC of positive *ROS-1*, showing that ORR was 56%; the 8- and 16-week DCR was 76% and 60% respectively; and the median PFS has not yet reached at the time in 2013 ASCO. This study re-demonstrated the effectiveness of Crizotinib for the treatment of *ROS-1* positive advanced NSCLC patients (44).

Conclusions: crizotinib is recommended for advanced NSCLC patients harboring positive ALK or ROS-1 fusion genes.

Angiogenesis inhibitors

Two phase III randomized studies demonstrated the

therapeutic effect of the angiogenesis inhibitor Bevacizumab in combination with chemotherapy as the first-line treatment for non-squamous NSCLC patients (45,46). In the study group, Bevacizumab was continued as maintenance therapy after chemotherapy until disease progression or the occurrence of intolerable drug toxicity. The E4599 study showed that the protocol using Carboplatin/Paclitaxel in combination with Bevacizumab (15 mg/kg/3w) improved OS, PFS and ORR of the patients: 12.3 months, 6.2 months and 35% *vs.* 10.3 months (HR =0.79, P=0.003), 4.5 months (HR =0.66, P<0.001) and 15% (P<0.001) respectively as compared with the control group (46). The AVAIL study demonstrated that the protocol of bevacizumab 7.5 or 15 mg/kg/3w in combination with cisplatin/gemcitabine improved PFS and ORR of the patients as compared with the protocol of placebo in combination with cisplatin/gemcitabine, though OS was not prolonged significantly (45). The most common adverse reactions of Bevacizumab include hypertension, proteinuria and hemorrhage, but the occurrence of grade 3 hypertension, grade 4 hypertension, grade 4 proteinuria and hemorrhage was lower than 4%, 0.5%, 0.5% and 2% respectively. Bevacizumab is not recommended in case of the following conditions: (I) squamous cell carcinoma or mixed-type lung cancer dominated by squamous cell carcinoma; (II) tumor invasion into major vessels; (III) history of hemoptysis (>2.5 mL at a time); and (IV) uncontrollable primary hypertension and other cardiovascular diseases.

The result of a randomized phase III clinical trial conducted in Mainland China showed that recombinant human endostatin (rh-Endo) in combination with Vinorelbine/Cisplatin significantly improved ORR and time to progression (TTP) in advanced NSCLC patients as compared with placebo + vinorelbine/cisplatin (35.4% *vs.* 19.5%, P=0.0003; 6.3 *vs.* 3.6 months, P<0.0001). In addition, there was no significant difference in the occurrence of adverse reactions between the two groups (47).

Conclusions: (I) the addition of bevacizumab to the basis of first-line chemotherapy (carboplatin/paclitaxel or cisplatin/gemcitabine) is recommended for non-squamous advanced NSCLC patients with PS 0-1 without significant signs of hemoptysis and major vessel invasion. Although there is no lung cancer indication for Bevacizumab in Mainland China for the time being, it is expected to be approved by the CFDA in the future; (II) vinorelbine/cisplatin in combination with rh-Endostatin can be considered in advanced NSCLC patients.

Group members of the Chinese Expert Consensus on

Molecularly Targeted Therapy for Advanced NSCLC include: BAI Chunxue, HONG Qunying and HU Jie (Zhongshan Hospital of Fudan University, China); CHEN Lian'an (CPLA General Hospital, China); HAN Baohui (Chest Hospital of Shanghai Jiaotong University, China); HU Chengping (Xiangya Hospital of Central South University, China); HUANG Jian'an (1st affiliated hospital of Suzhou University, China); LI Qiang (Changhai Hospital of the Second Military Medical University, China); ZHONG Nanshan and LI Shiyue (Guangzhou Institute of Respiratory Disease, China); LI Weimin (Huaxi Hospital of Sichuan University, China); JIN Faguang (Tangdu Hospital of the Fourth Military Medical University, China); QIAN Guisheng and WU Guoming (Xinqiao Hospital of the Third Military Medical University, China); SONG Yong (General Hospital of Nanjing Military Command Region, China); WU Yilong (Guangdong Provincial People's Hospital, China); XIE Canmao (1st affiliated Hospital of Zhongshan University, China); YANG Shuanying (2nd affiliated hospital of Xi'an Jiaotong University, China); ZHOU Caicun (Pulmonary Hospital of Tongji University, China); ZHOU Jianying (1st affiliated hospital of Zhejiang University School of Medicine, China); ZHANG Li (Beijing Union Hospital, China).

Acknowledgements

The authors are on behalf of Respiratory Disease Branch Lung Cancer Study Group of the Chinese Medical Association, Chinese Alliance against Lung Cancer.

This work is supported by National Key Scientific & Technology Support Program: Collaborative innovation of Clinical Research for chronic obstructive pulmonary disease and lung cancer, NO. 2013BAI09B09.

Disclosure: The authors declare no conflict of interest.

References

1. Peters S, Adjei AA, Gridelli C, et al. Metastatic non-small-cell lung cancer (NSCLC): ESMO Clinical Practice Guidelines for diagnosis, treatment and follow-up. *Ann Oncol* 2012;23 Suppl 7:vii56-64.
2. Stravodimou A, Peters S. Personalized Treatment of Advanced Non-small Cell Lung Cancer: EGFR Tyrosine Kinase Inhibitors as a Standard of Care. *The Journal of OncoPathology* 2014;1:63-71.
3. Wu YL, Zhong WZ, Li LY, et al. Epidermal growth factor receptor mutations and their correlation with gefitinib

- therapy in patients with non-small cell lung cancer: a meta-analysis based on updated individual patient data from six medical centers in mainland China. *J Thorac Oncol* 2007;2:430-9.
4. Chinese expert group of EGFR gene mutation detection in NSCLC patients. Chinese expert consensus on EGFR gene mutation detection in NSCLC patients. *Chin J Pathol* 2011;40:700-2.
 5. Beasley MB, Milton DT. ASCO Provisional Clinical Opinion: Epidermal Growth Factor Receptor Mutation Testing in Practice. *J Oncol Pract* 2011;7:202-4.
 6. Zhang XC, Lu S, Zhang L, et al. Chinese expert consensus on the diagnosis of NSCLC with positive ALK (2013 Ed). *Chin J Pathol* 2013;42:402-6.
 7. Bergethon K, Shaw AT, Ou SH, et al. ROS1 rearrangements define a unique molecular class of lung cancers. *J Clin Oncol* 2012;30:863-70.
 8. Mok TS, Wu YL, Thongprasert S, et al. Gefitinib or carboplatin-paclitaxel in pulmonary adenocarcinoma. *N Engl J Med* 2009;361:947-57.
 9. Mitsudomi T, Morita S, Yatabe Y, et al. Gefitinib versus cisplatin plus docetaxel in patients with non-small-cell lung cancer harbouring mutations of the epidermal growth factor receptor (WJTOG3405): an open label, randomised phase 3 trial. *Lancet Oncol* 2010;11:121-8.
 10. Maemondo M, Inoue A, Kobayashi K, et al. Gefitinib or chemotherapy for non-small-cell lung cancer with mutated EGFR. *N Engl J Med* 2010;362:2380-8.
 11. Zhou C, Wu YL, Chen G, et al. Erlotinib versus chemotherapy as first-line treatment for patients with advanced EGFR mutation-positive non-small-cell lung cancer (OPTIMAL, CTONG-0802): a multicentre, open-label, randomised, phase 3 study. *Lancet Oncol* 2011;12:735-42.
 12. Zhou C, Wu YL, Liu X, et al. Overall survival (OS) results from OPTIMAL (CTONG0802), a phase III trial of erlotinib (E) versus carboplatin plus gemcitabine (GC) as first-line treatment for Chinese patients with EGFR mutation-positive advanced non-small cell lung cancer (NSCLC). *J Clin Oncol* 2012;30:abstr 7520.
 13. Rosell R, Carcereny E, Gervais R, et al. Erlotinib versus standard chemotherapy as first-line treatment for European patients with advanced EGFR mutation-positive non-small-cell lung cancer (EURTAC): a multicentre, open-label, randomised phase 3 trial. *Lancet Oncol* 2012;13:239-46.
 14. Wu YL, Lee JS, Thongprasert S, et al. Intercalated combination of chemotherapy and erlotinib for patients with advanced stage non-small-cell lung cancer (FASTACT-2): a randomised, double-blind trial. *Lancet Oncol* 2013;14:777-86.
 15. Sequist LV, Yang JC, Yamamoto N, et al. Phase III study of afatinib or cisplatin plus pemetrexed in patients with metastatic lung adenocarcinoma with EGFR mutations. *J Clin Oncol* 2013;31:3327-34.
 16. Wu YL, Zhou C, Hu CP, et al. LUX-Lung 6: A randomized, open-label, Phase III study of afatinib (A) vs. gemcitabine/cisplatin (GC) as first-line treatment for Asian patients (pts.) with EGFR mutation-positive (EGFR M+) advanced adenocarcinoma of the lung. *J Clin Oncol* 2013;31:Abstract 8016.
 17. Zhang L, Ma S, Song X, et al. Gefitinib versus placebo as maintenance therapy in patients with locally advanced or metastatic non-small-cell lung cancer (INFORM; C-TONG 0804): a multicentre, double-blind randomised phase 3 trial. *Lancet Oncol* 2012;13:466-75.
 18. Takeda K, Hida T, Sato T, et al. Randomized phase III trial of platinum-doublet chemotherapy followed by gefitinib compared with continued platinum-doublet chemotherapy in Japanese patients with advanced non-small-cell lung cancer: results of a west Japan thoracic oncology group trial (WJTOG0203). *J Clin Oncol* 2010;28:753-60.
 19. Petrelli F, Borgonovo K, Cabiddu M, et al. Erlotinib as maintenance therapy in patients with advanced non-small cell lung cancer: a pooled analysis of three randomized trials. *Anticancer Drugs* 2011;22:1010-9.
 20. Cappuzzo F, Ciuleanu T, Stelmakh L, et al. Erlotinib as maintenance treatment in advanced non-small-cell lung cancer: a multicentre, randomised, placebo-controlled phase 3 study. *Lancet Oncol* 2010;11:521-9.
 21. Coudert B, Ciuleanu T, Park K, et al. Survival benefit with erlotinib maintenance therapy in patients with advanced non-small-cell lung cancer (NSCLC) according to response to first-line chemotherapy. *Ann Oncol* 2012;23:388-94.
 22. Shepherd FA, Douillard J, Fukuoka M, et al. Comparison of gefitinib and docetaxel in patients with pretreated advanced non-small cell lung cancer (NSCLC): Meta-analysis from four clinical trials. *J Clin Oncol* 2009;27:abstr 8011.
 23. Sun Y, Wu YL, Li LY, et al. Clinical analysis on failure of gefitinib or docetaxel as first-line chemotherapy for the treatment of NSCLC. *Chin J Oncol* 2011;33:377-80.
 24. Sun JM, Lee KH, Kim SW, et al. Gefitinib versus pemetrexed as second-line treatment in patients with nonsmall cell lung cancer previously treated with

- platinum-based chemotherapy (KCSG-LU08-01): an open-label, phase 3 trial. *Cancer* 2012;118:6234-42.
25. Shepherd FA, Rodrigues Pereira J, Ciuleanu T, et al. Erlotinib in previously treated non-small-cell lung cancer. *N Engl J Med* 2005;353:123-32.
 26. Ciuleanu T, Stelmakh L, Cicenias S, et al. Efficacy and safety of erlotinib versus chemotherapy in second-line treatment of patients with advanced, non-small-cell lung cancer with poor prognosis (TITAN): a randomised multicentre, open-label, phase 3 study. *Lancet Oncol* 2012;13:300-8.
 27. Vamvakas L, Kentepozidis NK, Karampeazis A, et al. Pemetrexed (mta) compared with erlotinib (erl) in pretreated patients with advanced non-small cell lung cancer (NSCLC): Results of a randomized phase III Hellenic Oncology Research Group trial. *J Clin Oncol* 2010;28:abstr 7519.
 28. Shi Y, Zhang L, Liu X, et al. Icotinib versus gefitinib in previously treated advanced non-small-cell lung cancer (ICOGEN): a randomised, double-blind phase 3 non-inferiority trial. *Lancet Oncol* 2013;14:953-61.
 29. Kim ST, Uhm JE, Lee J, et al. Randomized phase II study of gefitinib versus erlotinib in patients with advanced non-small cell lung cancer who failed previous chemotherapy. *Lung Cancer* 2012;75:82-8.
 30. Wu JY, Wu SG, Yang CH, et al. Comparison of gefitinib and erlotinib in advanced NSCLC and the effect of EGFR mutations. *Lung Cancer* 2011;72:205-12.
 31. Garassino MC, Martelli O, Brogini M, et al. Erlotinib versus docetaxel as second-line treatment of patients with advanced non-small-cell lung cancer and wild-type EGFR tumours (TAILOR): a randomised controlled trial. *Lancet Oncol* 2013;14:981-8.
 32. Okano Y, Ando M, Asami K, et al. Randomized phase III trial of erlotinib (E) versus docetaxel (D) as second- or third-line therapy in patients with advanced non-small cell lung cancer (NSCLC) who have wild-type or mutant epidermal growth factor receptor (EGFR): Docetaxel and Erlotinib Lung Cancer Trial (DELTA). *J Clin Oncol* 2013;31:abstr 8006.
 33. Yang JJ, Cheng Y, Zhao M, et al. A phase II trial comparing pemetrexed with gefitinib as the second-line treatment of nonsquamous NSCLC patients with wild-type EGFR (CTONG0806). *J Clin Oncol* 2013;31:abstr 8042.
 34. Narumi S, Inoue A, Morikawa N, et al. First-line gefitinib for elderly patients with advanced non-small cell lung cancer (NSCLC) harboring EGFR mutations: A combined analysis of NEJ studies. *J Clin Oncol* 2012;30:abstr 7563.
 35. Lee SM, Khan I, Upadhyay S, et al. First-line erlotinib in patients with advanced non-small-cell lung cancer unsuitable for chemotherapy (TOPICAL): a double-blind, placebo-controlled, phase 3 trial. *Lancet Oncol* 2012;13:1161-70.
 36. Liu S, Wang D, Chen B, et al. The safety and efficacy of EGFR TKIs monotherapy versus single-agent chemotherapy using third-generation cytotoxics as the first-line treatment for patients with advanced non-small cell lung cancer and poor performance status. *Lung Cancer* 2011;73:203-10.
 37. Kobayashi M, Matsui K, Katakami N, et al. Phase II study of gefitinib as a first-line therapy in elderly patients with pulmonary adenocarcinoma: West Japan Thoracic Oncology Group Study 0402. *Jpn J Clin Oncol* 2011;41:948-52.
 38. Yang JJ, Chen HJ, Yan HH, et al. Clinical modes of EGFR tyrosine kinase inhibitor failure and subsequent management in advanced non-small cell lung cancer. *Lung Cancer* 2013;79:33-9.
 39. Goldberg SB, Oxnard GR, Digumarthy S, et al. Chemotherapy with erlotinib or chemotherapy alone in advanced NSCLC with acquired resistance to EGFR tyrosine kinase inhibitors (TKI). *J Clin Oncol* 2012;30:abstr 7524.
 40. Camidge DR, Bang YJ, Kwak EL, et al. Activity and safety of crizotinib in patients with ALK-positive non-small-cell lung cancer: updated results from a phase 1 study. *Lancet Oncol* 2012;13:1011-9.
 41. Crinò L, Kim D, Riely GJ, et al. Initial phase II results with crizotinib in advanced ALK-positive non-small cell lung cancer (NSCLC): PROFILE 1005. *J Clin Oncol* 2011;29:abstr 7514.
 42. Shaw AT, Kim DW, Nakagawa K, et al. Crizotinib versus chemotherapy in advanced ALK-positive lung cancer. *N Engl J Med* 2013;368:2385-94.
 43. Shaw AT, Camidge DR, Engelman JA, et al. Clinical activity of crizotinib in advanced non-small cell lung cancer (NSCLC) harboring ROS1 gene rearrangement. *J Clin Oncol* 2012;30:abstr 7508.
 44. Ou SH, Bang YJ, Camidge DR, et al. Efficacy and safety of crizotinib in patients with advanced ROS1-rearranged non-small cell lung cancer (NSCLC). *J Clin Oncol* 2013;31:abstr 8032.
 45. Reck M, von Pawel J, Zatloukal P, et al. Overall survival with cisplatin-gemcitabine and bevacizumab or placebo

- as first-line therapy for nonsquamous non-small-cell lung cancer: results from a randomised phase III trial (AVAiL). *Ann Oncol* 2010;21:1804-9.
46. Sandler A, Gray R, Perry MC, et al. Paclitaxel-carboplatin

- alone or with bevacizumab for non-small-cell lung cancer. *N Engl J Med* 2006;355:2542-50.
47. Wang JW, Sun Y. Phase III clinical trial on recombinant human endostatin. *Chin J Front Med Sci* 2006;(8):87-90.

Cite this article as: Wu G, Zhou C, Bai C, Qian G. Chinese expert consensus on molecularly targeted therapy for advanced non-small cell lung cancer (2013 edition). *J Thorac Dis* 2014;6(10):1489-1498. doi: 10.3978/j.issn.2072-1439.2014.09.20

Microsatellite alteration in multiple primary lung cancer

Cheng Shen, Xin Wang, Long Tian, Guowei Che

Department of Thoracic Surgery, West-China Hospital, Sichuan University, Chengdu 610041, China

Correspondence to: Prof. Guowei Che. Department of Thoracic Surgery, West-China Hospital, Sichuan University, Chengdu 610041, China.

Email: cheguowei_hx@aliyun.com.

Abstract: Patients with pulmonary neoplasms have an increased risk for developing a second tumor of the lung, either at the same time or different times. It is important to determine if the second tumor represents an independent primary tumor or recurrence/metastasis, because it will significantly change the management and prognosis. Microsatellite instability (MSI) and loss of heterozygosity (LOH) represents molecular disorders acquired by the cell during neoplastic transformation. Both are associated with genetic instability. Functional silencing of tumour suppressor genes may be the consequence of genomic instability, particularly of the globally occurring LOH phenomenon. Numerous studies have confirmed the role of MSI/LOH at both the early and the late stages of multiple primary lung cancer. This paper reviews the published literatures focused on the role of MSI/LOH significance in multiple primary lung cancer. Additionally, a new method based on the allelic variations at polymorphic microsatellite markers was offered that it does not rely on collection of normal tissue, performed with minimal tumor sample, and will complement clinical criteria for diagnostic discrimination between multiple primary cancers versus solitary metastatic diseases.

Keywords: Microsatellite instability (MSI); loss of heterozygosity (LOH); multiple primary lung cancer

Submitted May 09, 2014. Accepted for publication Aug 28, 2014.

doi: 10.3978/j.issn.2072-1439.2014.09.14

View this article at: <http://dx.doi.org/10.3978/j.issn.2072-1439.2014.09.14>

Introduction

Lung cancer is the most common cause of cancer death in both males and females in the world. In clinical practice, it is not common to encounter patients with multiple anatomically isolate but histologically similar lung tumors. The incidence of this condition has been reported to range from 0.2% to 2.0% in patients with primary lung cancer (1-3). Coexisting lung cancers in a patient can be characterized as either synchronous or metachronous. The incidence of synchronous lung carcinomas is variably reported between 1% and 16% (4). Metachronous primary lung cancers are likely more common, representing 40-60% of all patients with multiple lung cancers (5). Two different theories have been proposed to explain the multifocality of lung tumors by Slaughter and his colleges. The first is that multifocal tumors arise separately from anatomically distinct malignant progenitor cells that independently undergo different genetic alterations, leading to neoplastic transformation. The second is that these tumors are of monoclonal origin, arising

from a single malignant cell that forms a neoplasm, which metastasizes to other regions of the lung parenchyma (6). This phenomenon has been related to the chronic exposure of the bronchial tree to carcinogens through a so-called "field cancerization" process (7). Distinguishing between these two possible mechanisms for the development of multifocal lesions has important surgical, therapeutic, and prognostic implications.

Molecular analysis of microsatellite markers is a method that has been used to assess clonality (8). Microsatellite markers, or tandem simple sequence repeats (SSR), are abundant across genomes and show high levels of polymorphism. Genomic microsatellites, iterations of 1-6 bp nucleotide motifs, have been detected in the genomes of every organism analyzed so far, and are often found at frequencies much higher than would be predicted purely on the grounds of base composition (9). Microsatellite alterations include microsatellite instability (MSI) and loss of heterozygosity (LOH). The relevance of genomic imbalance is further underscored by the association between

aneuploidy with disease aggressiveness in cancers of many tissues.

This review summarizes molecular analysis of allelic variations at microsatellite markers with the MSI or LOH can be used to determine lineage relationships between multiple tumors. At the same time, a new method based on the allelic variations at polymorphic microsatellite markers was offered that it does not rely on collection of normal tissue, performed with minimal tumor sample, and will complement clinical criteria for diagnostic discrimination between multiple primary cancers versus solitary metastatic disease.

MSI in multiple primary lung cancer

MSI describes a genomic imbalance occurring because of alterations in the length of microsatellites due to small deletions or expansions, which consists of long, tandem repeats of between one and six nucleotides. The number of nucleotide repeats varies, ranging from 5 to 100 segments, with a total length of repetitive DNA of 100–600 bp. Defective DNA mismatch repair (MMR) leading to MSI has been implicated in tumorigenesis (10). The primary function of the MMR is to eliminate base–base mismatches and insertion/deletion loops that arise as a consequence of DNA polymerase slippage during DNA synthesis (11,12). MSI was initially noted in colon cancers of patients with the hereditary nonpolyposis colon cancer (HNPCC) which is the most common hereditary colorectal cancer syndrome and is associated with a spectrum of extracolonic malignancies (13–15). The most common MMR gene germline mutations identified in HNPCC involve MSH2, MLH1, PMS2 and MSH6 (16,17).

A total of 52 sporadic primary non-small-cell lung cancers (NSCLC) were examined for MSI by Lawes and his colleagues (18). Six different microsatellite markers localized on chromosomes 2, 5, 8, 10, 11 and 17 were used. In their research, a total of 27 primary squamous-cell carcinomas, 15 adenocarcinomas (ADC), 7 bronchiolo-alveolar carcinomas and 3 anaplastic carcinomas were investigated for occurrence of MSI with 6 anonymous microsatellite markers from 6 different chromosomes. The instability was evidenced by the appearance of additional bands in tumor DNA compared with normal DNA and consisted of either expansion or compression of a single band or a “ladder” of bands. Genomic instability was observed in 35% (18/52) of NSCLC at single or multiple loci. At the same time, they collected the histopathological

data regarding size, histotype, stage, grade and lymph-node metastasis were available for each tumors. Statistical evaluation of the possible correlation between MSI and pathological feature of each tumor showed no kind of correlation. As their report showed that the genomic instability observed as MSI is probably due to a mechanism other than mismatch-repair defect, even if it cannot be excluded that inactivation of one of the DNA-repair genes may occur as a later event in the progression of a subset of NSCLC, as demonstrated by Wieland *et al.* (19). Canney reported a case of a 59-year-old man who presented mucinous ADC of his ascending colon. Four years later the patient presented with a biopsy proven metachronous ADC in his descending colon. While undergoing clinical staging, two additional lesions were identified in the right lung: one in the upper lobe and a second in the middle lobe. CT-guided biopsy of one of the lesions confirmed an invasive moderately differentiated ADC and the patient proceeded to have wedge resections of both lesions (20). In their research, immunohistochemical studies of both lung lesions showed positivity for thyroid transcription factor 1, with negative staining for cytokeratin 20 and CDX2; this immunoprofile supported a primary lung origin for both tumours. MMR protein immunocytochemistry showed loss of MSH2 and MSH6 proteins in both colonic carcinomas and the right middle lobe lung tumour, with retention of MLH1 and PMS2. Expression of all four MMR proteins was retained in the second lung tumour.

Little is known about the role of MMR genes in lung cancer and the literature is conflicting regarding the pattern and frequency of MSI in lung neoplasms. There is evidence to suggest that MLH1 and MSH2 gene inactivation occurs in NSCLC, and that it is likely to be related to DNA promoter methylation (21). Hsu *et al.* demonstrated significantly lower overall survival and cancer-specific survival rates in a population of non-smoking female patients with NSCLC showing promoter hypermethylation of the HSMH2 gene (22). Xinarianos *et al.* showed a greater frequency of reduced MSH2 expression in lung ADC; however, no significant association was identified between MSH2 expression and prognostic factors such as T stage and nodal metastasis (23).

LOH in multiple primary lung cancer

LOH is a phenomenon contrary to MSI and is frequently seen in cancer cells and is thought to occur through genetic instability at a chromosomal or similar level. In this genetic

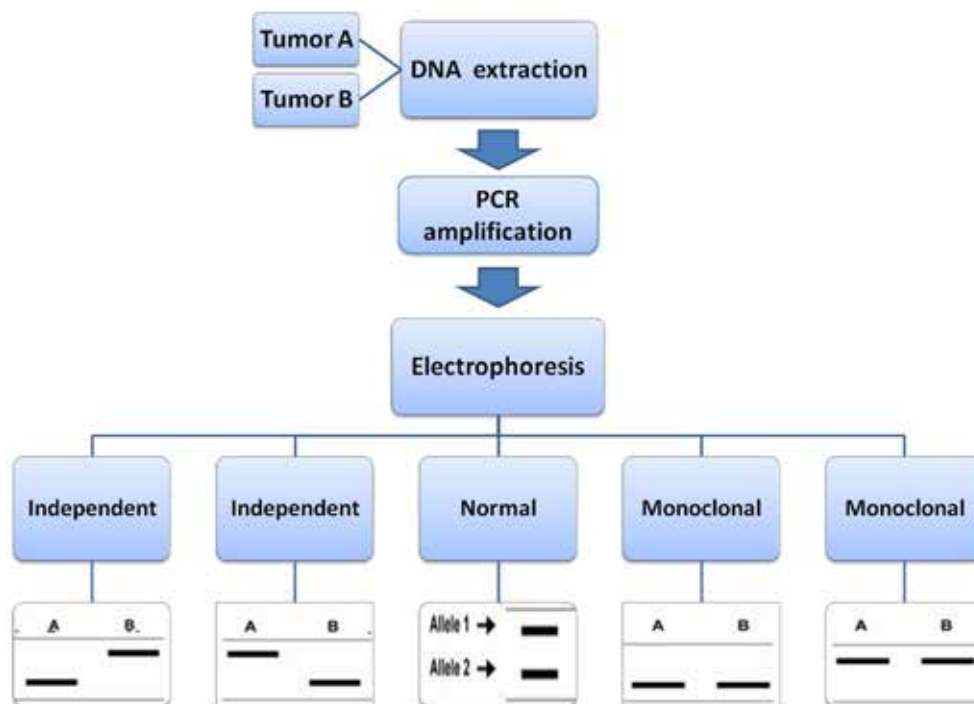


Figure 1 The procedure for determination of allele loss patterns in LOH. Tumors with different allele loss patterns would be grouped in independent clonal origin, whereas tumors with same allele loss patterns are grouped in a monoclonal origin. LOH, loss of heterozygosity.

disorder, one of the gene alleles is lost in a neoplastic cell (24). The mechanism of LOH is chromosome-specific, and it may concern the entire chromosome. However, loss of genetic material is more often associated with deletion of a fragment of chromosome, leading to LOH regarded as a generalised form of allelic imbalance. Loss of function of suppressor as well as mutator genes may be a functional consequence of the globally occurring LOH (25).

Two conventional methods are widely used for LOH analysis: polymerase chain reaction (PCR)-based assays and fluorescence *in situ* hybridization (FISH). PCR-based LOH assays with polymorphic markers are commonly used to detect LOH regions. Tumor genotypes at certain polymorphic regions are compared with normal cells from the patient. A disadvantage of this assay is the need for normal control DNA and multiple markers, as not every marker is always informative. However, we can easily select and design primers as appropriate polymorphic markers for specific regions. Furthermore, experiments with single nucleotide polymorphisms (SNPs) instead of microsatellite markers allow more quantitative and detailed analysis for LOH (26,27). These assays detect “allelic imbalance” without detailed information on the gene copy

number, thus including LOH as well as trisomy or local gene amplifications. Snuderl *et al.* recently reported that polysomy at 1p/19q may predict the clinical course of gliomas (28).

In 2001, using microdissection and LOH analysis, Huang *et al.* studied specimens from patients with multiple pulmonary neoplasms to determine if modern techniques can help us distinguish true independent primary from recurrence or metastasis (29). Among the four synchronous pulmonary tumors, the paired tumors in two cases appeared to be genetically different because they had very different profiles of LOH and the procedures for how to detect LOH was showed in *Figure 1*. Therefore, they probably represent true synchronous tumors. The two tumors in one case appeared to have identical patterns of LOH and may actually represent the same clone. A total of 25 patients in whom there was a suspicion of solitary metastasis or second primary tumor were evaluated by van der Sijp and his colleagues (30). In all 25 patients, LOH was detected in all tumors with at least three of the markers used. LOH in different tumors from one patient was regarded as identical when the same markers demonstrated loss of the same allele. LOH was regarded as different when in different

tumors from one patient different markers showed LOH or when the same marker had loss of different alleles. In the 15 patients with a second primary tumor, clinical decision making was influenced in 10 patients.

To distinguish a metastasis from a second primary tumor in patients with a history of head and neck squamous cell carcinoma and subsequent pulmonary squamous cell carcinoma, in another research, 44 patients were analysed with clinical data, histology, and LOH (31). Using these clinical criteria, 6 patients were considered to be likely to have a second primary lung tumor, whereas 38 patients were thought to have lung metastasis. With the analysis of LOH, 11 tumor pairs were classified as metastasis and 8 as probable metastases. A total of 22 cases were classified as certain and 3 as probable second primary tumors. In one case, the LOH analysis was inconclusive. In this case, there was not enough concordant or discordant LOH to draw any conclusions. Then, a case of three different synchronous primary lung tumours that two nodules were located in the upper lobe and consisted of an ADC, an endobronchial poorly differentiated squamous cell carcinoma (SCC) and a third nodule of the lower lobe corresponded to a small cell neuroendocrine carcinoma (SCLC) was reported by Froio *et al.* (32). They examined all three independent lung neoplasms for LOH by the analysis of 40 microsatellite markers. Of these, 29 out of 38 were informative for LOH analysis (76.3%). No MSI was observed in any tumour component. Distinction of multiple primary lung carcinomas from intrapulmonary metastases using empiric clinical and histopathologic criteria can be difficult. Recent advances have provided several molecular markers that can be used for clonal analysis of separate tumor nodules and enhance tumor staging and subsequent treatment and prognosis. To address this issue, Dacic and his workmates performed a microdissection based allelotyping of 20 cases of histologically similar ADC (33). By observation, the patients could be discriminated in survivors and nonsurvivors if the percentage of discordant microsatellite markers within primary tumor was equal or less than 40% or above 40%, respectively. Using 40% as a cutoff in a validation cohort of pathologic stage T4 cases, each tumor was identified as having a number of discordances above or below this percentage. If the percentage of discordances for all microsatellite markers was equal or less than 40%, the pattern of LOH for this particular tumor was defined as "homogenous". On the other hand, when the percentage of discordances was greater than 40%, the pattern of LOH status was defined as "heterogenous". In their study,

molecularly homogenous tumors were more frequently associated with angiolymphatic invasion, although that difference did not reach statistical significance. This suggests that molecularly homogenous tumors may actually represent intrapulmonary metastases, rather than independent lung cancers. Furthermore, visceral pleural invasion, which is a known adverse prognostic factor in non-small cell carcinoma, was more commonly seen in the molecularly homogenous group. These two features, which are clearly associated with biologically more aggressive lung tumors, support an idea of possible monoclonal origin of molecularly homogenous synchronous lung tumors.

The results of all the studies above concerning the role of LOH in the process of neoplastic transformation of multiple primary lung cancer have demonstrated that inactivation of various genes by deletions in their loci is already present in preneoplastic lesions, being associated with the process of carcinogenesis initiation in the lung. However, the role of that phenomenon varies, depending on chromosomal region and the significance of the LOH-affected loci in the physiology of the lung.

"Different trend" in multiple primary lung cancer

An interesting hypothesis as to the molecular sequence of genetic events in carcinogenesis in the multiple primary lung cancer was proposed by Mercer *et al.* (34). Since genomic instability is a common feature of cancer, they hypothesized that independently arising neoplasm in an individual patient would exhibit measurable genomic variation, enabling discrimination of tumor lineage and relatedness. Allelic variation between neoplasms often reflects accumulation of differential chromosomal deletion events. These chromosomal deletions are tolerated (non-lethal), but distinct from the molecular alterations that drive tumorigenesis, which will be common to most/all tumors of a specific type. Comparison of molecular signatures between two (or more) tumors from a single individual facilitates identification of common and unique genetic alterations. In the study, they described a molecular approach for analysis of genetic variation among multiple tumors from a single patient that does not rely on collection of normal tissue, and which can be performed with minimal tumor samples. A total of 25 paraffin-embedded human tissues corresponding to 14 squamous cell carcinomas of the H/N, 10 squamous cell carcinomas of the lung were selected for inclusion in this study. In addition to these 10 patients, tumor samples from a patient presenting with squamous cell carcinoma

of the larynx that was metastatic to the lymph nodes of the neck was also included. The tumor samples corresponding to this patient have a known lineage relationship: primary squamous cell carcinoma of the H/N and metastatic squamous cell carcinoma of a proximal lymph node and its consequence was regarded as the contrast standard. Of the 20 microsatellite markers evaluated, 18 (90%) detected allelic imbalance or allelic variation among multiple tumors from at least one patient. D20S171 and D21S1432 detected no differences between tumors for any of the patients examined. The lack of detectable allelic variation at these loci may be related to their specific chromosomal locations and/or their proximity to genes that are essential for cell survival. The other 18 microsatellite markers examined identified allelic variation in 10-80% of patients, and the majority of microsatellite markers (14/20, 70%) detected allelic differences in tumors from 10-50% of patients examined. The results presented in this study demonstrate that molecular analysis of allelic variations at polymorphic microsatellite markers can be used to determine lineage relationships between multiple tumors, facilitating the discrimination of second primary cancer versus metastatic disease.

In 2013, Shen *et al.* offered a new concept that the “unique trend” and the “contradictory trend” (35). The “unique trend” that represents metastasis cancers and the “contradictory trend” that represents primary multiple tumors are useful in the diagnosis between tumors found at the same time in the pulmonary even diagnosed with the histopathological evaluation. This study enrolled 13 patients, with multiple primary lung cancers demonstrating with the histology and 10 patients who were diagnosed as metastasis disease during the same period for comparison purposes. Genomic DNA from lung cancers from individual patients was analyzed by six microsatellites (D2S1363, D6S1056, D7S1824, D10S1239, D15S822, and D22S689) with PCR to identify discordant allelic variation. In the report, all of the 10 patients with distant metastasis showed a consistent consequence that was called “unique trend” between primary tumor and distant metastasis. The “trend” means that all alleles corresponding to six microsatellite markers were detected in DNA from primary tumors but were reduced or not observed in DNA from metastatic tumors. In the group of synchronous lung tumor with different histological types, the result showed a “contradictory trend”. Some alleles were detected in DNA from primary tumors but were reduced or not observed in DNA from metastatic tumors and other alleles

corresponding to six microsatellite markers were detected in DNA from metastatic tumors but were reduced or not observed in DNA from primary tumors. This approach is rapid and sensitive. It is paramount that such a test be amenable to the utilization of DNA samples from formalin-fixed paraffin-embedded tissues since these may be the only available source of DNA for the prior cancer.

Conclusions

LOH seems to be a more frequent phenomenon than MSI, inducing genetic instability in lung neoplasms in many chromosomal regions. MSI may be causatively associated with the initiation of molecular changes only, which may later lead to neoplasia, whereas the incidence of LOH overtly increases with tumour progression. This phenomenon increases with the degree of neoplastic progression, which indicates a successive accumulation of molecular disorders in cells and a coincidence of LOH/ mutations in multiple primary lung cancer. The new methods of Mercer *et al.* and Shen *et al.* studies, which were ideal for clinical use given that the methodology is straightforward, rapid, and inexpensive, were to refine a molecular method to analyze multiple tumors that does not rely on collection of normal tissue, can be performed with minimal tumor sample, and will complement clinical criteria for diagnostic discrimination between multiple primary cancer versus solitary metastatic disease.

Acknowledgements

We greatly appreciate the assistance of the staff of the Department of Thoracic Surgery, West-China Hospital, Sichuan University, and thank them for their efforts.

Funding: This work supported by the National Science Foundation (No: 81071929, to Guowei Che) and National Science Foundation (No: 81272595, to Guowei Che).

Disclosure: The authors declare no conflict of interest.

References

1. Wu SC, Lin ZQ, Xu CW, et al. Multiple primary lung cancers. *Chest* 1987;92:892-6.
2. Ferguson MK, DeMeester TR, DesLauriers J, et al. Diagnosis and management of synchronous lung cancers. *J Thorac Cardiovasc Surg* 1985;89:378-85.
3. Carey FA, Donnelly SC, Walker WS, et al. Synchronous primary lung cancers: prevalence in surgical material and

- clinical implications. *Thorax* 1993;48:344-6.
4. Flynn MJ, Rassl D, El Shahira A, et al. Metachronous and synchronous lung tumors: five malignant lung pathologies in 1 patient during 7 years. *Ann Thorac Surg* 2004;78:2154-5.
 5. Okada M, Tsubota N, Yoshimura M, et al. Operative approach for multiple primary lung carcinomas. *J Thorac Cardiovasc Surg* 1998;115:836-40.
 6. Ninomiya H, Nomura K, Satoh Y, et al. Genetic instability in lung cancer: concurrent analysis of chromosomal, mini- and microsatellite instability and loss of heterozygosity. *Br J Cancer* 2006;94:1485-91.
 7. Sikkink SK, Liloglou T, Maloney P, et al. In-depth analysis of molecular alterations within normal and tumour tissue from an entire bronchial tree. *Int J Oncol* 2003;22:589-95.
 8. Silk AD, Zasadil LM, Holland AJ, et al. Chromosome missegregation rate predicts whether aneuploidy will promote or suppress tumors. *Proc Natl Acad Sci U S A* 2013;110:E4134-41.
 9. Epplen C, Melmer G, Siedlaczek I, et al. On the essence of "meaningless" simple repetitive DNA in eukaryote genomes. *EXS* 1993;67:29-45.
 10. Chang IY, Kim SH, Cho HJ, et al. Human AP endonuclease suppresses DNA mismatch repair activity leading to microsatellite instability. *Nucleic Acids Res* 2005;33:5073-81.
 11. Buermeier AB, Deschênes SM, Baker SM, et al. Mammalian DNA mismatch repair. *Annu Rev Genet* 1999;33:533-64.
 12. Jiricny J, Nyström-Lahti M. Mismatch repair defects in cancer. *Curr Opin Genet Dev* 2000;10:157-61.
 13. Søreide K, Janssen EA, Söiland H, et al. Microsatellite instability in colorectal cancer. *Br J Surg* 2006;93:395-406.
 14. Ionov Y, Peinado MA, Malkhosyan S, et al. Ubiquitous somatic mutations in simple repeated sequences reveal a new mechanism for colonic carcinogenesis. *Nature* 1993;363:558-61.
 15. Subramanian S, Mishra RK, Singh L. Genome-wide analysis of microsatellite repeats in humans: their abundance and density in specific genomic regions. *Genome Biol* 2003;4:R13.
 16. Rouprêt M, Yates DR, Comperat E, et al. Upper urinary tract urothelial cell carcinomas and other urological malignancies involved in the hereditary nonpolyposis colorectal cancer (lynch syndrome) tumor spectrum. *Eur Urol* 2008;54:1226-36.
 17. Hendriks YM, de Jong AE, Morreau H, et al. Diagnostic approach and management of Lynch syndrome (hereditary nonpolyposis colorectal carcinoma): a guide for clinicians. *CA Cancer J Clin* 2006;56:213-25.
 18. Lawes DA, SenGupta S, Boulos PB. The clinical importance and prognostic implications of microsatellite instability in sporadic cancer. *Eur J Surg Oncol* 2003;29:201-12.
 19. Wieland I, Ammermüller T, Böhm M, et al. Microsatellite instability and loss of heterozygosity at the hMLH1 locus on chromosome 3p21 occur in a subset of nonsmall cell lung carcinomas. *Oncol Res* 1996;8:1-5.
 20. Canney A, Sheahan K, Keegan D, et al. Synchronous lung tumours in a patient with metachronous colorectal carcinoma and a germline MSH2 mutation. *J Clin Pathol* 2009;62:471-3.
 21. Fong KM, Zimmerman PV, Smith PJ. Microsatellite instability and other molecular abnormalities in non-small cell lung cancer. *Cancer Res* 1995;55:28-30.
 22. Hsu HS, Wen CK, Tang YA, et al. Promoter hypermethylation is the predominant mechanism in hMLH1 and hMSH2 deregulation and is a poor prognostic factor in nonsmoking lung cancer. *Clin Cancer Res* 2005;11:5410-16.
 23. Xinarianos G, Liloglou T, Prime W, et al. hMLH1 and hMSH2 expression correlates with allelic imbalance on chromosome 3p in non-small cell lung carcinomas. *Cancer Res* 2000;60:4216-21.
 24. Boland CR, Thibodeau SN, Hamilton SR, et al. A National Cancer Institute Workshop on Microsatellite Instability for cancer detection and familial predisposition: development of international criteria for the determination of microsatellite instability in colorectal cancer. *Cancer Res* 1998;58:5248-57.
 25. Devilee P, Cleton-Jansen AM, Cornelisse CJ. Ever since Knudson. *Trends Genet* 2001;17:569-73.
 26. Hata N, Yoshimoto K, Yokoyama N, et al. Allelic losses of chromosome 10 in glioma tissues detected by quantitative single-strand conformation polymorphism analysis. *Clin Chem* 2006;52:370-8.
 27. Guan Y, Hata N, Kuga D, et al. Narrowing of the regions of allelic losses of chromosome 1p36 in meningioma tissues by an improved SSCP analysis. *Int J Cancer* 2008;122:1820-6.
 28. Snuderl M, Eichler AF, Ligon KL, et al. Polysomy for chromosomes 1 and 19 predicts earlier recurrence in anaplastic oligodendrogliomas with concurrent 1p/19q loss. *Clin Cancer Res* 2009;15:6430-7.
 29. Huang J, Behrens C, Wistuba I, et al. Molecular analysis of synchronous and metachronous tumors of the lung:

- impact on management and prognosis. *Ann Diagn Pathol* 2001;5:321-9.
30. van der Sijp JR, van Meerbeeck JP, Maat AP, et al. Determination of the molecular relationship between multiple tumors within one patient is of clinical importance. *J Clin Oncol* 2002;20:1105-14.
 31. Geurts TW, Nederlof PM, van den Brekel MW, et al. Pulmonary squamous cell carcinoma following head and neck squamous cell carcinoma: metastasis or second primary? *Clin Cancer Res* 2005;11:6608-14.
 32. Froio E, D'Adda T, Fellegara G, et al. Three different synchronous primary lung tumours: a case report with extensive genetic analysis and review of the literature. *Lung Cancer* 2008;59:395-402.
 33. Dacic S, Ionescu DN, Finkelstein S, et al. Patterns of allelic loss of synchronous adenocarcinomas of the lung. *Am J Surg Pathol* 2005;29:897-902.
 34. Mercer RR, Lucas NC, Simmons AN, et al. Molecular discrimination of multiple primary versus metastatic squamous cell cancers of the head/neck and lung. *Exp Mol Pathol* 2009;86:1-9.
 35. Shen C, Xu H, Liu L, et al. "Unique trend" and "contradictory trend" in discrimination of primary synchronous lung cancer and metastatic lung cancer. *BMC Cancer* 2013;13:467.

Cite this article as: Shen C, Wang X, Tian L, Che G. Microsatellite alteration in multiple primary lung cancer. *J Thorac Dis* 2014;6(10):1499-1505. doi: 10.3978/j.issn.2072-1439.2014.09.14

Experimental studies in the bronchial circulation. Which is the ideal animal model?

Christophoros Kotoulas^{1,2}, Ioannis Panagiotou¹, Panteleimon Tsipas¹, Maria Melachrinou², Dimitrios Alexopoulos², Dimitrios Dougenis²

¹Department of Cardiothoracic Surgery, Army General Hospital of Athens, Athens, Greece; ²School of Medicine, University of Patras, Patras, Greece

Correspondence to: Christophoros Kotoulas, PhD, FETCS, FCCP. Kifissias Ave 38, Ampelokipoi, Athens, GR-11526, Greece. Email: info@kotoulas.com.

Background: The importance of the role of bronchial arteries is notable in modern days thoracic surgery. The significance of their anastomoses with adjusted structures has not yet been sufficiently rated, especially in cases of haemoptysis, heart-lung transplantations and treatment of aneurysms of the thoracic aorta. The need of a thorough study is more relevant than ever and appropriate laboratory animals are required.

Methods: We review the literature in order to highlight the ideal experimental animal for the implementation of pilot programs relative to the bronchial circulation. A comparative analysis of the anatomy of the bronchial arterial system in humans along with these of pigs, dogs, rats, and birds, as being the most commonly used laboratory animals, is presented in details.

Results: The pig has the advantage that the broncho-oesophageal artery usually originates from the aorta as a single vessel, which makes the recognition and dissection of the artery easy to perform. In dogs, there is significant anatomical variation of the origin of the bronchial arteries. In rats, bronchial artery coming from the aorta is a rare event while in birds the pattern of the bronchial artery tree is clearly different from the human analog.

Conclusions: The pig is anatomically and physiologically suited for experimental studies on the bronchial circulation. The suitable bronchial anatomy and physiology along with the undeniable usefulness of the pig in experimental research and the low maintenance cost make the pig the ideal model for experiments in bronchial circulation.

Keywords: Bronchial artery; pig; experimental study; anatomy; cardiorespiratory system cancer

Submitted May 12, 2014. Accepted for publication Sep 09, 2014.

doi: 10.3978/j.issn.2072-1439.2014.09.32

View this article at: <http://dx.doi.org/10.3978/j.issn.2072-1439.2014.09.32>

Introduction

Pulmonary circulation carries deoxygenated blood away from the heart to the lungs, and returns oxygenated blood back to the heart. The separate system is known as the bronchial circulation supplies blood to the tissue of the larger airways of the lung. The first reference to some small arteries in the lungs was made by Galen (1). Many years later, in 1513, Leonardo Da Vinci, described the bronchial arterial system as subsidiary of pulmonary vessels (2). In 1721, Ruysch presented the first illustration and made a more detailed description of the bronchial arteries as a

separate vascular network of the pulmonary vasculature with anastomoses between the two networks (3). In 1747, Albertus Haller gave a precise description of the origin, course and the variations of bronchial arteries in his masterpiece “Icorum Anatomicarum” (4).

Today, the importance of the bronchial arteries is recognized by the scientific community, especially in cases of massive haemoptysis and chemotherapy of lung cancer (5,6). Their revascularization seems to contribute to the reduction of postoperative complications in cases of heart-lung or single lung transplantation (7). In addition, the potential benefit from their embolism in cases of surgical

treatment of thoracic aneurysms of the descending aorta are still under investigation.

The ideal experimental studies should be made in models that show the greatest similarity to the human anatomy and physiology. Although, the most experimental studies in cardiopulmonary system take place mainly in the pigs. The anatomy of the porcine bronchial system has not yet been fully explored. Our aim is to explore which is the ideal experimental model for the bronchial circulation studies.

Methods

A thorough description and a comparative analysis of the anatomy of the bronchial system in human, pigs and other laboratory animals is presented in order to highlight the ideal animal model for experiments in the bronchial circulation.

The human bronchial circulation

Both left and right bronchial arteries originate from the aorta in 90%. More specifically in 80%, they originate between the upper border of the 5th and the lower border of the 6th thoracic vertebrae (T5-T6) with most of them arising from the level of the carina or slightly inferiorly (8,9). In the remaining cases, it has been described the origin of the bronchial arteries from all thoracic arterial structures, even from the coronary arteries (10). Cauldwell *et al.*, based on a large human cadaveric study, classified the variations in the number of bronchial arteries in nine categories (11). In most cases, the right bronchial artery is one of the branches of the intercostobronchial trunk that originates from the aorta.

In their origin, the diameter of the bronchial arteries is about 1.5 mm, decreasing to 0.5-0.6 mm when enter the pulmonary hilum (12). In cases of chronic pulmonary diseases, especially when haemoptysis is present, hypertrophy and increase in the arterial diameter more than 1.5 mm have been observed (9,13).

In their path from the aorta to the hilum, the bronchial arteries give branches to adjacent organs and structures. Small parietal branches may supply muscles, vertebrae, ligaments and pleura. Visceral branches supply the esophagus, the lower third of the trachea and pericardium. Vascular branches supply the aorta, the pulmonary vasculature, the azygous vein and the vena cava. There are also branches to intrathoracic nerves, such as to the vagus nerve, the sympathetic plexus and their branches. In a few studies, branches to mediastinal lymph nodes and

an anastomotic plexus with the coronary circulation are described (14-16).

The bronchial arteries enter the lung to the hilum. They form a communicating arc round the main bronchi from which the bronchial arterial divisions radiates along the major bronchi. They adhered closely to the bronchial wall and appeared to follow the same course to the level of the terminal bronchioles where finally anastomosed to the pulmonary vasculature (17). They bifurcated with the bronchi and give two to three divisions along each bronchus which tend to form an intercommunicating network in the fibrous coat of the bronchus. Smaller twigs penetrate the muscular layer and reach the bronchial mucosa forming a similar network in the submucosa. In this way, the bronchial arteries are responsible for the nourishment of the whole thickness of the bronchial wall till the level of terminal bronchioles. In the way down to the alveoli, the bronchial arterioles form an anastomotic network with pulmonary arterioles. These anastomotic branches, which named bronchopulmonary arteries, have been observed in both newborns and adults drain via the pulmonary veins into the left atrium (17-19). Tobin *et al.* described that there are two types of anastomoses, the short-narrow (length 1-2 mm, diameter 50-100 microns) and the long-wide (length 10-40 mm, diameter 300-400 microns) (20).

The short anastomotic vessels have spiral shape, achieving in this way the self-regulation of the flow to the pulmonary bronchial network and vice versa. Under normal conditions, these anastomoses are functionally closed but under pathologic conditions, such as in chronic thromboembolic pulmonary hypertension, they open and new anastomoses are formed (12,21,22).

Counterparts to the bronchial arteries are the bronchial veins. However, they only carry a small amount of the blood flow of the bronchial arteries while the remaining blood is returned to the heart via the pulmonary veins. The bronchial veins return blood from the larger bronchi and structures at the hilum of the lungs. The right side drains into the azygous vein, while the left side drains into the left superior intercostal vein or the accessory hemiazygous vein (17).

Comparative study of the bronchial circulation in laboratory animals

McLaughlin thoroughly described the pulmonary anatomy of 10 mammalian species and the human, classifying them into three groups according to their similarities in lung anatomy and physiology (23,24). In the first group belong

Table 1 Comparative study of the bronchial arteries among the different mammals

Variables	Pig	Dog	Rat	Human
Pleura	-	-	-	+
Septa	+	-	-	+
Bronchi	+	+	+	+
Terminal bronchioles	+	-	+	+
Alveoli	-	-	-	+
Hilar nodes	+	+	+	+
VASA vasorum	+	+	+	+
Bronchial artery-pulmonary anastomoses	+/-	-	+	+
General bronchovascular relationship	Pulmonary vein close to bronchus from periphery to hilum	Pulmonary vein follows independent course from periphery to hilum	Pulmonary vein follows independent course from periphery to hilum	Pulmonary vein near bronchus at periphery, apart at hilum

the cow, the sheep and the pig. In the second group belong the dog, the cat and the monkey. The rabbit, the rat and the guinea-pig could be considered a subcategory of the second group due to their minimum differences. Finally, in the third group belong the horse and the human.

In the following presentation a representative from each group has been chosen based on the ease to perform experiments on this and the lower cost of its maintenance. Thus, the bronchial circulation of the pig, the dog and the rat is described along with this of birds as being the most commonly used laboratory animals. The differences among the bronchial circulation of the human, the pig, the rat and the dog are presented in the *Table 1*.

Bronchial circulation of the pig

Calka *et al.*, Gade *et al.*, and more recently Lorentziadis *et al.*, demonstrated the most detailed descriptions of the anatomy of the porcine bronchial tree (25-27). The bronchial artery is the continuation of the bronchoesophageal artery which almost always originates from the aorta as a single vessel (28).

In 91-100% has a single origin from the aorta (*Figure 1*). In about 85% originates from the medial or anteromedial aspect of the descending aorta just distal to the ductus arteriosus ligament but cranial to the azygos vein crossing the aorta. In about 15% the origin is more mediadorsal or just cranial to the ductus arteriosus ligament. The orifice is normally 1-2 mm wide and approximately 3 cm from the slightly larger orifices of the intercostal arteries (25). The bronchoesophageal artery soon divides into 2-3 branches towards the lung hilum and the esophagus, while three different patterns of branching in the way to the main

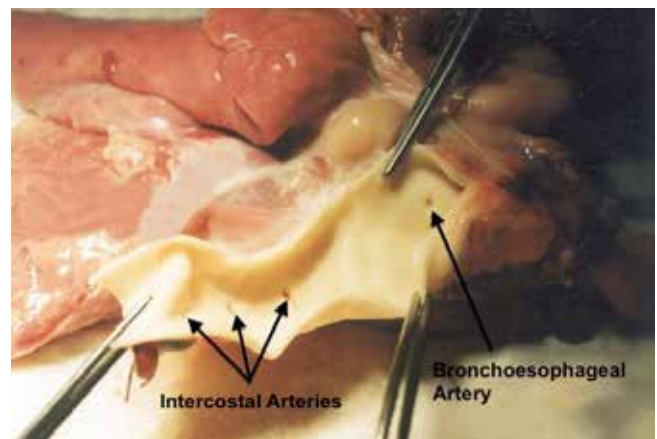


Figure 1 Relationship between the broncho-esophageal artery and the mediastinal arteries in a heart-lung porcine block.

bronchi have been described (22) (*Figure 2*).

In details, the bronchoesophageal artery is divided to a carinal branch, a left lateral branch and a smaller branch for the cranial lobe. The carinal branch crosses the carina ventrally and ramified further into a right lateral, a right medial and a left medial branch. The right lateral and right medial branches provide blood supply to the right main bronchus while the left lateral and left medial branches provide blood supply to the left main bronchus. According to the pattern described, each main bronchus of the pig is accompanied by two major bronchial artery branches named in accordance with their anatomical localization (26). Instead of this, the segmental bronchi are accompanied by a single bronchial branch, which finally disappeared 1-2 cm

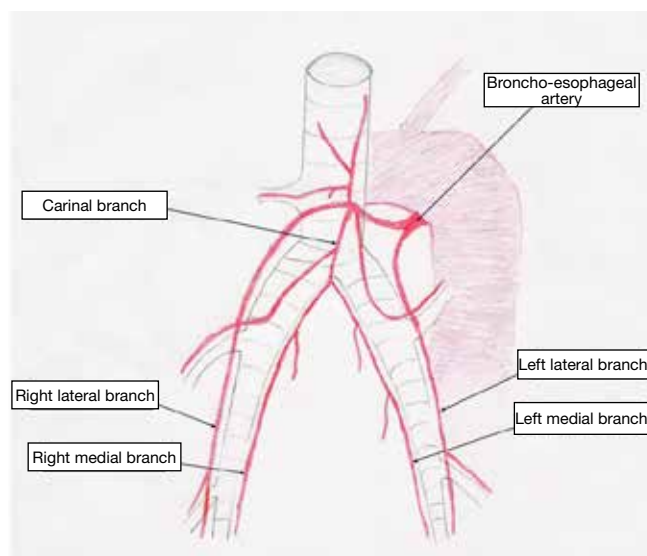


Figure 2 Nomenclature of branches of the bronchial artery in pig.

before the edge of the lung. All branches of the bronchial artery are in close proximity to the adjacent bronchi.

Communications between the bronchial branches and other structures are demonstrated in different levels. In the way to the hilum, small twigs develop an anastomotic plexus with most of the mediastinal structures including the esophagus, the pericardium, lymph nodes and vasa vasorum to the pulmonary artery (23,29). The existence of an anastomotic plexus with the pulmonary artery is still under question. Gade *et al.* demonstrated that broncho-pulmonary shunts must exist but it is likely to occur via the lung capillaries (26), though other investigations failed to demonstrate bronchial to pulmonary artery communications probably due to limitations in methodology. Other studies suggested that the communication between the two systems is via small pulmonary arterioles (23).

Of main importance is the anastomotic plexus with the esophagus along its entire intrathoracic length (30) while the existence of an anastomotic network between the bronchial branches and the coronary vessels of the heart has been described (31,32).

Bronchial circulation of the dog

There is significant anatomical variation of the origin of the bronchial arteries in dogs (33). The bronchial artery could be branch of the right 5th, 6th or 7th intercostal artery. These intercostal arteries always arise from the

thoracic aorta. In the majority of dogs the parent trunk is the bronchoesophageal artery, which arises from the right fifth intercostal artery close to its origin from the aorta (34). The course followed by the bronchial artery is also subject to considerable variation. In the majority of dogs the bronchoesophageal artery crosses the left side of the esophagus and contributes an esophageal branch before entering the hilum of the lung (34). In addition, small bronchial vessels that supply the hilum of the lung and arise from the pericardiophrenic or internal thoracic arteries are described. At the level of the respiratory bronchiole the bronchial artery terminates in a capillary bed that is continuous with that of the pulmonary artery (35).

True bronchial veins are found only at the hilum of the lung. They empty into the azygos vein or the intercostal vein at the level of the seventh thoracic vertebra (34).

Bronchial circulation of the rat

There are two bronchial arteries, the right and the left, which originate either from the subclavian arteries or from their primary branches (36). Each of the bronchial arteries has a long caudal course through the mediastinum, supplying several thoracic structures other than the bronchi. The left bronchial artery always originates from the internal thoracic artery. The right bronchial artery had a variable origin: the costocervical trunk, the right subclavian artery, or the internal thoracic artery (37). After emerging from the internal thoracic artery, the left bronchial artery runs caudally on the ventral surface of the aortic arch, where it gives off branches to the thymus, the trachea and the left recurrent laryngeal nerve. At the dorsal level of the left bronchus, the left bronchial artery originates esophageal and bronchial arteries. One or two branches run down along the main bronchus. The right bronchial artery gives off branches to the trachea, right cranial vena cava, and phrenic nerve. At the level of the carina, it originates 1-3 branches to the cranial bronchus and numerous transverse branches to the esophagus (38). Intrapulmonary branches of bronchial arteries form a peribronchial plexus made up of anastomosing arterioles giving off branches that passed through the muscular layer to form a second layer under the epithelium. Finally, precapillary anastomoses between bronchial arteries and pulmonary vessels exist resembling what occurs in humans (39).

Bronchial circulation of birds

General studies of the avian arterial system (40,41) have indicated that bronchial arteries arise from

the oesophagotracheobronchial branch of each common carotid artery in many species of birds. Each oesophagotracheobronchial artery passes caudally and forms more or less symmetrically, three or four branches supplying the caudal end of the trachea, the syrinx, and the oesophagus. It also gives rise to several small bronchial arteries which supply the extrapulmonary part of the primary bronchus. The largest and most caudal of these bronchial arteries passes caudally along the dorsal wall of its primary bronchus and enters the hilum of the lung. On reaching the opening of the first medioventral secondary bronchus it divides into two terminal branches which continue caudally on either side of the openings of the medioventral secondary bronchi, forming a network of small anastomosing branches. In the goose, duck, and turkey several small bronchial arteries supplied the whole length of each primary bronchus, including the orifices of the secondary bronchi. In the guinea-fowl and quail similar bronchial arteries supplied only the extrapulmonary part of the primary bronchus. In the pigeon a single true bronchial artery supplied the extrapulmonary part of each primary bronchus. There were no branches to the exchange tissue in any species. In all species the bronchial veins of the extra-pulmonary part of the primary bronchus drained via esophageal veins, whereas those of the intrapulmonary part emptied into branches of the pulmonary vein (40,41).

Results and discussion

The ideal experimental model should demonstrate the maximum similarity to the humans, in both anatomy and physiology. Lungs of all mammals share a common general structure consisting of a branching system of airways terminating in thin-walled alveolar spaces where gas exchange occurs but there are variations among species (23). Pigs, sheep and cows having “type I” lungs characterized by extremely well developed lobulation of lung parenchyma, a thick visceral pleura and absence of alveoli. The pulmonary artery supplies the distal portion of the airways. The bronchial artery supplies the hilar lymph nodes, pulmonary artery and vein, bronchi and terminal airways, but it also supplies the interlobular septae and pleura.

Dogs, cats and monkeys having a “type II” lungs characterized by the absence of secondary lobules within lobes, ill-defined intraparenchymal connective tissue support and a thin membranous pleura. The pulmonary artery supplies the distal portion of the respiratory bronchiole, the alveolar duct, alveoli and pleura. The

bronchial artery, except for a few short branches near the hilum contributes none of the pleural supply, but does supply the hilar lymph nodes, pulmonary artery and vein, bronchi and bronchioles and terminates in a common capillary bed with the pulmonary artery at the respiratory bronchioles. Rats, rabbits and guinea-pigs differ slightly as they have well-developed precapillary anastomoses.

human and horse having “type III” lungs characterized by partially developed secondary lobules with well-defined but haphazardly arranged interlobular septae and a thick vascular pleura. The pulmonary artery supplies the alveoli with only occasional anastomoses with bronchial artery at the terminal bronchial level. The bronchial artery supplies the hilar lymph nodes, pulmonary artery and vein bronchi and terminal airways, but it also supplies the interlobular septae and pleura. The bronchial artery contributes blood directly to the alveolar capillary network by the terminal bronchioles, interlobular septae and pleural network in areas lying close to the pleura.

Even if the horse has the same bronchial and pulmonary anatomy to humans its experimental use is extremely difficult because of its size, maintenance costs and animal testing regulations and laws.

In dogs, there is significant anatomical variation of the origin of the bronchial arteries and the course followed by the bronchial artery is also subject to considerable variation (33,34). There is also difficulty in isolation of the true bronchial arteries from their widespread anastomoses with the mediastinal and pericardial vessels (33).

As previously described the right bronchial artery of the rat concealed by the right vena cava and the phrenic nerve rendered its identification by dissection difficult (37). Additionally in rat, bronchial artery coming from the aorta is a rare event and correspond to a supernumerary artery, thus it is clear that the origin of bronchial arteries is clearly different in the rat and humans. On the other hand the presence of extrapulmonary branches of bronchial artery especially to the pericardium and myocardium is an important fact that suggests the existence of anastomoses between bronchial artery and the coronary circulation in the rat. This vascular arrangement may work as a collateral source of blood that reaches the myocardium (42). Thus, the rat may offer a model of coronary-bronchial arterial anastomoses that may be of interest to study the role of these anastomoses in heart and lung disorders in humans.

In birds, the bronchial arteries come from the bronchoesophageal artery, a branch of the common carotid artery and they express characteristic symmetry to their

origin and their distribution (41). This pattern is clearly different to the human analog.

The pig and the sheep have the advantage that the broncho-oesophageal artery usually originates from the aorta as a single vessel (25,26,43). The relative constancy of a single arterial trunk makes the recognition and dissection of the artery easy to perform. In this way it is also easy to perform physiological and rheometric studies requiring catheterization of the vessel (32). The extrapulmonary topographic anatomy of bronchial arteries in pigs exhibits similarities to that of humans. The principal bronchi of the pig are each accompanied by two major bronchial artery branches. Two bronchial arteries for each lung is also a common finding in human. Furthermore, the growth of the heart and cardiovascular system from birth to 4 months of age is analogous to the growth of the same system in humans into the mid-teens (26).

Conclusions

The above mentioned, suggest that the pig and the sheep are anatomically and physiologically suited for experimental studies on the bronchial circulation. The bronchial artery of the pig is similar to this of human concerning the origin, the course, the branches and the blood supply. The suitable bronchial anatomy and physiology along with the undeniable usefulness of the pig in experimental research and the low maintenance cost make the pig the ideal model for experiments in bronchial circulation.

Acknowledgements

The authors would like to express their gratitude to Mrs Alexia Agrogianni for her invaluable help in the creation of the figure of this manuscript.

Disclosure: The authors declare no conflict of interest.

References

1. Galen C. *Tracta Frobeniana*. Book 6. Basel: 1562.
2. Cudkowicz L. Leonardo de Vinci and the bronchial circulation. *Br J Tuberc Dis Chest* 1953;47:23-5.
3. Ruysch F. eds. *Opera omnia anatomico-medico-chirurgica*. Vol I: *Dilucidatio Valvularum*, chap. 4, obs 15, 19-22, fig. 9. Amstelodami: Janssonio-Waesbergios, 1721.
4. Haller Albertus. eds. *Icorum anatomicarum quibus praecipuae partes corporis humani*. Gottingen: 1747:35-7.
5. Osaki T, Hanagiri T, Nakanishi R, et al. Bronchial arterial infusion is an effective therapeutic modality for centrally located early-stage lung cancer: results of a pilot study. *Chest* 1999;115:1424-8.
6. Yoon W, Kim JK, Kim YH, et al. Bronchial and nonbronchial systemic artery embolization for life-threatening hemoptysis: a comprehensive review. *Radiographics* 2002;22:1395-409.
7. Kamler M, Nowak K, Bock M, et al. Bronchial artery revascularization restores peribronchial tissue oxygenation after lung transplantation. *J Heart Lung Transplant* 2004;23:763-6.
8. Moberg A. Anatomical and functional aspects of extracardial anastomoses to the coronary arteries. *Pathol Microbiol (Basel)* 1967;30:689-94.
9. Remy-Jardin M, Bouaziz N, Dumont P, et al. Bronchial and nonbronchial systemic arteries at multi-detector row CT angiography: comparison with conventional angiography. *Radiology* 2004;233:741-9.
10. Liebow AA. Patterns of origin and distribution of the major bronchial arteries in man. *Am J Anat* 1965;117:19-32.
11. Cauldwell EW, Siekert RG, et al. The bronchial arteries; an anatomic study of 150 human cadavers. *Surg Gynecol Obstet* 1948;86:395-412.
12. Pump KK. Distribution of bronchial arteries in the human lung. *Chest* 1972;62:447-451.
13. Petelenz T. Non-coronary anastomoses of bronchial arteries. *Cardiologia* 1967;50:43-55.
14. Björk L. Angiographic demonstration of extracardial anastomoses to the coronary arteries. *Radiology* 1966;87:274-7.
15. Moberg A. Anatomical and functional aspects of extracardial anastomoses to the coronary arteries. *Pathol Microbiol (Basel)* 1967;30:689-94.
16. Dupont P, Riquet M. The bronchial arteries. A review of their anatomy and their anastomoses with the coronary arteries. *Surg Radiol Anat* 1991;13:69-71.
17. Deffebach ME, Charan NB, Lakshminarayan S, et al. The bronchial circulation. Small, but a vital attribute of the lung. *Am Rev Respir Dis* 1987;135:463-81.
18. Wagenvoort CA, Wagenvoort N. Arterial anastomoses, bronchopulmonary arteries, and pulmobronchial arteries in perinatal lungs. *Lab Invest* 1967;16:13-24.
19. Pump KK. The bronchial arteries and their anastomoses in the human lung. *Dis Chest* 1963;43:245-55.
20. Tobin CE. The bronchial arteries and their connections with other vessels in the human lung. *Surg Gynecol Obstet* 1952;95:741-50.
21. Viamonte M Jr, Viamonte M, Camacho M, et al.

- Corrosion cast studies of the bronchial arteries. *Surg Radiol Anat* 1989;11:215-9.
22. Baile EM. The anatomy and physiology of the bronchial circulation. *J Aerosol Med* 1996;9:1-6.
 23. McLaughlin RF, Tyler WS, Canada RO. A study of the subgross pulmonary anatomy in various mammals. *Am J Anat* 1961;108:149-65.
 24. Magno M. Comparative anatomy of the tracheobronchial circulation. *Eur Respir J Suppl* 1990;12:557s-62s; discussion 562s-3s.
 25. Calka W. Extrapulmonary course of the bronchial and bronchoesophageal arteries in the domestic pig. *Folia Morphol (Warsz)* 1975;34:59-67.
 26. Gade J, Norgaard MA, Andersen CB, et al. The porcine bronchial artery: surgical and angiographic anatomy. *J Anat* 1999;194:241-7.
 27. Lorentziadis M, Chamogeorgakis T, Toumpoulis IK, et al. Topographic anatomy of bronchial arteries in the pig: a corrosion cast study. *J Anat* 2005;207:427-32.
 28. Nathan H, Orda R, Barkay M. The right bronchial artery. Anatomical considerations and surgical approach. *Thorax* 1970;25:328-33.
 29. Remy J, Deschildre F, Artaud D, et al. Bronchial arteries in the pig before and after permanent pulmonary artery occlusion. *Invest Radiol* 1997;32:218-24.
 30. Gade J, Norgaard MA, Andersen CB, et al. The porcine bronchial artery. Anastomoses with oesophageal, coronary and intercostal arteries. *J Anat* 1999;195:65-73.
 31. White FC, Carroll SM, Magnet A, et al. Coronary collateral development in swine after coronary artery occlusion. *Circ Res* 1992;71:1490-500.
 32. Kotoulas C, Karnabatidis D, Kalogeropoulou C, et al. Anastomoses between bronchial and coronary circulation in a porcine model: computed tomographic and angiographic demonstration. *Hellenic J Cardiol* 2006;47:206-10.
 33. Collier PS. Bronchial arteries of the dog—a pharmacological study. *J Anat* 1979;128:887-8.
 34. Evans HE, De Lahundra A. eds. *Miller's anatomy of the dog*. Fourth ed. Philadelphia: Elsevier Saunders, 2013:359.
 35. Notkovich H. The anatomy of the bronchial arteries of the dog. *J Thorac Surg* 1957;33:242-53.
 36. Hebel R, Strobberg MW. Circulatory system. In: Hebel R, Strobberg MW. eds. *Anatomy of the laboratory rat*. Baltimore: Williams & Wilkins, 1976:91.
 37. Ferreira PG, Silva AC, Aguas AP, et al. Detailed arrangement of the bronchial arteries in the Wistar rat: A study using vascular injection and scanning electron microscopy. *Eur J Anat* 2001;5:67-76.
 38. Deffebach M, Widdicombe J. The bronchial circulation. In: Crystal RG, West JB, Barnes PJ, et al. eds. *The Lung: Scientific Foundations*. New York: Raven Press, 1991:741-57.
 39. Peão MN, Aguas AP, de Sá CM, et al. Neof ormation of blood vessels in association with rat lung fibrosis induced by bleomycin. *Anat Rec* 1994;238:57-67.
 40. Glenn FH. Modifications of pattern in the aortic arch system of birds and their phylogenetic significance. *Proc U S Natl Mus* 1955;104:525-621.
 41. Abdalla MA, King AS. The avian bronchial arteries: species variations. *J Anat* 1977;123:697-704.
 42. Moberg A. Anastomoses between extracardiac vessels and coronary arteries. 3. Microangiographic appearance. *Acta Radiol Diagn (Stockh)* 1968;7:33-47.
 43. Nazari S, Prati U, Berti A, et al. Successful bronchial revascularization in experimental single lung transplantation. *Eur J Cardiothorac Surg* 1990;4:561-6; discussion 567.

Cite this article as: Kotoulas C, Panagiotou I, Tsipas P, Melachrinou M, Alexopoulos D, Dougenis D. Experimental studies in the bronchial circulation. Which is the ideal animal model? *J Thorac Dis* 2014;6(10):1506-1512. doi: 10.3978/j.issn.2072-1439.2014.09.32

L-BLP25 as a peptide vaccine therapy in non-small cell lung cancer: a review

Wenjie Xia^{1,2}, Jie Wang¹, Youtao Xu^{1,3}, Feng Jiang^{1*}, Lin Xu^{1*}

¹Department of Thoracic Surgery, Nanjing Medical University Affiliated Cancer Hospital, Jiangsu Key Laboratory of Molecular and Translational Cancer Research, Cancer Institute of Jiangsu Province, Baiziting 42, Nanjing 210009, China; ²The Fourth Clinical College of Nanjing Medical University, Nanjing 210000, China; ³The First Clinical College of Nanjing Medical University, Nanjing 210000, China

*These authors contributed equally to this work.

Correspondence to: Lin Xu; Feng Jiang. Department of Thoracic Surgery, Nanjing Medical University Affiliated Cancer Hospital, Jiangsu Key Laboratory of Molecular and Translational Cancer Research, Cancer Institute of Jiangsu Province, Baiziting 42, Nanjing 210009, China. Email: xulin83cn@gmail.com; zengnljf@hotmail.com.

Abstract: Lung cancer is one of the most prevalent malignancies worldwide and the leading cause of cancer-related death. Most cases are non-small cell lung cancer (NSCLC). The median overall survival of patients with advanced stage undergoing current standard chemotherapy is approximately 10 months. The addition of new compounds, including targeted agents, to standard first-line cytotoxic doublets, which are administered concurrently and/or as maintenance therapy in patients who have not experienced disease progression after first-line treatment, has shown potential in improving the efficacy in patients with advanced disease. L-BLP25 is a mucin 1 (MUC1) antigen-specific immunotherapy induces a T-cell response to MUC1 in both a preclinical MUC1-transgenic lung cancer mouse model and patients. This review is aimed at introducing the mechanism by which L-BLP25 targets MUC1, summarizing the achievements gained in the completed clinical trials with L-BLP25 administered as maintenance therapy in the treatment of unresectable stage III/IV NSCLC, and discussing the research trends.

Keywords: L-BLP25; mucin 1 (MUC1); non-small cell lung cancer (NSCLC); clinical trial; cancer vaccines

Submitted Apr 24, 2014. Accepted for publication Jul 03, 2014.

doi: 10.3978/j.issn.2072-1439.2014.08.17

View this article at: <http://dx.doi.org/10.3978/j.issn.2072-1439.2014.08.17>

Introduction

As one of the most prevalent malignancies worldwide, lung cancer is the leading cause of cancer-related death worldwide (1). There were 334,800 deaths due to lung cancer in 2006 in Europe (2) and 753,800 deaths in 2008 in Asia (3). The vast majority of cases (80-95%) are non-small cell lung cancer (NSCLC) (4). Patients with early-stage NSCLC may be cured by surgical resection, followed by adjuvant chemotherapy, which significantly improves the relapse-free and overall survival compared with surgery alone (5). However, a substantial proportion of patients with NSCLC are initially diagnosed with stage III disease (6).

Platinum-based chemotherapy together with concurrent thoracic radiotherapy is the first-line treatment for patients

with unresectable stage IIIB NSCLC (4), but progress with this approach has reached an efficacy plateau, with few patients surviving beyond 5 years. Currently, attention has turned to whether incorporating consolidation or maintenance therapy into treatment regimens for stage III disease might improve the clinical outcome, but recent attempts to improve the outcome for stage III NSCLC patients have had limited success. Subsequent to the Southwest Oncology Group (SWOG) S9504 phase II study, which demonstrated the feasibility and tolerability of docetaxel as consolidation therapy following concurrent chemoradiotherapy in patients with stage IIIB disease (7), the potential of this approach was further investigated in a phase III study conducted by the Hoosier Oncology Group and US Oncology. However, it failed to improve survival,

and even worse, it significantly increased toxicity (8). In another trial, maintenance therapy with gefitinib after concurrent chemoradiation therapy had a negative effect on survival in the SWOG 0023 trial (9).

Immunotherapy is a potential method for providing an improved therapeutic index by improving treatment tolerability (10). Modulation of the immune system, via vaccination or immunity checkpoint inhibition, has gained interest as a potential treatment pathway for NSCLC, particularly in view of successes with immunotherapy in melanoma and castration-resistant prostate cancer (11,12). The mucin 1 (MUC1) glycoprotein is overexpressed and abnormally glycosylated in NSCLC and other cancers (13,14). MUC1 promotes tumor cell growth, survival, and metastasis as a result of its high level of expression on the cell surface; the immunosuppressive properties of its released ectodomain; and its anti-adhesive properties, which prevent cell-cell adhesion and encourage metastasis (15,16). A number of factors make MUC1 a good target for immunotherapy, including high-level cell surface expression (17), antigenic epitopes (18) and aberrant glycosylation (19).

Rationale for immunotherapy with a MUC1 vaccine (L-BLP25)

L-BLP25 is a liposome-based vaccine consisting of a synthetic 25-amino acid lipopeptide derived from the tandem repeat region of MUC1, together with the nonspecific adjuvant monophosphoryl lipid A and three different lipids (15). Monophosphoryl lipid A serves as an adjuvant to induce a cellular immune response. The use of a liposome-based delivery system was intended to facilitate uptake of the antigenic peptide by antigen-presenting cells, such that lipopeptide is delivered into the intracellular space for presentation to Class I MHC. This presentation leads to an antigen-specific T-cell immune response that acts on MUC1-expressing tumors. Cytotoxic T lymphocytes specific to the MUC1 peptide sequence have been isolated from the peripheral blood or lymph nodes of adenocarcinoma patients with breast, pancreatic, and ovarian cancers (20-22). Stimulation of peripheral blood lymphocytes *in vitro* with L-BLP25 results in the generation of a strong MUC1-specific CTL response.

Cytotoxic T lymphocytes are specialized T lymphocytes that destroy cancer cells. T-cell receptors (TCRs) that are expressed on cytotoxic T cells can recognize a specific antigen. The antigen, which is often produced by cancer cells or viruses, can stimulate an immune response. A special antigen

inside a cell is bound to a class I MHC molecule and brought to the surface of the cell by the class I MHC molecule, where it can be recognized by the T cell. If the TCR is specific for that antigen, it binds to the complex of the class I MHC molecules and the antigen. Then, the T cell destroys the cell.

Although the vaccine was designed to generate a primarily cell-mediated immune response, a humoral response may also be involved. Subgroups of breast cancer patients have been identified who have IgG antibodies specific to the MUC1 core peptide (23). *Figure 1* shows the mechanism of action for L-BLP25 on MUC1.

A single low dose of intravenous cyclophosphamide (300 mg/m² to a maximum 600 mg) is administered prior to vaccination. MUC1 is highly immunosuppressive, and the low dose cyclophosphamide can overcome tolerance and enhance the effect of immunotherapy (24). Cyclophosphamide administered after immunization is immunosuppressive; thus, it is only given before the vaccination schedule is initiated. Cyclophosphamide plays a key role in the immunization strategy. Immune tolerance to self-antigens is a significant problem that must be overcome for many vaccine strategies to be effective (25). CD4+/25+ regulatory T cells are involved in the process of tumor-induced tolerance. Lutsiak *et al.* demonstrated that a single, low-dose parenteral administration of cyclophosphamide in female C57BL/6 mice leads to a decrease in both the number and functionality of T regs, enhancing apoptosis and the homeostatic proliferation of these cells (26). Similar findings have been noted using cyclophosphamide in a low dose, chronic daily dosing regimen, which is referred to as metronomic therapy (27).

As a MUC1 antigen specific immunotherapy, L-BLP25 induces a T-cell response to MUC1 in both a preclinical MUC1-transgenic lung cancer mouse model and patients (28-30), and preclinical studies have found that L-BLP25 is indeed capable of inducing a cellular immune response in mice (31). The 1-year survival rate is higher in patients with NSCLC who have high compared with low levels of natural MUC1 antibodies (32). Such observations provide the biological rationale, suggesting that inducing an anticancer immune response to MUC1 using a vaccination strategy might be an effective approach in the treatment of NSCLC.

In December 2013, Charles Butts and colleagues reported the results of the START trial (33), which was restricted to stage III NSCLC. The START trial is the first phase III trial of immunotherapy maintenance in patients with stage III NSCLC. Although the results did not show a survival improvement with tecemotide (consisting of the MUC1-derived 25-aminoacid BLP25 lipopeptide,

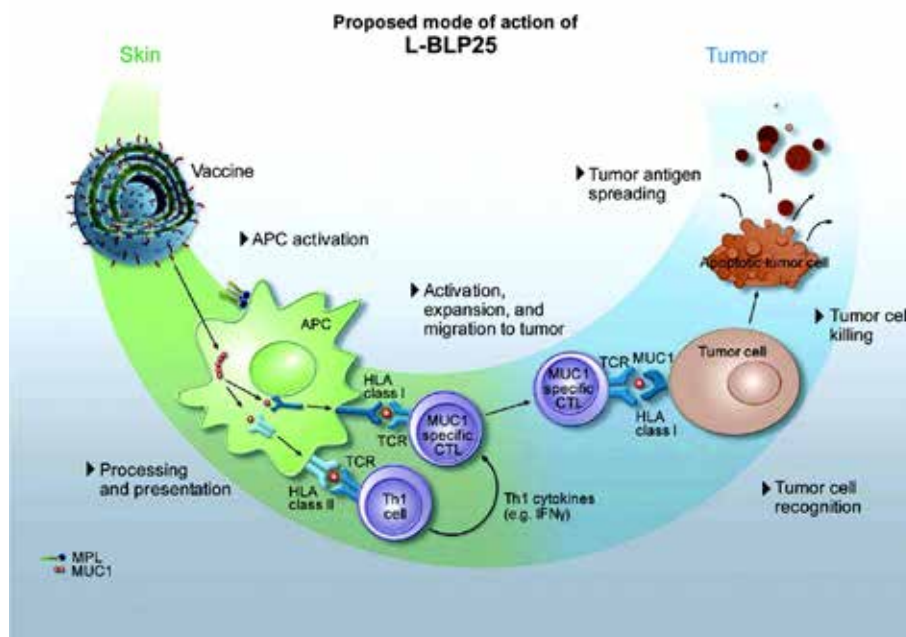


Figure 1 Proposed mechanism of action of L-BLP25. APC, antigen-presenting cell; CTL, cytotoxic T lymphocyte; HLA, human leukocyte antigen; IFN- γ , interferon gamma; MPL, monophosphoryl lipid A; MUC1, mucin 1; Th1, T-helper lymphocyte; TCR, T-cell receptor.

the immunoadjuvant monophosphoryl lipid A, and three liposome-forming lipids) in all assigned patients, their data suggest that the subgroup of patients who received previous concurrent chemoradiotherapy might benefit from maintenance tecemotide.

To provide a foundation for ongoing and future clinical trials, a summary of the achievements gained in the completed clinical trials involving BLP25 administered as maintenance therapy for the treatment of unresectable stage III/IV NSCLC is necessary.

Preclinical study and phase I clinical trial

In preclinical murine studies, L-BLP25 induced a cellular immune response that is characterized by antigen-specific T-cell proliferation and the production of IFN- γ (31,34). Ultimately, this response led to early phase I and II clinical trials to assess its safety profile and efficacy. Last year, Wurz and his colleagues (35) evaluated the effects of L-BLP25 combined with low-dose cyclophosphamide pretreatment on Th1/Th2 cytokines using a novel human MUC1 transgenic (hMUC1.Tg) lung cancer mouse model. They found that the antitumor response to L-BLP25 requires at least two cycles and pre-treatment with cyclophosphamide. In addition, monitoring pro-inflammatory serum cytokines

may be useful as a biomarker for the L-BLP25 response.

An initial phase I study in patients with NSCLC showed that the vaccine could be administered with minimal toxicity (36). Survival in the patients with advanced NSCLC who received L-BLP25 was sufficiently encouraging for proceeding with a phase II randomized study. In addition, an open-label, non-randomized phase I study combined with a double-blind, randomized, placebo-controlled phase II study was conducted in Japanese patients with unresectable stage III NSCLC after primary chemoradiotherapy. Their preliminary phase I safety data reported that L-BLP25 is well tolerated in Japanese patients, and the safety profile is consistent with that seen in previous studies.

Phase II clinical trials

Two foremost phase II trials established the dose and schedule of L-BLP25 and showed the ability of the vaccine to elicit a T-cell proliferative response (37). An open-label, randomized phase II trial in patients with stage IIIB or IV NSCLC who had undergone any first-line chemotherapy was undertaken to test the efficacy of L-BLP25. This trial recruited 171 patients from 17 centers in Canada and the United Kingdom. Patients were randomly assigned to either L-BLP25 plus the best supportive care (BSC) or

the BSC alone. Patients in the L-BLP25 arm received a single intravenous injection dose of cyclophosphamide (300 mg/m²) followed by 8 consecutive weekly subcutaneous injections of L-BLP25 (1,000 µg). Subsequent immunizations were administered at 6-week intervals. The overall survival showed a trend toward longer survival with L-BLP25 plus the BSC *vs.* BSC alone [median: 17.4 *vs.* 13.0 months; adjusted hazard ratio (HR): 0.739, 95% CI: 0.509-1.073; P=0.112], with a post hoc subgroup analysis (n=65) suggesting a greater survival benefit in patients with stage IIIB locoregional disease. An updated analysis confirmed the survival benefit in this subgroup of patients (median: 30.6 months for L-BLP25 plus BSC *vs.* 13.3 months for BSC alone; adjusted HR: 0.548; 95% CI: 0.301-0.999) (38). No significant toxicity was reported in the L-BLP25 arm of this study; grade 1 flu-like symptoms and adverse events related to cyclophosphamide were the most frequent side effects. The quality of life (QoL) analysis revealed a clear advantage for the L-BLP25 arm over the BSC alone arm; more patients in the vaccine arm had clinically meaningful improvement or no change in the QoL, and more patients in the BSC arm had clinically meaningful worsening in the trial outcome index (28).

These safety findings are supported by a subgroup analysis of 16 patients who received L-BLP25 for at least 2 years (39). The safety of the new formulation of BLP25 has also been evaluated in a single-arm, multicenter open-label phase II study enrolling 22 patients, wherein there was a similar safety profile as for the original formulation (30). The results of this phase II study showed that maintenance therapy with L-BLP25 in patients with unresectable locoregional stage IIIB NSCLC is at least feasible and may prolong survival in this patient group.

Phase III clinical trials

To determine whether the L-BLP25 vaccine enhances the survival of patients with stage III NSCLC who have received treatment with curative intent, Charles Butts and his colleagues started an international, randomized, double-blind phase III trial, which they called START (Stimulating Targeted Antigenic Response To NSCLC). In over 4 years of this trial, 1,513 patients (274 of them were excluded because of a clinical hold) with unresectable stage III NSCLC were enrolled. The patients had completed first-line treatment with chemoradiation, either concurrently or sequentially, and had stable disease or an objective clinical response. Randomly, 829 patients were assigned

to receive tecemotide, and 410 were assigned to placebo on a double-blind basis at a 2:1 ratio after the modified intention-to-treat analysis. Incipiently, the study drug was given for 8 consecutive weekly subcutaneous injections of tecemotide (806 µg lipopeptide) or placebo, followed by an injection once every 6 weeks until disease progression. The primary endpoint was overall survival; however, the overall survival in patients who received tecemotide after chemoradiotherapy was not significantly different from those who received placebo [25.6 months (95% CI: 22.5-29.2) with tecemotide *vs.* 22.3 months (95% CI: 19.6-25.5) with placebo; HR: 0.88; 95% CI: 0.75-1.03; P=0.123]. Interestingly, subgroup analysis revealed that there was a remarkable improvement in the patients who received previous concurrent chemoradiotherapy. The median overall survival for 538 (65%) of the 829 patients assigned to tecemotide was 30.8 months (95% CI: 25.6-36.8) compared with 20.6 months (95% CI: 17.4-23.9) for the 268 (65%) of 410 patients assigned to placebo (adjusted HR: 0.78; 95% CI: 0.64-0.95; P=0.016). Currently, Charles Butts and his colleagues are planning a confirmatory randomized trial of tecemotide for patients with stage III NSCLC after concurrent chemoradiotherapy.

The biological rationale for such a difference in the response to tecemotide of NSCLC patients who previously received concurrent as opposed to sequential CRT remains unclear. A hypothesis was recently raised that the success of concurrent chemoradiotherapy in different solid tumors might be explained by the achievement of immunogenic cell death (40). Chiao-Jung Kao and his colleagues are trying to build preclinical animal models to accurately evaluate the effects of tecemotide in a preclinical setting. The mouse model may help explain the biological rationale for such a difference in the response to tecemotide of NSCLC patients who were previously receiving concurrent as opposed to sequential CRT (41).

There is an ongoing phase III trial, INSPIRE (Stimuvax Trial in Asian NSCLC Patients: Stimulating Immune Response), that is being conducted by Professor Wu to gain valuable insight into the potential role of L-BLP25 as maintenance therapy for East-Asian patients with unresectable stage III NSCLC. Currently, approximately 40 trial sites are contributing to the study to achieve a population of 420 patients. *Figures 2 and 3* describe the overall survival from the phase III trial.

Conclusions

The theme within vaccine trials for NSCLC is a trend

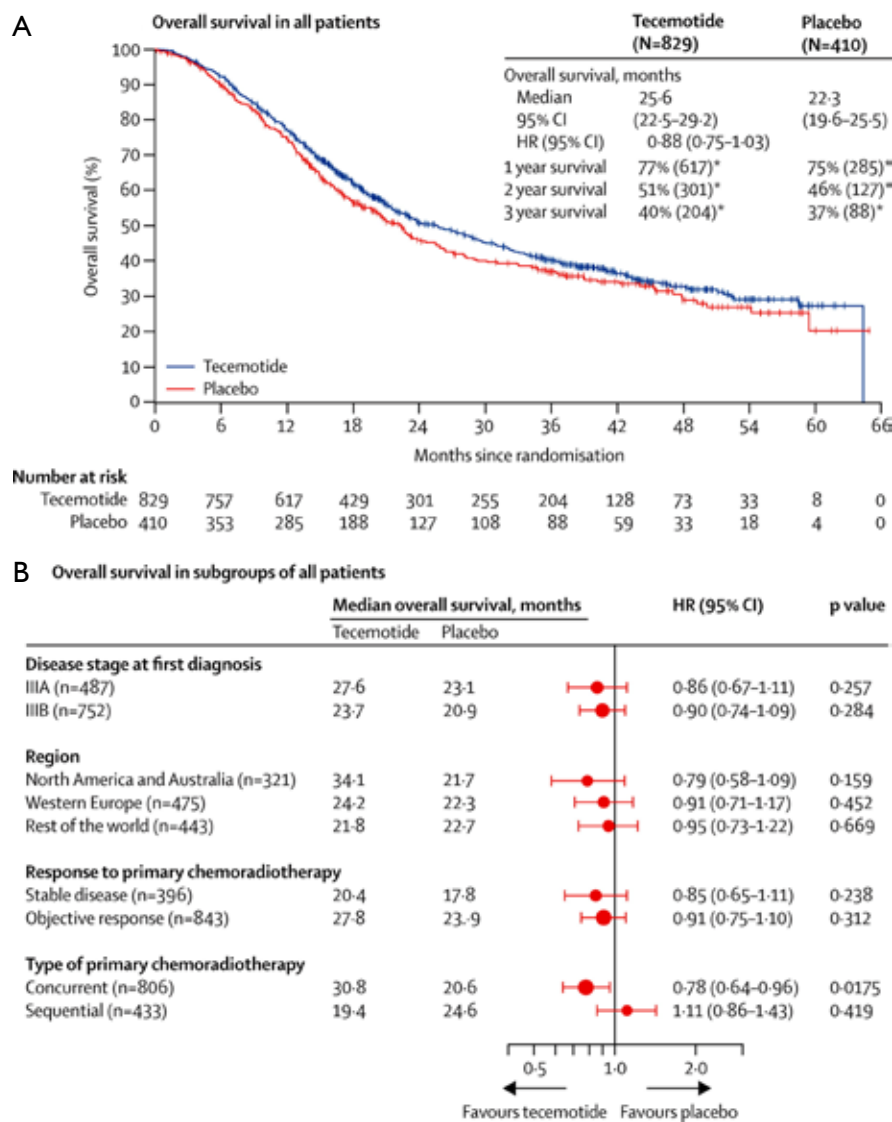


Figure 2 The overall survival in the modified intention-to-treat population and by randomization strata (33). (A) Kaplan-Meier curve of the overall survival in the primary analysis (modified intention-to-treat) population; (B) the overall survival in each of the four randomization strata in the modified intention-to-treat population. HR, hazard ratio; *, numbers in parentheses show the number at risk.

toward a benefit, but there is a general inability to achieve primary endpoints. However, in view of the results of clinical trials, it seems premature to think that targeting a single tumor-associated antigen is an invalid approach against NSCLC (42). The results of START should be considered a guide to understanding the interaction between antigen-specific immunotherapy and prior CRT. Numerous trials are underway internationally to determine whether novel immunotherapies can generate meaningful improvements in key clinical outcomes (such as the median overall survival and progression-free survival) in

patients with lung cancer. Defining patient populations that will attain the greatest benefit to treatment with immunotherapeutics and determining the best time in a patient's treatment course to administer immunotherapy remain open questions that require further exploration in phase III clinical trials.

One area for improvement in vaccine development is how to best design vaccines that generate both an immune response and a correlative clinical response. Perhaps the next phase of development should focus on the achievement of greater knowledge about the importance of MUC1 in

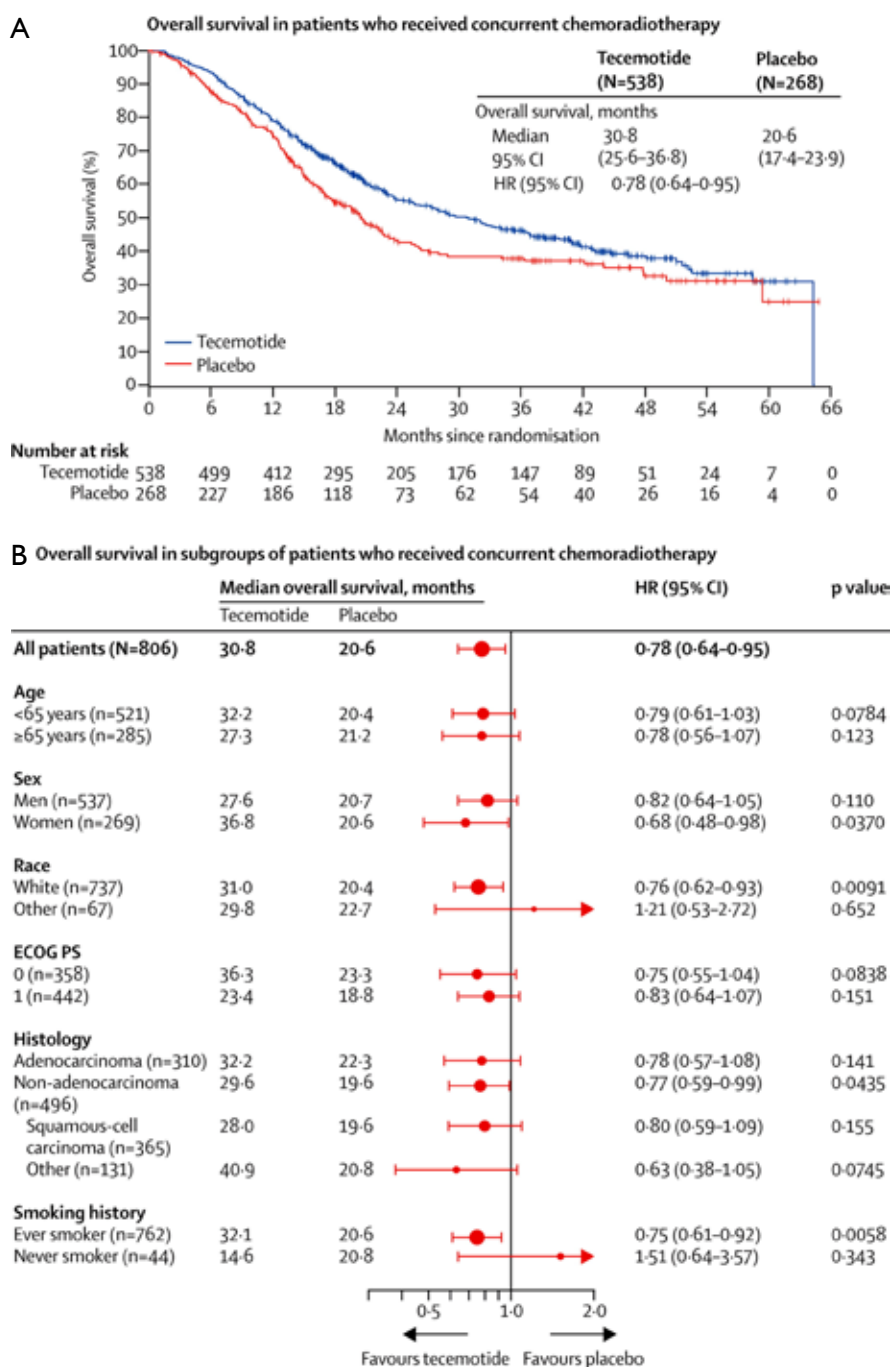


Figure 3 The overall survival in patients who received concurrent chemoradiotherapy (33). (A) Kaplan-Meier curve of the overall survival in the subgroup of patients who received initial concurrent chemoradiotherapy; (B) the overall survival according to the baseline characteristics in the concurrent chemoradiotherapy subgroup. ECOG PS, Eastern Cooperative Oncology Group performance status; HR, hazard ratio.

NSCLC as well as on the identification of biomarkers that predict tecemotide efficacy (43). It may be important to monitor the immune response of cancer patients receiving immunotherapy over time and identify the parameters that

correlate with survival. For example, it may be worthwhile to investigate an indicator of antigen-specific immune responses, such as the circulating levels of IFN- γ 24-48 h post-treatment, which might ensure that a given patient is

at least exhibiting an immunological response. The trials should be conducted in prospectively defined subgroups in ongoing and future clinical trials. Efforts to enhance the ability of a vaccine to generate immune responses in a greater percentage of patients and to identify patient factors that predict a greater likelihood of achieving a measurable immune response are necessary for maximizing the vaccine immunotherapy's ability to improve patient outcomes. The questions raised by START will hopefully be explained soon with substantial effort placed into the study of tecemotide.

Acknowledgements

Funding: This work was supported by the Natural Science Foundation of Jiangsu Province [grant number: BK2012482] and Jiangsu Provincial Special Program of Medical Science [grant number. BL2012030].

Disclosure: The authors declare no conflict of interest.

References

1. Ferlay J, Shin HR, Bray F, et al. Estimates of worldwide burden of cancer in 2008: GLOBOCAN 2008. *Int J Cancer* 2010;127:2893-917.
2. Ferlay J, Autier P, Boniol M, et al. Estimates of the cancer incidence and mortality in Europe in 2006. *Ann Oncol* 2007;18:581-92.
3. Chen W, Zhang S, Zou X. Evaluation on the incidence, mortality and tendency of lung cancer in China. *Thoracic Cancer* 2010;1:35-40.
4. Crinò L, Weder W, van Meerbeeck J, et al. Early stage and locally advanced (non-metastatic) non-small-cell lung cancer: ESMO Clinical Practice Guidelines for diagnosis, treatment and follow-up. *Ann Oncol* 2010;21 Suppl 5:v103-15.
5. Winton T, Livingston R, Johnson D, et al. Vinorelbine plus cisplatin vs. observation in resected non-small-cell lung cancer. *N Engl J Med* 2005;352:2589-97.
6. van Meerbeeck JP. Staging of non-small cell lung cancer: consensus, controversies and challenges. *Lung Cancer* 2001;34 Suppl 2:S95-107.
7. Gandara DR, Chansky K, Albain KS, et al. Consolidation docetaxel after concurrent chemoradiotherapy in stage IIIB non-small-cell lung cancer: phase II Southwest Oncology Group Study S9504. *J Clin Oncol* 2003;21:2004-10.
8. Hanna N, Neubauer M, Yiannoutsos C, et al. Phase III study of cisplatin, etoposide, and concurrent chest radiation with or without consolidation docetaxel in patients with inoperable stage III non-small-cell lung cancer: the Hoosier Oncology Group and U.S. Oncology. *J Clin Oncol* 2008;26:5755-60.
9. Kelly K, Chansky K, Gaspar LE, et al. Phase III trial of maintenance gefitinib or placebo after concurrent chemoradiotherapy and docetaxel consolidation in inoperable stage III non-small-cell lung cancer: SWOG S0023. *J Clin Oncol* 2008;26:2450-6.
10. Bradbury PA, Shepherd FA. Immunotherapy for lung cancer. *J Thorac Oncol* 2008;3:S164-70.
11. Forde PM, Reiss KA, Zeidan AM, et al. What lies within: novel strategies in immunotherapy for non-small cell lung cancer. *Oncologist* 2013;18:1203-13.
12. Hall RD, Gray JE, Chiappori AA. Beyond the standard of care: a review of novel immunotherapy trials for the treatment of lung cancer. *Cancer Control* 2013;20:22-31.
13. Bafna S, Kaur S, Batra SK. Membrane-bound mucins: the mechanistic basis for alterations in the growth and survival of cancer cells. *Oncogene* 2010;29:2893-904.
14. Raina D, Kosugi M, Ahmad R, et al. Dependence on the MUC1-C oncoprotein in non-small cell lung cancer cells. *Mol Cancer Ther* 2011;10:806-16.
15. Sangha R, Butts C. L-BLP25: a peptide vaccine strategy in non small cell lung cancer. *Clin Cancer Res* 2007;13:s4652-4.
16. Tang CK, Apostolopoulos V. Strategies used for MUC1 immunotherapy: preclinical studies. *Expert Rev Vaccines* 2008;7:951-62.
17. Apostolopoulos V, Pietersz GA, McKenzie IF. MUC1 and breast cancer. *Curr Opin Mol Ther* 1999;1:98-103.
18. Ho SB, Niehans GA, Lyftogt C, et al. Heterogeneity of mucin gene expression in normal and neoplastic tissues. *Cancer Res* 1993;53:641-51.
19. Hull SR, Bright A, Carraway KL, et al. Oligosaccharide differences in the DF3 sialomucin antigen from normal human milk and the BT-20 human breast carcinoma cell line. *Cancer Commun* 1989;1:261-7.
20. Jerome KR, Barnd DL, Bendt KM, et al. Cytotoxic T-lymphocytes derived from patients with breast adenocarcinoma recognize an epitope present on the protein core of a mucin molecule preferentially expressed by malignant cells. *Cancer Res* 1991;51:2908-16.
21. Berd D, Maguire HC Jr, McCue P, et al. Treatment of metastatic melanoma with an autologous tumor-cell vaccine: clinical and immunologic results in 64 patients. *J Clin Oncol* 1990;8:1858-67.
22. Ioannides CG, Fisk B, Jerome KR, et al. Cytotoxic T cells from ovarian malignant tumors can recognize

- polymorphic epithelial mucin core peptides. *J Immunol* 1993;151:3693-703.
23. Jerome KR, Domenech N, Finn OJ. Tumor-specific cytotoxic T cell clones from patients with breast and pancreatic adenocarcinoma recognize EBV-immortalized B cells transfected with polymorphic epithelial mucin complementary DNA. *J Immunol* 1993;151:1654-62.
 24. Mastrangelo MJ, Berd D, Maguire H Jr. The immunoaugmenting effects of cancer chemotherapeutic agents. *Semin Oncol* 1986;13:186-94.
 25. Ko HJ, Kim YJ, Kim YS, et al. A combination of chemoimmunotherapies can efficiently break self-tolerance and induce antitumor immunity in a tolerogenic murine tumor model. *Cancer Res* 2007;67:7477-86.
 26. Lutsiak ME, Semnani RT, De Pascalis R, et al. Inhibition of CD4(+)/25+ T regulatory cell function implicated in enhanced immune response by low-dose cyclophosphamide. *Blood* 2005;105:2862-8.
 27. Ghiringhelli F, Menard C, Puig PE, et al. Metronomic cyclophosphamide regimen selectively depletes CD4+CD25+ regulatory T cells and restores T and NK effector functions in end stage cancer patients. *Cancer Immunol Immunother* 2007;56:641-8.
 28. Butts C, Murray N, Maksymiuk A, et al. Randomized phase IIB trial of BLP25 liposome vaccine in stage IIIB and IV non-small-cell lung cancer. *J Clin Oncol* 2005;23:6674-81.
 29. Butts C, Maksymiuk A, Goss G, et al. Updated survival analysis in patients with stage IIIB or IV non-small-cell lung cancer receiving BLP25 liposome vaccine (L-BLP25): phase IIB randomized, multicenter, open-label trial. *J Cancer Res Clin Oncol* 2011;137:1337-42.
 30. Butts C, Murray RN, Smith CJ, et al. A multicenter open-label study to assess the safety of a new formulation of BLP25 liposome vaccine in patients with unresectable stage III non-small-cell lung cancer. *Clin Lung Cancer* 2010;11:391-5.
 31. Guan HH, Budzynski W, Koganty RR, et al. Liposomal formulations of synthetic MUC1 peptides: effects of encapsulation versus surface display of peptides on immune responses. *Bioconjug Chem* 1998;9:451-8.
 32. Hirasawa Y, Kohno N, Yokoyama A, et al. Natural autoantibody to MUC1 is a prognostic indicator for non-small cell lung cancer. *Am J Respir Crit Care Med* 2000;161:589-94.
 33. Butts C, Socinski MA, Mitchell PL, et al. Tecemotide (L-BLP25) versus placebo after chemoradiotherapy for stage III non-small-cell lung cancer (START): a randomised, double-blind, phase 3 trial. *Lancet Oncol* 2014;15:59-68.
 34. Agrawal B, Krantz MJ, Reddish MA, et al. Rapid induction of primary human CD4+ and CD8+ T cell responses against cancer-associated MUC1 peptide epitopes. *Int Immunol* 1998;10:1907-16.
 35. Wurz GT, Gutierrez AM, Greenberg BE, et al. Antitumor effects of L-BLP25 Antigen-Specific tumor immunotherapy in a novel human MUC1 transgenic lung cancer mouse model. *J Transl Med* 2013;11:64.
 36. Palmer M, Parker J, Modi S, et al. Phase I study of the BLP25 (MUC1 peptide) liposomal vaccine for active specific immunotherapy in stage IIIB/IV non-small-cell lung cancer. *Clin Lung Cancer* 2001;3:49-57; discussion 58.
 37. North S, Butts C. Vaccination with BLP25 liposome vaccine to treat non-small cell lung and prostate cancers. *Expert Rev Vaccines* 2005;4:249-57.
 38. Butts C, Maksymiuk A, Goss G, et al. A multi-centre phase IIB randomized controlled study of BLP25 liposome vaccine (L-BLP25 or Stimuvax) for active specific immunotherapy of non-small cell lung cancer (NSCLC): updated survival analysis. *J Thorac Oncol* 2007;2:s332-3.
 39. Butts C, Anderson H, Maksymiuk A, et al. Long-term safety of BLP25 liposome vaccine (L-BLP25) in patients (pts) with stage IIIB/IV non-small cell lung cancer (NSCLC). *J Clin Oncol* 2009;27:3055.
 40. Formenti SC, Demaria S. Combining radiotherapy and cancer immunotherapy: a paradigm shift. *J Natl Cancer Inst* 2013;105:256-65.
 41. Kao CJ, Wurz GT, Schröder A, et al. Clarifying the pharmacodynamics of tecemotide (L-BLP25)-based combination therapy. *Oncoimmunology* 2013;2:e26285.
 42. Kroemer G, Zitvogel L, Galluzzi L. Victories and deceptions in tumor immunology: Stimuvax®. *Oncoimmunology* 2013;2:e23687.
 43. Situ D, Wang J, Ma Y, et al. Expression and prognostic relevance of MUC1 in stage IB non-small cell lung cancer. *Med Oncol* 2011;28 Suppl 1:S596-604.

Cite this article as: Xia W, Wang J, Xu Y, Jiang F, Xu L. L-BLP25 as a peptide vaccine therapy in non-small cell lung cancer: a review. *J Thorac Dis* 2014;6(10):1513-1520. doi: 10.3978/j.issn.2072-1439.2014.08.17

Emergency operation of a patient with spontaneous rupture and massive hemorrhage of pleural solitary fibrous tumor

Feng Shao, Rusong Yang, Yanqing Pan

Department of Thoracic Surgery, Nanjing Chest Hospital, Nanjing 210000, China

Correspondence to: Rusong Yang. Department of Thoracic Surgery, Nanjing Chest Hospital, Nanjing 210000, China. Email: njyrs_md@188.com

Abstract: Solitary fibrous tumor (SFT) is a rare pleural disease with asymptomatic clinical course. We report a case of a patient with spontaneous rupture and massive hemorrhage of pleural SFT, which was treated by emergency operation.

Keywords: Solitary fibrous tumor (SFT); spontaneous rupture; hemorrhage; surgery

Submitted Feb 19, 2014. Accepted for publication May 31, 2014.

doi: 10.3978/j.issn.2072-1439.2014.08.22

View this article at: <http://dx.doi.org/10.3978/j.issn.2072-1439.2014.08.22>

Solitary fibrous tumor (SFT) is a rare pleural disease with asymptomatic clinical course. A case of pleural SFT with spontaneous rupture and massive hemorrhage, which was treated by emergency operation, is described.

Case report

A tumor was found in a 48-year-old woman's left thorax by routine physical examination. Her medical history was unremarkable without exposure to asbestos. Chest computed tomography (CT) scan showed a mass of 2.8 cm × 2.5 cm near the descending aorta in the left thorax without hydrothorax (*Figure 1A*). She refused consent for the operation at first. After two months she was sent to the hospital again for sudden dyspnea and chest pain. Chest CT scan showed the mass with the same size and moderate amount of pleural effusion (*Figure 1B*). Closed thoracic drainage in the left thorax was taken and massive bloody fluid was revealed. Hemoglobin in blood routine test gradually descended from 46 to 43 g/L despite blood transfusion. Enhanced chest CT scan showed large amount of pleural effusion in the left thorax, mediastinum was compressed to the right side, with no sign of aorta rupture or dissection (*Figure 1C,D*). Left posterolateral thoracotomy through the fifth intercostal spaces was performed immediately for hemostasis and resection of the tumor. About 2,500 mL blood was sucked in the left thorax. The left lung was normal. The tumor was found originated from the parietal pleura, the diameter

was 3 cm, top of the it was ruptured and bleeding. We completely resected the tumor and the parietal pleura on the chest wall between the fourth and fifth ribs near the descending aorta (*Figures 2,3*). The tumor was not connected with the visceral pleura and lung. Hemoglobin rose to 106 g/L by blood transfusion after surgery.

Histopathologically, spindle-shaped cells with demarcated nuclear membranes and dispersed chromatin in vesicular nuclei were observed. Mitoses were rare. Immunohistochemical staining showed that the tumor was expressing vimentin, CD34, CD31, and Bcl-2, cytokeratin was negative (*Figure 4A,B*). The tumor was pathologically diagnosed as benign localized pleural SFT. The patient discharged eight days after the operation. She is currently healthy after surgery.

Discussion

Solitary fibrous pleural tumor is a rare form of pleural disease. SFT represents less than 5% of pleural tumors and occurs most often in the visceral (80%) and parietal pleura (20%). It is considered to be originated from the mesenchymal cells of the sub-mesothelial connective tissue of the pleura. According to immunohistochemical analysis, vimentin, CD34, CD99 and Bcl-2 are positive in pleural SFT, which are markers of mesenchymal cells; however, cytokeratin is negative, which is found in mesotheliomas. These results indicate that SFT originates from mesenchymal cells rather

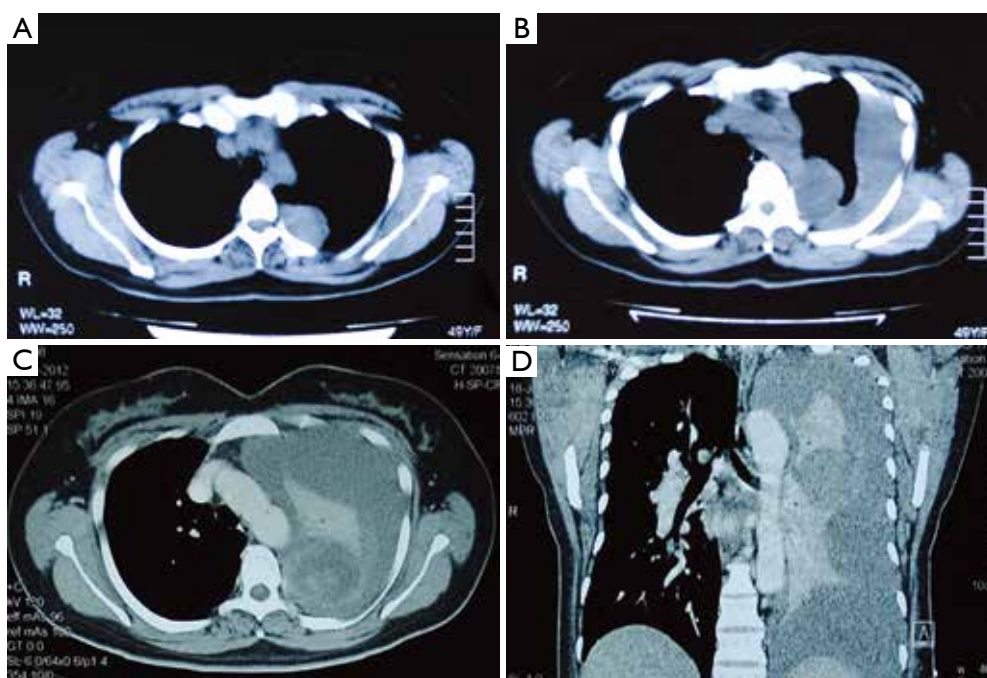


Figure 1 (A) Thoracic computed tomographic scan: a mass of 2.8 cm × 2.5 cm without hydrothorax; (B) tumor of 2.8 cm × 2.5 cm with middle hydrothorax; (C) and (D) enhanced computed tomography (CT) scan: abundant hydrothorax in the left thorax, organs in mediastinum are compressed, the aorta is normal and no sign of rupture.



Figure 2 The tumor between the fourth and fifth ribs was seen with rupture and bleeding on the top, the aorta was normal.



Figure 3 The tumor with spontaneous rupture and a hole was seen on the top because of necrosis and falling off in it.

than mesothelial cells (1). In our case, immunohistochemical analysis showed vimentin, CD34 and Bcl-2 were positive, which was the identical character of SFT.

SFTs often have an asymptomatic clinical course. The tumor usually grow into a huge mass before local compression symptoms developed, especially in patients without routine physical examinations. Tumors larger than 10 cm would occupy a large space and compress other

thoracic structures, which may cause symptoms such as dyspnea, chest pain, cough, and fatigue. About 50% of patients reported in the literature are symptomatic (2). Uncommonly hypertrophic pulmonary osteoarthropathy and hypoglycemia are also caused. Hypertrophic osteoarthropathy, called Pierre Marie-Bamberger syndrome, is associated with the abnormal production of hyaluronic acid by the tumors. Hypoglycemia is caused by

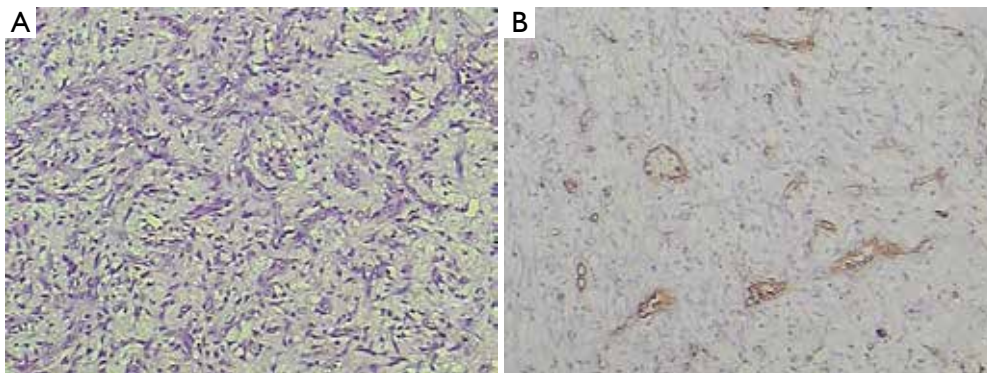


Figure 4 (A) The biopsy demonstrated a varying proportion of spindle-shaped cells and collagen in the tumor (hematoxylin and eosin, original magnification $\times 100$); (B) immunohistochemical analysis showed the tumor was positive for Bcl-2.

the insulin-like growth factor 2, which is secreted by the tumors (3). In our case, the patient had no symptom at first. When the tumor ruptured spontaneously, dyspnea and chest pain appeared until the operation was done to remove the tumor and relieve the compression of hemorrhage in her left thorax. The cause of spontaneous rupture is not clear. The only blood supply may come from vessels in the partial pleura and chest wall. One possible reason is that the top of the tumor tends to necrosis and bleeding because of insufficient blood supply along with growing of the tumor.

Occasional recurrences have been reported not only in malignant cases but also in benign cases, even though it is small percentage (1.4%) (4). Now the patient recovers very well after emergency operation, close follow-up is indicated because of the possibility of recurrence.

Conclusions

We report a case of a patient with spontaneous rupture and massive hemorrhage of pleural SFT. Although the tumor is small and benign, surgical resection could be considered for bleeding could be caused and presented as

dyspnea and chest pain.

Acknowledgements

Disclosure: The authors declare no conflict of interest.

References

1. Harrison-Phipps KM, Nichols FC, Schleck CD, et al. Solitary fibrous tumors of the pleura: results of surgical treatment and long-term prognosis. *J Thorac Cardiovasc Surg* 2009;138:19-25.
2. Guo J, Chu X, Sun YE, et al. Giant solitary fibrous tumor of the pleura: an analysis of five patients. *World J Surg* 2010;34:2553-7.
3. Shaker W, Meatchi T, Dusser D, et al. An unusual presentation of solitary fibrous tumour of the pleura: right atrium and inferior vena cava compression. *Eur J Cardiothorac Surg* 2002;22:640-2.
4. Magdeleinat P, Alifano M, Petino A, et al. Solitary fibrous tumors of the pleura: clinical characteristics, surgical treatment and outcome. *Eur J Cardiothorac Surg* 2002;21:1087-93.

Cite this article as: Shao F, Yang R, Pan Y. Emergency operation of a patient with spontaneous rupture and massive hemorrhage of pleural solitary fibrous tumor. *J Thorac Dis* 2014;6(10):E209-E211. doi: 10.3978/j.issn.2072-1439.2014.08.22

Caution for acute submassive pulmonary embolism with syncope as initial symptom: a case report

Sheng-Yu Wang, Hui Chen, Li-Gai Di

Pulmonary and Critical Care Department, Affiliated Hospital of Xi'an Medical University, Xi'an 710077, China

Correspondence to: Sheng-Yu Wang. Pulmonary and Critical Care Department, Affiliated Hospital of Xi'an Medical University, Xi'an 710077, China.

Email: wangshengyu@yeah.net.

Abstract: Pulmonary embolism (PE) may escape prompt diagnosis since clinical symptoms and signs are nonspecific. The occurrence of syncope as the sole initial symptom in a previously healthy patient with no predisposing factors to embolism and no hemodynamic instability is extremely rare, which may have been a factor in the delayed diagnosis. We describe a case of acute submassive PE with syncope as the initial symptom. A 62-year-old previously healthy female was admitted to our hospital for transitory episode of syncope. Following admission, chest computed tomography demonstrated embolism in the right main pulmonary and left inferior pulmonary arteries. Following the final diagnosis, the patient was successfully treated with thrombolytic therapy with systemic urokinase. We consider that raised awareness and early diagnosis and treatment were key factors in ensuring a satisfactory prognosis.

Keywords: Pulmonary embolism (PE); syncope; thrombolysis

Submitted Mar 09, 2014. Accepted for publication Jun 30, 2014.

doi: 10.3978/j.issn.2072-1439.2014.08.11

View this article at: <http://dx.doi.org/10.3978/j.issn.2072-1439.2014.08.11>

Introduction

Pulmonary embolism (PE) may escape prompt diagnosis since clinical symptoms and signs are nonspecific. It is estimated that approximately 650,000 cases occur annually in the United States (1). Clinically, PE mainly manifests as chest pain, shock and hypotension, and only about 10% of patients have syncope as the initial symptom (2,3). Syncope as the presenting symptom of PE has proven to be a difficult clinical correlation to make. We report on the diagnosis and treatment of a patient with PE with syncope as the initial symptom.

Case report

A 62-year-old woman with no history of disease was admitted to emergency department of Affiliated Hospital of Xi'an Medical University after she had a syncopal episode in her home. The patient kept her right upper limb inactive for 1 week because of right clavicle's fracture until she suddenly collapsed while standing and lost consciousness for

approximately ten minutes. She recovered spontaneously but was extremely weak and dyspneic. She was also diaphoretic and tachypneic, but denied any associated chest pain or palpitations. No seizures were witnessed, and she experienced no incontinence.

On admission to Pulmonary Department, physical examination revealed a diaphoretic and dyspneic patient without focal neurologic findings. Her heart rate was regular at 96 beats per minute, her blood pressure was 131/82 mmHg without orthostatic changes, and her respiratory rate was 32 breaths per minute. The room air oxygen saturation was 86-90%, and arterial blood gas analysis in room air revealed hypoxemia ($PO_2 = 47$ mmHg) with an elevated alveoli-arterial oxygen gradient (A-a O_2 gradient). Examination of her head and neck was normal. The results of chest wall examination revealed normal breath sounds bilaterally. The findings of heart, abdominal and central nervous system examinations were unremarkable. There were no edemas in lower extremities. Levels of serum electrolytes, glucose, blood urea and creatinine, and complete blood counts were normal. Results of a computed tomographic

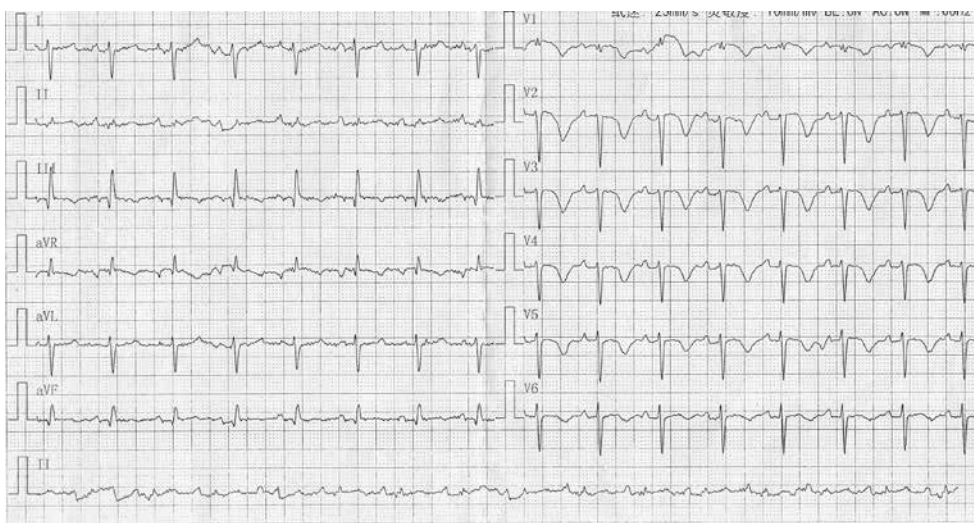


Figure 1 Electrocardiogram at pretreatment shows Q and T waves in lead III and an S wave in lead I, T wave inversion in precordial leads.

scan of her head were negative for bleeding, aneurysm or an embolic event. A Doppler scan of the legs was normal. An electrocardiogram showed a regular rhythm consistent with sinus rhythm; there were Q and T waves in lead III and an S wave in lead I, T wave inversion in lead V1-V6 (*Figure 1*). Because PE cannot be excluded and anticoagulant with low molecular weight heparin was performed immediately. A transthoracic echocardiogram revealed normal left ventricle function without a patent foramen ovale, an atrial septal defect or a ventricular septal defect and normal right ventricle function. The level of D-dimer was 1.5 mg/L (normal value 0-1 mg/L). The value of BNP was 170 pg/mL (normal level 0-100 pg/mL) and troponin was 0.1 mL (normal level 0-0.04 mL). An enhanced chest computed tomography (CT) scan revealed filling defects in the right main pulmonary and left inferior pulmonary arteries (*Figure 2*).

With a diagnosis of acute submassive PE (4), the patient underwent thrombolytic therapy with urokinase 1,000,000 IU over a 2-hour period, which brought about immediate improvement in the patient's condition. Anticoagulant with low molecular weight heparin and an oral anticoagulant were continued when APTT decreased within two times of normal value. The following days, the electrocardiograms showed Q and T waves in lead III and an S wave in lead I were improved, T wave in lead V5-V6 were normal (*Figure 3*). Her symptoms improved dramatically, her respiratory rate decreased and her O₂ saturation rose from 85% to 95%. An enhanced chest CT scan reexamination showed filling defects in the right main pulmonary and left inferior pulmonary

arteries were remarkably improved after 12 days (*Figure 4*). After a 16-day course of hospital treatment, she was discharged on oral warfarin therapy. The patient's long-term follow-up was performed by Pulmonary Department, and we learned that the patient was well for four months after that episode without any evidence of recurrent syncope or PE.

Discussion

The diagnosis of acute PE is amongst the most challenging problems encountered in clinical practice. Clinical assessment is necessary to estimate a pre-test probability of PE and determine what (if any) diagnostic testing is required. The most common symptoms of PE are dyspnea (82%), pleuritic chest pain (49%), and cough (20%) (5). Syncope is an uncommon presentation of PE, occurring in only 10% of patients. However, no clinical features can be used to rule in or rule out PE without further testing (6). There are several possible reasons why cause syncope: (I) acute right heart failure and damaged pulmonary blood perfusion causing decreased filling of the left ventricle, with resulting hypotension, bradycardia and cerebral circulation disturbance (7); (II) reflex syncope caused by bradycardia due to vagal stimulation and by peripheral vascular distention due to suppression of sympathetic nerves (8); and (III) syncope caused by an atrioventricular block induced by MPE (9).

Embolus of PE can be from superior vena cava or inferior vena cava. However, ~79% of patients who present with PE have evidence of deep venous thrombosis in their

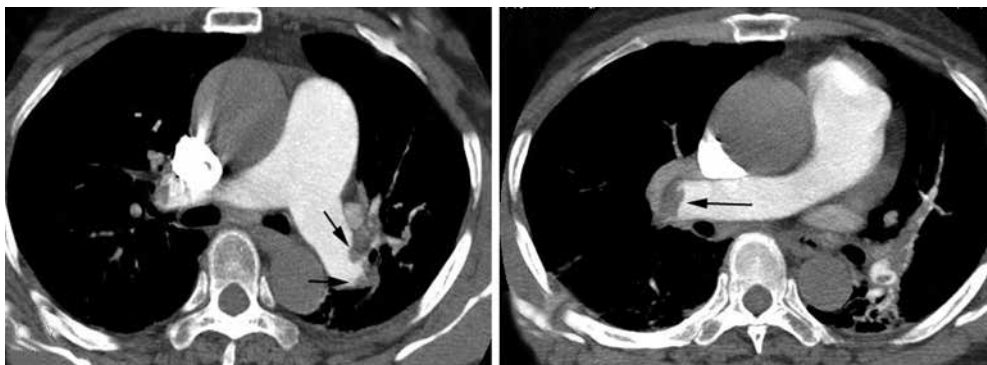


Figure 2 Enhanced chest computed tomography (CT) scan at pretreatment shows filling defects in the right main pulmonary and left inferior pulmonary arteries. Black arrows point embolus.

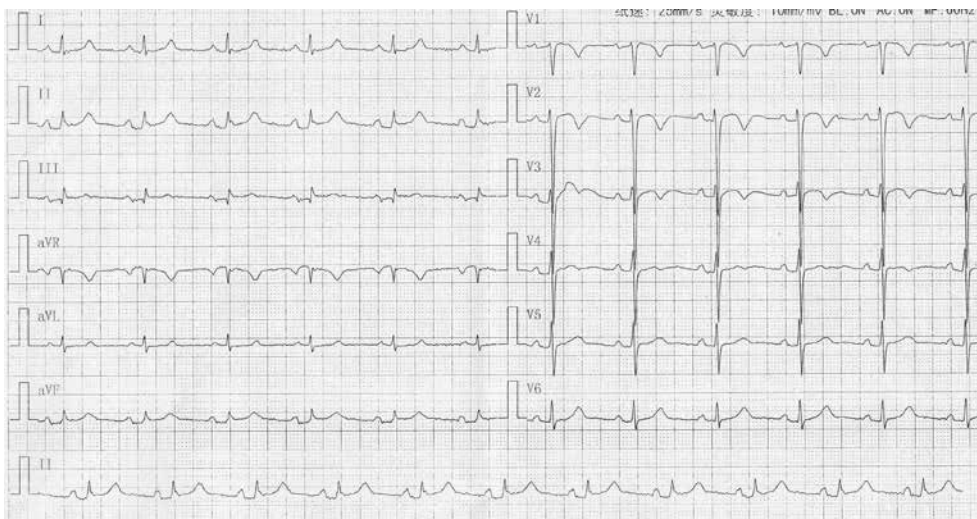


Figure 3 Electrocardiogram at post treatment shows Q and T waves in lead III and an S wave in lead I were improved, T wave in lead V5-V6 are normal.

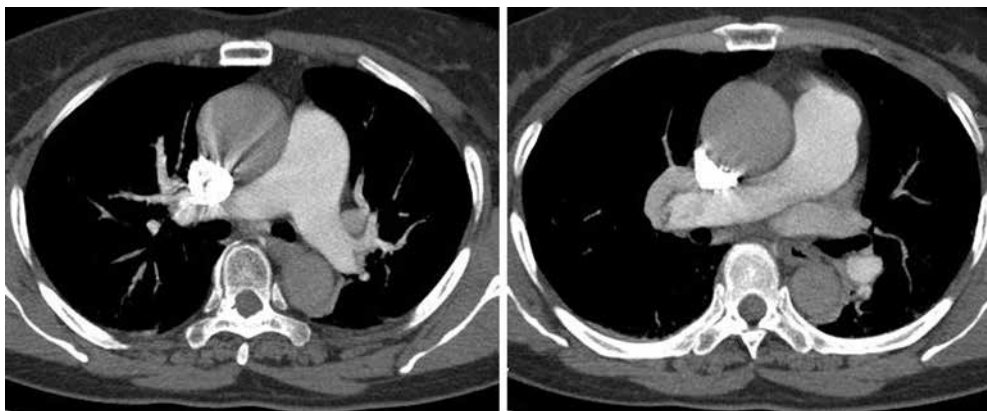


Figure 4 Enhanced chest CT scan at post treatment shows filling defects in the right main pulmonary and left inferior pulmonary arteries are improved.

legs, if deep venous thrombosis is not detected in such patients, it is likely that the whole thrombus has already detached (10). The exact number of the symptoms and signs of deep vein thrombosis in patients with a diagnosis of PE is not clear, but one study reported deep vein thrombosis in 62% of patients with PE (11). The patient lacked activities for one week because of right clavicle's fracture, it is possible embolus existed in inferior vena cava and whole thrombus detached from blood vessel, so it was not detected by ultrasound.

The electrocardiograph (ECG) is still simple, easy to use and useful in the diagnosis of acute PE. Surface ECG readings are altered in about 70% of PE (12). Numerous ECG findings have been reported, with sinus tachycardia being the most common (13). Findings such as the S1Q3T3 pattern lack sensitivity and specificity, and also show no correlation with the severity of PE (13,14). Several studies have stated that T-wave inversion in lead III, aVF and precordial leads is most often associated with massive PE and/or PE with right ventricle (RV) dysfunction, ascribing a high sensitivity, specificity, positive and negative predictive value to these findings (14-17). Negative T waves in both leads III and V1 have been reported to accurately differentiate acute PE from acute coronary syndrome (15). The changes between the initial and posttreatment ECG from this patient are obvious, the role of ECG on diagnosing PE is not ignored by clinicians.

Management with anticoagulants alone is typically sufficient for low-risk patients, more aggressive treatments such as thrombolysis, embolectomy, and inferior vena cava (IVC) filters are recommended for higher-risk patients. Thrombolytic therapy should be considered in all patients with massive PE and hypotension associated with deep vein thrombosis in the popliteal area or higher (18). The main indications for thrombolytic therapy include ongoing hypoxia, respiratory distress, pulmonary hypertension, and right heart failure because thrombolytic therapy often achieves an impressive and almost an immediate clinical benefit in these clinical settings (19). Our patient had emerged ongoing hypoxia and breathlessness on admission, so she had the indications for thrombolytic therapy. In fact her symptoms were improved dramatically after thrombolysis.

In conclusion, the occurrence of syncope as the sole initial symptom in a previously healthy patient with no hemodynamic instability following admission is extremely rare. In this situation, the raised awareness of diagnosis and knowledge concerning the clinical presentation of

pulmonary thromboembolism are key factors in ensuring an immediate diagnosis and adequate intervention.

Acknowledgements

Disclosure: The authors declare no conflict of interest.

References

1. Wolfe TR, Allen TL. Syncope as an emergency department presentation of pulmonary embolism. *J Emerg Med* 1998;16:27-31.
2. Calvo-Romero JM, Pérez-Miranda M, Bureo-Dacal P. Syncope in acute pulmonary embolism. *Eur J Emerg Med* 2004;11:208-9.
3. Blaho KE, Merigian KS, Winbery SL, et al. Foreign body ingestions in the Emergency Department: case reports and review of treatment. *J Emerg Med* 1998;16:21-6.
4. Jaff MR, McMurtry MS, Archer SL, et al. Management of massive and submassive pulmonary embolism, iliofemoral deep vein thrombosis, and chronic thromboembolic pulmonary hypertension: a scientific statement from the American Heart Association. *Circulation* 2011;123:1788-830.
5. Goldhaber SZ, Visani L, De Rosa M. Acute pulmonary embolism: clinical outcomes in the International Cooperative Pulmonary Embolism Registry (ICOPER). *Lancet* 1999;353:1386-9.
6. West J, Goodacre S, Sampson F. The value of clinical features in the diagnosis of acute pulmonary embolism: systematic review and meta-analysis. *QJM* 2007;100:763-9.
7. Gossage JR. Early intervention in massive pulmonary embolism. A guide to diagnosis and triage for the critical first hour. *Postgrad Med* 2002;111:27-8, 33-4, 39-40 passim.
8. Eldadah ZA, Najjar SS, Ziegelstein RC. A patient with syncope, only "vaguely" related to the heart. *Chest* 2000;117:1801-3.
9. Elias J, Kuniyoshi R, Moulin B, et al. Syncope and complete atrioventricular block related to pulmonary thromboembolism. *Arq Bras Cardiol* 2004;83:438-41; 434-7.
10. Tapson VF. Acute pulmonary embolism. *N Engl J Med* 2008;358:1037-52.
11. Köhn H, Mostbeck A, Bachmayr S, et al. 99mTc-DTPA aerosol for same-day post-perfusion ventilation imaging: results of a multicentre study. *Eur J Nucl Med* 1993;20:4-9.
12. Kosuge M, Kimura K, Ishikawa T, et al. Electrocardiographic differentiation between acute

- pulmonary embolism and acute coronary syndromes on the basis of negative T waves. *Am J Cardiol* 2007;99:817-21.
13. Laack TA, Goyal DG. Pulmonary embolism: an unsuspected killer. *Emerg Med Clin North Am* 2004;22:961-83.
 14. Cheng AS, Money-Kyrle A. Instructive ECG series in massive bilateral pulmonary embolism. *Heart* 2005;91:860-2.
 15. Punukollu G, Gowda RM, Vasavada BC, et al. Role of electrocardiography in identifying right ventricular dysfunction in acute pulmonary embolism. *Am J Cardiol* 2005;96:450-2.
 16. Sarin S, Elmi F, Nassef L. Inverted T waves on electrocardiogram: myocardial ischemia versus pulmonary embolism. *J Electrocardiol* 2005;38:361-3.
 17. Torbicki A, Perrier A, Stavros K, et al. Guidelines on the diagnosis and management of acute pulmonary embolism. *G Ital Cardiol (Rome)* 2009;10:303-47.
 18. Linn BJ, Mazza JJ, Friedenbergr WR. Treatment of venous thromboembolic disease. A pragmatic approach to anticoagulation and thrombolysis. *Postgrad Med* 1986;79:171-80.
 19. Gallus AS. Thrombolytic therapy for venous thrombosis and pulmonary embolism. *Baillieres Clin Haematol* 1998;11:663-73.

Cite this article as: Wang SY, Chen H, Di LG. Caution for acute submassive pulmonary embolism with syncope as initial symptom: a case report. *J Thorac Dis* 2014;6(10):E212-E216. doi: 10.3978/j.issn.2072-1439.2014.08.11

Rapid growing huge teratoma: complete surgical resection

Dohun Kim, Si-Wook Kim, Jong-Myeon Hong

Department of Thoracic and Cardiovascular Surgery, College of medicine, Chungbuk National University, Cheongju-si, Korea

Correspondence to: Jong-Myeon Hong, MD, PhD. Department of Thoracic and Cardiovascular, Surgery, College of Medicine, Chungbuk National University, 410 Sungbong-Ro, Heungduk-Gu, Cheongju, Chungbuk, 361-763, Korea. Email: hongjm@chungbuk.ac.kr

Abstract: We report successful total resection of a huge mediastinal teratoma. An 11-year-old male underwent chest computed tomography that revealed a 14-cm mediastinal mass occupying the right thoracic cavity. The mass was successfully removed without any postoperative complication.

Keywords: Mediastinal mass; thoracic surgery; teratoma

Submitted Apr 01, 2014. Accepted for publication Jul 24, 2014.

doi: 10.3978/j.issn.2072-1439.2014.08.05

View this article at: <http://dx.doi.org/10.3978/j.issn.2072-1439.2014.08.05>

Introduction

The most common causes of anterior mediastinal tumor include thymoma, germ cell tumor, thyroid disease, and lymphoma (1). Germ cell tumors are found in young adults and represent 15% of anterior mediastinal masses. Most common germ cell tumors are benign teratomas that grow very slowly (2). Complete surgical resection is the treatment of choice for such tumors, although this is sometimes difficult and requires careful attention in the case of larger tumors (2). We report our successful experience with complete resection of a large mediastinal teratoma showing rapid growth.

Case

An 11-year-old male with frequent upper respiratory symptoms visited our hospital for chest computed tomography. Chest radiography performed in a local hospital revealed a large mass occupying the right thoracic cavity (*Figure 1A*). A chest radiograph from three years prior also demonstrated a mediastinal mass neighboring the right cardiac border (*Figure 1B*). However, no further work-up was performed at that time. Chest computed tomography in our hospital revealed a mediastinal mass, measuring 14 cm in largest diameter, occupying most of the right thoracic cavity (*Figure 2A*). The tumor showing a heterogeneous nature compressed the right lung parenchyma, but it had not become totally atelectatic. There was no prominent

evidence of local invasion into neighboring organs. However, the mass compressed the right atrium and inferior vena cava (*Figure 2A*).

Preparation

The decision was made to remove the tumor. Left decubitus position was simulated before surgery to anticipate the mass effect on the inferior vena cava and right atrium. Fortunately, the patient had stable vital signs and did not complain of any other symptoms. A single lumen endotracheal tube with endobronchial blocker was prepared for single-lung ventilation. Forestalling the possibility of adhesions or invasions to the mediastinal organs or lungs, extracorporeal membrane oxygenation (ECMO) was utilized. A central line (6 Fr) via the internal jugular vein and two peripheral venous catheters (20 gauge) were prepared for unexpected bleeding or urgent intravenous medication. The vital signs were not changed after anesthesia, and surgery was performed with no extraordinary events.

Approach and pitfall

We selected the sixth intercostal space for our surgical approach. The mass seemed to have developed from the thymus or a thymus-neighboring organ based on comparison of the old and new chest X-rays (*Figure 1A,B*). Based on this finding, the fourth or fifth intercostal space would have been optimal for identifying the origin of the mass.

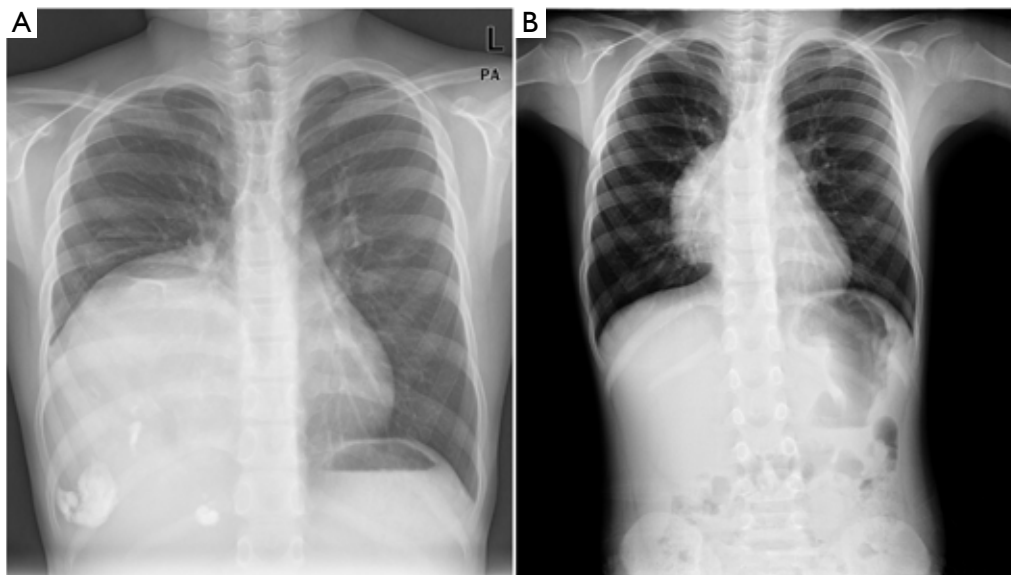


Figure 1 (A) Preoperative chest PA radiography; (B) chest radiography performed 3 years ago.

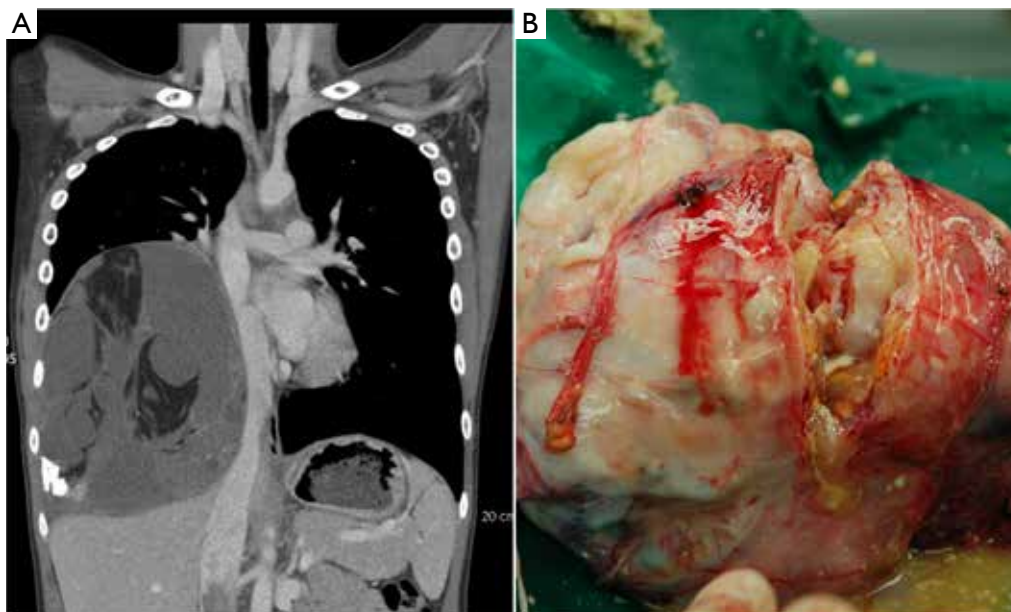


Figure 2 (A) The huge mass compressing the Inferior Vene Cava; (B) gross features of huge, firm mass.

However, the mass had occupied the end of the diaphragm and the costophrenic angle, and we could not guarantee absence of invasion or adhesion around the diaphragm space. Therefore, to anticipate dissection of the lower right thorax area, the sixth intercostal space was selected and easily widened without rib resection. There was no pleural adhesion or effusion. The mass was determined

to have originated from the thymus and was attached along the side of the phrenic nerve. Phrenic nerve sparing is important to preserve lung functions, especially in young patients. Thermal instrument use was avoided and meticulous dissection with Metzenbaum scissors was performed in order to not injure the nerve. Although there was no adhesion between the parietal pleura and the mass,

a fibrous band and adhesion was observed between the pericardial space and the mass. Finger palpation and blunt dissection were used because direct visualization was not possible. Tumor punctation could have provided additional information and simplified the surgery, especially if the tumor had been cystic. However, the outer surface was not cystic and was difficult to aspirate, so tumor punctation was not performed. After surgery, the lung was expanded to fill the space even if long term compression by the mass. The patient recovered without problems, and the chest tube was removed on postoperative day 3. The patient was discharged without complications. The pathological examination revealed a benign mature teratoma containing hair, teeth, and other sebaceous material (*Figure 2B*). The patient showed stable vital signs and normal chest X-ray in the outpatient clinic.

Discussion

Posterolateral thoracotomy was inevitable in this case. If the surgery had been performed when the mass was small, some minimally invasive surgical techniques including video-assisted thoracoscopic surgery or robotic surgery could have been utilized (3,4). However, by the time of presentation to our hospital, the mass had grown to a large size that prevented use of the technique. Median sternotomy with anterior thoracotomy was applied in a similar case (2). However, thoracotomy without a second incision was sufficient in this case, possibly due to the absence of tight adhesion or invasion between the mass and pleura. The flexible intercostal space of the 11-year-old boy also made this technique possible. In fact, rib resection or additional intercostal incision was not required even for extraction of the mass. Moreover, the patient did not complain of postoperative chest pain except tolerable discomfort.

Meticulous preoperative preparation might be also inevitable in such cases. Teratoma patients typically do not complain of major symptoms regardless of the size of the mass; however, the mass effect can be serious (2,5,6). In addition, surgery may be difficult in some cases (5,7). Therefore, preoperative simulation of the surgical position,

application of a central catheter, and even ECMO should be considered. A meticulous surgical technique is also imperative so as to not injure a mediastinal structure such as the phrenic nerve, vagus nerve, or hilar structures. Decisive dissection with finger palpation is required because direct visualization of all entire mass is sometimes impossible, especially with large masses.

In conclusion, resection of a very large mediastinal mass occupying the right hemithorax via posterolateral thoracotomy was performed in an 11-year-old boy. Our meticulous preoperative preparation and surgical technique were effective and resulted in no postoperative complications and favorable recovery.

Acknowledgements

Disclosure: The authors declare no conflict of interest.

References

1. Duwe BV, Sterman DH, Musani AI. Tumors of the mediastinum. *Chest* 2005;128:2893-909.
2. Yokoyama Y, Chen F, Date H. Surgical resection of a giant mediastinal teratoma occupying the entire left hemithorax. *Gen Thorac Cardiovasc Surg* 2013. [Epub ahead of print].
3. Melfi F, Fanucchi O, Davini F, et al. Ten-year experience of mediastinal robotic surgery in a single referral centre. *Eur J Cardiothorac Surg* 2012;41:847-51.
4. Rothermel L, Gilkeson R, Markowitz AH, et al. Thoracoscopic resection of a giant teratoma compressing the right heart. *Interact Cardiovasc Thorac Surg* 2013;17:594-7.
5. Zisis C, Rontogianni D, Stratakos G, et al. Teratoma occupying the left hemithorax. *World J Surg Oncol* 2005;3:76.
6. Avci A, Eren S. Life-threatening giant mediastinal cystic teratoma in a 4-month-old male baby. *Gen Thorac Cardiovasc Surg* 2009;57:389-91.
7. Miyazawa M, Yoshida K, Komatsu K, et al. Mediastinal mature teratoma with rupture into pleural cavity due to blunt trauma. *Ann Thorac Surg* 2012;93:990-2.

Cite this article as: Kim D, Kim SW, Hong JM. Rapid growing huge teratoma: complete surgical resection. *J Thorac Dis* 2014;6(10):E217-E219. doi: 10.3978/j.issn.2072-1439.2014.08.05

The challenging management of lung choriocarcinoma

Lasha Gvinianidze¹, Nikolaos Panagiotopoulos¹, Wen Ling Woo¹, Elaine Borg², David Lawrence¹

¹Department of Cardiothoracic Surgery, The Heart Hospital, University College London Hospitals (UCLH), London, UK; ²Department of Histopathology, University College London Hospitals (UCLH), London, UK

Correspondence to: Dr. Lasha Gvinianidze. Department of Cardiothoracic Surgery, The Heart Hospital, University College London Hospitals (UCLH), 16-18 Westmoreland Street, London W1G 8PH, UK. Email: lasha.gvinianidze@nhs.net.

Abstract: The purpose of this paper is to highlight the existence and the management of lung choriocarcinoma (CCA), a rare category of lung tumors. We present a 42-year-old female that presented to our department with a PET positive lesion in the left upper lobe and a history of pregnancy 6 months prior to onset of symptoms. CT guided biopsy was inconclusive for diagnosis and the patient underwent a left thoracotomy and lingula sparing upper lobectomy. Histology revealed CCA of the lung and subsequently blood results confirmed the elevated b-HCG. CCA of the lung is a clinical entity that should be considered in the differential diagnosis of lung lesions in women after pregnancy.

Keywords: Choriocarcinoma (CCA); lung metastases; pregnancy

Submitted Apr 28, 2014. Accepted for publication Aug 24, 2014.

doi: 10.3978/j.issn.2072-1439.2014.09.18

View this article at: <http://dx.doi.org/10.3978/j.issn.2072-1439.2014.09.18>

Introduction

As part of the group of pregnancy related tumors, choriocarcinoma (CCA) is a trophoblastic neoplasm arising from placenta with secondary haematogenous spread into lungs, brain, liver, kidneys, intestine, pelvis and vagina. It is characterized by a fast course with reasonably satisfactory prognosis. Symptoms can vary from cough, shortness of breath and haemoptysis to menorrhagia, gastrointestinal bleed and devastating neurological deterioration depending on the site of invasion of the metastatic disease. It is associated with notable and sometimes soaring levels of serum b-HCG. In addition to chemotherapy, surgical intervention would sometimes be indicated especially in sizeable distant lesions resistant to chemotherapy.

Case report

A 42-year-old female school teacher presented to our department with recent onset of cough, shortness of breath on physical exertion and haemoptysis. She had a smoking history of ten cigarettes per day for the last 15 years and a recent pregnancy giving birth to a healthy girl 6 months prior to onset of symptoms. Sputum sample was positive

for blood but negative for growth of microorganisms. CXR demonstrated an isolated left upper lobe lung lesion (*Figure 1*), confirmed on subsequent CT scan of the chest. A PET CT image revealed mild metabolic activity within the lung lesion (*Figure 2*). A CT guided biopsy of the lesion was inconclusive and the patient underwent a left thoracotomy with lingula sparing upper lobectomy and systematic lymph node dissection. The postoperative course was complicated by chylothorax that was treated conservatively with octreotide and a low fat diet. Histology report was extremely interesting demonstrating largely ischemic, ill-defined necrotic tumor with variable cellular component ranging from giant, irregular and symplastic cells with multiple hyperchromatic nuclei to the other, smaller and rounder cells with clear cytoplasm, well defined borders, central hyperchromatic nuclei and abundant atypical mitosis. The above represented syncytia and cytotrophoblastic cells, respectively and were strongly suggestive of the diagnosis of metastatic CCA possibly arising from a primary gestational endometrial carcinoma especially on the background of the recent pregnancy. Raised serum BHCG levels (3,200 UI/L) further confirmed the diagnosis. Further investigation from the gynaecology team including transvaginal ultrasound was negative for a lower



Figure 1 Chest X-ray demonstrating the lesion in the left upper lobe.



Figure 2 PET CT. Mild metabolic activity within the lung lesion.

abdominal or pelvic mass. At this point, she developed the loss of peripheral vision and the subsequent MRI scan of the brain showed 2 mm lesion in the brain. The neurosurgical opinion was sought that concluded no surgical intervention due to a very small lesion and the patient was commenced on the combined chemotherapy (low dose etoposide and cisplatin initially and EMA/CO on week 2). Patient underwent three courses of chemotherapy treatment with duration of 6 weeks resulting in a complete resolution of the physical symptoms and normalization of the BHCG serum levels. A repeat PET CT scan was negative and she was discharged home with a 6-month follow-up outpatient appointment and 2 weekly BHCG level monitoring by the GP in the community.

Discussion

Gestational trophoblastic diseases (GTD), as a broad term encompassing both benign and malignant growths arising from products of conception in the uterus, may be classified as hidatidiform moles (HM) which contain complete and partial HM and gestational trophoblastic neoplasia comprising invasive mole, CCA, placental site trophoblastic tumor (PSTT) and epithelioid trophoblastic tumor (ETT) (1,2). The reported incidence of GTD varies widely worldwide, from a low of 23 per 100,000 pregnancies (Paraguay) to a high of 1,299 per 100,000 pregnancies (Indonesia) (2). However, at least part of this variability is caused by differences in diagnostic criteria and reporting. The reported incidence in the United States is about 110 to 120 per 100,000 pregnancies. Some textbooks speculate more generalized idea that in Europe and North America the incidence of CCA is higher ranging from 1 in 40,000 pregnancies to 9.3 in 40,000 in South East Asia and Japan (3).

Variety of the risk factors have been implicated by different studies ranging from smoking, exogenous hormones and low body mass to associations between different maternal and paternal blood groups, genetic and environmental factors. However, on reviewing the modern literature, the most commonly described predisposing factors seem to be pregnancy, previous abortions or ectopic pregnancies with the biggest of them all being previous molar pregnancy and an early or late maternal age (2). Nevertheless, early identification of the high risk groups and decision for giving prophylactic chemotherapy remains a challenge as there is no clear cut indication for testing individuals extensively without presence of significant symptoms.

Immunohistochemical markers can further confirm the diagnosis of CCA with tumors staining strongly for HCG and inhibin alpha in the trophoblast, human placental lactogen (HPL) and inhibin alpha in intermediate trophoblast, and cytokeratin in all trophoblast cells (4). Approximately 75% of the CCA demonstrate distant body metastasis on diagnosis most commonly to lungs and brain.

The most commonly referred classifying and staging tool for GTD appears to be the WHO modifying scoring system adapted by FIGO anatomical staging (*Tables 1,2*) (5).

In our example, modified WHO score was 14, FIGO stage IV putting the patient in an exceptionally high risk. Ordinarily, in similar circumstances, treatment with polychemotherapy must be commenced with an immediate effect. There are no randomized trials comparing regimens in common use to establish superiority of one

Scores	0	1	2	4
Age	<40	>40	–	–
Antecedent pregnancy	Mole	Abortion	Term	–
Interval from pregnancy	<4 months	4-6 months	7-12 months	>12 months
Pretreatment serum HCG (IU/L)	<103	103-104	104-105	>105
Largest tumor size including uterus	<3 cm	3-4 cm	5 cm or more	–
Site of metastasis	Lung	Spleen, kidney	GI system	Liver, brain
Number of metastasis	–	1-4	5-8	>8
Previously failed chemotherapy	–	–	Single drug	2 or more drugs

I	Disease confined to uterus
II	GTN extending outside of the uterus but limited to the genital structures
III	GTN extends to the lungs with or without genital involvement
IV	Extension to the other sites of metastasis (brain, kidneys, liver etc.)

chemotherapeutic agent over another. Therefore, literature does not permit firm conclusions about the best therapeutic regimen (6). EMA/CO (etoposide, methotrexate and dactinomycin/cyclophosphamide and vincristine) is the most commonly used regimens (7,8). Concomitantly, vigorous serum BHCG level control must follow and close observation for potential symptoms to ensure initially falling, and then normal levels of HCG and possible need for surgical intervention in the event of debilitating recurrent metastatic disease resistant to chemotherapy.

All in all, it can be concluded that, all women post pregnancy and especially with the presence of significant risk factors (i.e., previous abortions, ectopic pregnancy, molar pregnancy, age more than 35) presenting with hemoptysis must be carefully worked up for CCA, or at the least it should be one of the main differential diagnosis.

Acknowledgements

Disclosure: The authors declare no conflict of interest.

References

1. Ngan HY, Kohorn EI, Cole LA, et al. Trophoblastic disease. *Int J Gynaecol Obstet* 2012;119:S130-6.
2. Altieri A, Franceschi S, Ferlay J, et al. Epidemiology and aetiology of gestational trophoblastic diseases. *Lancet Oncol* 2003;4:670-8.
3. Principles and practice of gynecologic oncology. In: Barakat RR, Berchuck A, Markman M, et al. eds. 6th Edition. Epidemiology of gynecologic cancers. Demographic patterns. Host Factors. Chapter 1:21.
4. Principles and practice of gynecologic oncology. In: Barakat RR, Berchuck A, Markman M, et al. eds. 6th Edition. Gestational trophoblastic disease: Molar pregnancy. Chapter 27:889-92.
5. FIGO Committee on Gynecologic Oncology. Current FIGO staging for cancer of the vagina, fallopian tube, ovary, and gestational trophoblastic neoplasia. *Int J Gynaecol Obstet* 2009;105:3-4.
6. Deng L, Yan X, Zhang J, et al. Combination chemotherapy for high-risk gestational trophoblastic tumour. *Cochrane Database Syst Rev* 2009;(2):CD005196.
7. Bower M, Newlands ES, Holden L, et al. EMA/CO for high-risk gestational trophoblastic tumors: results from a cohort of 272 patients. *J Clin Oncol* 1997;15:2636-43.
8. Lurain JR, Singh DK, Schink JC. Management of metastatic high-risk gestational trophoblastic neoplasia: FIGO stages II-IV: risk factor score > or = 7. *J Reprod Med* 2010;55:199-207.

Cite this article as: Gvinianidze L, Panagiotopoulos N, Woo WL, Borg E, Lawrence D. The challenging management of lung choriocarcinoma. *J Thorac Dis* 2014;6(10):E220-E222. doi: 10.3978/j.issn.2072-1439.2014.09.18

Primary mucoepidermoid carcinoma of the thymus presenting with myasthenia gravis

Wen Ling Woo¹, Nikolaos Panagiotopoulos¹, Lasha Gvinianidze¹, Ian Proctor², David Lawrence¹

¹Department of Cardiothoracic Surgery, The Heart Hospital, University College London Hospitals (UCLH), London, UK; ²Department of Histopathology, University College London Hospitals (UCLH), London, UK

Correspondence to: Dr. Lasha Gvinianidze. Department of Cardiothoracic Surgery, The Heart Hospital, University College London Hospitals (UCLH), 16-18 Westmoreland Street, London W1G 8PH, UK. Email: lasha.gvinianidze@nhs.net.

Abstract: Mucoepidermoid carcinoma (MEC) of the thymus is a rare malignant neoplasm of the anterior mediastinum. There are less than 30 cases described in the English literature. We report a case of a 47-year-old lady who presented with myasthenia gravis and was found to have a well-circumscribed anterior mediastinal mass in her medical work-up. This mass was surgically resected and subsequently found to be a primary MEC of the thymus. This is the first reported case of thymic MEC with concurrent myasthenia gravis. Her myasthenia symptoms have persisted following complete surgical resection of her tumour.

Keywords: Mucoepidermoid carcinoma (MEC); thymus; myasthenia gravis

Submitted Apr 28, 2014. Accepted for publication Aug 18, 2014.

doi: 10.3978/j.issn.2072-1439.2014.09.19

View this article at: <http://dx.doi.org/10.3978/j.issn.2072-1439.2014.09.19>

Case presentation

A 47-year-old female was referred for surgical resection of an anterior mediastinal mass which was found incidentally on a computed tomography pulmonary angiogram (CTPA). She presented with worsening shortness of breath and fatigue whilst under investigation for autoimmune hepatitis under the hepatologist. As part of the medical work up, she underwent a CTPA which ruled out a pulmonary embolus, but confirmed the presence of a well-rounded anterior mediastinal mass which was largely homogenous (*Figure 1*). In view of her ongoing symptoms of fatigue and breathlessness, she was also reviewed by the neurologists and was subsequently diagnosed with myasthenia gravis, confirmed on electromyography (EMG) and blood tests showing elevated titres of acetylcholine receptor antibodies.

She underwent surgical resection of her anterior mediastinal mass via median sternotomy without immediate complication. She had an uneventful recovery and was discharged on the sixth post-operative day.

Histological analysis revealed a 31 mm diameter unencapsulated tumor with an infiltrative margin (*Figure 2*). There was evidence of sheets and trabeculae of bland

squamous cells, large polygonal and columnar cells with eosinophilic cytoplasm, round nuclei with vascular chromatin and prominent nucleoli. Nuclear inclusions were present in occasional cells. Histological and immunochemical analysis were consistent with a well-differentiated mucoepidermoid carcinoma (MEC) (*Figure 3*). Background tissue was mostly atrophic with no evidence of a thymoma.

The patient then underwent magnetic resonance imaging (MRI), which excluded a head and neck primary, confirming a primary MEC of the thymus. She continues to have symptoms of myasthenia gravis which are well controlled with her pre-operative medication. The patient did not require any chemotherapy or radiotherapy post-operatively and remained well after the operation. She has been scheduled for a surveillance CT scan in 9 months.

Discussion

MEC are most commonly found in salivary glands as first described by Stewart *et al.* in 1945 (1), there has since been reports of these neoplasms arising in other sites including larynx, bronchus and oesophagus. Primary MEC of the

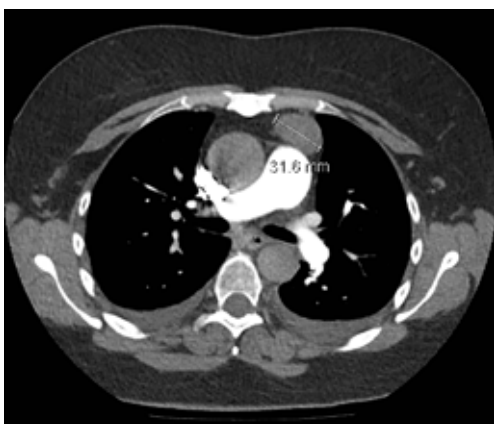


Figure 1 Computed tomography (CT) scan of the chest demonstrating the 31 mm lesion in the anterior mediastinum.

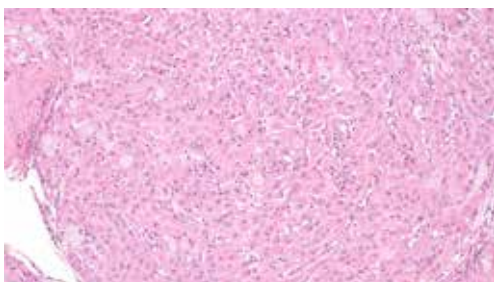


Figure 2 Mucoepidermoid carcinoma comprising a large epidermoid cells, intermediate cells and mucous cells seen with hematoxylin and eosin (H&E) stain at $\times 200$ magnification.

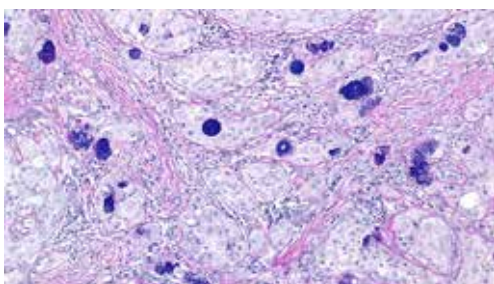


Figure 3 The presence of mucous cells are confirmed on staining with alcian blue-diastase periodic acid Schiff (AB-DPAS) stain at $\times 200$ magnification.

thymus is a rare malignant epithelial neoplasm and less than 30 cases have been reported in the literature (2-4). There are no apparent associations with other conditions or paraneoplastic syndromes. There has been only one

reported case of combined MEC of the thymus and thymoma with a background of myasthenia gravis (2), that patient's symptoms of myasthenia gravis resolved completely following resection of his combined thymic carcinoma and thymoma. There has been no reported case of MEC of the thymus alone with concurrent myasthenia gravis. It is uncertain why our patient has myasthenia gravis and if it is related to her thymic malignancy, or if it is purely a coincidence that she had a thymic mass and her myasthenia gravis may be related to other underlying autoimmune processes in view of her ongoing autoimmune hepatitis. In view of the rare nature of this condition, it appears difficult to draw any conclusive evidence at present.

Patients with MEC of the thymus commonly present with respiratory symptoms including exertional dyspnea and chest pain, others remain asymptomatic and are incidentally found to have an anterior mediastinal mass on routine chest radiography. Radiologically, MEC of the thymus are often well-circumscribed, homogenous masses in the anterior mediastinum with multi-locular cystic structures observed on computed tomography (CT) scans of the thorax (3). This can vary depending on tumor grade and there have been cases where local invasion to adjacent structures are observed (4,5). These tumors are characterized histologically by squamoid mucin-producing cells with intermediate type cells. Histological analysis also revealed that these tumors vary from well- to poorly-differentiated. Poorly-differentiated, high grade tumors have greater propensity for local invasion and distant metastasis and often have rapid progression of the disease despite aggressive subsequent treatment with chemotherapy resulting in mortality.

The Masaoka staging system for thymomas is also commonly used for thymic carcinomas. The stages are as follows: stage 1, grossly and microscopically encapsulated mass; stage 2, invasion of mass beyond thymic capsule; stage 3, macroscopic invasion of neighbouring organs; stage 4a, pleural or pericardial dissemination; stage 4b, haematogenous or lymphatic dissemination. This is often useful in determining prognosis as higher stage patients have much poorer 5-year survival rates.

Surgical resection is the mainstay of treatment for low-grade tumors, some requiring radiotherapy to prevent local recurrence or disease progression. In cases where complete surgical resection is not possible, treatment with local radiotherapy appears to have a positive prognosis for low-grade disease as well (6). There is also suggestion in the literature that thymic tumors may be chemosensitive

for high grade disease (7). However, as these tumors are fairly uncommon and vary greatly between cases, there is no established treatment regimen that has proven effective beyond anecdotal evidence.

Although extremely rare, MEC of the thymus should be considered in a list of differential diagnosis for anterior mediastinal masses. As it is difficult to achieve a diagnosis based on radiological findings alone, early surgical excision is recommended, not only to achieve histological diagnosis but also to prevent local invasion or further disease progression.

Acknowledgements

Disclosure: The authors declare no conflict of interest.

References

1. Stewart FW, Foote FW, Becker WF. Muco-Epidermoid Tumors of Salivary Glands. *Ann Surg* 1945;122:820-44.
2. Wu SG, Li Y, Li B, et al. Unusual combined thymic mucoepidermoid carcinoma and thymoma: a case report and review of literature. *Diagn Pathol* 2014;9:8.
3. Yasuda M, Yasukawa T, Ozaki D, et al. Mucoepidermoid carcinoma of the thymus. *Jpn J Thorac Cardiovasc Surg* 2006;54:23-6.
4. Nonaka D, Klimstra D, Rosai J. Thymic mucoepidermoid carcinomas: a clinicopathologic study of 10 cases and review of the literature. *Am J Surg Pathol* 2004;28:1526-31.
5. Kim GD, Kim HW, Oh JT, et al. Mucoepidermoid carcinoma of the thymus: a case report. *J Korean Med Sci* 2004;19:601-3.
6. Stefanou D, Goussia AC, Arkoumani E, et al. Mucoepidermoid carcinoma of the thymus: a case presentation and a literature review. *Pathol Res Pract* 2004;200:567-73.
7. Ogawa K, Toita T, Uno T, et al. Treatment and prognosis of thymic carcinoma: a retrospective analysis of 40 cases. *Cancer* 2002;94:3115-9.

Cite this article as: Woo WL, Panagiotopoulos N, Gvinianidze L, Proctor I, Lawrence D. Primary mucoepidermoid carcinoma of the thymus presenting with myasthenia gravis. *J Thorac Dis* 2014;6(10):E223-E225. doi: 10.3978/j.issn.2072-1439.2014.09.19

Right ventricle inflow obstructing mass proven to be a synovial sarcoma

Guang-Won Seo¹, Sang-Hoon Seol¹, Pil-Sang Song¹, Dong-Kie Kim¹, Ki-Hun Kim¹, Woo Gyeong Kim², Yeon Mee Kim², Sun Ju Oh³, Hee-Jae Jun⁴, Doo-Il Kim¹

¹Division of Cardiology, Department of Internal Medicine, ²Department of Pathology, Haeundae Paik Hospital, Inje University College of Medicine, Busan, Korea; ³Department of Pathology, Asan Medical Center, Seoul, Korea; ⁴Division of Thoracic and Cardiovascular Surgery, Haeundae Paik Hospital, Inje University College of Medicine, Busan, Korea

Correspondence to: Doo-Il Kim, M.D. Department of Medicine, Inje University College of Medicine, Haeundae Paik Hospital, 1435 Jwa-dong, Haeundae-gu, Busan, 612-030, Korea. Email: jo1216@inje.ac.kr.

Abstract: Soft tissue sarcoma is the most common malignant cardiac tumor. The chief modes of presentation are embolization, obstruction, and arrhythmogenesis. We describe an unusual case of a 27-year-old man who presented with nausea and dyspnea on exertion. Transthoracic echocardiography and computed tomography revealed a huge mass in the right heart that extended through the inferior vena cava and right renal vein to the right kidney. The cardiac mass was resected, and an immunohistochemical analysis revealed it to be a *TLE1*-positive synovial sarcoma. After surgery, the patient received serial adjuvant chemotherapy. We herein describe the case with a brief review.

Keywords: Cardiac tumor; cardiac mass; synovial sarcoma (SS); *SYT-SSX*; *TLE1*

Submitted Jun 06, 2014. Accepted for publication Aug 25, 2014.

doi: 10.3978/j.issn.2072-1439.2014.09.21

View this article at: <http://dx.doi.org/10.3978/j.issn.2072-1439.2014.09.21>

Introduction

Approximately one quarter of all cardiac tumors exhibit some features of malignancy. The majority of malignant primary cardiac tumors are sarcomas, usually angiosarcomas or rhabdomyosarcomas (1). Synovial sarcoma (SS) is a clinically and histomorphologically well-defined soft tissue tumor that is extremely uncommon in joint cavities and has no apparent relation to synovial structures. SSs have been described at other unusual sites including the heart, pleura, kidney, prostate, liver, mediastinum, gastrointestinal tract, and peripheral nerve (2-7). A SS arising primarily from heart is uncommon and is usually identified at a late stage because of its nonspecific presentation and difficulty in obtaining a biopsy from this site. Complete surgical resection combined with chemoradiotherapy continues to remain the fundamental strategy for sarcoma management. This case describes our experiences with the presentation, diagnosis, and management of a patient with SS of the heart.

Case

A 27-year-old man presented with a 1-month history of dyspnea on exertion, nausea, general weakness, and palpitations. He had no remarkable medical or family history. Vital signs at the time of the first admission revealed temperature, 36.5 °C; respiration, 27/min; pulse, 110/min; and blood pressure, 120/80 mmHg. An examination showed a faint continuous murmur with clear breathing sounds and mild peripheral pitting edema on both legs. Initial laboratory findings showed elevated levels of serum bilirubin, 2.2 mg/dL; aspartate aminotransferase, 194 IU/L; alanine aminotransferase, 343 IU/L; creatinine, 1.49 mg/dL; and pro-brain natriuretic peptide, 3267.2 pg/mL with prolonged prothrombin time. A chest X-ray showed cardiomegaly and pleural effusion. Transthoracic echocardiography revealed a large mass in the right heart that nearly obstructed the right ventricle inflow tract during systole and a small 0.4 cm sized patent ductus arteriosus (*Figure 1*). Subsequent computed tomography showed a heterogenous enhancing tumor like

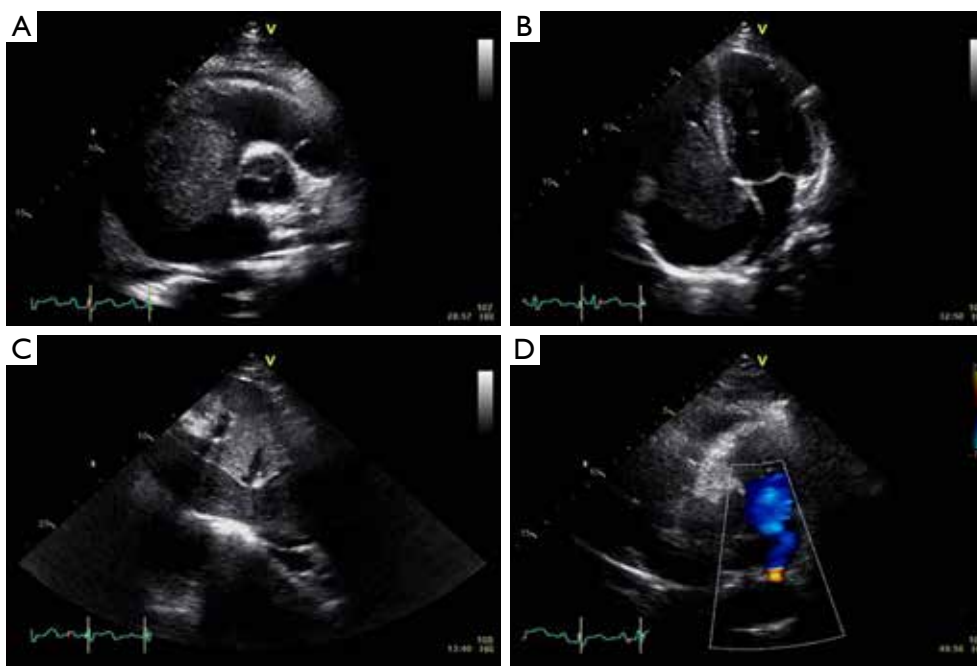


Figure 1 Transthoracic echocardiography shows a large mass in the right heart that is nearly obstructing the right ventricle inflow tract during systole and extending to the inferior vena cava (A-C). A small 0.4 cm sized patent ductus arteriosus (D).



Figure 2 Computed tomography shows heterogeneous enhancing tumor extending along the right ventricle to the upper pole of the right kidney.

lesion along the right ventricle, right atrium, inferior vena cava (IVC), right renal vein, and upper pole of the right kidney (Figure 2).

The decision was made to resect the mass for a definite diagnosis and to restore the right heart failure with congestive hepatopathy and nephropathy. Aggressive surgical management was done with radical nephrectomy, IVC mass excision, and intra-arterial tumor resection (Figure 3). The cardiac tumor was about 10.5 cm × 5.5 cm × 5.0 cm sized and connected to IVC mass without adhesion. There were no adhesion of the tumor at all and no lymph node enlargement, intra-atrial tumor was cut and removed from the near IVC and hepatic vein. From abdomen incision, after the incision of orifice of right renal vein that extend to the IVC, nephrectomy was done. The remained IVC tumor was removed totally.

Histological features revealed a monophasic SS, composed of fairly low uniform grade spindle cells. Immunohistochemical staining was positive for vimentin, C-kit, Bcl-2, and negative for cytokeratin (CK), smooth muscle actin, CD34, desmin, S100, CK7, and CK19. Transducin-like enhancer of split *TLE1* was positive with the characteristic t(X; 18) (p11.2; q11.2) translocation, the *SYT-SSX* fusion oncogene was not present (Figure 4).

The postoperative period was uneventful. He was discharged on postoperative day 10 by arrangement with an oncologist. He underwent four cycles of chemotherapy with

40 mg/m² of adriamycin and 5,000 mg/m² of ifosfamide. To date, he is alive with no significant clinical issues 5 months after primary surgery.

Discussion

Sarcomas are common between the third and fifth decades of life and the right atrium is the most frequently affected (1). They have a wide variety of morphologies due to their mesenchymal origin. The SS in this case was located from



Figure 3 Resected mass in right atrium.

the right ventricle to the right kidney. Except the kidney and adjacent large vessels, no definite adhesions or extensions were found. However the exact origin of this patient's SS is still uncertain because of the side of uncertified microvascular invasion and the possibility of a widely distributed origin. SS is typically an aggressive tumor, and survival is usually less than nine months, even with surgery and adjuvant chemoradiotherapy. As with all malignant tumors of the heart, the characteristics of a SS can be life-threatening because of obstructed intracardiac blood flow, interference with valve function, and rhythm disturbances, as well as pericardial tamponade resulting from local invasion (8). Because cardiac SSs are rare, prognostic factors are hard to ascertain, but younger age at diagnosis, absence of complex chromosomal abnormalities, and origin of the tumor from the pericardium seem to be favorable factors (9).

SSs have biphasic and monophasic histological patterns. The classic biphasic SS has mixed epithelial and spindle cell components, whereas the monophasic SS has only the spindle cell component. In most cases of biphasic SSs, the expression of both CK and vimentin is seen, and almost always at least one epithelial cell marker is expressed, although expression may be focal. In monophasic SS, tumor cells stain diffusely positive for vimentin and variably positive for epithelial

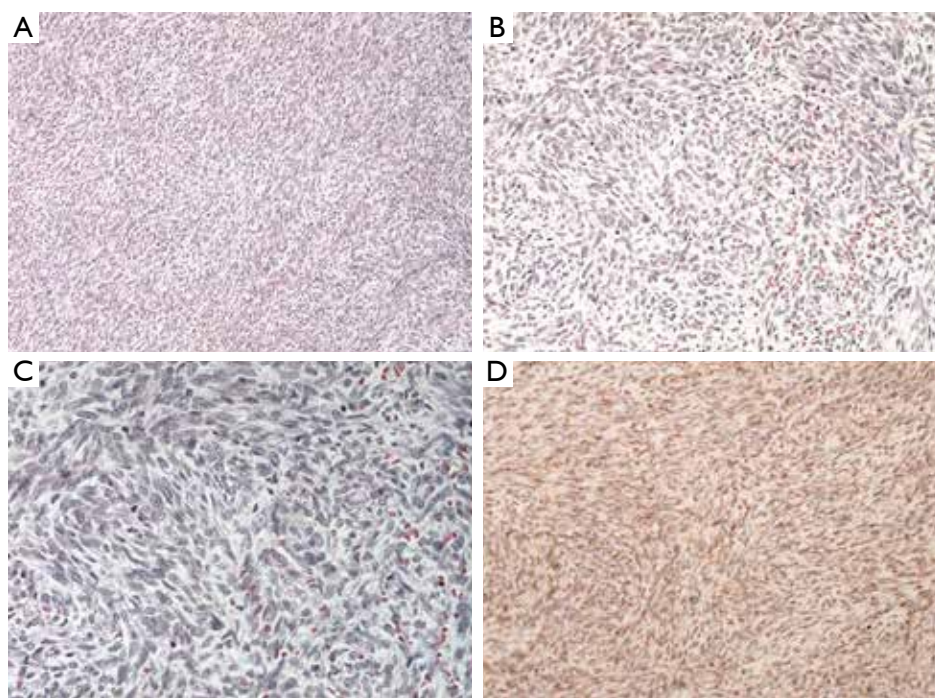


Figure 4 Solid and compact sheets of relatively well oriented plump spindle cells of uniform appearance with prominent nuclei [(A), (H&E, $\times 200$); (B), (H&E, $\times 400$); (C), (H&E, $\times 600$)]. Nuclear positivity for the transducing-like enhancer of split (TLE)1 antibody [(D), (IHC, $\times 200$)].

proteins. The hallmark of the SS diagnosis is detection of the translocated chromosome t(X; 18) (p11.2;q11.2), the *SYT-SSX* fusion oncogene, which is present in more than 90% of the SSs (10). *TLE1* is one of four TLE genes that encode human transcriptional repressors homologous to the *Drosophila* corepressor *groucho* (11). *TLE1* is a sensitive and specific immunohistochemical marker for SS, performing better than other known immunohistochemical markers, and can significantly aid in the pathologic diagnosis (12). We confirmed the diagnosis in this case using ancillary diagnostic methods such as cytogenetics and fluorescence *in situ* hybridization and validated that *TLE1* was positive even though the *SYT-SSX* fusion oncogene was negative.

Treatment for SS is a combination of surgical resection, radiotherapy, and chemotherapy. Radical resection is the mainstay of treatment, although complete resection is seldom possible. Adjuvant radiotherapy is usually recommended in cases of extensive resection of a large tumor or incomplete resection. Adjuvant chemotherapy is needed but no standard medical therapy exists due to the rarity of SS. Therefore, more aggressive and complete surgical resection allows the best chance for palliation and survival due to SS.

We herein reported a case of cardiac SS immunohistochemically confirmed by *TLE1* treated with surgical resection and adjuvant chemotherapy.

Acknowledgements

Disclosure: The authors declare no conflict of interest.

References

- Shapiro LM. Cardiac tumours: diagnosis and management. *Heart* 2001;85:218-22.
- Wang JG, Li NN. Primary cardiac synovial sarcoma. *Ann Thorac Surg* 2013;95:2202-9.
- Tuncer ON, Erbasan O, Golbasi I. Primary intravascular synovial sarcoma: case report. *Heart Surg Forum* 2012;15:E297-9.
- Sheu CC, Lin SF, Chiu CC, et al. Left atrial sarcoma mimicking obstructive pulmonary disease. *J Clin Oncol* 2007;25:1277-9.
- Kang MK, Cho KH, Lee YH, et al. Primary synovial sarcoma of the parietal pleura: a case report. *Korean J Thorac Cardiovasc Surg* 2013;46:159-61.
- Hussain S, Khan AA, Khan Q. Synovial sarcoma of the heart. *J Coll Physicians Surg Pak* 2012;22:723-5.
- de Zwaan C, Bekkers SC, van Garsse LA, et al. Primary monophasic mediastinal, cardiac and pericardial synovial sarcoma: a young man in distress. *Neth Heart J* 2007;15:226-8.
- Alsara O, Rayamajhi S, Ghanem F, et al. Primary cardiac pleomorphic sarcoma presenting as back pain in an 18-year-old man. *Tex Heart Inst J* 2013;40:339-42.
- Varma T, Adegboyega P. Primary cardiac synovial sarcoma. *Arch Pathol Lab Med* 2012;136:454-8.
- Sandberg AA, Bridge JA. Updates on the cytogenetics and molecular genetics of bone and soft tissue tumors. *Synovial sarcoma. Cancer Genet Cytogenet* 2002;133:1-23.
- Stifani S, Blaumueller CM, Redhead NJ, et al. Human homologs of a *Drosophila* Enhancer of split gene product define a novel family of nuclear proteins. *Nat Genet* 1992;2:119-27.
- Terry J, Saito T, Subramanian S, et al. *TLE1* as a diagnostic immunohistochemical marker for synovial sarcoma emerging from gene expression profiling studies. *Am J Surg Pathol* 2007;31:240-6.

Cite this article as: Seo GW, Seol SH, Song PS, Kim DK, Kim KH, Kim WG, Kim YM, Oh SJ, Jun HJ, Kim DI. Right ventricle inflow obstructing mass proven to be a synovial sarcoma. *J Thorac Dis* 2014;6(10):E226-E229. doi: 10.3978/j.issn.2072-1439.2014.09.21

Chondrosarcoma of the anterior chest wall: surgical resection and reconstruction with titanium mesh

Elçin Ersöz, Serdar Eyman, Levent Alpay, Mustafa Akyıl, Mustafa Vayvada, Deniz Gürer, Serkan Bayram, Çağatay Tezel

Department of Thoracic Surgery, Süreyyapaşa Training and Research Hospital, Istanbul, Turkey

Correspondence to: Çağatay Tezel. Associate Professor, Thoracic Surgery Department, Süreyyapaşa Göğüs Hastalıkları ve Göğüs Cerrahisi, Eğitim ve Araştırma Hastanesi, D blok Başbüyük Maltepe İstanbul, Turkey. Email: cagataytezel@hotmail.com.

Abstract: Primary malignant tumors of the chest wall are uncommon. Chondrosarcoma is the most common malignancy of the sternum. The current therapy for chondrosarcoma requires adequate surgical excision. A 52-year-old man presented with a lower-sternal mass. Thorax computed tomography (CT) revealed a well-lined, hypodense and round mass, which highly suggested the sarcoma of the chest wall. The tumor involved 1/3 distal part of the corpus sterni. Incisional biopsy of the mass was reported as chondrosarcoma. In order to obtain disease-free surgical margins, 1/3 distal part of the sternum with costochondral junctions was resected and reconstruction of anterior chest wall was performed with titanium mesh. The postoperative course was uneventful. The titanium mesh provided the essential rigidity and minimal elasticity over the surgical wound. Our findings show that this technique is adequate even for reconstructing extensive defects of the anterior chest wall.

Keywords: Chondrosarcoma; reconstruction; sternum; titanium mesh

Submitted Jul 27, 2013. Accepted for publication Sep 12, 2014.

doi: 10.3978/j.issn.2072-1439.2014.09.30

View this article at: <http://dx.doi.org/10.3978/j.issn.2072-1439.2014.09.30>

Background

Primary malignant tumors of the chest wall are a heterogeneous group of uncommon tumors developing from the bones, cartilages or the soft tissues (1). Chondrosarcoma is the most common primary malignancy of the sternum, and the successful treatment of choice includes en-bloc removal of the tumor with the surrounding tissue with a minimum clear margin of 2 to 6 cm (2,3). Reconstruction of an oversized defect can be difficult, and sometimes needs the use of a synthetic prosthesis. Hereby, our experience with titanium mesh reconstruction of a large anterior chest wall defect is presented.

Case presentation

A 52-year-old man admitted to our clinic with progressive pain and swelling on the anterior chest wall. Past medical history was unremarkable. Physical examination showed a large solid mass fixed to the sternum. Thorax computed

tomography (CT) demonstrated a hypodense 6×7 cm round mass located on the lower part of corpus sterni, with no sign of subcutaneous invasion radiologically (*Figure 1A*). Incisional biopsy revealed as chondrosarcoma. Positron emission tomography (PET-CT) scan demonstrated 66×46×74 mm mass originating from the 1/3 lower part of corpus sterni, with a fluorodeoxyglucose (FDG) maximum standard uptake value of 3.8, with no other sign of distant organ or lymphatic metastasis (*Figure 1B*).

The patient underwent an en-bloc resection of the lower half of sternum with approximately 4-5 cm of the 5th to 8th ribs, bilaterally. In order to reconstruct and recuperate the stability of the thoracic wall, a titanium mesh was placed and fixed to the edges of the remaining sternum and the ribs over a polypropylene mesh placed beneath, to protect the lung parenchyma from direct contact with the rigid titanium mesh (*Figure 2*). It was then covered with the pectoral muscle and the subcutaneous tissue. The postoperative course was uneventful, and the patient was

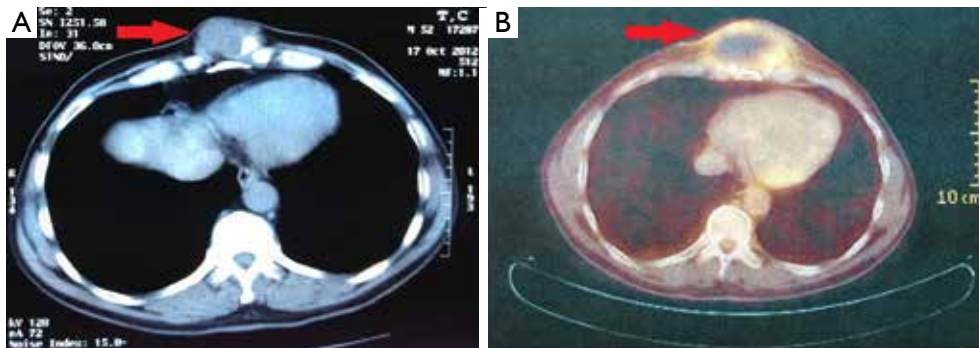


Figure 1 (A) Chest computed tomography (CT), showing 6x7 cm mass adjacent to the sternum; (B) positron emission tomography revealing intermediate metabolic activity in the mass, with the suspicion of bone/soft tissue malignancy.

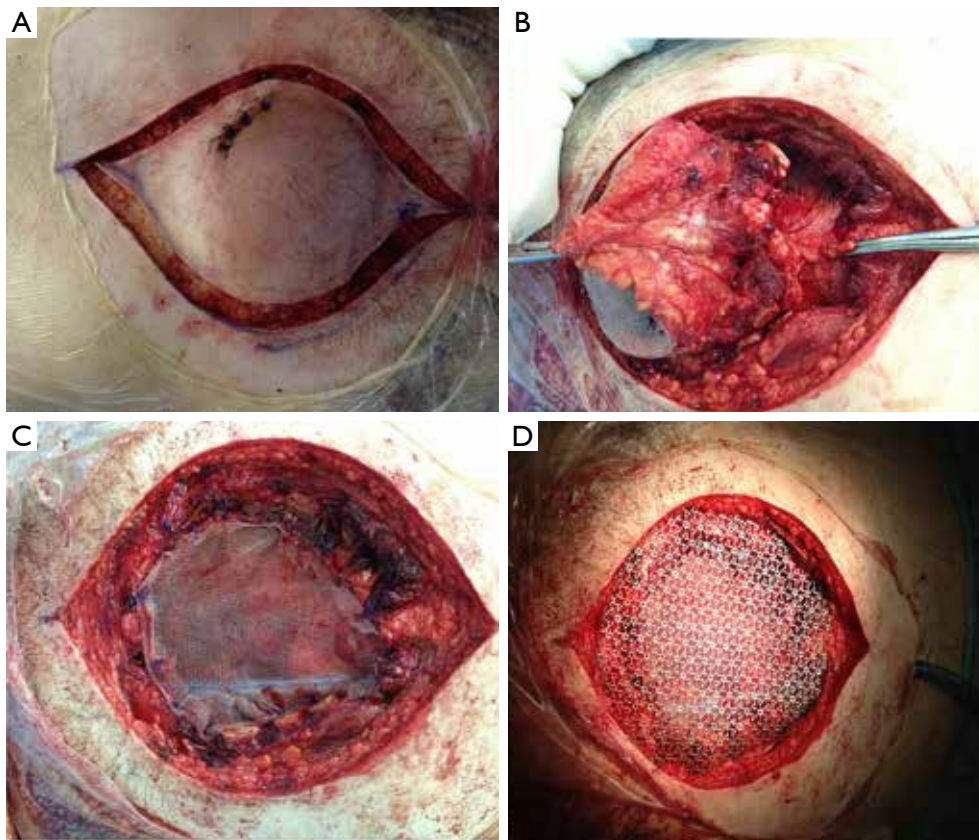


Figure 2 (A) Fish mouth wide skin incision of the tumor with previous incisional biopsy site; (B) En-bloc resection of lower-half of sternum and bilateral 5th to 8th ribs, with the involved superficial tissue; (C) parenchyma protective polypropylene mesh reconstruction under the titanium plates; (D) titanium plate coverage, with screws fixed over the remaining rib edges.

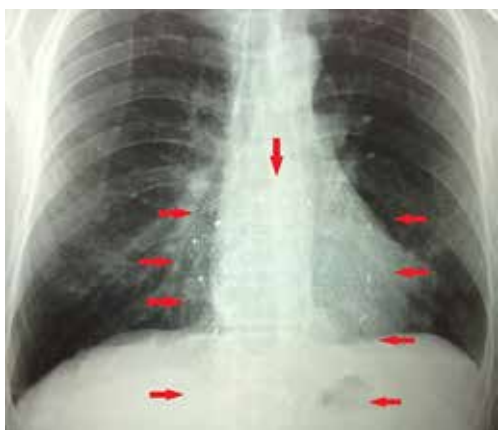


Figure 3 Post-operative chest X-ray, arrows showing the screwed mesh plate over the resection area.

discharged on the postoperative day 8, with mesh present in proper location on chest X-ray (*Figure 3*). He is still being followed-up on 37th month, asymptotically, without adjuvant chemo or radiotherapy.

Discussion

Tumors are rare, forge almost 0.5% to 1% of the primary bone tumors, with chondrosarcoma being the most common subtype. It mostly arises after the 6th decade of life, and has a slight male predominance (3,4). It is usually presented with a gradually growing, solid and fixed mass on the sternum, occasionally with concomitant chest pain, which is a sign of bad prognosis (3).

Chest wall resection and reconstruction procedures require adequate radical resection associated with the maintenance of chest stability, adequate lung function, and an acceptable cosmetic result (5).

Surgery is still accepted as the major treatment of primary malignant chest wall tumors, since they tend to be resistant to chemo or radiotherapy. The purpose of adequate radical surgery is removal of the tumor with a wide disease-free margin along with maintenance of chest wall stability. Inadequate tumor resection is associated with a high incidence of recurrence. Total sternectomy must be avoided if the sternum is not entirely involved. Subtotal resection is recommended, whenever possible, in order to partially preserve the chest wall stability (5,6).

The treatment of sternal tumors may be complicated because of anatomical proximity to vital neurovascular structures which can limit the surgical margins. The optimal

incision should be 2 to 6 cm from the margin of tumor, in order to minimize the risk of local recurrence (7).

Reconstruction is essential to maintain original respiratory functions and protect other mediastinal organs. These reconstruction techniques include pedicled skin and muscle flaps, free skin grafts, and autologous bone transplants. The choice of reconstruction technique depends on the extent and localization of the defect. If the defect is less than 5cm, then the skeletal reconstruction is not necessary. Muscle flap reconstruction may be used alone in cases with sole upper-half sternal resections. Resection of the lower sternum requires synthetic materials to stabilize the rigid chest wall, in order to protect the vital organs (2-4,8).

The prosthetic material used during the reconstruction should have sufficient rigidity to prevent paradoxical chest motion, must have adequate radiolucency to allow radiographic follow-up, and must be a biocompatible structure which allows growth of fibrous tissue, without causing any infection (1,4). It is not always possible to use autologous tissue for reconstruction of large chest wall defects because of possible surface area limitation, lack of adequate rigidity, and extended operation time. Surgical prosthetic materials may be preferred for thoracic reconstruction, but they are either too weak to provide sufficient stability, or excessively rigid with risk of erosion of neighboring structures, or causing restriction in the movements of the chest. Polypropylene mesh (Marlex[®]) is usually used for the reconstruction of large defects in the chest wall. It is relatively cheap and has a high affinity for tissue growth, but its lack of rigidity in patients with extensive defects may result in paradoxical motion of the chest wall (9).

Titanium mesh is more rigid, flexible, biocompatible and osteoconductive than polypropylene mesh, but it may as well be complicated by infection or fragmentation of the graft. It is quite rigid like a methyl methacrylate mesh, but relatively easier to shape, minimally elastic, less opaque on radiological examinations, and incorporates well with adjacent soft tissues, therefore cause minimal trauma (10). Shorter operation time through fast and easy instillation with no need for additional autologous tissue transplantation is other advantages of the titanium mesh.

Hereby, we described a rare chondrosarcoma case that has undergone subtotal sternal resection and reconstruction of the sternum. Reconstruction of large defects on the anterior chest wall with titanium mesh can rapidly, safely, and effectively be performed on patients with large malignant lesions of the sternum, with ideal rigidity and biocompatibility.

Acknowledgements

The written informed consent was obtained from the patient for publication of this case report and all accompanying images. A copy of the written consent is available for review by the Editor-in-chief of this journal.

Disclosure: The authors declare no conflict of interest.

References

1. Gonfiotti A, Santini PF, Campanacci D, et al. Malignant primary chest-wall tumours: techniques of reconstruction and survival. *Eur J Cardiothorac Surg* 2010;38:39-45.
2. Nosotti M, Rosso L, Mendogni P, et al. Sternal reconstruction for unusual chondrosarcoma: innovative technique. *J Cardiothorac Surg* 2012;7:40.
3. Pairolero PC. Chest wall tumors. In: Shields TW, LoCicero J 3rd, Ponn RB. eds. *General thoracic surg.* 5th ed. Philadelphia, Lippincott Williams & Wilkins, 2000;589-98.
4. Koto K, Sakabe T, Horie N, et al. Chondrosarcoma from the sternum: reconstruction with titanium mesh and a transverse rectus abdominis myocutaneous flap after subtotal sternal excision. *Med Sci Monit* 2012;18:CS77-81.
5. Incarbone M, Pastorino U. Surgical treatment of chest wall tumors. *World J Surg* 2001;25:218-30.
6. Chapelier AR, Missana MC, Couturaud B, et al. Sternal resection and reconstruction for primary malignant tumors. *Ann Thorac Surg* 2004;77:1001-6; discussion 1006-7.
7. Martini N, Huvos AG, Burt ME, et al. Predictors of survival in malignant tumors of the sternum. *J Thorac Cardiovasc Surg* 1996;111:96-105; discussion 105-6.
8. Carbognani P, Vagliasindi A, Costa P, et al. Surgical treatment of primary and metastatic sternal tumours. *J Cardiovasc Surg (Torino)* 2001;42:411-4.
9. Matsumoto K, Sano I, Nakamura A, et al. Anterior chest wall reconstruction with titanium plate sandwiched between two polypropylene sheets. *Gen Thorac Cardiovasc Surg* 2012;60:590-2.
10. Horio H, Ohtsuka T, Kubota Y, et al. Large chest wall reconstruction using titanium micromesh and a pedicled latissimus dorsi musculocutaneous flap: report of a case. *Surg Today* 2005;35:73-5.

Cite this article as: Ersöz E, Evman S, Alpay L, Akyıl M, Vayvada M, Güreş D, Bayram S, Tezel Ç. Chondrosarcoma of the anterior chest wall: surgical resection and reconstruction with titanium mesh. *J Thorac Dis* 2014;6(10):E230-E233. doi: 10.3978/j.issn.2072-1439.2014.09.30

Large cell carcinoma on the bullous wall detected in a specimen from a patient with spontaneous pneumothorax: report of a case

Toshinari Ema

Department of Thoracic Surgery, Meirikai Central Medical Center, 3-2-11 Higasijyujo Kita-Ku, Tokyo, 174-0051, Japan

Correspondence to: Toshinari Ema. Department of Thoracic Surgery, Meirikai Central Medical Center, 3-2-11 Higasijyujo Kita-Ku, Tokyo, 174-0051, Japan. Email: toshinariema09@yahoo.co.jp.

Abstract: Bullous emphysema has been proven to be an important risk factor for lung cancer. Some reports have described pneumothorax caused by rupture of an emphysematous bulla, following which cancer is found in the resected specimen. A 72-year-old male patient was referred to our hospital because of dyspnea and high fever. Chest radiography and computed tomography (CT) revealed right pneumothorax and emphysematous bullae. There was also effusion in the bullae and thoracic cavity. Based on the diagnosis of pneumothorax and a lung infection associated with bullous emphysema, we resected the bullae. Pathological examination of the specimen revealed a mass and large cell carcinoma.

Keywords: Pneumothorax; primary lung cancer; bullas emphysema; large cell; carcinoma

Submitted Jul 02, 2014. Accepted for publication Sep 12, 2014.

doi: 10.3978/j.issn.2072-1439.2014.09.29

View this article at: <http://dx.doi.org/10.3978/j.issn.2072-1439.2014.09.29>

Introduction

Bullous emphysema has been proven to be an important risk factor for lung cancer. Lung cancer, however, is rarely found during surgery for pneumothorax. In the reported case, lung cancer was incidentally discovered after the patient underwent surgery because of pneumothorax. We report a large cell carcinoma on the bullous wall detected in the specimen resected during an operation for spontaneous pneumothorax.

Case

A 72-year-old male patient with emphysema was admitted to our hospital complaining of dyspnea. He was found to have a high fever. The previous history of the patient was not significant. Chest radiography showed infectious bullae and pneumothorax as well as infectious effusion in the bullae (*Figure 1*). Computed tomography (CT) of the chest revealed bullae on the right upper lobe (*Figure 2*). We performed chest drainage, finding serous fluid and air in the drainage tube, removing them. Although chest drainage was instituted, the patient continued to have a persistent air leak. Furthermore, the intracystic infection did not



Figure 1 Chest radiography after chest drainage shows a bulla and intra-bulla fluid in the right upper lung field.

diminish. Therefore, we performed a right upper lobectomy because the bullae had spread over almost all of the right upper lobe. The postoperative course was uneventful, and the patient was discharged on the 6th postoperative day.

The pathological specimen contained a tumor that had developed from the thickened wall of a bulla (*Figure 3A*). The postoperative pathological diagnosis was large cell carcinoma arising from the wall of a bulla (*Figure 3B*).

Discussion

Bullous emphysema is an important risk factor for lung cancer (1-4). The incidence of lung cancer associated with emphysematous bullae has been reported to be 6.1%, which was times higher than that for patients without bullous disease (1). There are three possible explanations for lung cancer arising in a patient with bullous emphysema: (I) an occult cancer that has been present for some time, causing accumulation of material in the bullous area; (II) cancer arising from an area of squamous metaplasia; (III) cancer arising from a scar on the bullous wall (5).

Histologically, poorly differentiated adenocarcinoma and large cell carcinoma are most common. The prognosis is poor for each (6). It is rare that lung cancers are detected via the spontaneous pneumothorax (7,8). Cases of lung cancer whose first symptom is spontaneous pneumothorax are rare,

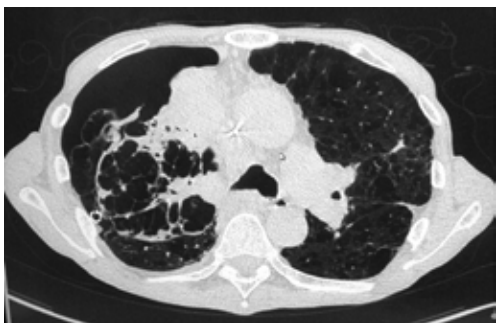


Figure 2 Chest computed tomography shows bullae spread over almost all of the right upper lung lobe.

having been reported in fewer than 1% of cases (9).

In this case, the patient was admitted to our hospital because of spontaneous pneumothorax. We performed surgery on him to resect bullae that exhibited air leakage or contained infectious fluid. During the operation, we could see the bullae spreading over almost all of the right upper lobe, so we decided to change the operation to right upper lobectomy. During the operation the cancerous lesion was not macroscopically evident. Fortunately, we completed the resection so it included removal of the occult cancer that was found later in the resected specimen. In medical practice, we see many patients with spontaneous pneumothorax caused by rupture of emphysematous bullae. Although our first thought is that the disease is probably caused by a weakened lung surface, we must not lose sight of the possible existence of cancer. Also, at the time of lung collapse it is common that various examinations (e.g., radiography and CT of the chest) indicate that the part of the lung that has collapsed has a nodular appearance. Thus, it is possible to misread the results of those examinations. Additionally, tumor associated with a lung cyst is almost always located in the distal portion of the lung. Hence, in most patients there are no symptoms that could be attributed to a cancer. This point makes it more difficult to suspect and then detect a tumor (5).

Conclusions

We reported a case of lung cancer detected in the operative specimen from a patient with diagnosed pneumothorax. Cases of lung cancer in which the first symptom is spontaneous pneumothorax are rare. Bullous emphysema, however, has been proven to be an important risk factor for lung cancer. It is therefore important to keep in mind the possible occurrence of lung cancer in the walls of bullae.

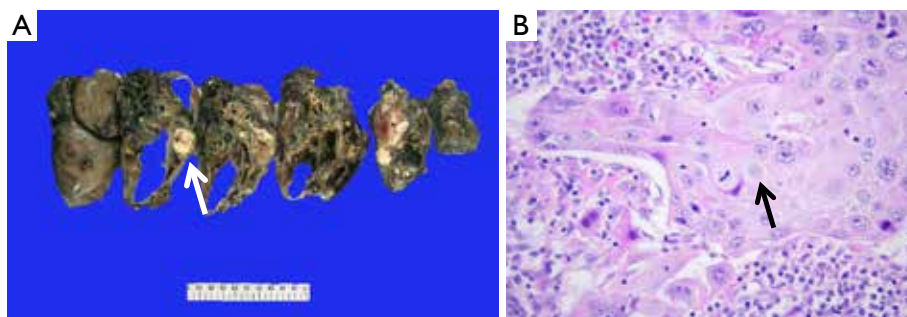


Figure 3 (A) Cut surface of the resected right upper lobe discloses a well-demarcated tumor nodule measuring 5.0 cm in greatest diameter. It is closely associated with bullous cystic lung tissue; (B) histological sections reveal solid nests of large cell carcinoma ($\times 600$).

Acknowledgements

Disclosure: The author declares no conflict of interest.

References

1. Stoloff IL, Kanofsky P, Magilner L. The risk of lung cancer in males with bullous disease of the lung. *Arch Environ Health* 1971;22:163-7.
2. Hanaoka N, Tanaka F, Otake Y, et al. Primary lung carcinoma arising from emphysematous bullae. *Lung Cancer* 2002;38:185-91.
3. Ogawa D, Shiota Y, Marukawa M, et al. Lung cancer associated with pulmonary bulla. case report and review of literature. *Respiration* 1999;66:555-8.
4. Hirai S, Hamanaka Y, Mitsui N, et al. Primary lung cancer arising from the wall of a giant bulla. *Ann Thorac Cardiovasc Surg* 2005;11:109-13.
5. Sakuraba M, Murasugi M, Adachi T, et al. Squamous cell carcinoma caused by dysplasia on the bullous wall. *Kyobu Geka* 2004;57:533-6.
6. Shin H, Oda M, Matsumoto I, et al. Lung adenocarcinoma originated from bulla wall accompanying spontaneous hemopneumothorax; report of a case. *Kyobu Geka* 2010;63:245-7.
7. Hiraoka S, Osaki T, Fukuda A, et al. Minute foci of adenocarcinoma detected in the operative specimen in a case of spontaneous pneumothorax. *J Jpn Surg Ass* 2005;66:2407-10.
8. Kaito A, Toyoda F, Nakamura T, et al. Large cell neuroendocrine cell carcinoma of the lung found incidentally during surgery for spontaneous pneumothorax. *J JpnSurg Ass* 2008;69:1902-5.
9. Tsukamoto T, Satoh T, Yamada K, et al. Primary lung cancer presenting as spontaneous pneumothorax. *Nihon Kyobu Shikkan Gakkai Zasshi* 1995;33:936-9.

Cite this article as: Ema T. Large cell carcinoma on the bullous wall detected in a specimen from a patient with spontaneous pneumothorax: report of a case. *J Thorac Dis* 2014;6(10):E234-E236. doi: 10.3978/j.issn.2072-1439.2014.09.29

A huge neoplasm occupying the right hemithorax in a pregnancy

Mei Yang*, Cheng Shen*, Heng Du, Yun Wang, Guowei Che

Department of Thoracic Surgery, West-China Hospital, Sichuan University, Chengdu 610041, China

*These authors contributed equally to this work.

Correspondence to: Guowei Che, MD. Department of Thoracic Surgery, West-China Hospital, Sichuan University, Chengdu 610041, China. Email: cheguowei_hx@aliyun.com.

Abstract: Germ cell tumors, like teratoma, typically occur in young adults in their second to fourth decade with equal sex distribution. We firstly report a very rare case of a huge tumor compressed the vital structures of the mediastinum that was diagnosed in a 21-year-old woman at 39 weeks of gestation during a routine prenatal examination. The patient underwent complete en-bloc resection and the size of the tumor was extremely large although no invasion to the vessels or to the airway had occurred. Adherence to the adjacent right pulmonary artery and right main bronchus was present, but without erosion or fistulization. The patient has remained well for over 2 months after the treatment without any signs of disease recurrence.

Keywords: Teratoma; surgery

Submitted Aug 12, 2014. Accepted for publication Aug 14, 2014.

doi: 10.3978/j.issn.2072-1439.2014.08.46

View this article at: <http://dx.doi.org/10.3978/j.issn.2072-1439.2014.08.46>

Introduction

Germ cell tumors typically occur in young adults. Female ascendency has been reported by some authors with a ratio of 1.27-2.05 for female to male (1-3). In 1953, Willis defined the teratomas as true tumors composed of tissues that are foreign to the part or organ of the body (4). Anterior mediastinum is the most frequent site of occurrence of the tumors in thorax, and benign teratomas constitute about 3-12% (5). According to another review, 3-8% is located in the posterior portion of the visceral compartment (6). The incidence given for germ cell tumors complicating pregnancy varies in the literatures (7,8). We firstly report a very rare case of a huge tumor compressed the vital structures of the mediastinum that was diagnosed in a 21-year-old woman at 39 weeks of gestation during a routine prenatal examination.

Case report

An ultrasound scan was performed at 39th gestational week in a 21-year-old primigravida which revealed a 10 cm × 10 cm × 8 cm smooth-walled, mixed echogenic mass with irregular inner contents in the right thorax and presented

to our hospital with cough for 2 weeks. A repeat scan four weeks later after she underwent a cesarean section, showed the same in the size of the mass. Physical examination showed dullness to percussion and diminished breath sounds on the right side of the chest. Laboratory data, including serum tumor markers were all within normal limits. Chest X-ray showed total atelectasis of the right lung and contained some calcified components in the middle of the thorax (*Figure 1*). The contrast-enhanced computed tomography (CT) scan revealed a large heterogeneous well-defined mass of 16 cm × 10 cm in size on the right side abutting the chest wall and extended to the whole right pleural space (*Figure 2*). The mass showed heterogeneous density containing soft tissue elements, fat, cystic areas and foci of calcification. The echocardiography showed squeezing of the right atrium (*Figure 3*).

The patient, however, refused to have the Computed tomography-guided percutaneous aspiration examination. As diagnosis was not established through imaging, surgical management was first in the priority list of therapeutic options. The patient was subjected to the right posterolateral thoracotomy through the fifth intercostal space. Many adhesions existed with the right pulmonary artery, the right main bronchus, the pericardium, the

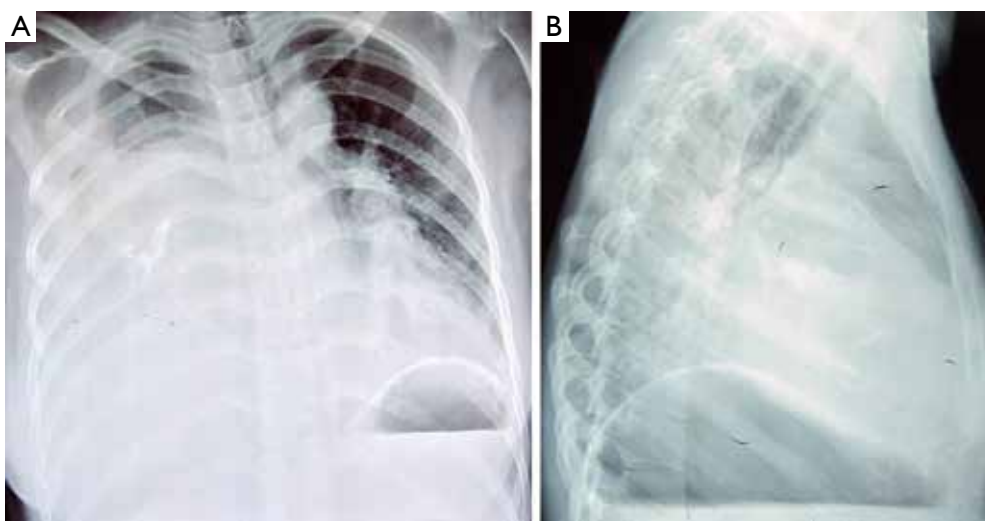


Figure 1 Chest X-ray of the case. Chest X-ray showed total atelectasis of the right lung and contained some calcified components in the middle of the thorax (A,B).

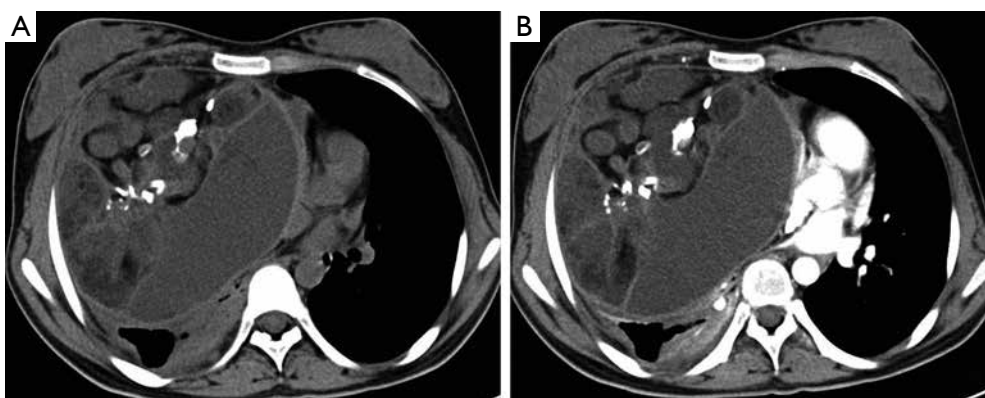


Figure 2 Contrast-enhanced CT features of the case. The contrast-enhanced CT scan revealed a large heterogeneous well-defined mass of 16 cm × 10 cm in size on the right thorax (A,B).

superior vena cava, and the diaphragm, and a combination of blunt and sharp dissection for the division was applied uneventfully. Because of difficulty in the mobilization of such a huge mass, a purse string suture permitted aspiration of sebaceous content via a small incision in the wall. As the size diminished, manipulation was facilitated. The tumor was completely resected and the collapsed right lung was easily re-expanded. Macroscopic examination of the resected tumor was white-gray colored, well circumscribed, and measured 16 cm × 13 cm × 10 cm in size. Histologically, it contained skin components with sebaceous glands, vessels, and fat, and muscles with bone, bone marrow, and gastrointestinal epithelium (*Figure 4*). No malignant or immature component was found. She is doing well without

evidence of tumor recurrence 2 months following her initial diagnosis.

Discussion

Teratomas are uncommon neoplasms comprised of mixed dermal elements derived from the three germ cell layers and are characterized by the presence of virtually any tissue type. According to the mediastinal germ cell tumor classification system proposed in 1986 by Mullen and Richardson, there are three categories: benign germ cell tumors, seminomas, and nonseminomatous germ cell tumors, also called malignant teratomas (9). Germ cell tumors comprise 15-20% of all anterior mediastinal tumors and benign

mediastinal teratomas accounts for 60% of all germ cell tumors (10). Benign mature teratomas contain components derived from more than one of the three primitive germ cell layers: ectoderm: hair, skin; mesoderm: bone, cartilage, muscle, fat; endoderm: bronchial, intestinal, pancreatic tissue (11). A PubMed searching of the period from 1990 to 2014 revealed little information on the “huge teratoma” of gravida as seen in our patient. We firstly report a very rare

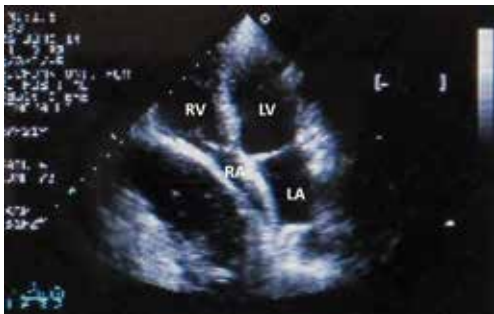


Figure 3 Echocardiography of the case. The echocardiography showed squeezing of the right atrium.

case of a huge teratoma that was diagnosed in a 21-year-old woman at 39 weeks of gestation.

Benign teratomas are usually asymptomatic and may be diagnosed as an incidental finding. Common presenting symptoms include chest or shoulder pain, dyspnea, cough, fever, pleural effusion, and bulging of the chest wall (12). In the case under discussion, the patient presented cough for two weeks. With regard to radiologic evaluation, the most characteristic radiologic finding of these neoplasms is identification of a complex mass containing a well-circumscribed fluid volume, fat-fluid level and calcifications. These findings are best identified by CT. CT offers superior identification of fat as either sebum or adipose tissue than by ultrasound. A fat-fluid level, however, has also been described in a case of well-differentiated liposarcoma of the retroperitoneum (13). There is also a word of caution in our case. Patient examined with chest X-ray showed total atelectasis of the right lung and contained some calcified components and the contrast-enhanced CT scan revealed a huge heterogeneous well-defined mass on the right side abutting the chest wall, which probably extended to the whole right pleural space. While CT was the standard for

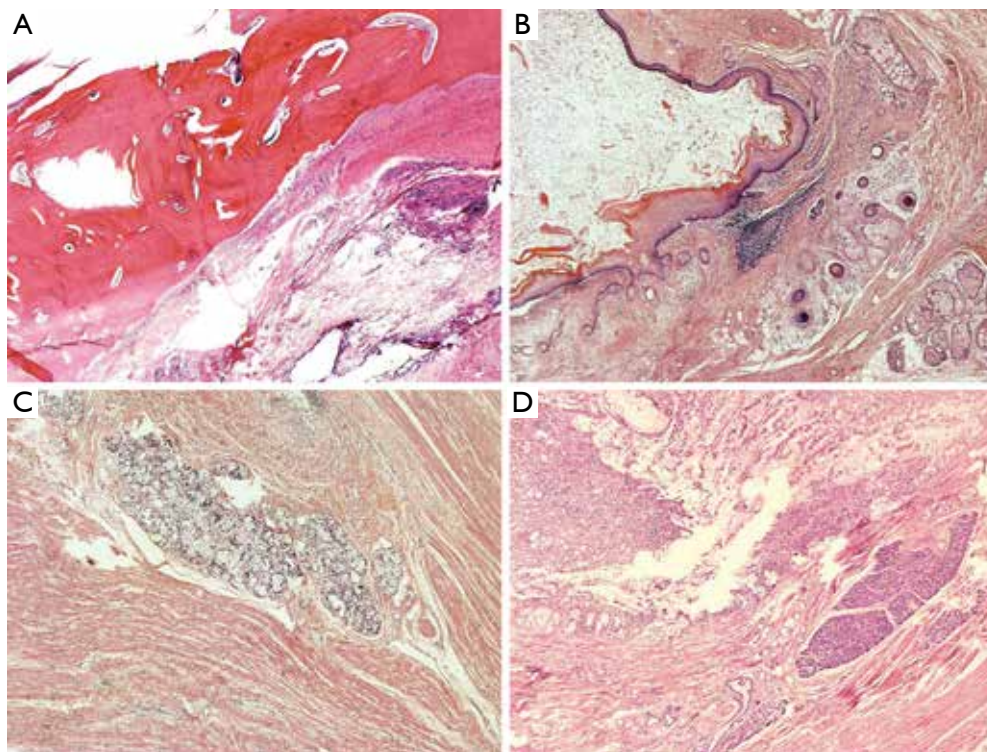


Figure 4 Histological and immunoistochemical features. Histologically, it contained skin components with bone marrow (A), sebaceous glands (B), muscles and muciparous glands (C) and gastrointestinal epithelium (D). (40×).

retroperitoneal imaging, MRI allows for improved soft tissue resolution. It is useful in assessing for encasement or invasion of blood vessels, which aids in the determination of malignant potential and resectability. Fat is suggested by high-intensity signal on T1-weighted images (14). In our case, the patient refused to have the examination of MRI for the high cost.

Macroscopically, there are two variants. Cystic teratomas are composed of fully mature elements and are usually benign. Solid teratomas are more likely to be malignant and formed of immature embryonic tissue, fibrous tissue, fat, cartilage, and bone (15). Microscopically, cysts lined by a variety of epithelia, calcification and ossification are often seen. Benign mature cystic teratomas include epidermis, brain and glial tissue, teeth, cartilage, peripheral nerve, smooth muscle, respiratory epithelium, connective tissue, and intestinal epithelium (16). The teratoma classification system introduced by Gonzalez-Crussi (17), allows for stratification based on the nature of the tissues present within the tumor, their proportion, and their characteristics.

The differential diagnosis of benign teratoma is malignant teratoma. Malignant transformation has been reported to occur in 1% to 2% of ovarian cystic teratomas and in a few cases of mediastinal teratoma, especially giant mediastinal teratoma (18). The possibility of malignant transformation should be considered in any cystic tumor with an invasive solid portion in the wall. Malignant teratomas tend to progress rapidly and are generally diagnosed at advanced stages when symptoms develop. Renato *et al.* (19) reviewed ten cases of malignant retroperitoneal teratomas and found that the most common presenting symptoms were abdominal pain, an abdominal mass, vomiting, weight loss, and fever. Germinomas, while malignant, are radiosensitive and multi-modality treatment (chemotherapy, radiation, and surgery) often leads to effective tumor control.

Surgical resection is the treatment of choice and radical extirpation secures a long survival out of recurrence. Chemotherapy and radiotherapy have relatively small roles in the management of these tumors. Median sternotomy is usually preferred for tumor removal, but access via either posterolateral or anteroposterior thoracotomy depends on the size, location, and expansion of the tumor. Difficulty in surgical maneuvers may be a result of the vital structures involved (20). In the case reported, right posterolateral access was chosen, as the tumor was almost entirely located into the right hemithorax, reaching and adherent to the left hemidiaphragm. Such a location precludes median

sternotomy, otherwise the preferred approach, as surgical manipulations are impossible on the lower lobe of the right lung and on the right hemidiaphragm. CT-scan revealed the relations with the mediastinum vital anatomical structures because it was critical to clarify whether there was an invasion or simply compression. At last, the tumor was completely resected and the collapsed right lung was easily re-expanded. Microscopic examination showed mature cystic teratoma.

Conclusions

Huge teratoma is rare neoplasm that is diagnosed in a pregnant woman. Teratoma is suggested by CT demonstrating a complex mass with a well-circumscribed fluid volume, fat-fluid level, and calcifications. While the majority of these neoplasms are benign, a variety of malignant components may be present or develop from clonal transformation. In the case reported, the primigravida presented only the cough for 2 weeks and the growth of the huge tumor has little influenced the pregnancy. Surgical resection and careful histologic evaluation is required for diagnosis. To facilitate the preoperative diagnosis and avoid the misdiagnosis of such rare disease, more cases will need to be reported.

Acknowledgements

We greatly appreciate the assistance of the staff of the Department of Thoracic Surgery, West-China Hospital, Sichuan University, and thank them for their efforts.

Disclosure: The authors declare no conflict of interest.

References

1. Takeda S, Miyoshi S, Ohta M, et al. Primary germ cell tumors in the mediastinum: a 50-year experience at a single Japanese institution. *Cancer* 2003;97:367-76.
2. Lewis BD, Hurt RD, Payne WS, et al. Benign teratomas of the mediastinum. *J Thorac Cardiovasc Surg* 1983;86:727-31.
3. Dulmet EM, Macchiarini P, Suc B, et al. Germ cell tumors of the mediastinum. A 30-year experience. *Cancer* 1993;72:1894-901.
4. Soysal Ö, Saraç K, Kutlu R, et al. A case of mediastinal teratoma presenting as a cystic lesion on chest wall. *East J Med* 1998;3:32-3.
5. Sinclair DS, Bolen MA, King MA. Mature teratoma within

- the posterior mediastinum. *J Thorac Imaging* 2003;18:53-5.
6. Shirodkar NP, Chopra PS, Marker M, et al. Conjoined gastric and mediastinal benign cystic teratomas. Case report of a rare occurrence and review of literature. *Clin Imaging* 1997;21:340-5.
 7. Walid D, Hamdi N, Ouerdiane N, et al. Huge cervico-facial teratoma. *Tunis Med* 2012;90:408-9.
 8. Jeong HC, Cha SJ, Kim GJ. Rapidly grown congenital fetal immature gastric teratoma causing severe neonatal respiratory distress. *J Obstet Gynaecol Res* 2012;38:449-51.
 9. Mullen B, Richardson JD. Primary anterior mediastinal tumors in children and adults. *Ann Thorac Surg* 1986;42:338-45.
 10. Lakhota S, Dewan RK. Benign cystic teratoma of mediastinum. *Indian J Surg* 2008;70:244-6.
 11. Duwe BV, Sterman DH, Musani AI. Tumors of the mediastinum. *Chest* 2005;128:2893-909.
 12. Wang RM, Chen CA. Primary retroperitoneal teratoma. *Acta Obstet Gynecol Scand* 2000;79:707-8.
 13. Schmidt M, Wolke S, Hübner A, et al. Successful treatment of a huge congenital cervical teratoma. *J Craniofac Surg* 2009;20:1277-80.
 14. Cadeddu MO, Mamazza J, Schlachta CM, et al. Laparoscopic excision of retroperitoneal tumors: technique and review of the laparoscopic experience. *Surg Laparosc Endosc Percutan Tech* 2001;11:144-7.
 15. Bruneton JN, Diard F, Drouillard JP, et al. Primary retroperitoneal teratoma in adults: presentation of two cases and review of the literature. *Radiology* 1980;134:613-6.
 16. Gupta N, Shah D, Singh U, et al. Antenatal diagnosis of large sacro-coccygeal teratoma with foetal cardiomegaly and hydrops. *Kathmandu Univ Med J (KUMJ)* 2008;6:383-5.
 17. Gonzalez-Crussi F. *Extragenital Teratomas*. Washington: AFIP, 1982.
 18. Yamaguchi K, Mandai M, Fukuhara K, et al. Malignant transformation of mature cystic teratoma of the ovary including three cases occurring during follow-up period. *Oncol Rep* 2008;19:705-11.
 19. Renato F, Paolo V, Girolamo M, et al. Malignant retroperitoneal teratoma: case report and literature review. *Acta Urol Belg* 1996;64:49-54.
 20. Zisis C, Rontogianni D, Stratakos G, et al. Teratoma occupying the left hemithorax. *World J Surg Oncol* 2005;3:76.

Cite this article as: Yang M, Shen C, Du H, Wang Y, Che G. A huge neoplasm occupying the right hemithorax in a pregnancy. *J Thorac Dis* 2014;6(10):E237-E241. doi: 10.3978/j.issn.2072-1439.2014.08.46

Primary intravascular large B-cell lymphoma of the lung: a review and case report

Yanfan Chen¹, Cheng Ding², Quan Lin², Kaiyan Yang³, Yuping Li², Shaoxian Chen²

¹Department of Respiration, Zhejiang Chinese Medical University, Hangzhou 310000, China; ²Department of Respiration, ³Department of Pathology, The First Affiliated Hospital of Wenzhou Medical University, Wenzhou 325000, China

Correspondence to: Yanfan Chen. Department of Respiration, Zhejiang Chinese Medical University, Hangzhou 310000, China. Email: chenyf2605@163.com.

Objective: To investigate the clinicopathological features of primary intravascular large B-cell lymphoma (IVLBCL) of the lung.

Methods: Histopathological and clinical data based on lung biopsy were analyzed and used to diagnose a patient with IVLBCL of the lung.

Results: Fever and respiratory symptoms were the main presentations, lung biopsy revealed lymphoma cells in the lumen of small blood vessels. Tumor cells expressed Bcl-2, the Bcl-6, CD20, Ki67, MUM-1, Pax5, CD, CD30, and vascular endothelial CD34.

Conclusions: Primary pulmonary IVLBCL of the lung is extremely rare, on chest CT it manifests as diffuse ground glass shadow, or nodular consolidations in the lung, lactate dehydrogenase and C-reactive protein was found to increase, fluorodeoxyglucose positron emission tomography/computed tomography (FDG-PET/CT) is an important and significant diagnostic modality in its early diagnosis. Also, bronchial lung biopsy has the advantage of less trauma and high sensitive rate. R-CHOP is the main treatment for lung primary pulmonary IVLBCL of the lung; however, its prognosis is relatively poor.

Keywords: Intravascular lymphoma; large B-cell; lung; case report

Submitted Apr 21, 2014. Accepted for publication Aug 14, 2014.

doi: 10.3978/j.issn.2072-1439.2014.08.45

View this article at: <http://dx.doi.org/10.3978/j.issn.2072-1439.2014.08.45>

Background

Intravascular large B-cell lymphoma (IVLBCL) of lung is a rare type of extranodal large B-cell lymphoma (LBCL) characterized by the selective growth of lymphoma cells within the lumina of vessels, particularly within capillaries, with sparing of larger arteries and veins. The clinical presentation is highly variable due to occlusion of small vessels or capillaries in different organ systems. This is an aggressive lymphoma with poor prognosis that in part reflects frequent delays in diagnosis due to above variable symptoms. The most common clinical manifestations involve central nervous system (CNS) presentations, cutaneous lesions, fever, or hemophagocytic syndrome. Although autopsy findings have revealed that pulmonary involvement is common in this disease, primary presentation in the lungs is distinctly uncommon and has been rarely described. Here we report a case with its predominant

clinical manifestation as interstitial lung disease, which was finally diagnosed as IVLBCL by biopsy. The clinical features, histopathological characteristics, and differential diagnosis of primary IVLBCL were also discussed in this article. Our patient was diagnosed with the help of the bronchial lung biopsy (TBLB). The clinical features, histopathological characteristics, and differential diagnosis of primary IVLBCL were also discussed in this article.

Case presentation

A 35-year-old, previously healthy woman presented to our hospital, with one-month history of cough, breathlessness and fever for two weeks. At a local hospital, based on the radiological findings, she was tentatively diagnosed with pulmonary infection and treated with various antibiotics and an intermittent use of methylprednisolone (40 mg/d). Her fever remained constant, and her breathlessness was

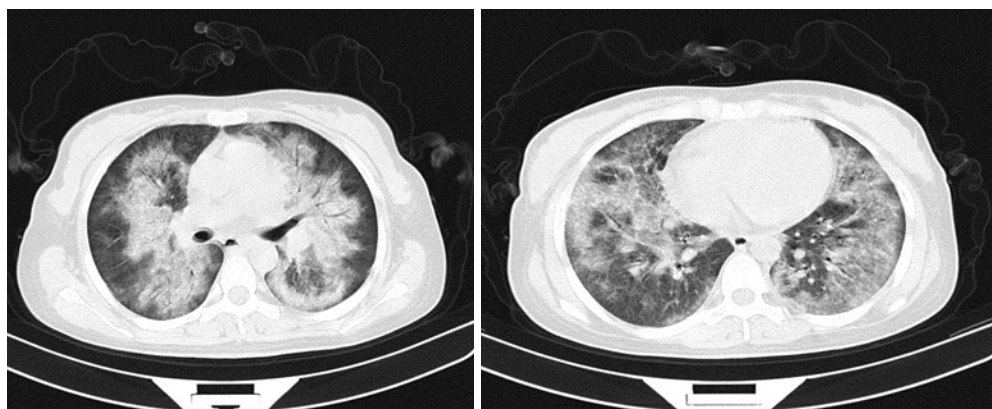


Figure 1 Chest CT-scan showing diffuse bilateral interstitial shadows with small granules and nodules. CT, computed tomography.

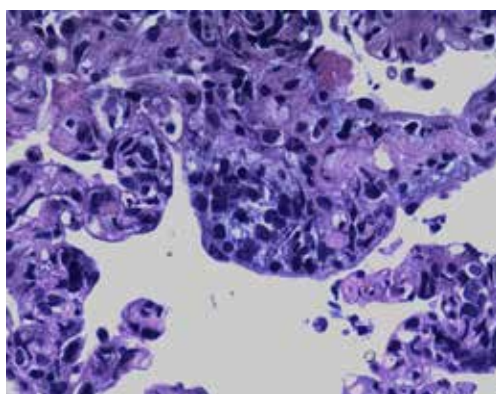


Figure 2 Hematoxylin-eosin staining of pulmonary interstitium intravascular lymphoma, (400 \times).

worsening even after treatment. She was a housekeeper and lived in Beijing for ten years. She denies any dust exposure or illicit drug use. At her initial presentation (day 1), she appeared well, and vital signs showed blood pressure of 106/54 mmHg, temperature 38.6 °C, heart rate 112 beats/min, respiratory rate 23 breaths/min and oxygen saturation 92-95% (FIO₂ = 5 L/min). Physical examination showed emaciation and no inspiratory fine crackles and superficial lymphadenopathy was noted. Serum laboratory examinations showed a mild decrease in leucocyte count (3,600 μ L); hemoglobin (72 g/L) and marked elevation of lactate dehydrogenase (LDH; 1,554 IU/L), C-reactive protein (175 U/L), procalcitonin (0.331 ng/mL), β 2 microglobulin (5.22 mL) and antinuclear antibodies, and antineutrophil cytoplasmic antibodies were negative. Blood gas analysis showed pH 7.406, PaCO₂ 33.5 mmHg, PaO₂ 64.2 mmHg. Chest CT-scan showed diffuse interstitial shadows (*Figure 1*).

Lung function test showed decline in diffusion and a mild restrictive ventilatory disorder.

Echocardiography showed moderate pulmonary hypertension (mean pulmonary artery pressure of 43 mmHg). After admission, prophylactic treatment was given, but her fever persisted intermittently (temperature range, 37-39 °C), with oxygen saturation fluctuations in the 92-95% (nasal 5 L/min). A TBLB was immediately performed. On HE staining, the biopsied specimen showed accumulation of abundant atypical lymphocytes in the capillary vessels (*Figure 2*). Immunohistochemical (IHC) staining showed cells were positive for CD20, Pax5 (*Figure 3A,B*), BCL2, BCL6 and MUM-1 and negative for CD3, CD10, CD2, CD30, CD34 (*Figure 4*), CD5, CD56, CD68, EBER, Syn, TTF-1, Granzyme B, and P63. The mean Ki-67 proliferation rate was 60% (*Figure 5*), indicating the tumour was in an active growing status. Bone marrow biopsy specimen revealed hyperplastic bone marrow, and atypical lymphocytes (9%) were also found (*Figure 6*).

Based on thorough history and investigation, the patient was diagnosed with IVLBCL. She was treated with R-CHOP (rituximab 600 mg, the day before chemotherapy, cyclophosphamide 1.0 g on day 1 + doxorubicin 60 mg on day 1 and day 2 + leucovorin 2 mg on day 1 + prednisone 60 mg from day 1 to day 9, daily) for one cycle.

Due to severe respiratory failure, the patient died from multiple organ failure a week after the diagnosis.

Discussion

Pfleger and Tappeiner first described IVLBCL in 1958. It is characterized by tumor cells located almost entirely in the intravascular, peripheral blood and bone marrow

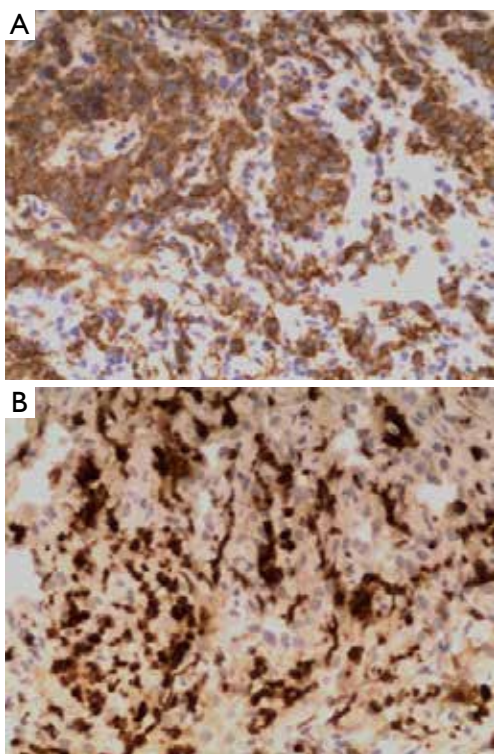


Figure 3 (A) CD20 immunostain of neoplastic intravascular B lymphocytes, (200×); (B) Pax5 immunostain showing the neoplastic lymphocytes, (200×).

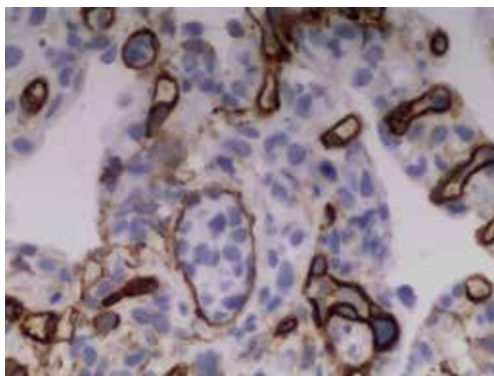


Figure 4 CD34 immunostain showing neoplastic lymphocytes located in the alveolar capillaries, (400×).

which makes it difficult to correctly differentiate from other tumors and it is regarded as a source of endothelial cells of the tumor. With the development of immunohistochemical and monoclonal antibody technology, it has been classified as a special type of lymphoma. In 2008 WHO identified it as a rare type of non-Hodgkins lymphoma (NHL). The

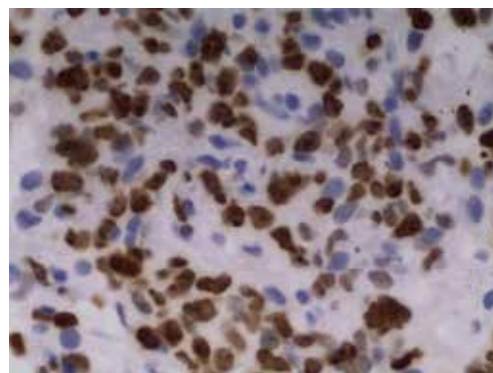


Figure 5 KI-67 immunostain highlighting the proliferation of intravascular lymphoma cells, (200×).

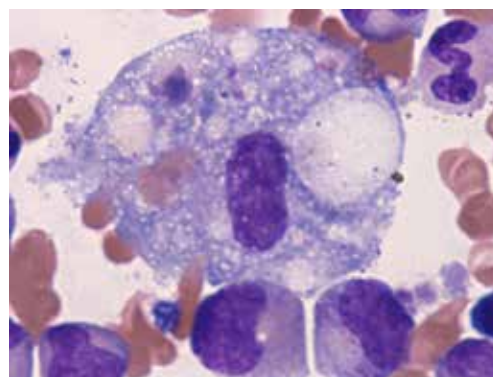


Figure 6 Bone marrow smear shows hemophagocytic syndrome (red cells are engulfed).

main characteristics of this type of lymphoma are diffuse, occlusive proliferation, especially in the capillaries, small arteries and veins (1). There's also the involvement of different organs and tissues including the CNS, skin, lung, kidney, but rarely affects the liver, spleen and lymph nodes. The pathogenesis of IVLBCL is unclear, however the splitting and translocation of chromosome maybe related with the pathogenesis of this disease (2).

The clinical manifestations of IVLBCL were nonspecific. Fever, weight loss and sweating (3) were the most common presentations. The main clinical findings were cough, sputum, hypoxaemia and dyspnea when lung was involved. Some patients also presented with hypercalcemia, pulmonary embolism, pulmonary hypertension or hemophagocytic syndrome as initial symptoms (3-5). In this case, pulmonary arterial hypertension was the main presentation with bone marrow hemophagocyte found on

histological examination.

An increased serum LDH, CRP and β 2-microglobulin interleukin-2R (IL-2R) were found in most cases, and close relation between increased LDH levels and the differentiation of tumor cells was observed, accompanied with anemia, decreased platelets and white blood cell count (6,7). The abnormal lung function usually seen in such cases was limitation of ventilation and diffusion dysfunction (8).

Thoracic computed tomography (CT) findings of the lung involvement of IVLBCL patients were diverse, including ground glass opacity (GGO), multiple centrilobular nodules, interlobular septal thickening, interstitial shadows and thickening of bronchovascular bundles, suggesting lymphatic and or haematological spread (8). Recently, FDG-PET has emerged as a powerful functional imaging tool in the assessment of patients with this type of NHL. Several authors have reported FDG-PET is useful in the diagnosis of IVLBCL when this type of lymphoma is clinically suspected. FDG-PET is a powerful tool for the early diagnosis of IVLBCL with pulmonary involvement, when there is a suspected possibility of the presence of this disease in a patient with respiratory symptoms without abnormal findings by CT (9).

The diagnosis is often delayed due to varied clinical presentations and limited understanding of the entity. Histopathology remains the gold standard for diagnosis, showing the classic appearance of large malignant lymphocytes filling small vascular lumina particularly in cases involving the lung; TBLB was a useful method in our diagnosis. If it cannot be confirmed with TBLB, it is necessary to perform an open lung biopsy or a thoracoscopy (10).

Treatment recommendations are extrapolated from results of trials of more common subtypes of lymphoma. Most cases of IVL are associated with poor prognosis and should be treated systemically with an anthracycline-based regimen. Anthracycline-based chemotherapy has been associated with a 60% response rate and a 3-year overall survival rate of more than 30%. CHOP (cyclophosphamide, doxorubicin, vincristin, prednisone) and CHOP-like regimens are also considered to be effective. The treatment of cases with lung involvement is similar to that of diffuse LBCL. Takahashi *et al.* (11) found that the effect of rituximab combined with CHOP was better than just the single CHOP regimen, through analysis of the effect on 1,221 cases involving the various organs in patients with LBCL.

Acknowledgements

Disclosure: The authors declare no conflict of interest.

References

1. Swerdlow SH, Campo E, Harris NL, et al. eds. WHO Classification of Tumours of Haematopoietic and Lymphoid Tissue. Geneva: World Health Organization, 2008.
2. Cui J, Liu Q, Cheng Y, et al. An intravascular large B-cell lymphoma with a t(3;14)(q27;q32) translocation. *J Clin Pathol* 2014;67:279-81.
3. Sinha N, Lantigua L, Niazi M, et al. An elderly lady with Fever of unknown etiology and severe pulmonary hypertension: intravascular lymphoma-an elusive diagnosis. *Case Rep Med* 2013;2013:153798.
4. Chinen Y, Nakao M, Sugitani-Yamamoto M, et al. Intravascular B-cell lymphoma with hypercalcemia as the initial presentation. *Int J Hematol* 2011;94:567-70.
5. Fung KM, Chakrabarty JH, Kern WF, et al. Intravascular large B-cell lymphoma with hemophagocytic syndrome (Asian variant) in a Caucasian patient. *Int J Clin Exp Pathol* 2012;5:448-54.
6. Anila KR, Nair RA, Koshy SM, et al. Primary intravascular large B-cell lymphoma of pituitary. *Indian J Pathol Microbiol* 2012;55:549-51.
7. Ponzoni M, Ferreri AJ. Intravascular large B cell lymphoma: widespread but not everywhere. *Acta Haematol* 2014;131:16-7.
8. Yu H, Chen G, Zhang R, et al. Primary intravascular large B-cell lymphoma of lung: a report of one case and review. *Diagn Pathol* 2012;7:70.
9. Yamashita H, Suzuki A, Takahashi Y, et al. Intravascular large B-cell lymphoma with diffuse FDG uptake in the lung by 18FDG-PET/CT without chest CT findings. *Ann Nucl Med* 2012;26:515-21.
10. Nishizawa T, Saraya T, Ishii H, et al. Antemortem diagnosis with multiple random skin biopsies and transbronchial lung biopsy in a patient with intravascular large B-cell lymphoma, the so-called Asian variant lymphoma. *BMJ Case Rep* 2014;2014.
11. Takahashi H, Tomita N, Yokoyama M, et al. Prognostic impact of extranodal involvement in diffuse large B-cell lymphoma in the rituximab era. *Cancer* 2012;118:4166-72.

Cite this article as: Chen Y, Ding C, Lin Q, Yang K, Li Y, Chen S. Primary intravascular large B-cell lymphoma of the lung: a review and case report. *J Thorac Dis* 2014;6(10):E242-E245. doi: 10.3978/j.issn.2072-1439.2014.08.45